

Effective-field theories for heavy quarkonium

Nora Brambilla

INFN and Dipartimento di Fisica dell'Università di Milano via Celoria 16, 20133 Milan, Italy

Antonio Pineda and Joan Soto

Departament d'Estructura i Constituents de la Matèria, Universitat de Barcelona, Diagonal 647, E-08028 Barcelona, Catalonia, Spain

Antonio Vairo

INFN and Dipartimento di Fisica dell'Università di Milano via Celoria 16, 20133 Milan, Italy

(Published 2 December 2005)

This article reviews recent theoretical developments in heavy-quarkonium physics from the point of view of effective-field theories of QCD. We discuss nonrelativistic QCD and concentrate on potential nonrelativistic QCD. The main goal will be to derive Schrödinger equations based on QCD that govern heavy-quarkonium physics in the weak- and strong-coupling regimes. Finally, the review discusses a selected set of applications, which include spectroscopy, inclusive decays, and electromagnetic threshold production.

CONTENTS

I. Introduction	1424	B. Renormalon-subtracted scheme and power counting	1458
II. NRQCD	1427	VI. (p)NRQCD: The Static Limit	1459
A. Degrees of freedom	1427	A. NRQCD in the static limit	1459
B. Power counting	1427	B. Static pNRQCD in the weak-coupling regime	1460
C. Lagrangian, currents, and symmetries	1428	C. The singlet static potential at short distances versus lattice	1461
D. Matching	1429	D. Gluelumps versus lattice	1462
E. Renormalization group	1432	VII. Potential NRQCD. The Strong-Coupling Regime	1463
F. Applications: spectrum and inclusive decay widths	1434	A. Degrees of freedom	1463
1. Spectra	1434	B. Power counting	1464
2. Inclusive decay widths	1435	C. Lagrangian and symmetries	1464
III. Potential NRQCD. The Physical Picture	1437	D. Matching: analytic and nonanalytic mass terms	1464
A. Weak-coupling regime	1437	E. Matching for $ \mathbf{p} \sim \Lambda_{\text{QCD}}$	1465
B. Strong-coupling regime	1438	1. Matching of the analytic terms:	
IV. Potential NRQCD. The Weak-Coupling Regime	1438	quantum-mechanical matching	1466
A. pNRQCD: the degrees of freedom	1438	2. Matching of the analytic terms: the real pNRQCD potential	1467
B. Power counting	1439	3. Matching of the analytic terms: the imaginary pNRQCD potential	1470
C. Lagrangian and symmetries	1439	4. Matching of the analytic terms: direct matching of Wilson-loop amplitudes	1471
D. Feynman rules	1442	5. Matching of the nonanalytic terms	1472
E. Matching: diagrammatic approach	1443	F. Matching for $ \mathbf{p} \gg \Lambda_{\text{QCD}} \gg E$	1474
1. Pinch singularities	1445	1. pNRQCD'	1474
2. Potentials	1445	2. Matching pNRQCD to pNRQCD'	1474
F. Matching: Wilson-loop approach	1447	G. Potentials and spectra: lattice and models	1477
1. Interpolating fields	1447	1. Potentials and spectrum from the lattice	1478
2. Matching at $\mathcal{O}(r^0, 1/m^0)$	1448	2. QCD vacuum models	1479
3. Matching at $\mathcal{O}(r^1, 1/m^0)$ and $\mathcal{O}(r^2, 1/m^0)$	1449	H. Inclusive decay widths into light particles	1480
4. Matching at order r^0 ($1/m, 1/m^2$, and beyond)	1450	VIII. Phenomenological Applications	1482
G. Observables: spectrum and inclusive decay widths	1450	A. Determinations of m_b and m_c from the 1S resonances	1482
1. Heavy-quarkonium mass	1452	B. Spectroscopy in the weak-coupling regime	1483
2. Inclusive decay widths	1453	C. Electromagnetic inclusive decay widths in the weak-coupling regime	1484
H. Renormalization group	1454	D. Inclusive decay widths in the strong-coupling regime	1485
V. Renormalons and the Definition of the Heavy-Quark Mass	1456	E. Nonrelativistic sum rules	1487
A. The pole mass and static singlet potential renormalon	1456	F. $t\bar{t}$ production near threshold	1488

G. Semi-inclusive radiative decays	1489
IX. Conclusions	1491
X. Prospects	1492
Acknowledgments	1493
Table of Acronyms	1493
References	1493

I. INTRODUCTION

In order to understand human-scale processes, a classical nonrelativistic (NR) picture of physics based on Galilean symmetry proves sufficient. Until the beginning of the last century, this picture, supplemented with electromagnetism, was enough to understand the majority of processes observed in nature. At the start of the quantum age, it was again a NR equation, the Schrödinger equation, which proved to be the most successful in explaining the atomic and nuclear spectra.

High-energy processes are far from human-scale processes. They are described in the present by relativistic quantum field theories (QFTs). Under some circumstances, however, high-energy processes develop a NR regime and produce bound states that behave very much like atoms.

The discovery of the J/ψ , a heavy resonance with a very narrow width, at Brookhaven and SLAC (Aubert *et al.*, 1974; Augustin *et al.*, 1974), which was later identified with a bound state of a new (heavy) quark, charm, and its antiquark, namely, a charmonium ($c\bar{c}$) state, opened up the possibility of using a NR picture in the realm of QCD, the fundamental QFT of strong interactions. This possibility was enhanced three years later by the discovery of the Y , an even heavier and narrower resonance, which was again interpreted as a bound state of a new (heavier) quark, bottom, and its antiquark, namely, a bottomonium ($b\bar{b}$) state (Herb *et al.*, 1977). In fact, the narrow width of these resonances proved to be crucial in establishing QCD as the sector of the Standard Model that describes the strong interaction (Appelquist and Politzer, 1974; De Rujula and Glashow, 1975). From that moment on, charmonia and bottomonia have been thoroughly studied and still are a subject of intensive theoretical and experimental research (see, for instance, Brambilla *et al.*, 2004 and Skwarnicki, 2004). They can indeed be classified in terms of the quantum numbers of a NR bound state, and the spacing of the radial excitations and of the fine and hyperfine splittings has a pattern similar to the ones in positronium, a well-studied QED NR bound state. A related system, the $b\bar{c}$ bound state (B_c), has also been found in nature (Abe *et al.*, 1998). The heaviest of the quarks, the top, which has recently been found at the Tevatron (Abe *et al.*, 1994), has a large decay width (due to weak interactions) and is not expected to form narrow $t\bar{t}$ resonances. However, the production of $t\bar{t}$ near threshold, namely, in the NR regime, will be one of the major programs at the International Linear Collider.

These systems will be denoted by *heavy quarkonia*. They are characterized by at least three widely sepa-

rated scales: the hard scale (the mass m of the heavy quarks), the soft scale (the relative momentum of the heavy quark–antiquark $|\mathbf{p}| \equiv p \sim mv$, $v \ll 1$), and the ultrasoft (US) scale (the typical kinetic energy $E \sim mv^2$ of the heavy quark and antiquark). Moreover, by the definition of heavy quark, m is large in comparison with the typical hadronic scale Λ_{QCD} . Hence processes that happen at the scale m are expected to be successfully described using perturbation theory, due to the asymptotic freedom of QCD. This explains why the narrow heavy-quarkonium widths could be qualitatively understood as a manifestation of asymptotic freedom. However, lower scales, such as $|\mathbf{p}|$ and E , which are responsible for the binding, may or may not be accessible to perturbation theory. The appearance of all these scales in the dynamics of heavy quarkonia makes its quantitative study extremely difficult. This is even so in the weak-coupling regime, where the system becomes Coulombic. Nevertheless, by exploiting the hierarchies $m \gg p \gg E$ and $m \gg \Lambda_{\text{QCD}}$ the problem can be considerably simplified. This may be done in any particular calculation for a given observable, or, alternatively, using effective-field theories (EFTs). In the latter, the hierarchies of scales are exploited at the action level producing universal results independent of particular observables, which is far more advantageous. The basic idea behind EFTs is that to describe observables of a particular (low) energy region, one can integrate out the degrees of freedom of the other regions. This produces an effective action (for the EFT) involving only the degrees of freedom in the region we are interested in. Calculating with the effective (EFT) or with the fundamental (QCD) action gives equivalent physical results as far as that particular region is concerned, but calculations are much simpler with the EFT. In heavy quarkonium, we are interested in physics at the low-energy scale E . Hence EFTs, which have energy scales larger than E integrated out, can be and have been built. They have led to major progress in our understanding of heavy quarkonium in recent years. We shall devote this review to these new developments. Before that, let us put this progress in a historical perspective.

The discovery of bottomonium and charmonium triggered the use of NR potential models (where the physics of the bound state is described by a Schrödinger equation). The main input in this approach is the potential introduced. At lowest order in the weak-coupling regime ($|\mathbf{p}| \gg \Lambda_{\text{QCD}}$), the potential is Coulombic. Higher-order corrections to the potential in perturbation theory were obtained over the years (Buchmüller *et al.*, 1981; Gupta and Radford, 1981, 1982; Pantaleone *et al.*, 1986; Titard and Yndurain, 1994) even though the computations were difficult due to the several scales involved. It was also not clear how to systematically incorporate US effects. For instance, we mention the infrared sensitivity found in the static potential (Appelquist *et al.*, 1978) or in the one-loop calculations of P -wave decays (Barbieri *et al.*, 1980). In any case, the observed bottomonium and charmonium spectra turned out not to be Coulombic

and phenomenologically fine-tuned potentials were necessary to reproduce them (Eichten *et al.*, 1978). See Brambilla and Vario (1999a) for more references. This motivated attempts to derive the heavy-quarkonium potential from QCD without relying on perturbation theory. The idea was to find gauge-invariant expressions for the potentials (within an expansion in $1/m$) in terms of the expectation values of Wilson loops. Several methods have been worked out over the years and expressions for the spin-dependent and spin-independent potentials up to $\mathcal{O}(1/m^2)$ were obtained (Wilson, 1974; Susskind, 1977; Brown and Weisberger, 1979; Eichten and Feinberg, 1981; Peskin, 1983; Gromes, 1984; Barchielli *et al.*, 1988, 1990; Szczepaniak and Swanson, 1997). All the obtained potentials have been investigated on the lattice (see Bali, 2001, for a recent review). However, these results had a number of shortcomings. Lucha *et al.* (1991) pointed out that if calculated in perturbation theory, the potentials obtained from the Wilson-loop approach missed the hard logarithms $\sim \ln m$ present in the potentials directly computed from QCD. More recently, Brambilla, Pineda, *et al.* (2001) also pointed out that not only hard logarithms, but some of the potentials, relevant at relative order α_s^2 in the spectrum, were missed as well. Finally, the infrared (IR) divergences in the perturbative computation of P -wave decays seemed impossible to accommodate in that framework. Overall, a more systematic and controlled derivation of the nonrelativistic dynamics from QCD was required.

Independent of the line of research above, nonrelativistic QED (NRQED) an EFT for NR leptons, was introduced (Caswell and Lepage, 1986). It turned out to be the first and decisive link in the chain of developments that we shall review here. NRQED is obtained from QED by integrating out the hard scale m . It is characterized by an UV cutoff much smaller than the mass m and much larger than any other scale. Nonrelativistic QCD (NRQCD), which also appears in the title of the article of Caswell and Lepage (1986), was introduced soon afterwards (Lepage and Thacker, 1988). The Lagrangian of NRQCD can be organized in powers of $1/m$, thus making explicit its nonrelativistic nature. A set of operators and matching coefficients are associated with each power of m . The operators encode the low-energy content of the theory and the coefficients encode the effects of the degrees of freedom with energy $\mathcal{O}(m)$ that have been integrated out. Namely, in NRQCD the contributions coming from the hard scale m are factorized. NRQCD had two major advantages that we would like to point out here: (i) it could be rigorously derived from QCD in a systematic manner providing an optimized framework for lattice simulations (Thacker and Lepage, 1991) and (ii) it solved the problem of the IR divergences of the P -wave decays of heavy quarkonium. This solution, however, came at the price of introducing the so-called color-octet matrix elements, which could not be incorporated in the Schrödinger-like formulations available at that time. In spite of this, it was noted by

Chen *et al.* (1995) that if the nonperturbative potentials were calculated starting from NRQCD instead of from QCD, the problem of the missing hard logarithms mentioned above disappeared.¹ This again raised some hope that NR potential models could eventually be regarded as EFTs of QCD. It also made it evident that the potential models available, even those in which the potentials were obtained in terms of Wilson loops, were not controlled derivations from QCD and that first-principles computations of heavy quarkonia should be done within the framework of NRQCD.

NRQCD itself was, however, not free of shortcomings. The main problem was related to the fact that both soft and US degrees of freedom were entangled. This affects the power-counting rules, which were not homogeneous. Namely, the power counting by Lepage *et al.* (1992) assumed $\Lambda_{\text{QCD}} \lesssim mv^2$, which catches the leading-order contribution but not the subleading contributions in v . Also perturbative calculations were difficult to perform due to the dependence on two scales. Another problem was that the first computations in NRQCD were based on cutoff regularization,² whereas the calculations in QCD are often done in dimensional regularization (DR). Attempts to perform the matching between QCD and NRQCD using DR had the drawback that the naive incorporation of the kinetic term in the quark propagator jeopardized the power-counting rules.

A solution to the last problem was first proposed by Manohar (1997). He argued that the matching between QCD and NRQCD in the bilinear sector of the theory in DR should be performed by treating the kinetic-energy term as a perturbation, as was done in heavy-quark effective theory (reviewed by Neubert, 1994). Along the same lines, the matching of QCD to NRQCD in the four-fermion sector, where the Coulomb pole enhancement starts playing a role, was performed soon after by Pineda and Soto (1998a, 1998c). The key point was that in order to carry out the matching, it is not so important to know the power counting of each term in the effective theory, but to know that the remaining dynamical scales of the effective theory are much lower than the mass: $m \gg |\mathbf{p}|, E, \Lambda_{\text{QCD}}$.

Returning to the main problem, the first works addressing the entanglement of the soft and US scales in NRQCD tried to classify the different momentum regions existing in a purely perturbative version of NRQCD and/or to reformulate NRQCD in such a way that some of these regions were explicitly displayed by introducing new fields in the NRQCD Lagrangian. In particular, we mention the article by Labelle (1998),

¹These are included in the matching coefficients of the theory and may be transferred to the potentials by expanding Green's functions in NRQCD instead of in QCD (Chen *et al.*, 1995; Bali *et al.*, 1997; Brambilla and Vairo, 1999b).

²In any case, the simplifications compared with purely relativistic Bethe-Salpeter-like (Bethe and Salpeter, 1951) computations were enormous and led to a plethora of new results in QED. See, for instance, Kinoshita and Nio, 1996; Hoang *et al.*, 1997; Labelle *et al.*, 1997; Hill and Lepage, 2000; Hill, 2001.

where a diagrammatic approach to NRQED was used and the subsequent work by Luke and Manohar (1997), Grinstein and Rothstein (1998), and Luke and Savage (1998) in NRQCD. All these early attempts turned out to be missing some relevant intermediate degrees of freedom.

The first complete solution came in the work of Pineda and Soto (1998a). The idea was to build an EFT containing only the degrees of freedom relevant for \bar{Q} - Q systems near threshold, i.e., those with $E \sim mv^2$ and as close as possible to a Schrödinger-like formulation [see also Lepage (1997)]. All other degrees of freedom were to be integrated out. The EFT, which was called potential NRQCD (pNRQCD), had roughly the following structure:

$$\mathcal{L} = \Phi(\mathbf{r})^\dagger \left(i\partial_0 - \frac{\mathbf{p}^2}{2m} - V^{(0)}(r) \right. \\ \left. + \text{corrections to the potential} \right. \\ \left. + \text{interactions with other low-} \right. \\ \left. \text{energy degrees of freedom} \right) \Phi(\mathbf{r}) \quad \left. \vphantom{\mathcal{L}} \right\} \text{pNRQCD,}$$

where $V^{(0)}(r)$ is the static potential ($-C_F\alpha_s/r$ in the perturbative case) and $\Phi(\mathbf{r})$ is the field associated with the \bar{Q} - Q state. This EFT turned out to meet all our expectations: it achieved the factorization between US and higher-energy modes, had a definite power counting (at least in the perturbative regime), and was very close to a NR Schrödinger-like formulation of the heavy-quarkonium dynamics. In the Lagrangian, potentials appear. These are the matching coefficients of the theory and are calculated by matching with NRQCD amplitudes, using either Feynman diagrams (see Beneke *et al.*, 1999; Czarnecki *et al.*, 1999b; Pineda and Soto, 1999; Kniehl, Penin, Steinhäuser, *et al.*, 2002 for specific examples in QCD and QED and Sec. IV.E for further details) or Wilson-loop amplitudes (Brambilla *et al.*, 1999b, 2000). In the perturbative regime, a confirmation that pNRQCD was able to catch all the relevant dynamical regions came from diagrammatic studies. Beneke and Smirnov (1998) made the most complete classification of (perturbative) momentum regions to date by a diagrammatic study called the *threshold expansion*. In the language of the threshold expansion, the matching between NRQCD and QCD corresponds to integrating out the hard region and pNRQCD is obtained from NRQCD by integrating out what are called soft quarks and gluons and potential gluons. Finally, we mention two later works which dealt with reformulating NRQCD within an effective Lagrangian formalism. In the article by Griesshammer (1998) all degrees of freedom of NRQCD were made explicit in the Lagrangian. In that of Luke *et al.* (2002) the question of how to obtain renormalization-group (RG) equations for NR systems was addressed for the first time. The resulting formalism is now known as velocity NRQCD. For a review on this theory, see Hoang (2002). All these formulations should be equivalent

to pNRQCD once the same degrees of freedom have been integrated out.

This closed the circle connecting QCD with a properly modified Schrödinger-like formulation in the weak-coupling regime. Compared with the traditional methods, perturbative computations are optimized since only one scale appears in each of the Feynman integrals. The interaction with US gluons is treated in a quantum-field-theory fashion yet everything can be encoded in a Schrödinger-like formulation. The applications of these ideas to QED have also been very successful. We refer to Sec. IV.G for references.

The natural question then was: What happens in the strong-coupling regime? The application of EFTs has led to a well-founded connection with QCD in this regime. The potentials are now understood as matching coefficients to be obtained by comparison with NRQCD. This along with new computational techniques has solved the problems mentioned before allowing the complete computation of the potential at $\mathcal{O}(1/m^2)$ (Brambilla, Pineda, *et al.*, 2001; Pineda and Vairo, 2001). Also with these techniques, new terms, nonanalytic in $1/m$, were identified (Brambilla *et al.*, 2004) and a solution was found for the IR sensitivity of the P -wave decays (Brambilla, Eiras, *et al.*, 2002). Again, the use of EFTs has allowed us to close the circle and connect QCD with a properly modified Schrödinger-like formulation in the strong-coupling regime.

Heavy quarkonium has been important in the history of QCD and maintains that role even today. In the early 1970s, its high-energy nature helped to establish asymptotic freedom and QCD as the fundamental theory of the strong interaction. Later on, its NR nature served as a testing ground for many models of the low-energy dynamics of QCD. Since the 1990s, due to the rise of EFTs for heavy quarks, heavy-quarkonium observables can be rigorously derived from QCD, low- and high-energy modes factorized, and large logarithms systematically resummed. From a conceptual point of view, the origin and exact meaning of a QCD Schrödinger equation has been clarified. In the weak-coupling regime, this opens up the possibility of having precise determinations of the Standard Model parameters to which heavy quarkonium is sensitive: α_s and the heavy-quark masses. In the strong-coupling regime, heavy quarkonia are, due to their wealth of scales, an ideal laboratory in which to probe the structure of the QCD vacuum.

It is our aim to review the recent developments in heavy-quarkonium physics from the point of view of EFTs. Our main goal will be to derive the QCD Schrödinger equation that governs heavy-quarkonium physics in the weak- and strong-coupling regimes. We shall not be exhaustive in most of the derivations but concentrate on the main ideas and general lines of development with some illustrative examples. Then we shall discuss a selected set of applications. The review is not exhaustive. For instance, we shall not discuss one of the major phenomenological successes of NRQCD: explaining the heavy-quarkonium production rate at the

Tevatron (Braaten *et al.*, 1996; Beneke, 1997; Krämer, 2001; Bodwin *et al.*, 2003).

Before moving to the main body of the review, we list here our main notational choices (Yndurain, 1999). The QCD Lagrangian density reads

$$\mathcal{L} = \sum_{i=1}^{N_f} \bar{q}_i (i\not{D} - m_i) q_i - \frac{1}{4} G^{\mu\nu a} G_{\mu\nu}^a, \quad (1)$$

where $D_\mu = \partial_\mu + igA_\mu$, $igG_{\mu\nu} = [D_\mu, D_\nu]$, q_i are the quark fields, and m_i their current masses. N_f is the total number of quark flavors. We shall often indicate with the capital letter Q_i the heavy-quark fields and always set to zero the light-quark masses. In the EFT, the heavy-quark masses will be also indicated by m_i , but always understood, if not differently specified, as pole masses. The strong-coupling constant $\alpha_s = g^2/4\pi$ in the presence of n_f light quarks runs, at energies below the heavy-quark thresholds, as

$$v \frac{d\alpha_s}{dv} = -2\alpha_s \left\{ \beta_0 \frac{\alpha_s}{4\pi} + \beta_1 \left(\frac{\alpha_s}{4\pi} \right)^2 + \dots \right\}, \quad (2)$$

where

$$\beta_0 = \frac{11}{3} C_A - \frac{4}{3} T_F n_f,$$

$$\beta_1 = \frac{34}{3} C_A^2 - \frac{20}{3} C_A T_F n_f - 4 C_F T_F n_f, \quad \dots,$$

and $C_A = N_c = 3$, $C_F = (N_c^2 - 1)/2N_c = 4/3$ and $T_F = 1/2$.

The basic computational techniques for perturbative QCD used throughout can be found in the book of Pасcual and Tarrach (1984).

II. NRQCD

A. Degrees of freedom

NRQCD is designed to describe the dynamics of a heavy quark and a heavy antiquark (not necessarily of the same flavor) at energy scales (in the center-of-mass frame) much smaller than their masses, which are assumed to be much larger than Λ_{QCD} , the typical hadronic scale. At these energies, further heavy-quark-antiquark pairs cannot be created so it is sufficient, and convenient, to use Pauli spinors for both the heavy-quark and heavy-antiquark degrees of freedom. We shall denote by $\psi(x)$ the Pauli spinor field that annihilates a quark and by $\chi(x)$ the one that creates an antiquark. Both $\psi(x)$ and $\chi(x)$ transform in the fundamental representation of color SU(3). The remaining (light) degrees of freedom are the same as in QCD, except for the UV cutoffs as we shall discuss below. In particular, the gluon fields will appear in covariant derivatives D_μ and field strengths $G_{\mu\nu}$. For instance, we shall see that the leading-order Lagrangian density for the heavy-quark and antiquark fields reads

$$\mathcal{L} = \psi^\dagger \left(iD_0 + \frac{1}{2m} \mathbf{D}^2 \right) \psi + \chi^\dagger \left(iD_0 - \frac{1}{2m} \mathbf{D}^2 \right) \chi. \quad (3)$$

In a NR frame, the energy and three-momentum of the heavy particles scale in a different way and hence a different UV cutoff may be introduced for each: ν_s and ν_p , respectively. However, NRQCD is usually considered as having a single UV cutoff $\nu_{\text{NR}} = \{\nu_p, \nu_s\}$ satisfying $E, p, \Lambda_{\text{QCD}} \ll \nu_{\text{NR}} \ll m$; ν_p is the UV cutoff of the relative three-momentum of the heavy quark and antiquark; ν_s is the UV cutoff of the energy of the heavy quark and the heavy antiquark, and of the four-momentum of the gluons and light quarks.

From a Wilson RG point of view, NRQCD is obtained from QCD by integrating out energy fluctuations about the heavy-quark (heavy-antiquark) mass and three-momentum fluctuations up to the scale ν_{NR} for the heavy-quark (heavy-antiquark) fields, and four-momentum fluctuations up to the same scale for the fields of the light degrees of freedom. Since $\nu_{\text{NR}} \gg \Lambda_{\text{QCD}}$, this can be carried out in practice perturbatively in $\alpha_s(\nu_{\text{NR}})$. Within the threshold expansion framework (Beneke and Smirnov, 1998), this corresponds to integrating out the *hard* modes of QCD.

If the quark and antiquark have the same flavor, they can annihilate into hard gluons, which have already been integrated out and are not present in the NRQCD Lagrangian. This implies that the QCD Lagrangian must contain imaginary Wilson coefficients. The non-Hermiticity of the NRQCD Lagrangian, which at first sight may appear rather unwelcome, if not disastrous, turns out to provide an extremely powerful tool for calculating inclusive decay widths to light particles.

B. Power counting

From the discussion above, it follows that the NRQCD Lagrangian can be organized as a power series in $1/m_Q$ (and $1/m_{\bar{Q}}$). The Wilson or *matching* coefficients of each operator depend logarithmically on m_Q ($m_{\bar{Q}}$), ν_{NR} and, as mentioned before, can be calculated in perturbation theory in $\alpha_s(\nu_{\text{NR}})$. Hence the importance of a given operator for a practical calculation depends not only on its size (power counting), which we shall briefly discuss next, but also on the leading power of α_s that its matching coefficient has.

Since several scales ($E, |\mathbf{p}|, \Lambda_{\text{QCD}}$) remain dynamical, it is not possible to assign a size to each operator unambiguously without extra assumptions: no homogeneous power counting exists. As we shall see, the introduction of pNRQCD facilitates this task. The original power counting introduced by Bodwin *et al.* (1995) assumes $\Lambda_{\text{QCD}} \sim E \sim mv^2$, and hence $|\mathbf{p}| \sim mv \gg \Lambda_{\text{QCD}}$, $v \sim \alpha_s(mv) \ll 1$, which implies that the bound state is Coulombic (positroniumlike). In this case homogeneous power-counting rules can be given using pNRQCD in the weak-coupling regime (Sec. IV). Nevertheless, it is unlikely that the whole heavy-quarkonium spectrum can be described by this power counting and alternatives

need to be explored. We only anticipate here that in the strong-coupling regime of pNRQCD the following scaling will be considered: $E \ll |\mathbf{p}| \sim \Lambda_{\text{QCD}}$. The issue of the power counting of NRQCD has also been addressed by Beneke (1997) and Fleming *et al.* (2001) (see also the discussion in Sec. II.F). In both cases, the authors allow for some freedom in the possible size of the NRQCD matrix elements by introducing a parameter λ that interpolates between different power countings.

C. Lagrangian, currents, and symmetries

The allowed operators in the Lagrangian are constrained by the symmetries of QCD. However, due to the particular kinematic region on which we are focusing, Lorentz invariance is not linearly realized in the heavy-quark sector, and it is not straightforward (though certainly possible, as will be discussed below) to implement. One has, in a first stage, to content oneself with implementing the rotational subgroup only. Including n_f light quarks, the NRQCD Lagrangian density for a quark of mass m_1 and an antiquark of mass m_2 ($m_1, m_2 \gg \Lambda_{\text{QCD}}$) reads at $\mathcal{O}(1/m^2)$,³ $m = m_1, m_2$ (Caswell and Lepage, 1986; Bodwin *et al.*, 1995; Manohar, 1997; Bauer and Manohar, 1998):

$$\mathcal{L}_{\text{NRQCD}} = \mathcal{L}_g + \mathcal{L}_l + \mathcal{L}_\psi + \mathcal{L}_\chi + \mathcal{L}_{\psi\chi}, \quad (4)$$

$$\mathcal{L}_g = -\frac{1}{4}G^{\mu\nu a}G_{\mu\nu}^a + \frac{1}{4}\left(\frac{c_1^{g(1)}}{m_1^2} + \frac{c_1^{g(2)}}{m_2^2}\right)gf_{abc}G_{\mu\nu}^aG_{\alpha}^{\mu b}G^{\nu ac}, \quad (5)$$

$$\begin{aligned} \mathcal{L}_l = & \sum_{i=1}^{n_f} \bar{q}_i i \not{D} q_i + \frac{1}{8}\left(\frac{c_1^{ll(1)}}{m_1^2} + \frac{c_1^{ll(2)}}{m_2^2}\right)g^2 \sum_{i,j=1}^{n_f} \bar{q}_i T^a \gamma^\mu q_i \bar{q}_j T^a \gamma_\mu q_j \\ & + \frac{1}{8}\left(\frac{c_2^{ll(1)}}{m_1^2} + \frac{c_2^{ll(2)}}{m_2^2}\right)g^2 \sum_{i,j=1}^{n_f} \bar{q}_i T^a \gamma^\mu \gamma_5 q_i \bar{q}_j T^a \gamma_\mu \gamma_5 q_j \\ & + \frac{1}{8}\left(\frac{c_3^{ll(1)}}{m_1^2} + \frac{c_3^{ll(2)}}{m_2^2}\right)g^2 \sum_{i,j=1}^{n_f} \bar{q}_i \gamma^\mu q_i \bar{q}_j \gamma_\mu q_j \\ & + \frac{1}{8}\left(\frac{c_4^{ll(1)}}{m_1^2} + \frac{c_4^{ll(2)}}{m_2^2}\right)g^2 \sum_{i,j=1}^{n_f} \bar{q}_i \gamma^\mu \gamma_5 q_i \bar{q}_j \gamma_\mu \gamma_5 q_j, \end{aligned} \quad (6)$$

$$\begin{aligned} \mathcal{L}_\psi = & \psi^\dagger \left\{ iD_0 + \frac{c_k^{(1)}}{2m_1} \mathbf{D}^2 + \frac{c_4^{(1)}}{8m_1^3} \mathbf{D}^4 + \frac{c_F^{(1)}}{2m_1} \boldsymbol{\sigma} \cdot \mathbf{gB} \right. \\ & + \frac{c_D^{(1)}}{8m_1^2} (\mathbf{D} \cdot \mathbf{gE} - \mathbf{gE} \cdot \mathbf{D}) + i \frac{c_S^{(1)}}{8m_1^2} \boldsymbol{\sigma} \cdot (\mathbf{D} \times \mathbf{gE} \\ & \left. - \mathbf{gE} \times \mathbf{D}) \right\} \psi + \frac{c_1^{hl(1)}}{8m_1^2} g^2 \sum_{i=1}^{n_f} \psi^\dagger T^a \psi \bar{q}_i \gamma_0 T^a q_i \\ & + \frac{c_2^{hl(1)}}{8m_1^2} g^2 \sum_{i=1}^{n_f} \psi^\dagger \boldsymbol{\sigma}^k T^a \psi \bar{q}_i \gamma_k \gamma_5 T^a q_i \end{aligned}$$

³We also include the $\mathbf{D}^4/8m^3$ terms since they will be necessary later on.

$$+ \frac{c_3^{hl(1)}}{8m_1^2} g^2 \sum_{i=1}^{n_f} \psi^\dagger \psi \bar{q}_i \gamma_0 q_i + \frac{c_4^{hl(1)}}{8m_1^2} g^2 \sum_{i=1}^{n_f} \psi^\dagger \boldsymbol{\sigma}^k \psi \bar{q}_i \gamma_k \gamma_5 q_i, \quad (7)$$

$$\mathcal{L}_\chi = \text{c.c. of } \mathcal{L}_\psi (1 \leftrightarrow 2),$$

$$\begin{aligned} \mathcal{L}_{\psi\chi} = & \frac{f_1(^1S_0)}{m_1 m_2} O_1(^1S_0) + \frac{f_1(^3S_1)}{m_1 m_2} O_1(^3S_1) + \frac{f_8(^1S_0)}{m_1 m_2} O_8(^1S_0) \\ & + \frac{f_8(^3S_1)}{m_1 m_2} O_8(^3S_1), \end{aligned} \quad (8)$$

where

$$O_1(^1S_0) = \psi^\dagger \chi \chi^\dagger \psi, \quad O_1(^3S_1) = \psi^\dagger \boldsymbol{\sigma} \chi \chi^\dagger \boldsymbol{\sigma} \psi, \quad (9)$$

$$O_8(^1S_0) = \psi^\dagger T^a \chi \chi^\dagger T^a \psi, \quad O_8(^3S_1) = \psi^\dagger T^a \boldsymbol{\sigma} \chi \chi^\dagger T^a \boldsymbol{\sigma} \psi. \quad (10)$$

The matching coefficients are symmetric under the exchange $m_1 \leftrightarrow m_2$, $\boldsymbol{\sigma}$ are the Pauli matrices, $iD^0 = i\partial^0 - gA^0$, $i\mathbf{D} = i\nabla + g\mathbf{A}$, $\mathbf{E}^i = G^{i0}$, $\mathbf{B}^i = -\epsilon_{ijk} G^{jk}/2$, ϵ_{ijk} being the usual three-dimensional antisymmetric tensor⁴ $[(\mathbf{a} \times \mathbf{b})^i \equiv \epsilon_{ijk} \mathbf{a}^j \mathbf{b}^k]$ with $\epsilon_{123} = 1$, and c.c. stands for charge conjugate ($\psi^c = -i\sigma^2 \chi^*$, $\chi^c = i\sigma^2 \psi^*$, and $A_\mu^c = -A_\mu^T$).

The NRQCD Lagrangian is defined up to field redefinitions. In the expression adopted here, we have made use of this freedom. Powers larger than one of iD_0 applied to the quark fields have been eliminated. We have also redefined the gluon fields in such a way that the coefficient in front of $-G^{\mu\nu a}G_{\mu\nu}^a/4$ in \mathcal{L}_g is 1. This turns out to be equivalent to redefining the coupling constant in such a way that it runs with $N_f - 2 = n_f$ flavors (for $m_1 \neq m_2$, $N_f - 1 = n_f$ for $m_1 = m_2$), where N_f are the flavors in QCD (Pineda and Soto, 1998c) [see also Griesshammer (2000) for a calculation of the β function in NRQCD]. A possible term $D^\mu G_{\mu\alpha}^a D_\nu G^{\nu\alpha a}$ has been eliminated through the identity (Manohar, 1997)

$$\begin{aligned} \int d^4x (2D^\mu G_{\mu\alpha}^a D_\nu G^{\nu\alpha a} + 2gf_{abc} G_{\mu\nu}^a G_{\alpha}^{\mu b} G^{\nu ac} \\ + G_{\mu\nu}^a D^2 G^{\mu\nu a}) = 0. \end{aligned} \quad (11)$$

Finally, a term like $cG_{\mu\nu}^a D^2 G^{\mu\nu a}$ has been eliminated through the field redefinition $A_\mu \rightarrow A_\mu + 2c[D^\alpha, G_{\alpha\mu}]$ (Pineda and Vairo, 2001).

The Wilson coefficients appearing in the NRQCD Lagrangian will be discussed in Sec. II.D. The $\mathcal{O}(1/m^3)$ Lagrangian (without the light-fermion sector) can be found in the paper by Manohar (1997). The Feynman rules associated with the first two lines of Eq. (7) can be found in the article by Bodwin and Chen (1999).

⁴In DR several prescriptions are possible for the ϵ_{ijk} tensors and $\boldsymbol{\sigma}$. Therefore if DR is used, one has to make sure that one uses the same procedure as that used to calculate the matching coefficients.

NR currents should also be considered since they appear in inclusive (electromagnetic) decays, NR sum rules, or $t\text{-}\bar{t}$ production near threshold. Similar to the Lagrangian, they can be written as an expansion in $1/m$ times some hard matching coefficients times some NR (local) operators. For instance, the electromagnetic vector and axial-vector currents read (see Hoang and Teubner, 1999)

$$j_k^v(x) = b_{1,\text{NR}}^v(\psi^\dagger \sigma_k \chi)(x) - \frac{b_{2,\text{NR}}^v}{6m^2} \left[\psi^\dagger \sigma_k \left(-\frac{i \overleftrightarrow{\mathbf{D}}}{2} \right)^2 \chi \right](x) + \dots, \quad (12)$$

$$j_k^a(x) = \frac{b_{1,\text{NR}}^a}{m} \left[\psi^\dagger \left(-\frac{i \overleftrightarrow{\mathbf{D}}}{2} \times \boldsymbol{\sigma} \right)_k \chi \right](x) + \dots, \quad (13)$$

where $\psi^\dagger \overleftrightarrow{\mathbf{D}} \chi \equiv \psi^\dagger (\mathbf{D}\chi) - (\mathbf{D}\psi)^\dagger \chi$ and the dots stand for corrections, which do not contribute at next-to-next-to leading order (NNLO) for S waves. In practice, most of the physical information can be extracted from the imaginary parts of the four-fermion operators, which are discussed in Sec. II.F.2. In particular, the matching coefficients $b_{1,\text{NR}}^v$ and $b_{2,\text{NR}}^v$ can be traded for the matching coefficients $\text{Im} f_{\text{EM}}(^3S_1)$ and $\text{Im} g_{\text{EM}}(^3S_1)$, respectively.

The QCD Lagrangian is invariant under Lorentz boosts. However, the NR expansion has destroyed the manifest invariance of the EFT under Lorentz boosts. Since the EFT is equivalent to QCD at any order of the strong-coupling and NR expansion, the invariance under Lorentz boosts is not lost but must be somehow incorporated into the EFT. Indeed, it imposes specific constraints on the form of the EFT itself.

Constraints imposed by the relativistic invariance were first worked out for heavy-quark effective theory (HQET), which coincides with NRQCD in the bilinear sector of the heavy-quark fields (Luke and Manohar, 1992; Manohar, 1997). In HQET the realization of the relativistic invariance is called reparametrization invariance. It imposes constraints on the Wilson coefficients of the EFT. For instance,

$$c_k = c_4 = 1, \quad 2c_F - c_S - 1 = 0, \quad (14)$$

where we have dropped the explicit indication of the flavor index.

An alternative derivation consists of imposing the Poincaré algebra on the generators H , \mathbf{P} , \mathbf{J} , and \mathbf{K} of time translations, space translations, rotations, and Lorentz-boosts transformations of NRQCD (Brambilla, Gromes, and Vairo, 2003). The idea originates from the work of Dirac (1949), and has been used to constrain the form of the relativistic corrections to phenomenological potentials (Foldy, 1961; Krajcik and Foldy, 1974; Sebastian and Yun, 1979). It was applied to NR EFTs by Brambilla, Gromes, and Vairo (2003) and Vairo (2004a). In a field theory, the Poincaré algebra has to be understood among fields quantized in accordance with the ca-

nonical equal-time commutation relations.⁵ The translation and rotation generators \mathbf{P} and \mathbf{J} may be derived from the NRQCD Lagrangian or by matching to the QCD generators. They are exact because translational and rotational invariance have not been explicitly broken in going to the EFT. The Lorentz-boost generators may be obtained by matching order by order in $1/m$ to the Lorentz-boost generators of QCD. They depend on some specific matching coefficients independent of those in the Lagrangian. The NRQCD Poincaré generators satisfy the Poincaré algebra if Eq. (14) is satisfied for each flavor up to $\mathcal{O}(1/m)$ and $\mathcal{O}(\nabla^2 \nabla/m^2)$ (plus some other constraints on the matching coefficients appearing in \mathbf{K}) (Brambilla, Gromes, and Vairo, 2003). Therefore at the considered order, one gets the same result as from reparametrization invariance. The calculation of constraints specific to NRQCD, i.e., involving four-fermion operators, has not been done in either approach yet. This would correspond to going to higher orders in $1/m$.

In general, we shall constrain the matching coefficients of the kinetic energy in accordance with Eq. (14). Occasionally, however, we shall keep them explicit for tracking purposes.

D. Matching

The calculation of the NRQCD Wilson coefficients is done through a procedure called *matching*. In a matching calculation suitable renormalized QCD and renormalized NRQCD Green's functions (or matrix elements) are imposed to be equal for scales below ν_{NR} at the desired order of α_s and $1/m$. In particular, the expansion of Green's functions in external energies E and three-momenta p must be equal. This fixes the matching coefficients, which will depend on the renormalization schemes used in QCD and in NRQCD. It greatly simplifies calculations if these expansions are done *before* the loop integrals are performed. However, doing so may introduce IR divergences and for the equality between QCD and NRQCD Green's functions to remain valid the same IR regulator must be used in both theories. It is very convenient to use DR as an IR regulator as well as an UV one. This is because all loop integrals in the NRQCD calculations will be scaleless and can be set to zero, as we shall argue below. Let us explain what will happen. Schematically (Manohar, 1997) one has

$$A_{\text{eff}} \left(\frac{1}{\epsilon_{\text{UV}}} - \frac{1}{\epsilon_{\text{IR}}} \right) \quad (15)$$

in the EFT, which is zero if $\epsilon_{\text{UV}} = \epsilon_{\text{IR}}$ in DR. Therefore we only have to calculate loop integrals in QCD that depend on a single scale (m). Typically we get

⁵More precisely, the algebra imposes relations among the bare fields and coupling constants. These relations are preserved in the renormalized theory if Poincaré invariance is not broken by quantum effects.

$$A \frac{1}{\epsilon_{UV}} + B \frac{1}{\epsilon_{IR}} + (A+B) \ln \frac{\nu}{m} + D. \quad (16)$$

Since the full and effective theories share the same IR behavior $B = -A_{\text{eff}}$. Moreover, the UV divergences are absorbed in the coefficients of both theories. In this way the difference between the full and effective theory is

$$(A+B) \ln \frac{\nu}{m} + D, \quad (17)$$

which provides the one-loop contribution to the matching coefficients for the effective theory. It is implicit in this procedure that the same renormalization scheme is used for both UV and IR divergences in NRQCD. In the QCD calculation both the UV and IR divergences can also be renormalized in the same way, for instance, using the minimal subtraction scheme, which is the standard one for QCD calculations. This fixes the UV renormalization scheme in NRQCD in which the Wilson coefficients have been calculated and means that for these Wilson coefficients to be consistently used in a NRQCD calculation, it must be carried out in the same scheme, for instance, in dimensional regularization and in the minimal subtraction (MS) scheme.

The matching calculation can be carried out in any gauge since both the QCD and NRQCD Lagrangians are manifestly gauge invariant. However, since most of the times one is matching gauge-dependent Green's functions, the same gauge must be chosen in QCD and NRQCD. Using different gauges or, in general, different ways to carry out the matching procedure, may lead to apparently different results for the matching coefficients (within the same regularization and renormalization scheme). These results must be related by local-field redefinitions. In other words, if both matching calculations had used the same minimal basis of operators, the results would have coincided. If the matching is carried out as described above, it is more convenient to choose a covariant gauge (i.e., Feynman gauge) since only QCD calculations, which are manifestly covariant, are to be carried out.

In the procedure described above, one may worry about the fact that the NR propagator $1/(p^0 - \mathbf{p}^2/m)$ contains the scale m , which spoils the usual argument (used in HQET, for instance) that loop integrals in the EFT contain no scales once one has expanded in the external energies and three-momenta. Let us argue in the following paragraphs that the procedure is indeed correct.

Consider first the single-quark or single-antiquark sector. In any diagram in NRQCD, one can always choose the momenta flowing along the heavy-quark line in the same direction. Then all heavy-quark propagators will have poles in either the lower or upper half of the complex plane only. Then, if all integrals over the energies flowing through the heavy-quark propagators are carried out by closing the contour around the opposite half-complex plane, these energies will be replaced by linear dependencies in the three-momenta in the NR quark propagators. These linear dependencies dominate over quadratic dependencies of the kinetic terms both in the

IR and in the UV. The latter is so because ν_{NR} is always smaller than m . Hence the kinetic term can be expanded and the integrals become dimensionless. In fact, in DR the kinetic term not only can but must be expanded since this is the only way to ensure that three-momenta remain smaller than ν_{NR} .

Consider next the quark-antiquark sector. Any fixed-order loop calculation may contain heavy-quark-antiquark irreducible diagrams (meaning diagrams which cannot be disconnected by cutting an internal quark line and an internal antiquark line) and heavy-quark-antiquark reducible ones.

Consider first a quark-antiquark irreducible diagram. The fact that at any point of an internal quark propagator there is always at least one gluon propagator (or two light-quark propagators) in addition to an antiquark propagator allows one to choose all momenta flowing both along the quark and along the antiquark propagator in the same direction. Hence the poles of both the quark and antiquark propagators are in the same complex half plane, and therefore the argument put forward for the single-quark sector also holds here.

Consider finally a quark-antiquark reducible diagram. It can always be written as a series of two-particle irreducible (2PI) diagrams linked by a quark and by an antiquark propagator. Let us choose the center-of-mass momentum to be zero and focus on one such 2PI block. If p (p') is the momentum flowing along the incoming (outgoing) quark line, then $-p$ ($-p'$) is necessarily the momentum flowing along the incoming (outgoing) antiquark line. p^0 (p'^0) has two relevant scalings, namely, $p^0 \sim |\mathbf{p}|$ and $p^0 \sim \mathbf{p}^2/2m$. If the scaling $p^0 \sim |\mathbf{p}|$ occurs, then kinetic terms $\sim \mathbf{p}^2/2m$ can be neglected in 2PI diagram and no further scale m will be introduced. If the scaling $p^0 \sim \mathbf{p}^2/2m$ occurs, then p^0 can be neglected in the gluon propagators and the only dependence in p^0 can be reduced to either the quark or antiquark propagator. Furthermore, the internal energies in the 2PI diagram eventually take the value of the three-momenta $|\mathbf{p}|$ and hence p^0 and $\mathbf{p}^2/2m$ can be expanded. In either case, no extra scales m are introduced in the 2PI diagrams and they can be set to zero. Consider now the link between two 2PI diagrams. If $p^0 \sim |\mathbf{p}|$, the kinetic term can be expanded and no further scale m is introduced. If $p^0 \sim \mathbf{p}^2/2m$, no further dependence on p^0 in the 2PI diagrams exists, and hence the integral over p^0 can be trivially done inducing a m/\mathbf{p}^2 propagator so that the m dependence factorizes trivially. In summary, two-particle reducible diagrams also become scaleless and can be set to zero.

One might be concerned about the appearance of pinch singularities when the kinetic terms are expanded in the links. Let us show that they are of no concern. Recall first that pinch singularities blow up only after the limit $\eta \rightarrow 0$ is taken, where $i\eta$ defines the causal propagator. We propose taking this limit at the end of the calculation. If no other dependence on p^0 existed, we could carry out all integrals except the one over p^0 . Since they have no scale, as argued before, and they

contain no pinch singularities, they can safely be set to zero, and the net result is zero. If there are further dependencies on p^0 , by fraction decomposition one can always isolate the pinch singularity in a term $1/(p^0 + i\eta)(-p^0 + i\eta)$ with no further dependencies on p^0 (plus other terms with no pinch singularity) and proceed as above.

Let us finally note that this matching procedure corresponds to taking the purely hard contribution in the threshold expansion for the NRQCD matching coefficients.

In order to address the matching calculation, we also need the relation between the QCD and NRQCD quark (antiquark) fields:

$$\begin{aligned} Q_1(x) &\rightarrow Z_1^{1/2} \frac{1 + \gamma_0}{2} e^{-im_1 t} \psi(x), \\ Q_2(x) &\rightarrow Z_2^{1/2} \frac{1 - \gamma_0}{2} e^{im_2 t} \chi(x). \end{aligned} \quad (18)$$

At one loop, one obtains for the wave-function renormalization constants

$$Z_i = 1 + C_F \frac{\alpha}{\pi} \left(\frac{3}{4} \ln \frac{m_i^2}{v^2} - 1 \right) + \mathcal{O}\left(\left(\frac{\alpha}{\pi}\right)^2\right), \quad i = 1, 2. \quad (19)$$

Notice also that the states are differently normalized in relativistic [$\langle \mathbf{p} | \mathbf{p}' \rangle = (2\pi)^3 2\sqrt{\mathbf{p}^2 + m^2} \delta^3(\mathbf{p} - \mathbf{p}')$] or NR [$\langle \mathbf{p} | \mathbf{p}' \rangle = (2\pi)^3 \delta^3(\mathbf{p} - \mathbf{p}')$] theories. Hence in order to compare the S -matrix elements between the two theories, a factor $(2\sqrt{\mathbf{p}^2 + m^2})^{1/2}$ has to be introduced for each external fermion.

For the single-quark (antiquark) sector as well as for the purely gluonic sector, the matching coefficients have been obtained at one loop up to $\mathcal{O}(1/m^2)$ in the background Feynman gauge by Manohar (1997). They read (similarly for $1 \rightarrow 2$)

$$\begin{aligned} c_F^{(1)} &= 1 + \frac{\alpha_s}{2\pi} \left[C_F + \left(1 - \ln \frac{m_1}{v}\right) C_A \right], \\ c_D^{(1)} &= 1 + \frac{\alpha_s}{\pi} \left[\left(\frac{8}{3} \ln \frac{m_1}{v}\right) C_F + \left(\frac{1}{2} + \frac{2}{3} \ln \frac{m_1}{v}\right) C_A \right] \\ &\quad - \frac{4}{15} \frac{\alpha_s}{\pi} T_F \left(\frac{m_1^2 + m_2^2}{m_2^2} \right), \\ c_S^{(1)} &= 1 + \frac{\alpha_s}{\pi} \left[C_F + \left(1 - \ln \frac{m_1}{v}\right) C_A \right], \\ c_1^{g(1)} &= \frac{\alpha_s}{360\pi} T_F \end{aligned} \quad (20)$$

($v = v_{\text{NR}}$). The complete $\mathcal{O}(\alpha_s^2)$ correction to c_F is also known (Czarnecki and Grozin, 1997).

For the quark-antiquark sector, they have been obtained at one loop up to $\mathcal{O}(1/m^2)$ by Pineda and Soto

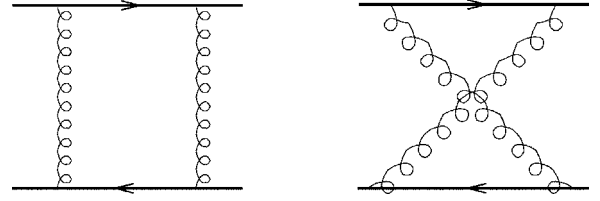


FIG. 1. Relevant one-loop diagrams for the matching of the four-fermion operators at order $\mathcal{O}(1/m^2)$ for the case of unequal masses. The incoming and outgoing particles are on shell and exactly at rest.

(1998c). For the nonannihilation diagrams, which are displayed in Fig. 1, it is convenient to use the following basis:

$$\begin{aligned} \mathcal{L}_{\psi\chi} &= \frac{d_{ss}}{m_1 m_2} \psi_1^\dagger \psi_1 \chi_2^\dagger \chi_2 + \frac{d_{sv}}{m_1 m_2} \psi_1^\dagger \boldsymbol{\sigma} \psi_1 \chi_2^\dagger \boldsymbol{\sigma} \chi_2 \\ &\quad + \frac{d_{vs}}{m_1 m_2} \psi_1^\dagger T^a \psi_1 \chi_2^\dagger T^a \chi_2 \\ &\quad + \frac{d_{vv}}{m_1 m_2} \psi_1^\dagger T^a \boldsymbol{\sigma} \psi_1 \chi_2^\dagger T^a \boldsymbol{\sigma} \chi_2, \end{aligned} \quad (21)$$

which is equivalent to the one in Eq. (8). The relation between them can be found (in four dimensions) in the article by Pineda and Soto (1998c). In this basis, for the case of the quark and antiquark having arbitrary flavor, the matching coefficients at one loop read in the Feynman gauge

$$\begin{aligned} d_{ss} &= -C_F \left(\frac{C_A}{2} - C_F \right) \frac{\alpha_s^2}{m_1^2 - m_2^2} \left[m_1^2 \left(\ln \frac{m_2^2}{v^2} + \frac{1}{3} \right) \right. \\ &\quad \left. - m_2^2 \left(\ln \frac{m_1^2}{v^2} + \frac{1}{3} \right) \right], \end{aligned} \quad (22)$$

$$d_{sv} = C_F \left(\frac{C_A}{2} - C_F \right) \frac{\alpha_s^2}{m_1^2 - m_2^2} m_1 m_2 \ln \frac{m_1^2}{m_2^2}, \quad (23)$$

$$\begin{aligned} d_{vs} &= -\frac{2C_F \alpha_s^2}{m_1^2 - m_2^2} \left[m_1^2 \left(\ln \frac{m_2^2}{v^2} + \frac{1}{3} \right) - m_2^2 \left(\ln \frac{m_1^2}{v^2} + \frac{1}{3} \right) \right] \\ &\quad + \frac{C_A \alpha_s^2}{4(m_1^2 - m_2^2)} \left\{ 3 \left[m_1^2 \left(\ln \frac{m_2^2}{v^2} + \frac{1}{3} \right) \right. \right. \\ &\quad \left. \left. - m_2^2 \left(\ln \frac{m_1^2}{v^2} + \frac{1}{3} \right) \right] + \frac{1}{m_1 m_2} \left[m_1^4 \left(\ln \frac{m_2^2}{v^2} + \frac{10}{3} \right) \right. \right. \\ &\quad \left. \left. - m_2^4 \left(\ln \frac{m_1^2}{v^2} + \frac{10}{3} \right) \right] \right\}, \end{aligned} \quad (24)$$

$$\begin{aligned} d_{vv} &= \frac{2C_F \alpha_s^2}{m_1^2 - m_2^2} m_1 m_2 \ln \frac{m_1^2}{m_2^2} + \frac{C_A \alpha_s^2}{4(m_1^2 - m_2^2)} \left\{ \left[m_1^2 \left(\ln \frac{m_2^2}{v^2} + 3 \right) \right. \right. \\ &\quad \left. \left. - m_2^2 \left(\ln \frac{m_1^2}{v^2} + 3 \right) \right] - 3m_1 m_2 \ln \frac{m_1^2}{m_2^2} \right\} \end{aligned} \quad (25)$$

($v = v_{\text{NR}}$). The v -independent pieces of d_{vv} depend on the procedure for reducing the D -dimensional Dirac matrices.

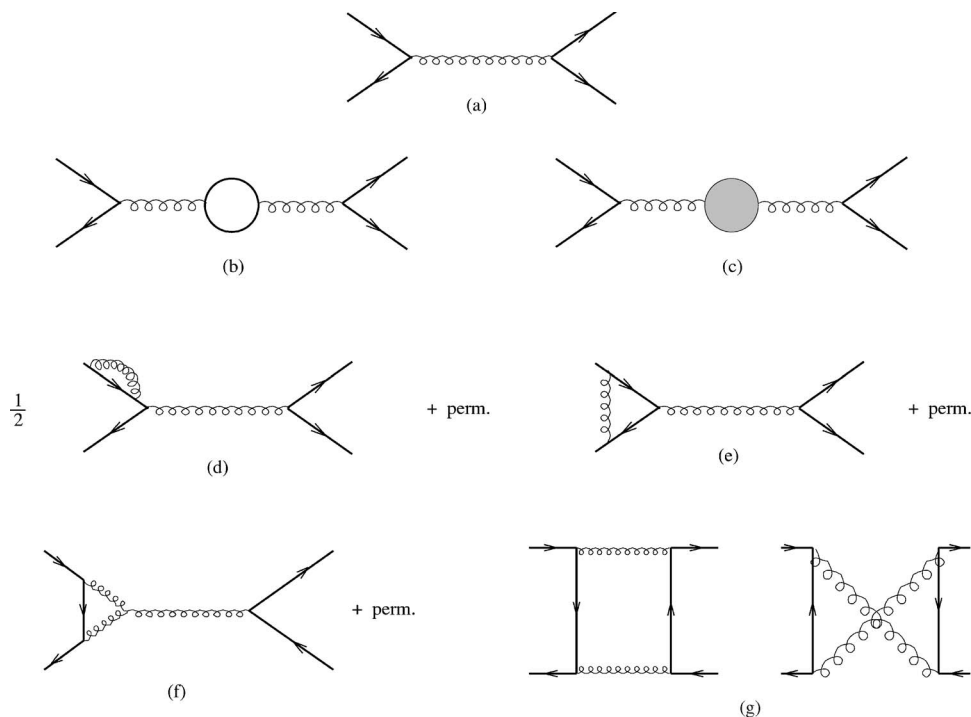


FIG. 2. Relevant diagrams for the matching of the four-fermion operators at order $\mathcal{O}(1/m^2)$ and one loop that only appear for the equal-mass case. The incoming and outgoing particles are on shell and exactly at rest.

ces to Pauli matrices. Note that we have used the prescription for the dimensionally regulated spin matrices of Pineda and Soto (1998c), which differs from the more standard 't Hooft–Veltman scheme.

The contribution of the diagrams in Fig. 1 to the case of equal flavor is obtained by taking the limit $m_1 \rightarrow m_2 = m$. Explicit formulas for this case can be found in the article by Pineda and Soto (1998c). In this case, however, annihilation processes are allowed and they should be taken into account. The relevant annihilation diagrams up to one loop are displayed in Fig. 2.

One obtains

$$f_1(^1S_0) = \alpha_s^2 C_F \left(\frac{C_A}{2} - C_F \right) (2 - 2 \ln 2 + i\pi), \quad (26)$$

$$f_1(^3S_1) = 0, \quad (27)$$

$$f_8(^1S_0) = \frac{\alpha_s^2}{2} \left(-\frac{3}{2} C_A + 4 C_F \right) (2 - 2 \ln 2 + i\pi), \quad (28)$$

$$f_8(^3S_1) = -\pi \alpha_s(m) \left(1 + \frac{\alpha_s}{\pi} \left[T_F \left[\frac{n_f}{3} \left(2 \ln 2 - \frac{5}{3} - i\pi \right) - \frac{8}{9} \right] + \frac{109}{36} C_A - 4 C_F \right] \right). \quad (29)$$

Recall that we have to add to the annihilation contributions above the contributions (22)–(25) in the $m_1 \rightarrow m_2 = m$ limit. Note that imaginary contributions appear, which are relevant for the calculation of inclusive decay widths. The calculation of corrections of higher order in α_s to the imaginary parts of the four-fermion matching coefficients has a long history (Barbieri *et al.*, 1979, 1980, 1981; Hagiwara *et al.*, 1981; Mackenzie and Lepage,

1981; Bodwin *et al.*, 1995; Beneke *et al.*, 1998; Czarnecki and Melnikov, 1998; Petrelli *et al.*, 1998; Maltoni, 1999). An updated list of them and a summary of the state of the art can be found in the article by Vairo (2004b). No further matching calculations beyond the order reported here have been carried out for the real part of four-quark operators.

The ν dependence of the matching coefficients is eventually traded for a lower scale ($|\mathbf{p}|, E, \Lambda_{\text{QCD}}$). This may introduce large logarithms that ought to be summed up, as discussed in Sec. II.E. When higher-order terms in α_s are calculated, it may occur that large numerical factors lead to poor convergence of the perturbative series. This is often related to so-called renormalon singularities, which are discussed in Sec. V.

E. Renormalization group

Once the EFT has been built, one may try to work out the RG improvement of the matching coefficients. This has proven to be a nontrivial task for NRQCD, which is related to the fact that different kinds of degrees of freedom are encoded in the same fields. In other words, the soft and US physics have not been disentangled at the NRQCD Lagrangian level. This means that obtaining the RG improvement at the NRQCD level becomes an ill-defined problem. We shall see later on that the introduction of pNRQCD, which does factorize soft and US physics, indicates how this problem must be posed. Indeed, it is possible to obtain some results at this level (in fact it is even convenient) which will be used afterwards in order to obtain the RG equations in potential NRQCD (in the weak-coupling regime). The NRQCD matching coefficients are functions of $\nu_{\text{NR}} = \{\nu_p, \nu_s\}$. It is convenient to restrict ourselves to the derivation of RG

equations with respect to the scale ν_s since the RG equations with respect to the scale ν_p are obtained in a much simpler way using pNRQCD.

The matching coefficients of the terms bilinear in the heavy-quark fields and of the pure gluonic terms are just functions of ν_s , i.e., $c=c(\nu_s, m) \equiv c(\nu_s)$. This is due to the fact that the UV behavior of the Green's functions in this sector is only sensitive to the energy and not to the three-momentum of the heavy quarks, as can also be seen by explicit computations. Therefore the anomalous dimensions can be computed using the static propagator for the heavy quark, and coincide with those obtained for HQET. The complete leading-logarithm-order (LLO) running of these matching coefficients in the basis of operators (5)–(7) was calculated by Bauer and Manohar (1998) in the (background) Feynman gauge [some partial previous results already existed in the literature (Eichten and Hill, 1990; Falk *et al.*, 1991; Blok *et al.*, 1997)]. For the case of the only nontrivial matching coefficient at $\mathcal{O}(1/m)$, c_F , a next-to-leading-logarithm-order (NLL) evaluation is also available (Amoros *et al.*, 1997; Czarnecki and Grozin, 1997), which we explicitly display to illustrate the typical structure of the RG-improved matching coefficients:

$$c_F(m_i) = z^{-\gamma_0/2} \left[1 + \frac{\alpha_s(\nu_h)}{4\pi} \left(c_1 + \frac{\gamma_0}{2} \ln \frac{\nu_h^2}{m_i^2} \right) + \frac{\alpha_s(\nu_h) - \alpha_s(\nu_s)}{4\pi} \left(\frac{\gamma_1}{2\beta_0} - \frac{\gamma_0\beta_1}{2\beta_0^2} \right) + \dots \right], \quad (30)$$

where $z = [\alpha_s(\nu_s)/\alpha_s(\nu_h)]^{1/\beta_0}$, $\nu_h \sim m_i$ is the hard matching scale, $c_1 = 2(C_A + C_F)$, and the one- and two-loop anomalous dimensions are

$$\gamma_0 = 2C_A, \quad \gamma_1 = \frac{68}{9}C_A^2 - \frac{52}{9}C_A T_F n_f. \quad (31)$$

Complications appear when the four-heavy-quark operators $\{f\}$ are considered. As we have mentioned, they depend on both cutoffs: ν_p and ν_s . Nevertheless, at one loop, all the dependence of the matching coefficients is due only to ν_s , i.e., $f(\nu_p, \nu_s, m) \equiv f(\nu_p, \nu_s) \approx f(\nu_s)$. The dependence on ν_p appears at two loops or higher and will be discussed in Sec. IV. In any case, if one restricts oneself to the purely soft running (i.e., ν_s dependence only), it still makes sense to consider the (soft) RG running of the NRQCD matching coefficients including the four-heavy-fermion operators. In this approximation, one can always perform the computation with static propagators for the heavy quarks and order by order in $1/m$.

Formally, we can write the NRQCD Lagrangian as an expansion in $1/m$:

$$\mathcal{L}_{\text{NRQCD}} = \sum_{n=0}^{\infty} \frac{1}{m^n} \lambda_n O_n, \quad (32)$$

where the RG equations of the matching coefficients are

$$\nu_s \frac{d}{d\nu_s} \lambda = B_\lambda(\lambda). \quad (33)$$

The RG equations have a triangular structure (the standard structure one can see, for instance, in HQET RG equations):

$$\begin{aligned} \nu_s \frac{d}{d\nu_s} \lambda_0 &= B_0(\lambda_0), \\ \nu_s \frac{d}{d\nu_s} \lambda_1 &= B_1(\lambda_0) \lambda_1, \\ \nu_s \frac{d}{d\nu_s} \lambda_2 &= B_{2(2,1)}(\lambda_0) \lambda_2 + B_{2(1,2)}(\lambda_0) \lambda_1^2, \\ &\dots, \end{aligned} \quad (34)$$

where the different B 's can be expanded into a power series in λ_0 [λ_0 corresponds to the marginal operators (renormalizable interactions)]. For NRQCD we have $\lambda_0 = \alpha_s$ and $\lambda_1 = \{c_k, c_F\}$, $\lambda_2 = \{c_1^g, c_D, c_S, \{c^{hl}\}, \{f\}\}$.

As we have already mentioned, the LLO running for the $\{c\}$ in Feynman gauge can be read off from the results obtained by Bauer and Manohar (1998). The LLO running of the $\{f\}$ in Feynman gauge can be found in the article by Pineda (2002b).

At this stage, we would like to stress that we are working in a nonminimal basis of operators for the NRQCD Lagrangian. Consequently the values of (some of) the matching coefficients are ambiguous (only some combinations with physical meaning are unambiguous) and could depend upon the gauge in which the calculation has been performed. At the practical level, this means that they will depend on the specific basis of operators we have taken for the NRQCD Lagrangian and on the procedure used (in particular on the gauge). Therefore if working in a nonminimal basis, one should be careful to do the matching using the same gauge for all the operators (or at least for those that are potentially ambiguous). This affects the running of c_D , $f_8(^1S_0)$, and c_1^{hl} . Indeed, it has been shown by Bauer and Manohar (1998) that c_D can be absorbed into $f_8(^1S_0)$ and c_1^{hl} by using the equations of motion [$\mathbf{D} \cdot \mathbf{E}^a = g(\psi^\dagger T^a \psi + \chi^\dagger T^a \chi + \sum_{j=1}^{n_f} \bar{q}_j \gamma^0 T^a q_j)$].

Let us illustrate the point by considering the running of c_D and $f_8(^1S_0)$ in the equal-mass case and without light quarks. In Feynman gauge we obtain

$$\nu_s \frac{d}{d\nu_s} c_D = \frac{\alpha_s}{4\pi} \left[\frac{4C_A}{3} c_D - \left(\frac{2C_A}{3} + \frac{32C_F}{3} \right) c_k^2 - \frac{10C_A}{3} c_F^2 \right], \quad (35)$$

$$\nu_s \frac{d}{d\nu_s} f_8(^1S_0) = 4(C_F - C_A) \alpha_s^2 c_k^2 + \frac{3}{2} \alpha_s^2 C_A c_D, \quad (36)$$

while in Coulomb gauge we have

$$\begin{aligned}
v_s \frac{d}{dv_s} c_D(\text{Coulomb}) &= \frac{\alpha_s}{4\pi} \left[\frac{22C_A}{3} c_D - \left(\frac{32C_A}{3} \right. \right. \\
&\quad \left. \left. + \frac{32C_F}{3} \right) c_k^2 - \frac{10C_A}{3} c_F^2 \right], \\
v_s \frac{d}{dv_s} f_8(^1S_0)(\text{Coulomb}) &= \left(4C_F - \frac{3C_A}{2} \right) \alpha_s^2 c_k^2.
\end{aligned} \tag{37}$$

Clearly, the running of c_D and $f_8(^1S_0)$ is gauge dependent, but the running of the combination $\alpha_s c_D + (1/\pi) f_8(^1S_0)$ is not, reflecting the fact that c_D can be absorbed into $f_8(^1S_0)$ by means of a suitable field redefinition.

F. Applications: spectrum and inclusive decay widths

NRQCD has been applied over the last 12 years to a large number of observables related to heavy-quarkonium physics. Here we shall briefly discuss two kinds of observables: spectra and inclusive decay widths. Concerning the spectra, we shall mention the state of the art relevant to the lattice determination of the bottomonium levels. We shall keep a continuum EFT point of view since a discussion of lattice NRQCD is beyond the scope of the present work [see Kronfeld (2004) and Lepage (2005) for some recent reviews]. We shall, however, give a more detailed discussion of the inclusive decay width. We have chosen these observables because they are amenable to rather clean theoretical derivations. They will also be addressed in the following sections dedicated to pNRQCD.

Before proceeding, we have to establish a power counting for NRQCD. As was mentioned in Sec. II.B, since the scales $(E, |\mathbf{p}|, \Lambda_{\text{QCD}})$ remain dynamical, it is not possible to give a homogeneous counting for each operator. In other words, in contrast to pNRQCD, we shall not be able to disentangle the contributions coming from the different scales. In order to be on the safe side, we have to assume the most conservative counting where each operator counts as $(mv)^d$, d being its dimension, with the exception of iD_0 which counts as mv^2 ($v \sim |\mathbf{p}|/m \sim E/|\mathbf{p}|$).⁶ To count matrix elements of color singlet operators between quarkonium states is rather simple. Since the quarkonium states are normalized, it is sufficient to count the dimension of the gluon field operators and covariant derivatives. For color octet operators,⁷ one has to take into account that they give a nonvanishing contribution between quarkonium states if at least two extra $1/m$ operators are inserted. Hence

⁶In principle, at least another scale is relevant for quarkonium: $\sqrt{m}\Lambda_{\text{QCD}}$. Since this scale is larger than E , $|\mathbf{p}|$, and Λ_{QCD} , it may, in principle, change our counting. We discuss this in Sec. VII.

⁷This applies to the pure octet content of the octet operators $(O_8, \mathcal{P}_8, \dots)$ defined in Eq. (39), which starting from $\mathcal{O}(1/m^4)$ may also contain singlet parts.

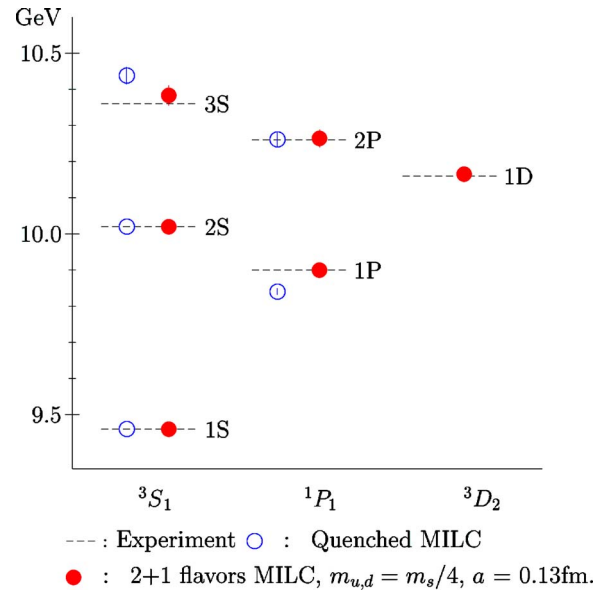


FIG. 3. (Color online) Radial and orbital splittings in the Y system from lattice QCD in the quenched approximation (open circles) and including dynamical u , d , and s quarks (filled circles). The lattice spacing has been fixed by the radial splitting between $Y(2S)$ and $Y(1S)$. The b -quark mass has been tuned to get the Y mass correct. From Lepage and Davies, 2004.

using the above rules, one has to add 2 to the dimension of the gluon field operators and covariant derivatives. This counting, which we call the *conservative counting*, differs from the “original counting” of NRQCD introduced by Lepage *et al.* (1992). We refer to Sec. II.B for further details.

1. Spectra

The idea to put NRQCD on the lattice was a very early one (Lepage *et al.*, 1992). The advantages with respect to full QCD are obvious. The lattice spacing a and the dimension L of the lattice have to fulfill the requirement $1/a \gg Q \gg q \gg 1/L$, where Q is the largest and q the smallest scale of the system under study. In full QCD we have $Q \sim m$ while in NRQCD $Q \sim |\mathbf{p}| \ll m$. NRQCD therefore does not require such a fine lattice as full QCD, which means that much more economical simulations are sufficient. The drawback is that the continuum scaling window will not be reached and much more care has to be taken in order to extrapolate from the discrete simulations to the continuum physics.

Some recent results obtained in the lattice version of NRQCD can be found in the article by Lepage and Davies (2004). As a consequence of the rather precise data, for the heavy-quarkonium spectra all levels below the open-flavor threshold have been obtained from multiexponential fits to suitable correlation functions. In Fig. 3 we show some recent quenched and unquenched results for the radial and orbital splittings in the bottomonium system (Gray *et al.*, 2003).

Here we comment on the theoretical limits of precise lattice results. We neglect all complications and uncertainties connected with the numerical simulations and continuum extrapolations. The version of the NRQCD Lagrangian used in all lattice simulations contains, apart from the Yang-Mills term, only bilinear terms in the heavy-quark fields. The matching coefficients are taken at tree level. This is due to the fact that their calculation in a lattice regularization scheme turns out to be quite cumbersome so that, up to now, only some preliminary numerical estimates are available (Trottier and Lepage, 1998). As a consequence, regardless of how many operators have been added to the bilinear sector of the Lagrangian, the theoretical limit on the precision of the radial splittings is of relative order $\alpha_s v^2 \approx 0.2 \times 0.1 \approx 2\%$ in the original power counting described in the article of Lepage *et al.* (1992) [$\alpha_s v \approx 0.2 \times 0.3 \approx 6\%$ in the conservative counting introduced above], while for the fine and hyperfine splittings it is of relative order $\alpha_s \approx 0.2 \approx 20\%$. We have assumed for the bottomonium case $v^2 \approx 0.1$ and $\alpha_s(m_b) \approx 0.2$.⁸ In any case, the precision in the radial splittings is rather good, while it is worse by an order of magnitude in the fine and hyperfine splittings. In the charmonium case, $v^2 \approx 0.3$ and $\alpha_s(m_c) \approx 0.35$, which means that the theoretical limit on the precision of the radial splittings is not smaller than 10% in the original counting (20% in the conservative counting). In order to improve the present precision, it is therefore crucial to calculate the one-loop corrections to the Wilson coefficients in the NRQCD Lagrangian in a consistent lattice regularization and renormalization scheme. In this sense, the recent work by Becher and Melnikov (2002, 2003) seems to be rather promising. Note that at order $\alpha_s v^4$ ($\alpha_s v^3$ in the conservative counting), $1/m^2$ corrections to the Yang-Mills sector of the NRQCD Lagrangian and four-fermion operators also have to be taken into account.

2. Inclusive decay widths

Let us consider heavy quarkonia made out of a quark and an antiquark of the same flavor ($m_1 = m_2 = m$). Annihilation processes happen in QCD at the scale of the mass m . Therefore integrating out these scales in the matching from QCD to NRQCD produces imaginary terms in the matching coefficients of the 4-four-fermion operators of the NRQCD Lagrangian as we have seen in Sec. II.D. Therefore the annihilation width of a heavy quarkonium H into light particles is given by (Bodwin *et al.*, 1995)

⁸It seems too optimistic to replace α_s with α_s/π , as suggested by Lepage *et al.* (1992), since several α_s corrections appear with large coefficients [compare with the explicit expressions given in the previous section and with the discussion in the article by Brambilla and Vairo (1999b)]. Moreover, large logarithms could also deteriorate the convergence.

$$\Gamma(H \rightarrow \text{light particles}) = 2 \text{Im}\langle H | \mathcal{L}_{\psi\chi} | H \rangle, \quad (38)$$

where $|H\rangle$ is a normalized eigenstate of the NRQCD Hamiltonian with the quantum numbers of the considered quarkonium in its center-of-mass frame.⁹ In Eq. (8) we have given $\mathcal{L}_{\psi\chi}$ up to order $1/m^2$, here we need it up to order $1/m^4$:

$$\begin{aligned} \mathcal{L}_{\psi\chi} = & \frac{f_1(^1S_0)}{m^2} O_1(^1S_0) + \frac{f_1(^3S_1)}{m^2} O_1(^3S_1) \\ & + \frac{f_8(^1S_0)}{m^2} O_8(^1S_0) + \frac{f_8(^3S_1)}{m^2} O_8(^3S_1) \\ & + \frac{f_1(^1P_1)}{m^4} O_1(^1P_1) + \frac{f_1(^3P_0)}{m^4} O_1(^3P_0) \\ & + \frac{f_1(^3P_1)}{m^4} O_1(^3P_1) + \frac{f_1(^3P_2)}{m^4} O_1(^3P_2) \\ & + \frac{g_1(^1S_0)}{m^4} \mathcal{P}_1(^1S_0) + \frac{g_1(^3S_1)}{m^4} \mathcal{P}_1(^3S_1) \\ & + \frac{g_1(^3S_1, ^3D_1)}{m^4} \mathcal{P}_1(^3S_1, ^3D_1) \\ & + [O_1 \rightarrow O_8, \mathcal{P}_1 \rightarrow \mathcal{P}_8, f_1 \rightarrow f_8, g_1 \rightarrow g_8], \quad (39) \end{aligned}$$

where the explicit expressions for the operators in the first line can be found in Eq. (10) and for the remaining operators in the paper by Bodwin *et al.* (1995).

The NRQCD factorization formula for the inclusive heavy-quarkonium annihilation width into light particles reads (d_n denotes the dimension of the generic four-fermion operator $O^{(n)}$)

$$\Gamma(H \rightarrow \text{LH}) = \sum_n \frac{2 \text{Im} f^{(n)}}{m^{d_n-4}} \langle H | O^{(n)} | H \rangle, \quad (40)$$

$$\Gamma(H \rightarrow \text{EM}) = \sum_n \frac{2 \text{Im} f_{\text{EM}}^{(n)}}{m^{d_n-4}} \langle H | O_{\text{EM}}^{(n)} | H \rangle, \quad (41)$$

where we have distinguished between electromagnetic decay widths and decay widths into light hadrons (LH). The information needed in order to describe decays into hard electromagnetic particles is encoded in the electromagnetic contributions to the matching coefficients that we denote by $f_{\text{EM}}, g_{\text{EM}}, \dots$. We do not use a special symbol to denote the purely hadronic component of the matching coefficients, which is the dominant one. The purely electromagnetic component of the inclusive decay width may be singled out by projecting the four-fermion operators onto the QCD vacuum state $|\text{vac}\rangle$ according to $\psi^\dagger \dots \chi \chi^\dagger \dots \psi \rightarrow \psi^\dagger \dots \chi |\text{vac}\rangle \langle \text{vac}| \chi^\dagger \dots \psi$. The

⁹This expression only holds at leading order (LO) in the imaginary terms. The exact expression, which has not been necessary for applications so far, reads $\Gamma(H \rightarrow \text{light particles}) = -2 \text{Im}(\langle \tilde{H} | H | H \rangle / \langle \tilde{H} | H \rangle)$, where H is the NRQCD Hamiltonian and $|\tilde{H}\rangle$ ($\neq |H\rangle$ in general) is the corresponding eigenstate of H^\dagger .

projected operators are denoted by $O_{EM}, \mathcal{P}_{EM}, \dots$. For instance, $O_{EM}(^1S_0) = \psi^\dagger \chi | \text{vac} \rangle \langle \text{vac} | \chi^\dagger \psi$. The inclusive annihilation width into light hadrons may be obtained from the full annihilation width by switching off the electromagnetic interaction. The factorization formulas (40) and (41) have been rigorously proven and shown diagrammatically in the article by Bodwin *et al.* (1995).

Working out Eqs. (40) and (41), the explicit expressions for the decay widths of S - and P -wave quarkonium up to $\mathcal{O}(\text{Im} f \times mv^5)$ are

$$\begin{aligned} \Gamma(V_Q(nS) \rightarrow \text{LH}) &= \frac{2}{m^2} \left(\text{Im} f_1(^3S_1) \langle V_Q(nS) | O_1(^3S_1) | V_Q(nS) \rangle \right. \\ &+ \text{Im} f_8(^3S_1) \langle V_Q(nS) | O_8(^3S_1) | V_Q(nS) \rangle \\ &+ \text{Im} f_8(^1S_0) \langle V_Q(nS) | O_8(^1S_0) | V_Q(nS) \rangle \\ &+ \text{Im} g_1(^3S_1) \frac{\langle V_Q(nS) | \mathcal{P}_1(^3S_1) | V_Q(nS) \rangle}{m^2} \\ &+ \text{Im} f_8(^3P_0) \frac{\langle V_Q(nS) | O_8(^3P_0) | V_Q(nS) \rangle}{m^2} \\ &+ \text{Im} f_8(^3P_1) \frac{\langle V_Q(nS) | O_8(^3P_1) | V_Q(nS) \rangle}{m^2} \\ &\left. + \text{Im} f_8(^3P_2) \frac{\langle V_Q(nS) | O_8(^3P_2) | V_Q(nS) \rangle}{m^2} \right), \quad (42) \end{aligned}$$

$$\begin{aligned} \Gamma(P_Q(nS) \rightarrow \text{LH}) &= \frac{2}{m^2} \left(\text{Im} f_1(^1S_0) \langle P_Q(nS) | O_1(^1S_0) | P_Q(nS) \rangle \right. \\ &+ \text{Im} f_8(^1S_0) \langle P_Q(nS) | O_8(^1S_0) | P_Q(nS) \rangle \\ &+ \text{Im} f_8(^3S_1) \langle P_Q(nS) | O_8(^3S_1) | P_Q(nS) \rangle \\ &+ \text{Im} g_1(^1S_0) \frac{\langle P_Q(nS) | \mathcal{P}_1(^1S_0) | P_Q(nS) \rangle}{m^2} \\ &\left. + \text{Im} f_8(^1P_1) \frac{\langle P_Q(nS) | O_8(^1P_1) | P_Q(nS) \rangle}{m^2} \right), \quad (43) \end{aligned}$$

$$\begin{aligned} \Gamma(\chi_Q(nJS) \rightarrow \text{LH}) &= \frac{2}{m^2} \left(\text{Im} f_1(^{2S+1}P_J) \frac{\langle \chi_Q(nJS) | O_1(^{2S+1}P_J) | \chi_Q(nJS) \rangle}{m^2} \right. \\ &\left. + \text{Im} f_8(^{2S+1}S_S) \langle \chi_Q(nJS) | O_8(^1S_0) | \chi_Q(nJS) \rangle \right), \quad (44) \end{aligned}$$

$$\begin{aligned} \Gamma(V_Q(nS) \rightarrow e^+e^-) &= \frac{2}{m^2} \left(\text{Im} f_{ee}(^3S_1) \langle V_Q(nS) | O_{EM}(^3S_1) | V_Q(nS) \rangle \right. \\ &\left. + \text{Im} g_{ee}(^3S_1) \frac{\langle V_Q(nS) | \mathcal{P}_{EM}(^3S_1) | V_Q(nS) \rangle}{m^2} \right), \quad (45) \end{aligned}$$

$$\begin{aligned} \Gamma(P_Q(nS) \rightarrow \gamma\gamma) &= \frac{2}{m^2} \left(\text{Im} f_{\gamma\gamma}(^1S_0) \langle P_Q(nS) | O_{EM}(^1S_0) | P_Q(nS) \rangle \right. \\ &\left. + \text{Im} g_{\gamma\gamma}(^1S_0) \frac{\langle P_Q(nS) | \mathcal{P}_{EM}(^1S_0) | P_Q(nS) \rangle}{m^2} \right), \quad (46) \end{aligned}$$

$$\begin{aligned} \Gamma(\chi_Q(nJ1) \rightarrow \gamma\gamma) &= 2 \text{Im} f_{\gamma\gamma}(^3P_J) \frac{\langle \chi_Q(nJ1) | O_{EM}(^3P_J) | \chi_Q(nJ1) \rangle}{m^4} \\ &\text{for } J=0,2, \quad (47) \end{aligned}$$

where the symbols V and P stand for the vector and pseudoscalar S -wave heavy quarkonium and the symbol χ for the generic P -wave quarkonium (the states $\chi(n10)$ and $\chi(nJ1)$ are usually called $h[(n-1)P]$ and $\chi_J[(n-1)P]$, respectively).

Looking at Eqs. (42)–(47), the first obvious observation is that in the hadronic decay widths singlet as well as octet matrix elements occur. In the case of the hadronic P -wave decay widths the color octet matrix elements are of the same order as the singlet matrix elements. This means that a description of heavy quarkonium in terms of a color-singlet bound state of a heavy quark and antiquark necessarily fails at some point: for P -wave decay this point is the leading order! There is another way to understand the role of the octet matrix elements. The singlet matching coefficients are plagued by IR divergences. The coefficients $\text{Im} f(^3P_0)$ and $\text{Im} f(^3P_2)$ are IR divergent at next-to-leading order (NLO) (Barbieri *et al.*, 1976). These divergences are precisely canceled by the octet contributions (Bodwin *et al.*, 1992). Therefore the inclusion of the octet matrix elements is crucial to making Eq. (44) physical, i.e., independent of the cutoff. For S -wave decays, note that in the original NRQCD power counting used by Lepage *et al.* (1992) the octet matrix elements are $\mathcal{O}(v^4)$ suppressed compared with the leading order. This is not so within the conservative power counting adopted here, where they are $\mathcal{O}(v^2)$. This may be of phenomenological relevance for $\Gamma(V \rightarrow \text{LH})$ since $\text{Im} f_1(^3S_1)$ is $\mathcal{O}(\alpha_s)$ suppressed with respect to $\text{Im} f_8(S)$.

Despite the fact that the NRQCD factorization formulas for inclusive decay widths are theoretically solid and have provided a solution to the long-standing problem of the cancellation of the IR divergences, their practical relevance in calculating inclusive or electromagnetic decay widths of quarkonia has been rather limited. This is mainly due to the following reasons:

(i) NRQCD matrix elements may be fitted on the experimental decay data (Maltoni, 2003) or calculated on the lattice (Bodwin *et al.*, 1996, 2002). The matrix elements of singlet operators can be linked at leading order to the Schrödinger wave functions at the origin (Bodwin *et al.*, 1995) and therefore may be evaluated by means of potential models (Eichten and Quigg, 1995). In general, however, NRQCD matrix elements, in particular of

higher dimensionality, are poorly known or completely unknown.

(ii) The formulas depend on a large number of matrix elements. In the bottomonium system, 14 S - and P -wave states lie below the open-flavor threshold [$Y(nS)$ and $\eta_b(nS)$ with $n=1,2,3$; $h_b(nP)$ and $\chi_{bj}(nP)$ with $n=1,2$ and $J=0,1,2$] and in the charmonium system 8 [$\psi(nS)$ and $\eta_c(nS)$ with $n=1,2$; $h_c(1P)$ and $\chi_{cj}(1P)$ with $J=0,1,2$]. For these states, Eqs. (42)–(47) describe the decay widths into light hadrons and into photons or e^+e^- in terms of 46 NRQCD matrix elements (40 for the S -wave decays and 6 for the P -wave decays). More matrix elements are needed if higher-order operators have to be included. Indeed, Ma and Wang (2002) and Bodwin and Petrelli (2002) have stated that higher-order operators not included in Eqs. (42)–(47), even if parametrically suppressed, may turn out to give sizable contributions to the decay widths. This may be the case, in particular, for charmonium, where $v^2 \sim 0.3$, so that relativistic corrections are large and for P -wave decays, where the above formulas provide only the leading-order contribution in the velocity expansion. In fact it was pointed out by Ma and Wang (2002) and Vairo (2002) that if no special cancellations among the matrix elements occur, then the order v^2 relativistic corrections to the electromagnetic decays $\chi_{c0} \rightarrow \gamma\gamma$ and $\chi_{c2} \rightarrow \gamma\gamma$ may be as large as the leading terms. Finally, it was noted by Maltoni (2003) that the relevance of higher-order matrix elements may be enhanced (or suppressed) by the multiplying matching coefficients.

(iii) The convergence of the perturbative series of the four-fermion matching coefficients is often poor [see, for instance, the examples in the article by Vairo (2002)]. This limits, in general, the reliability and stability of the results. Some classes of large perturbative contributions have been resummed for S -wave annihilation decays by Braaten and Chen (1998) and Bodwin and Chen (1999, 2001) improving the convergence of the series.

III. POTENTIAL NRQCD. THE PHYSICAL PICTURE

Of the full hierarchy of scales in heavy quarkonium, NRQCD takes advantage of the fact that m is much larger than the remaining ones ($|\mathbf{p}|, E, \Lambda_{\text{QCD}}, \dots$) only. This means that if we are interested in physics at the scale of the binding energy E , NRQCD contains degrees of freedom that can never appear as physical states at that scale. These are, in particular, light degrees of freedom of energy $\sim |\mathbf{p}| \gg E$ and heavy quarks with energy fluctuations of the same order. Therefore within the philosophy of EFTs, these degrees of freedom should be integrated out. The implementation of this idea gives rise to a new effective theory called pNRQCD (Pineda and Soto, 1998a). The appropriate description of the remaining degrees of freedom and how this integration can actually be carried out will clearly depend on the relative size of Λ_{QCD} compared to the scales $|\mathbf{p}|$ and E . We consider the different possibilities in the next two sections. In pNRQCD it is the large scale $|\mathbf{p}|$ that limits

the UV cutoff of the energy fluctuations. Even if its typical value in a bound state can be associated with mv , its fluctuations may reach up to the scale m , which is the UV cutoff for the three-momentum fluctuations of the heavy quarks, $|\mathbf{p}|$.

A. Weak-coupling regime

If $|\mathbf{p}| \gg \Lambda_{\text{QCD}}$, the integration of degrees of freedom of energy scale $|\mathbf{p}|$ can be done in perturbation theory. Hence we do not expect a qualitative change in the degrees of freedom but only a lowering of their energy cutoff. Let us call the resulting EFT pNRQCD'. pNRQCD' is thus defined by the same particle content as NRQCD and the cutoffs $\nu_{\text{pNR}} = \{\nu_p, \nu_{us}\}$, where ν_p is the cutoff of the relative three-momentum of the heavy quarks and ν_{us} is the cutoff of energy fluctuations of the heavy quarks and of the four-momenta of the gluons and light quarks. They satisfy the following inequalities: $|\mathbf{p}| \ll \nu_p \ll m$ and $\mathbf{p}^2/m \ll \nu_{us} \ll |\mathbf{p}|$. The Wilson coefficients of pNRQCD' will then depend on \mathbf{p} and \mathbf{p}' , the three-momenta of the heavy quark and antiquark, respectively, usually through the combination $\mathbf{k} = \mathbf{p} - \mathbf{p}'$. Hence nonlocal terms (potentials) in real space are produced. Indeed, these potentials encode the nonanalytic behavior in the momentum transfer \mathbf{k} of the heavy quark, which is of the order of the relative three-momentum of the heavy quarks. This is again a peculiar feature of pNRQCD which had not been observed in any EFT before. It provides an appealing interpretation of the usual potentials in quantum mechanics within an EFT framework.

In order to take advantage of the fact that the three-momentum of the heavy quarks is always larger than the four-momentum of the light degrees of freedom, it is very convenient to use fields in which the relative coordinate (conjugate to the relative momentum) appears explicitly. We define the center-of-mass coordinate of the $Q-\bar{Q}$ system $\mathbf{R} \equiv (\mathbf{x}_1 + \mathbf{x}_2)/2$ and the relative coordinate $\mathbf{r} \equiv \mathbf{x}_1 - \mathbf{x}_2$. A $Q-\bar{Q}$ state can be decomposed into a singlet state $S(\mathbf{r}, \mathbf{R}, t)$ and an octet state $O(\mathbf{r}, \mathbf{R}, t)$ in relation to color gauge transformation with respect to the center-of-mass coordinate. (We notice that in QED only the state analogous to the singlet appears.) The gauge fields are evaluated in \mathbf{R} and t , i.e., $A_\mu = A_\mu(\mathbf{R}, t)$. They do not depend on \mathbf{r} due to the fact that, since the typical size of \mathbf{r} is the inverse of the soft scale, gluon fields are multipole expanded with respect to this variable.

If the binding energy E is larger than or of the same order as Λ_{QCD} , we have accomplished our goal and the EFT we are looking for, namely, pNRQCD in the weak-coupling regime, coincides with pNRQCD'. If, on the contrary, $\Lambda_{\text{QCD}} \gg E$, we still have to integrate out the energy scale Λ_{QCD} and its associated three-momentum scale $\sqrt{\Lambda_{\text{QCD}} m}$ in order to obtain pNRQCD. This cannot be done perturbatively in α_s anymore, but one can definitely continue exploiting the hierarchy of scales, as will be discussed in the following section.

B. Strong-coupling regime

For illustration purposes, let us first consider the particular case $|\mathbf{p}| \gg \Lambda_{\text{QCD}} \gg E$, which was discussed in the previous section. We have to figure out what happens to the pNRQCD' degrees of freedom after integrating out those of energy $\sim \Lambda_{\text{QCD}}$. Below the scale Λ_{QCD} , it is better to think in terms of hadronic degrees of freedom, which are color-singlet states. Hence the octet field is not acceptable in the final EFT and must be integrated out. Since it couples to gluons of energy $\sim \Lambda_{\text{QCD}}$, it is also expected that it develops a mass gap of the same order. Therefore in pure gluodynamics the only degree of freedom left is the singlet field interacting with a potential, which also has nonperturbative contributions from the integration of degrees of freedom of order Λ_{QCD} . In real QCD, pseudo-Goldstone bosons, which have masses smaller than Λ_{QCD} , should also be included. These are the expected degrees of freedom of pNRQCD in the strong-coupling regime (Brambilla *et al.*, 2000).

In the general case $|\mathbf{p}| \gtrsim \Lambda_{\text{QCD}}$, we cannot integrate out energy degrees of freedom at the scale $|\mathbf{p}|$ in perturbation theory in α_s . Still the relevant energy scales are at a lower scale $E \ll |\mathbf{p}| \sim \Lambda_{\text{QCD}}$ and one can in principle build an EFT at that scale, as we have done above in a particular case. This is pNRQCD in the strong-coupling regime. At scales $E \ll \Lambda_{\text{QCD}}$, QCD becomes strongly coupled and it is again better to think in terms of hadronic degrees of freedom, which are color-singlet states. Hence the most likely degrees of freedom in this regime are a singlet field and pseudo-Goldstone bosons. This is supported by our knowledge of the static limit of QCD as will be argued below.

In the static limit, there is an energy gap between the ground state and the first excited state. In the nonstatic case there will be a set of states $\{n_{us}\}$ whose energies $E_{n_{us}}$ lie much below the energy of the first excited state in the static case. We denote these states as US. The aim of pNRQCD is to describe the behavior of the US states. Therefore all the physical degrees of freedom in NRQCD with energies larger than $E_{n_{us}}$ can be integrated out in order to obtain pNRQCD. The available lattice calculations of the static spectrum (see Fig. 4) clearly show that from small to moderately large values of \mathbf{r} there is an energy gap between the ground state and higher excitations. The ground-state energy is known as the static QCD potential. If the binding energy of the heavy-quarkonium state we are interested in is much lower than the first excitation of the static limit, we can integrate out all higher excitations of this limit and keep only the ground state, which will be represented by a singlet field whose static energy is given by the static QCD potential.

Note finally that for heavy-quarkonium states whose binding energy is close to or above the region where higher excitations occur, the use of pNRQCD is not justified and one should stay at the NRQCD level. In the case of real QCD, the heavy-light meson pair threshold plays the role of a higher excitation.

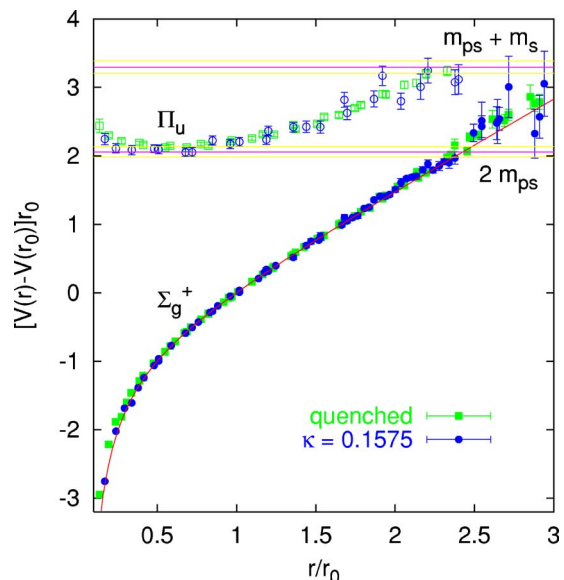


FIG. 4. (Color online) Mass gap between the singlet and hybrid fields. From Bali *et al.*, 2000.

IV. POTENTIAL NRQCD. THE WEAK-COUPLING REGIME

A. pNRQCD: the degrees of freedom

The degrees of freedom of pNRQCD in the weak-coupling regime ($|\mathbf{p}| \gg E \gtrsim \Lambda_{\text{QCD}}$) are a quark-antiquark pair, gluons, and light quarks with the cutoffs $\nu_{\text{pNR}} = \{\nu_p, \nu_{us}\}$. ν_p is the cutoff of the relative three-momentum of the heavy quarks and ν_{us} is the cutoff of the energy of the heavy-quark-antiquark pair and of the four-momentum of the gluons and light quarks. They satisfy the following inequalities: $|\mathbf{p}| \ll \nu_p \ll m$ and $\mathbf{p}^2/m \ll \nu_{us} \ll |\mathbf{p}|$.

The degrees of freedom of pNRQCD can be represented by the same fields as in NRQCD. The main difference with respect to the NRQCD Lagrangian will be that now nonlocal terms in space (namely, potentials) are allowed. This representation is suitable for explicit perturbative matching calculations. However, in order to establish a power counting, it is more convenient to represent the quark-antiquark pair by a wave-function field

$$\begin{aligned} \Psi(\mathbf{x}_1, \mathbf{x}_2, t)_{\alpha\beta} &\sim \psi_\alpha(\mathbf{x}_1, t) \chi_\beta^\dagger(\mathbf{x}_2, t) \\ &\sim \frac{1}{N_c} \delta_{\alpha\beta} \psi_\sigma(\mathbf{x}_1, t) \chi_\sigma^\dagger(\mathbf{x}_2, t) \\ &\quad + \frac{1}{T_F} T_{\alpha\beta}^a T_{\rho\sigma}^a \psi_\sigma(\mathbf{x}_1, t) \chi_\rho^\dagger(\mathbf{x}_2, t). \end{aligned} \quad (48)$$

This can be rigorously achieved in a NR system: (i) time is universal, and hence one can constrain oneself to calculating correlators in which the time coordinate of the quark field coincides with the time coordinate of the antiquark field; (ii) since particle and antiparticle numbers are separately conserved, if we are interested in the one-heavy-quark one-heavy-antiquark sector, there is no loss of generality if we project our theory to that subspace of the Fock space which is described by the wave-

function field $\Psi(\mathbf{x}_1, \mathbf{x}_2, t)$. Furthermore, this wavefunction field can be uniquely decomposed into singlet- and octet-field components with homogeneous (US) gauge transformations with respect to the center-of-mass coordinate:

$$\Psi(\mathbf{x}_1, \mathbf{x}_2, t) = P[e^{ig\int_{\mathbf{x}_2}^{\mathbf{x}_1} \mathbf{A} \cdot d\mathbf{x}}]S(\mathbf{r}, \mathbf{R}, t) + P[e^{ig\int_{\mathbf{R}}^{\mathbf{x}_1} \mathbf{A} \cdot d\mathbf{x}}]O(\mathbf{r}, \mathbf{R}, t)P[e^{ig\int_{\mathbf{x}_2}^{\mathbf{R}} \mathbf{A} \cdot d\mathbf{x}}]. \quad (49)$$

P stands for path ordered. Under (US) color gauge transformations $[g(\mathbf{R}, t)]$, we have

$$S(\mathbf{r}, \mathbf{R}, t) \rightarrow S(\mathbf{r}, \mathbf{R}, t), \quad (50)$$

$$O(\mathbf{r}, \mathbf{R}, t) \rightarrow g(\mathbf{R}, t)O(\mathbf{r}, \mathbf{R}, t)g^{-1}(\mathbf{R}, t).$$

Using these fields has the advantage that the relative coordinate \mathbf{r} is explicit, and the fact that \mathbf{r} is much smaller than the typical length of the light degrees of freedom can be easily implemented via a multipole expansion. This implies that the gluon fields will always appear evaluated at the center-of-mass coordinate. Note that this is nothing but translating to real space the constraint $v_p \gg v_{us}$. In addition, if we restrict ourselves to the singlet field only, we are left with a theory which is totally equivalent to a quantum-mechanical Hamiltonian. The whole theory, however, will contain singlet-to-octet transitions mediated by the emission of an US gluon, which cannot be encoded in any quantum-mechanical Hamiltonian.

B. Power counting

The power counting of the pNRQCD Lagrangian is easier to establish when it is written in terms of singlet and octet fields. Since quark and antiquark particle numbers are separately conserved, the Lagrangian will be bilinear in these fields and we only have to estimate the size of the terms multiplying those bilinears. m and $\alpha_s(m)$, inherited from the hard matching coefficients, have well-known values. Derivatives with respect to the relative coordinate $i\nabla_{\mathbf{r}}$ and $1/r \sim k$ (the transfer momentum) must be assigned the soft scale $\sim |\mathbf{p}|$. Time derivatives $i\partial_0$, center-of-mass derivatives $i\nabla_{\mathbf{R}}$, and the fields of the light degrees of freedom must be assigned the US scale $E \sim \mathbf{p}^2/m$. The α_s arising in the matching calculation from NRQCD, namely, those in the potentials, must be assigned the size $\alpha_s(1/r)$ and those associated with the light degrees of freedom (gluons, at lower orders) the size $\alpha_s(E)$. If Λ_{QCD} did not exist (as in QED) this would provide a homogeneous counting in which each term has a well-defined size. If $E \sim \Lambda_{\text{QCD}}$ [recall that then $\alpha_s(E) \sim 1$] this is also true, but calculations at the US scale cannot be done in perturbation theory in $\alpha_s(E)$ anymore. If $E \gg \Lambda_{\text{QCD}}$, the counting becomes inhomogeneous (i.e., it is not possible to assign *a priori* a unique size to each term) since the light degrees of freedom may have contributions both at the scale E and at the scale Λ_{QCD} (see Sec. IV.G). Nevertheless, the largest size a term can have can be estimated identically as before.

C. Lagrangian and symmetries

The degrees of freedom of pNRQCD can be arranged in several ways and so accordingly can the pNRQCD Lagrangian. We first write it in terms of quarks and gluons, which allows a smooth connection with the NRQCD section. One of the most distinct features of the pNRQCD Lagrangian is the appearance of the terms V , nonlocal in r , as matching coefficients of four-fermion operators:

$$L_{\text{pot}} = - \int d^3\mathbf{x}_1 d^3\mathbf{x}_2 \psi^\dagger(t, \mathbf{x}_1) \chi(t, \mathbf{x}_2) V(\mathbf{r}, \mathbf{p}_1, \mathbf{p}_2, \mathbf{S}_1, \mathbf{S}_2) \times (\text{US gluon fields}) \chi^\dagger(t, \mathbf{x}_2) \psi(t, \mathbf{x}_1), \quad (51)$$

where $\mathbf{p}_j = -i\nabla_{\mathbf{x}_j}$, for $j=1,2$, and $\mathbf{S}_1 = \boldsymbol{\sigma}_1/2$, $\mathbf{S}_2 = \boldsymbol{\sigma}_2/2$ act on the fermion and antifermion, respectively (the fermion and antifermion spin indices are contracted with the indices of V , which are not explicitly displayed). Typically, US gluon fields show up at higher order. With this new term the pNRQCD Lagrangian can be written in the following way:

$$L_{\text{pNRQCD}} = L_{\text{NRQCD}}^{\text{US}} + L_{\text{pot}}, \quad (52)$$

where $L_{\text{NRQCD}}^{\text{US}}$ has the form of the NRQCD Lagrangian but all the gluons must be understood as US. This way of writing the pNRQCD Lagrangian is advantageous for calculating the matching potentials straightforwardly by means of standard Feynman-diagram techniques. On the other hand, for the study of heavy quarkonium, it is convenient, before calculating physical quantities, to project the above Lagrangian onto the quark-antiquark sector of the Fock space. This makes the multipole expansion explicit at the Lagrangian level and it may also be useful at the matching level, depending on how it is done. An example is the matching via Wilson loops discussed in Sec. IV.F. The projection onto the quark-antiquark sector is easily done at the Hamiltonian level by projecting onto the subspace spanned by

$$\int d^3\mathbf{x}_1 d^3\mathbf{x}_2 \Psi(\mathbf{x}_1, \mathbf{x}_2) \psi^\dagger(\mathbf{x}_1) \chi(\mathbf{x}_2) |\text{US gluons}\rangle, \quad (53)$$

where $|\text{US gluons}\rangle$ is a generic state belonging to the Fock subspace with no quarks and antiquarks but an arbitrary number of ultrasoft gluons. The pNRQCD Lagrangian then has the form

$$L_{\text{pNRQCD}} = \int d^3\mathbf{x}_1 d^3\mathbf{x}_2 \text{Tr} \left\{ \Psi^\dagger(t, \mathbf{x}_1, \mathbf{x}_2) \left(iD_0 + \frac{\mathbf{D}_{\mathbf{x}_1}^2}{2m_1} + \frac{\mathbf{D}_{\mathbf{x}_2}^2}{2m_2} + \dots \right) \Psi(t, \mathbf{x}_1, \mathbf{x}_2) \right\} - \int d^3x \frac{1}{4} G_{\mu\nu}^a(x) G^{\mu\nu a}(x) + \int d^3x \sum_{i=1}^{n_f} \bar{q}_i(x) i\not{D} q_i(x) + \dots$$

$$\begin{aligned}
& + \int d^3\mathbf{x}_1 d^3\mathbf{x}_2 \text{Tr}\{\Psi^\dagger(t, \mathbf{x}_1, \mathbf{x}_2) \\
& \times V(\mathbf{r}, \mathbf{p}_1, \mathbf{p}_2, \mathbf{S}_1, \mathbf{S}_2) \\
& \times (\text{US gluon fields})\Psi(t, \mathbf{x}_1, \mathbf{x}_2)\}, \quad (54)
\end{aligned}$$

where the first four lines stand for the NRQCD Lagrangian projected onto the quark-antiquark sector and

$$\begin{aligned}
iD_0\Psi(t, \mathbf{x}_1, \mathbf{x}_2) &= i\partial_0\Psi(t, \mathbf{x}_1, \mathbf{x}_2) - gA_0(t, \mathbf{x}_1)\Psi(t, \mathbf{x}_1, \mathbf{x}_2) \\
&+ \Psi(t, \mathbf{x}_1, \mathbf{x}_2)gA_0(t, \mathbf{x}_2). \quad (55)
\end{aligned}$$

The dots in Eq. (54) stand for higher terms in the $1/m$ expansion. The last four lines contain the four-fermion terms specific to pNRQCD. In general US gluon fields may also appear there, but the leading term (in α_s , $1/m$, and in the multipole expansion) is simply given by the Coulomb law (one gluon exchange):

$$\frac{\alpha_s}{|\mathbf{x}_1 - \mathbf{x}_2|} \text{Tr}[T^a\Psi^\dagger(t, \mathbf{x}_1, \mathbf{x}_2)T^a\Psi(t, \mathbf{x}_1, \mathbf{x}_2)]. \quad (56)$$

We can enforce that the gluons be US by multipole expanding them in \mathbf{r} . In the case of the covariant derivatives in Eq. (54) this corresponds to

$$\begin{aligned}
iD_0\Psi(t, \mathbf{x}_1, \mathbf{x}_2) &= i\partial_0\Psi(t, \mathbf{x}_1, \mathbf{x}_2) - [gA_0(t, \mathbf{R}), \Psi(t, \mathbf{x}_1, \mathbf{x}_2)] \\
&- \frac{1}{2}\mathbf{r}^i(g\partial_i A_0(t, \mathbf{R}))\Psi(t, \mathbf{x}_1, \mathbf{x}_2) \\
&- \frac{1}{2}\mathbf{r}^i\Psi(t, \mathbf{x}_1, \mathbf{x}_2)(g\partial_i A_0(t, \mathbf{R})) + \mathcal{O}(r^2), \quad (57)
\end{aligned}$$

$$\begin{aligned}
i\mathbf{D}_{\mathbf{x}_1}\Psi(t, \mathbf{x}_1, \mathbf{x}_2) &= \left(i\nabla_{\mathbf{r}} + \frac{i}{2}\nabla_{\mathbf{R}} + g\mathbf{A}(t, \mathbf{R}) \right. \\
&\left. + \frac{\mathbf{r}^i}{2}(g\partial_i \mathbf{A}(t, \mathbf{R})) \right) \Psi(t, \mathbf{x}_1, \mathbf{x}_2) + \mathcal{O}(r^2). \quad (58)
\end{aligned}$$

$$\begin{aligned}
i\mathbf{D}_{\mathbf{x}_2}\Psi(t, \mathbf{x}_1, \mathbf{x}_2) &= \left(-i\nabla_{\mathbf{r}} + \frac{i}{2}\nabla_{\mathbf{R}} \right) \Psi(t, \mathbf{x}_1, \mathbf{x}_2) \\
&+ \Psi(t, \mathbf{x}_1, \mathbf{x}_2) \left(-g\mathbf{A}(t, \mathbf{R}) \right. \\
&\left. + \frac{\mathbf{r}^i}{2}g(\partial_i \mathbf{A}(t, \mathbf{R})) \right) + \mathcal{O}(r^2).
\end{aligned}$$

From now on, all the gluon (and light-quark) fields will be understood as functions of t and \mathbf{R} . We shall not always explicitly display this dependence. According to the power counting given in the previous section, the multipole expansion makes explicit the size of each term in the Lagrangian. On the other hand, expansions like Eqs. (57) and (58) spoil the manifest gauge invariance of the Lagrangian. This may be restored by introducing singlet and octet fields as in Eq. (49). We choose the following normalization with respect to color:

$$S = S\mathbf{1}_c/\sqrt{N_c}, \quad O = O^a T^a/\sqrt{T_F}. \quad (59)$$

We shall not always explicitly display their dependence on \mathbf{R} , \mathbf{r} , and t in the following. After multipole expansion, the pNRQCD Lagrangian may be organized as an expansion in $1/m$ and r (and α_s). The most general pNRQCD Lagrangian density, compatible with the symmetries of QCD, that can be constructed with a singlet field, an octet field, and US gluon fields up to order p^3/m^2 (see Sec. IV.B) has the form

$$\begin{aligned}
\mathcal{L}_{\text{pNRQCD}} &= \int d^3\mathbf{r} \text{Tr}\{S^\dagger[i\partial_0 - h_s(\mathbf{r}, \mathbf{p}, \mathbf{P}_{\mathbf{R}}, \mathbf{S}_1, \mathbf{S}_2)]S \\
&+ O^\dagger[iD_0 - h_o(\mathbf{r}, \mathbf{p}, \mathbf{P}_{\mathbf{R}}, \mathbf{S}_1, \mathbf{S}_2)]O\} \\
&+ V_A(r)\text{Tr}\{O^\dagger\mathbf{r} \cdot g\mathbf{E}S + S^\dagger\mathbf{r} \cdot g\mathbf{E}O\} \\
&+ \frac{V_B(r)}{2}\text{Tr}\{O^\dagger\mathbf{r} \cdot g\mathbf{E}O + O^\dagger O\mathbf{r} \cdot g\mathbf{E}\} \\
&- \frac{1}{4}G_{\mu\nu}^a G^{\mu\nu a} + \sum_{i=1}^{n_f} \bar{q}_i i\not{D}q_i, \quad (60)
\end{aligned}$$

$$\begin{aligned}
h_s(\mathbf{r}, \mathbf{p}, \mathbf{P}_{\mathbf{R}}, \mathbf{S}_1, \mathbf{S}_2) &= \left\{ c_S^{(1,-2)}(r), \frac{\mathbf{p}^2}{2m_{\text{red}}} \right\} + c_S^{(1,0)}(r) \frac{\mathbf{P}_{\mathbf{R}}^2}{2m_{\text{tot}}} \\
&+ V_s(\mathbf{r}, \mathbf{p}, \mathbf{P}_{\mathbf{R}}, \mathbf{S}_1, \mathbf{S}_2), \quad (61)
\end{aligned}$$

$$\begin{aligned}
h_o(\mathbf{r}, \mathbf{p}, \mathbf{P}_{\mathbf{R}}, \mathbf{S}_1, \mathbf{S}_2) &= \left\{ c_O^{(1,-2)}(r), \frac{\mathbf{p}^2}{2m_{\text{red}}} \right\} + c_O^{(1,0)}(r) \frac{\mathbf{P}_{\mathbf{R}}^2}{2m_{\text{tot}}} \\
&+ V_o(\mathbf{r}, \mathbf{p}, \mathbf{P}_{\mathbf{R}}, \mathbf{S}_1, \mathbf{S}_2), \quad (62)
\end{aligned}$$

$$V_s = V_s^{(0)} + \frac{V_s^{(1,0)}}{m_1} + \frac{V_s^{(0,1)}}{m_2} + \frac{V_s^{(2,0)}}{m_1^2} + \frac{V_s^{(0,2)}}{m_2^2} + \frac{V_s^{(1,1)}}{m_1 m_2}, \quad (63)$$

$$V_o = V_o^{(0)} + \frac{V_o^{(1,0)}}{m_1} + \frac{V_o^{(0,1)}}{m_2} + \frac{V_o^{(2,0)}}{m_1^2} + \frac{V_o^{(0,2)}}{m_2^2} + \frac{V_o^{(1,1)}}{m_1 m_2}, \quad (64)$$

where $iD_0 O \equiv i\partial_0 O - g[A_0(\mathbf{R}, t), O]$, $\mathbf{P}_{\mathbf{R}} = -i\mathbf{D}_{\mathbf{R}}$, $\mathbf{p} = -i\nabla_{\mathbf{r}}$, $m_{\text{red}} = m_1 m_2 / m_{\text{tot}}$, and $m_{\text{tot}} = m_1 + m_2$. When acting between singlet fields, the color trace reduces $\mathbf{P}_{\mathbf{R}}$ to $-i\nabla_{\mathbf{R}}$. According to the order at which we are working, the potentials have been displayed up to terms of order $1/m^2$. The static and the $1/m$ potentials are real-valued functions of r only. The $1/m^2$ potentials have an imaginary part proportional to $\delta^{(3)}(\mathbf{r})$ and a real part that may be decomposed as (we drop the labels s and o for singlet and octet which have to be understood)

$$V^{(2,0)} = V_{SD}^{(2,0)} + V_{SI}^{(2,0)}, \quad V^{(0,2)} = V_{SD}^{(0,2)} + V_{SI}^{(0,2)}, \quad (65)$$

$$V^{(1,1)} = V_{SD}^{(1,1)} + V_{SI}^{(1,1)},$$

$$V_{SI}^{(2,0)} = \frac{1}{2}\{\mathbf{p}_1^2, V_{\mathbf{p}^2}^{(2,0)}(r)\} + \frac{V_{\mathbf{L}^2}^{(2,0)}(r)}{r^2} \mathbf{L}_1^2 + V_r^{(2,0)}(r), \quad (66)$$

$$V_{SI}^{(0,2)} = \frac{1}{2}\{\mathbf{p}_2^2, V_{\mathbf{p}_2^2}^{(0,2)}(r)\} + \frac{V_{\mathbf{L}^2}^{(0,2)}(r)}{r^2}\mathbf{L}_2^2 + V_r^{(0,2)}(r), \quad (67)$$

$$V_{SI}^{(1,1)} = -\frac{1}{2}\{\mathbf{p}_1 \cdot \mathbf{p}_2, V_{\mathbf{p}_2^2}^{(1,1)}(r)\} - \frac{V_{\mathbf{L}^2}^{(1,1)}(r)}{2r^2} \\ \times (\mathbf{L}_1 \cdot \mathbf{L}_2 + \mathbf{L}_2 \cdot \mathbf{L}_1) + V_r^{(1,1)}(r), \quad (68)$$

$$V_{SD}^{(2,0)} = V_{LS}^{(2,0)}(r)\mathbf{L}_1 \cdot \mathbf{S}_1, \quad (69)$$

$$V_{SD}^{(0,2)} = -V_{LS}^{(0,2)}(r)\mathbf{L}_2 \cdot \mathbf{S}_2, \quad (70)$$

$$V_{SD}^{(1,1)} = V_{L_1S_2}^{(1,1)}(r)\mathbf{L}_1 \cdot \mathbf{S}_2 - V_{L_2S_1}^{(1,1)}(r)\mathbf{L}_2 \cdot \mathbf{S}_1 \\ + V_{S_1^2}^{(1,1)}(r)\mathbf{S}_1 \cdot \mathbf{S}_2 + V_{S_{12}}^{(1,1)}(r)\mathbf{S}_{12}(\hat{\mathbf{r}}), \quad (71)$$

where $\mathbf{S}_1 = \boldsymbol{\sigma}_1/2$, $\mathbf{S}_2 = \boldsymbol{\sigma}_2/2$, $\mathbf{L}_1 \equiv \mathbf{r} \times \mathbf{p}_1$, $\mathbf{L}_2 \equiv \mathbf{r} \times \mathbf{p}_2$, and $\mathbf{S}_{12}(\hat{\mathbf{r}}) \equiv 3\hat{\mathbf{r}} \cdot \boldsymbol{\sigma}_1 \hat{\mathbf{r}} \cdot \boldsymbol{\sigma}_2 - \boldsymbol{\sigma}_1 \cdot \boldsymbol{\sigma}_2$. The pNRQCD Lagrangian density at order r^2/m^0 , r^0/m , $(r/m)\mathbf{P}_R$, and $(r^0/m^2)\mathbf{P}_R$ and the corresponding matching coefficients at tree level can be found in the article by Brambilla, Gromes, and Vairo (2003).

For the case $m_1 = m_2 = m$, the potential has the following structure:

$$V(r) = V^{(0)}(r) + \frac{V^{(1)}(r)}{m} + \frac{V^{(2)}(r)}{m^2} + \dots, \\ V^{(2)} = V_{SD}^{(2)} + V_{SI}^{(2)}, \quad (72) \\ V_{SI}^{(2)} = \frac{1}{8}\{\mathbf{P}_R^2, V_{\mathbf{p}^2, \text{CM}}^{(2)}(r)\} + \frac{(\mathbf{r} \times \mathbf{P}_R)^2}{4r^2}V_{\mathbf{L}^2, \text{CM}}^{(2)}(r) \\ + \frac{1}{2}\{\mathbf{p}^2, V_{\mathbf{p}^2}^{(2)}(r)\} + \frac{V_{\mathbf{L}^2}^{(2)}(r)}{r^2}\mathbf{L}^2 + V_r^{(2)}(r), \\ V_{SD}^{(2)} = \frac{(\mathbf{r} \times \mathbf{P}_R) \cdot (\mathbf{S}_1 - \mathbf{S}_2)}{2}V_{LS, \text{CM}}^{(2)}(r) + V_{LS}^{(2)}(r)\mathbf{L} \cdot \mathbf{S} \\ + V_{S_1^2}^{(2)}(r)\mathbf{S}^2 + V_{S_{12}}^{(2)}(r)\mathbf{S}_{12}(\hat{\mathbf{r}}),$$

$\mathbf{S} = \mathbf{S}_1 + \mathbf{S}_2$ and $\mathbf{L} = \mathbf{r} \times \mathbf{p}$. Other forms of the potential can be brought to the one above by using unitary transformations, or the relation

$$-\left\{\frac{1}{r}, \mathbf{p}^2\right\} + \frac{1}{r^3}\mathbf{L}^2 + 4\pi\delta^{(3)}(\mathbf{r}) = -\frac{1}{r}\left(\mathbf{p}^2 + \frac{1}{r^2}\mathbf{r} \cdot (\mathbf{r} \cdot \mathbf{p})\mathbf{p}\right). \quad (73)$$

From Eq. (60) we see that the relative coordinate \mathbf{r} plays the role of a continuous parameter which specifies different fields. Moreover, we note that the Lagrangian is now in an explicitly gauge-invariant form. This is a consequence of the transformation properties (50) of the singlet and octet fields and of the fact that the gluon fields depend on t and \mathbf{R} only. The functions V_s , V_o , $c_S^{(1,-2)}$, $c_O^{(1,-2)}$, $c_S^{(1,0)}$, $c_O^{(1,0)}$, V_A , and V_B are the matching coefficients of the effective theory. At leading order it

follows from Eq. (57) that $V_A = V_B = 1$, from Eq. (58) that $c_S^{(1,-2)} = c_O^{(1,-2)} = c_S^{(1,0)} = c_O^{(1,0)} = 1$, and from Eq. (56) that $V_s^{(0)} = -C_F\alpha_s/r$ and $V_o^{(0)} = (1/2N_c)\alpha_s/r$.

Equations (52), (54), and (60) provide three different ways to write the pNRQCD Lagrangian. We have also shown how to derive one from the other. This works (and is useful) at tree level. In general, each form of the pNRQCD Lagrangian may be constructed independently of the others by identifying the degrees of freedom, using symmetry arguments, and matching directly to NRQCD.

The expressions for the currents in pNRQCD are equal to those of NRQCD with the replacements: NR \rightarrow pNR and $\nu \rightarrow \nu_{\text{pNR}}$. In particular, this applies to Eqs. (12) and (13). As in NRQCD, most of the physical information can be extracted from the imaginary part of the potentials, which are proportional to the imaginary part of the NRQCD four-fermion matching coefficients. Therefore the imaginary part of the (singlet or octet) potential will have the following structure (with only local potentials, delta functions, or derivatives of delta functions):

$$\text{Im } V = \frac{\text{Im } V^{(2)}}{m^2} + \frac{\text{Im } V^{(4)}}{m^4} + \dots, \quad (74)$$

where the explicit expressions for $\text{Im } V^{(2)}$ and $\text{Im } V^{(4)}$ are

$$\text{Im } V^{(2)} = -\frac{C_A}{2}\delta^{(3)}(\mathbf{r})\{4 \text{Im } f_1^{\text{pNR}}(1S_0) \\ - 2\mathbf{S}^2[\text{Im } f_1^{\text{pNR}}(1S_0) - \text{Im } f_1^{\text{pNR}}(3S_1)] \\ + 4 \text{Im } f_{\text{EM}}^{\text{pNR}}(1S_0) - 2\mathbf{S}^2[\text{Im } f_{\text{EM}}^{\text{pNR}}(1S_0) \\ - \text{Im } f_{\text{EM}}^{\text{pNR}}(3S_1)]\}, \quad (75)$$

$$\text{Im } V^{(4)} = C_A T_{Sj}^{ij} \nabla_{\mathbf{r}}^i \delta^{(3)}(\mathbf{r}) \nabla_{\mathbf{r}}^j [\text{Im } f_1^{\text{pNR}}(2S+1P_j) \\ + \text{Im } f_{\text{EM}}^{\text{pNR}}(2S+1P_j)] + \frac{C_A}{2} \Omega_{Sj}^{ij} \{\nabla_{\mathbf{r}}^i \nabla_{\mathbf{r}}^j \delta^{(3)}(\mathbf{r})\} \\ \times [\text{Im } g_1^{\text{pNR}}(2S+1S_j) + \text{Im } g_{\text{EM}}^{\text{pNR}}(2S+1S_j)], \quad (76)$$

$$T_{01}^{ij} = \delta_{ij}(2\mathbf{1} - \mathbf{S}^2), \quad (77)$$

$$T_{10}^{ij} = \frac{1}{3}\mathbf{S}^i \mathbf{S}^j, \quad (78)$$

$$T_{11}^{ij} = \frac{1}{2}\epsilon_{kil}\epsilon_{kjl}\mathbf{S}^k \mathbf{S}^l, \quad (79)$$

$$T_{12}^{ij} = \left(\frac{\delta_{ik}\mathbf{S}^k + \delta_{il}\mathbf{S}^k}{2} - \frac{\mathbf{S}^i \delta_{kl}}{3}\right) \left(\frac{\delta_{jk}\mathbf{S}^k + \delta_{jl}\mathbf{S}^k}{2} - \frac{\mathbf{S}^j \delta_{kl}}{3}\right), \quad (80)$$

$$\Omega_{00}^{ij} = \delta_{ij}(2\mathbf{1} - \mathbf{S}^2), \quad \Omega_{11}^{ij} = \delta_{ij}\mathbf{S}^2, \quad (81)$$

and we have omitted the labels singlet and octet in the matching coefficients for simplicity. Note that we use a notation for the matching coefficients similar to the one

used in NRQCD, but this does not imply that the matching coefficients are equal.

The pNRQCD Lagrangian is invariant under charge conjugation plus $1 \leftrightarrow 2$ exchange (82), time reversal (83), and parity (84). In particular singlet, octet, and gluon fields transform under these as

$$S(\mathbf{r}, \mathbf{R}, t) \rightarrow \sigma^2 S(-\mathbf{r}, \mathbf{R}, t)^T \sigma^2, \quad (82)$$

$$O(\mathbf{r}, \mathbf{R}, t) \rightarrow \sigma^2 O(-\mathbf{r}, \mathbf{R}, t)^T \sigma^2,$$

$$A_\mu(\mathbf{R}, t) \rightarrow -A_\mu(\mathbf{R}, t)^T,$$

$$S(\mathbf{r}, \mathbf{R}, t) \rightarrow \sigma^2 S(\mathbf{r}, \mathbf{R}, -t) \sigma^2, \quad (83)$$

$$O(\mathbf{r}, \mathbf{R}, t) \rightarrow \sigma^2 O(\mathbf{r}, \mathbf{R}, -t) \sigma^2,$$

$$A_\mu(\mathbf{R}, t) \rightarrow A^\mu(\mathbf{R}, -t),$$

$$S(\mathbf{r}, \mathbf{R}, t) \rightarrow -S(-\mathbf{r}, -\mathbf{R}, t), \quad (84)$$

$$O(\mathbf{r}, \mathbf{R}, t) \rightarrow -O(-\mathbf{r}, -\mathbf{R}, t),$$

$$A_\mu(\mathbf{R}, t) \rightarrow A^\mu(-\mathbf{R}, t).$$

Singlet- and octet-field transformations may be derived from Eq. (48).

The discrete symmetries constrain the form of the Lagrangian. As an example we observe that the charge conjugate of $\int d^3\mathbf{r} \text{Tr}\{O^\dagger \mathbf{r} \cdot g\mathbf{E} O\}$ is $\int d^3\mathbf{r} \text{Tr}\{O^\dagger O \mathbf{r} \cdot g\mathbf{E}\}$ and therefore only the sum of the two appears in the Lagrangian. For a similar reason the term $\int d^3\mathbf{r} \text{Tr}\{S^\dagger(\mathbf{r} \times \mathbf{p} \cdot g\mathbf{B}) S\}/m$ cannot appear, while the combination $\int d^3\mathbf{r} \text{Tr}\{O^\dagger(\mathbf{r} \times \mathbf{p} \cdot g\mathbf{B}) O - O^\dagger O(\mathbf{r} \times \mathbf{p} \cdot g\mathbf{B})\}/m$ is possible.

As in NRQCD, the form of the pNRQCD Lagrangian may also be constrained by imposing the Poincaré algebra of the generators H , \mathbf{P} , \mathbf{J} , and \mathbf{K} of time translations, space translations, rotations, and Lorentz boosts of the EFT (Brambilla, Gromes, and Vairo, 2003). H is the pNRQCD Hamiltonian. The translation and rotation generators \mathbf{P} and \mathbf{J} may be derived from the pNRQCD Lagrangian or by matching to the NRQCD generators. They are exact because translational and rotational invariance have not been broken in going to the EFT. The Lorentz-boost generators may be obtained by matching to the Lorentz-boost generators of NRQCD. As can be seen from the explicit expressions given by Brambilla, Gromes, and Vairo (2003), they depend on some specific matching coefficient independent of those in the Lagrangian. The tree-level matching may be performed by multipole expanding the NRQCD Lorentz-boost generators and projecting onto singlet and octet two-particles states. Loop corrections can, in principle, be calculated as has been done for the matching coefficients of the pNRQCD Lagrangian.

Imposing the Poincaré algebra on the above generators constrains the form of the pNRQCD Lagrangian. For the constraints on the Lorentz-boost generators, see Brambilla, Gromes, and Vairo (2003). For the Lagrangian, the constraints

$$c_S^{(1,0)} = c_O^{(1,0)} = 1 \quad (85)$$

fix the center-of-mass kinetic energy to $\mathbf{P}_R^2/4m$. The coefficient of the kinetic energy \mathbf{p}^2/m , $c_S^{(1,-2)}$, is not fixed by Poincaré invariance. However, one may argue that because no other momentum-dependent operator than the kinetic energy of NRQCD, $-\psi^\dagger \nabla^2/(2m)\psi + \chi^\dagger \nabla^2/(2m)\chi$, may contribute to the kinetic energy of pNRQCD, the coefficients $c_S^{(1,0)}$ and $c_S^{(1,-2)}$ have to be equal. It follows then that $c_S^{(1,-2)}=1$ (analogously for $c_O^{(1,-2)}$).¹⁰ In the singlet- and octet-potential sectors we obtain

$$\frac{V_{LS,CM}}{V^{(0)'}} = -\frac{1}{2r}, \quad V_{L^2,CM} + \frac{rV^{(0)'}}{2} = 0, \quad (86)$$

$$V_{\mathbf{p}^2,CM} + V_{L^2,CM} + \frac{V^{(0)'}}{2} = 0,$$

where $V' = dV/dr$. We shall come back to the relations between the singlet potentials in the strong-coupling regime in Sec. VII.E.2. Finally, in the singlet-octet and octet-octet sectors of the Lagrangian, the chromoelectric fields are constrained to enter in the combination

$$\mathbf{r} \cdot \left(g\mathbf{E} + \frac{1}{2} \left\{ \frac{\mathbf{P}_R}{2m} \times, g\mathbf{B} \right\} \right), \quad (87)$$

i.e., as in the Lorentz force. Further constraints can be found in the article by Brambilla, Gromes, and Vairo (2003).

D. Feynman rules

The Feynman rules of pNRQCD for the static limit were given by Brambilla *et al.* (2000) in terms of the time variable and background gluon fields. However, for computations in pNRQCD using Feynman diagrams, it is sometimes more useful to consider the Feynman rules in US momentum space (even if preserving the relative distance \mathbf{r} between the heavy quarks in position space). The propagator of the singlet is

$$\frac{i}{E - h_s}. \quad (88)$$

This expression contains subleading terms in the velocity expansion. In order to have homogeneous power counting, it is convenient to expand it about the Coulomb Green's function G_c defined in Fig. 5, which scales as $1/mv^2$, and similarly for the octet. The complete set of Feynman rules at the order displayed in Eq. (60) is shown in Fig. 5.

¹⁰One may also obtain $c_S^{(1,-2)}=1$ by a direct nonperturbative matching computation as done by Brambilla, Pineda, *et al.* (2001). The relevant steps of that calculation are reproduced in Eqs. (270)–(272). The kinetic-energy operator may be read from the ratio of the $1/m$ Green's function (272) and the zeroth-order one (270).

$$\text{---} = -iG_c(E) = \frac{i}{E - h_s^{(0)}} = \frac{i}{E - \mathbf{p}^2/m - C_F \alpha_s/\tau}$$

$$\text{---} \equiv \delta V_s = -i\delta V_s$$

$$\text{---} \equiv \delta V_o = -i\delta V_o$$

$$\text{---} = -iG_c^o(E)\delta_{ab} = \frac{i\delta_{ab}}{E - h_o^{(0)}} = \frac{i\delta_{ab}}{E - \mathbf{p}^2/m - (1/(2N_c))\alpha_s/\tau}$$

$$\text{---} = -gV_A \sqrt{\frac{T_F}{N_c}} \delta_{ca} \boldsymbol{\tau} P^0$$

$$\text{---} = gV_A \sqrt{\frac{T_F}{N_c}} \delta_{ca} \mathbf{r} \cdot \mathbf{P}$$

$$\text{---} = -ig^2 V_A \sqrt{\frac{T_F}{N_c}} f_{abc}$$

$$\text{---} = -g \frac{V_B}{2} d^{abc} \boldsymbol{\tau} P^0$$

$$\text{---} = g \frac{V_B}{2} d^{abc} \mathbf{r} \cdot \mathbf{P}$$

$$\text{---} = -ig^2 \frac{V_B}{2} d^{abc} f_{cde} \mathbf{r}$$

$$\text{---} = g f^{abc}$$

FIG. 5. Propagators and vertices of the pNRQCD Lagrangian (60). Dashed lines represent longitudinal gluons and curly lines transverse gluons. P^μ represents the gluon incoming momentum.

E. Matching: diagrammatic approach

We discuss here how the matching between NRQCD and pNRQCD [in the formulation of Eq. (52)] within a diagrammatic approach is made along the lines of that shown in Pineda and Soto (1998a, 1998b, 1999). This procedure is especially convenient for obtaining the potentials order by order in α_s since the whole technology of Feynman diagrams can be used.

A practical way of obtaining the matching coefficients of pNRQCD is by enforcing that two- and four-fermion Green's functions with arbitrary US external gluons be equal to those of NRQCD at any desired order in E/k . It is convenient to expand the energy of the external quark and the energy and momenta of the US gluons around zero before carrying out the loop integrals so that the integrals become homogeneous in the soft scale and hence are easier to evaluate. This may produce IR divergences which are most conveniently (but not necessarily) regulated in DR in the same way as the UV divergences are. Since the IR behavior of NRQCD and pNRQCD is the same, these divergences will cancel out in the matching provided that the same IR regulator is used in both theories. The UV divergences of NRQCD must be renormalized in the MS scheme if we want to use the matching coefficients of the NRQCD Lagrangian computed themselves in this scheme. We still have a choice in the renormalization scheme of pNRQCD. However, it is most advantageous to again use the MS scheme. Indeed, with this choice we can blindly subtract

any divergence regardless of whether it is UV or IR in the matching calculation. For the UV divergences of NRQCD and pNRQCD, this just corresponds to our choice of scheme, and for the IR divergences this is possible since as long as we use the same treatment in both theories, their IR behavior is the same. This allows us to set integrals with no scale equal to zero.

Notice that we demand that off-shell Green's functions in NRQCD and pNRQCD be equal and not on-shell Green's functions (or on-shell matrix elements) as is usual in many matching calculations, in particular, in matching calculations from QCD to NRQCD. This is due to the fact that we are eventually interested in bound states, and particles in a bound state are typically off shell. More precisely, the equations of motion at lowest order are not those of the free particles. The equations of motion of pNRQCD (with potential terms included) or local-field redefinitions may be consistently used later on to remove time derivatives in higher-order terms and to write the pNRQCD Lagrangian in a standard form, in the philosophy advocated by Scherer and Fearing (1995) [see also Balzereit (1999)]. It has actually been checked by Pineda and Soto (1999)¹¹ that this pro-

¹¹However, there is still some freedom in the choice of the wave-function field due to time-independent unitary transformations which commute with the leading terms in the pNRQCD Lagrangian. Therefore, in general, it is not expected that the standard forms of the pNRQCD Lagrangian calcu-

cedure produces gauge-independent results at $\mathcal{O}(m\alpha_s^4)$ in the computation of the positronium spectrum.

The remaining important step for carrying out the matching efficiently is the use of static (HQET) propagators for the fermions. This can be justified as follows. When $p^0 \sim |\mathbf{p}|$ we are in the kinematical region we wish to integrate out, and the cutoffs of both NRQCD and pNRQCD ensure that the kinetic term $\mathbf{p}^2/2m$ be sub-leading with respect to the energy irrespective of the value of $|\mathbf{p}|$. This fact is not automatically implemented in DR. When DR is used, the correct UV behavior of NRQCD is only obtained when expanding about the static propagator. When $p^0 \sim \mathbf{p}^2/2m$, we are in a kinematical region which still exists in pNRQCD, and it should not be integrated out. The simplest way to avoid this kinematical region is, again, by expanding the kinetic term. After all these simplifications the computations in the NRQCD side reduce to diagrams with only one scale inside loops. In short, one would have (where E generically denotes the external momentum or the kinetic term \mathbf{p}^2/m)

$$\int d^D q f(q, k, E) = \int d^D q f(q, k, 0) + \mathcal{O}\left(\frac{E}{k}\right). \quad (89)$$

Now we are in a position to prove that no pNRQCD diagram containing a loop contributes to the matching calculation. Consider first the two-fermion Green's function with an arbitrary number of US legs. For potential terms to contribute at least a four-fermion Green's function are needed and hence we only care about US gluons. If we put a momentum $\sim |\mathbf{p}|$ in the fermion line, it cannot flow out through any external US gluon line (by definition of US). Thus it must flow through the fermion line, which is a series of static propagators insensitive to the momentum flowing through them. Upon expanding about external fermion energies and external energies and momenta of the US gluons there is no scale left in any of the integrals and therefore any loop contribution vanishes. In fact, exactly the same argument can be used for the NRQCD calculation. We conclude that the terms bilinear in fermions are exactly the same in NRQCD and pNRQCD. However, we have to keep in mind that the latter (by definition) must be understood as containing ultrasoft gluons only.

Consider next the four-fermion Green's function in pNRQCD containing several potential terms but no US gluons. Since no energy can flow through the potentials and the static propagators are insensitive to the momentum, upon expanding about the US external energy, the integrals over internal energies have no scale. However, these integrals have IR (pinch) singularities which are not regulated by standard DR. How to rigorously deal with them is discussed in Sec. IV.E.1. Since the IR behavior of pNRQCD and NRQCD is the same, the same

lated with different gauges coincide, but that they are only related by one such unitary transformation. This explains the different expressions for the potential that one may find in the literature but which still lead to the same physics.

kind of integrals appears in the NRQCD calculation. If we consistently set them to zero, we obtain the correct potential terms. It is important to keep in mind that the Wilson coefficients compensate the different UV behavior of the effective theory (pNRQCD) with respect to that of the more “fundamental” theory (NRQCD). Hence they are not sensitive to the details of the IR behavior, which legitimates the prescription above. Then any loop diagram in pNRQCD with no US gluons can be set to zero. This still holds if an arbitrary number of US gluon lines is included in the diagram. Indeed, any potential line in the diagram may now also contain US momenta from the gluon lines. These, however, can be expanded about zero since they are (by definition) much smaller than the momentum transfer in the potential. Hence the integrals over US gluon energies and momenta contain no scale (again upon expanding the US external energy in the fermion static propagators) and can also be set to zero. In short, loops in pNRQCD will have the following structure in general:

$$\int d^D q f(q, E) = \int d^D q f(q, 0) + \mathcal{O}\left(\frac{E}{k}\right) = 0. \quad (90)$$

In brief, we can directly identify the potential terms from a calculation in NRQCD. We stress again the similarity in the procedure with the matching between QCD and NRQCD as carried out before. The potential terms in pNRQCD play the role of Wilson coefficients in the matching procedure. As a summary, the final set of rules is the following:

- Compute (off-shell) NRQCD Feynman diagrams within an expansion in α_s , $1/m$, and E . In case loops appear, they have to be computed using static propagators for the heavy quark and antiquark, which makes the integrals depend on k only.
- Match the resulting expression to the *tree-level* expression in pNRQCD (i.e., the potentials that appear in the pNRQCD Lagrangian) to the required order in α_s , $1/m$, and E .
- Isolate pinch singularities, if they appear, in expressions which are identical to those which appear in the pNRQCD computation and set them to zero. Or, alternatively, one may just subtract the pNRQCD diagrams with the same pinch singularity, as discussed in Sec. IV.E.1.

Let us mention here that when this procedure is used to match local NRQCD four-fermion operators, these do not get any loop correction. Indeed, due to the use of HQET propagators, all NRQCD integrals become scaleless and hence vanish. We often say that they are *inherited* in pNRQCD.

A word of caution is necessary concerning the procedure above. It relies heavily on the fact that there are no further scales other than m , k , and E . If, for instance, an energy scale m' such that $E \ll m' \sim k \ll m$ enters the picture, it would be convenient to take $v_{us} \ll m'$ rather than $v_{us} \ll k$ and hence $v_p \ll \sqrt{mm'}$ rather than $v_p \ll m$. Then, in the matching calculation we should also integrate out

quarks with energy $\sim m'$ and three-momentum $\sim \sqrt{mm'}$, which cannot be done anymore in the static approximation. A careful analysis of the integration regions along the lines of the threshold expansion discussed below should be carried out in this case. Incidentally, this situation is of physical relevance for the $Y(1S)$ system, where the charm-quark mass plays the role of m' .

It is also possible to perform the matching to pNRQCD using the threshold expansion (Beneke and Smirnov, 1998). This procedure has been followed by several groups (Beneke *et al.*, 1999; Kniehl *et al.*, 2002a, 2002b). Typically (although not always), the procedure consists of taking one specific diagram of NRQCD and splitting it into the different existing regions of momenta. According to this terminology, the modes (and correspondingly the regions of momenta) that appear in NRQCD are the following:

- (i) *Soft modes.* Quarks and gluons with energy and three-momenta of $\mathcal{O}(mv)$ (the quarks are off-shell in this situation).
- (ii) *Potential modes.* Quarks and gluons with energy of $\mathcal{O}(mv^2)$ and three-momenta of $\mathcal{O}(mv)$ (the gluons are off-shell in this situation).
- (iii) *US modes.* Quarks and gluons with energy and three-momenta of $\mathcal{O}(mv^2)$ (in practice, it does not seem there are quarks in this situation).

Integrating out soft modes and potential gluons corresponds to matching NRQCD to pNRQCD. In some cases, it is customary to perform the matching using (free) on-shell quarks. This has the consequence that loops in pNRQCD do not vanish (since the energy is not left as a free parameter in which one can expand) and have to be subtracted accordingly. In addition, the on-shell condition may set to zero some terms in the (off-shell) potential. When these terms enter into a NRQCD subdiagram of a higher-loop matching calculation, they may give rise to new contributions to the potential due to quark potential loops. This never occurs if the procedure described above is used. In any case, the potentials obtained by using different methods can be related to each other by unitary transformations.

1. Pinch singularities

Let us now discuss the issue of the so-called pinch singularity. We illustrate this discussion with the diagram (in the Coulomb gauge) in Fig. 6. Actually, such a diagram appears in the computation of the positronium spectrum at $\mathcal{O}(m\alpha^5)$ carried out in the article by Pineda and Soto (1999). The one-loop integral of this diagram reads

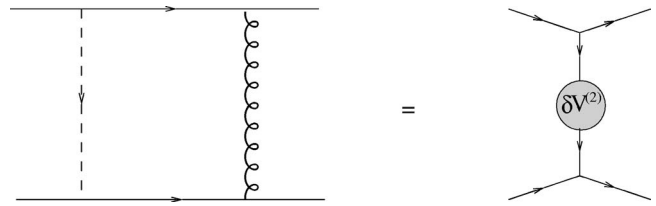


FIG. 6. Matching between NRQCD and pNRQCD without considering pinch singularities. The dashed and curly lines represent the longitudinal and transverse gluon exchanges, respectively.

$$I \sim \int \frac{d^D q}{(2\pi)^D} \frac{1}{(\mathbf{q}-\mathbf{k})^2} \frac{1}{q^0 + i\epsilon} \frac{1}{-q^0 + i\epsilon} \frac{1}{q^2} \left(\delta_{ij} - \frac{\mathbf{q}^i \mathbf{q}^j}{\mathbf{q}^2} \right) \times (\dots), \quad (91)$$

where (\dots) stands for a q_0 -independent term. We see that it has two singularities at $q_0 = \pm i\epsilon$. This is usually referred to as the pinch singularity. The rigorous procedure employed to eliminate the pinch singularity comes from the matching computation. Previously we mentioned that loops in pNRQCD could be set to zero as far as the matching computation was concerned, but that required that the same kind of pinch-singularity diagrams were set to zero in NRQCD. The implementation of this idea can be translated into a simple solution: since for any NRQCD diagram with a pinch singularity there must be a pNRQCD diagram with the same pinch singularity, just subtract it (see Fig. 7). Therefore the actual integral to be computed is

$$I \sim \int \frac{d^D q}{(2\pi)^D} \frac{1}{(\mathbf{q}-\mathbf{k})^2} \frac{1}{q^0 + i\epsilon} \frac{1}{-q^0 + i\epsilon} \left(\frac{1}{q^2} + \frac{1}{\mathbf{q}^2} \right) \times \left(\delta_{ij} - \frac{\mathbf{q}^i \mathbf{q}^j}{\mathbf{q}^2} \right) (\dots). \quad (92)$$

We can see how the pinch singularity disappears, and the resulting integral provides new contributions to the potential only.

Pinch singularities also appear in computations using the threshold expansion. We have seen here that understanding the pinch singularities within the EFT framework provides a consistent prescription to eliminate them in each case.

2. Potentials

The general structure of the potentials has been given in Sec. IV.C. We shall focus on the equal-mass case, Eq. (72). By dimensional analysis, $V^{(1)}$ scales like $1/r^2$, $V_{\mathbf{p}^2}^{(2)}$ like $1/r$, $V_r^{(2)}$ like $1/r^3$ or $\delta^{(3)}(\mathbf{r})$, and so on. They are

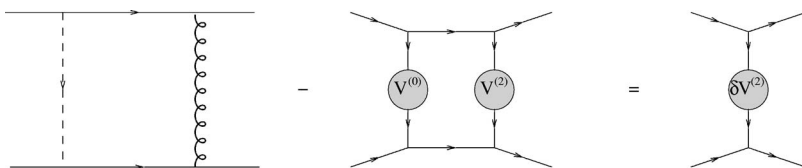


FIG. 7. Matching between NRQCD and pNRQCD taking into account pinch singularities. In pNRQCD the loop regulates the pinch singularity.

$$V_s^{(0)}(r) = -C_F \frac{\alpha_{V_s}(r)}{r}, \quad (93)$$

$$V_s^{(1)}(r) = -\frac{C_F C_A D_s^{(1)}}{2r^2}, \quad (94)$$

$$V_{\mathbf{p}^2, s}^{(2)}(r) = -C_F D_{1, s}^{(2)}, \quad (95)$$

$$V_{\mathbf{L}^2, s}^{(2)}(r) = \frac{C_F D_{2, s}^{(2)}}{2} \frac{1}{r}, \quad (96)$$

$$V_{r, s}^{(2)}(r) = \pi C_F D_{d, s}^{(2)} \delta^{(3)}(\mathbf{r}), \quad (97)$$

$$V_{S^2, s}^{(2)}(r) = \frac{4\pi C_F D_{S^2, s}^{(2)}}{3} \delta^{(3)}(\mathbf{r}), \quad (98)$$

$$V_{LS, s}^{(2)}(r) = \frac{3C_F D_{LS, s}^{(2)}}{2} \frac{1}{r^3}, \quad (99)$$

$$V_{S_{12}, s}^{(2)}(r) = \frac{C_F D_{S_{12}, s}^{(2)}}{4} \frac{1}{r^3}, \quad (100)$$

where α_{V_s} and the various D 's depend logarithmically on r and the renormalization scale ν_{pNR} . In order to obtain the spectrum at order $m\alpha_s^4$, α_{V_s} has to be calculated to order α_s^3 (two loops), $V_s^{(1)}$ to order α_s^2 (one loop), and the remaining potentials to order α_s (tree level). They are

$$\alpha_{V_s} = \alpha_s(r) \left\{ 1 + (a_1 + 2\gamma_E \beta_0) \frac{\alpha_s(r)}{4\pi} + \left[\gamma_E (4a_1 \beta_0 + 2\beta_1) + \left(\frac{\pi^2}{3} + 4\gamma_E^2 \right) \beta_0^2 + a_2 \right] \frac{\alpha_s^2(r)}{16\pi^2} \right\}, \quad (101)$$

$$D_s^{(1)} = \alpha_s^2(r),$$

$$D_{1, s}^{(2)} = D_{2, s}^{(2)} = D_{d, s}^{(2)} = D_{S^2, s}^{(2)} = D_{LS, s}^{(2)} = D_{S_{12}, s}^{(2)} = \alpha_s(r). \quad (102)$$

a_1 was computed by Fischler (1977) and a_2 by Peter (1997) and Schröder (1999b). If one wishes to have the spectrum to one order higher, namely, $m\alpha_s^5$, all these potentials must be calculated to one more power in α_s . For α_{V_s} , only the logarithmic contributions are known (Brambilla *et al.*, 1999b; Kniehl and Penin, 1999) [Padé approximant (Chishtie and Elias, 2001) and renormalon-based (Pineda, 2001) estimates are also available]. $V_s^{(1)}$ was calculated by Kniehl, Penin, Steinauser, *et al.* (2002) (the logarithmic corrections were computed by Brambilla *et al.*, 1999a and Kniehl and Penin, 1999) and the complete $V_s^{(2)}$ have been computed over the years (Buchmüller *et al.*, 1981; Gupta and Radford, 1981, 1982; Pantaleone *et al.*, 1986; Titard and Yndurain, 1994; Brambilla *et al.*, 1999a; Pineda and Soto, 1999; Manohar and Stewart, 2000b; Kniehl *et al.*, 2002a) and can be found in the article by Kniehl *et al.* (2002a). Several com-

ments are in order concerning these calculations.

(1) The potentials in the matching calculation appear naturally in momentum space, and so they are given in many of the references above. The real-space potentials, which are better suited for bound-state calculations, are obtained by Fourier transforming the momentum-space potentials. At lower orders, it is enough to take the Fourier transform in three dimensions in the sense of distributions (Titard and Yndurain, 1994). At higher orders, it must be taken in d dimensions, as discussed below.

(2) In different papers, the results displayed for each of the potentials may vary, even if the same basis (72) is used. This does not mean *a priori* that there are inconsistencies. The basis (72) is overcomplete and hence apparently different results may be related to each other by unitary transformations. In particular, $V_s^{(1)}$ can be totally reshuffled into $1/m^2$ potentials.

(3) In earlier papers, the potentials were calculated directly from QCD without expanding in the kinetic energy. In that case there are contributions from the pNRQCD side to the matching calculation due to the fact that the kinetic term in the pNRQCD Hamiltonian cannot be expanded anymore. In this framework, the integrals involved in the calculation have more than one scale and are harder to evaluate.

(4) In higher-order calculations, quantum-mechanical perturbation theory requires regularization and renormalization. The UV divergences are renormalized by local potentials inherited from NRQCD and the scale dependence is compensated by the one in the NRQCD matching coefficients. In order to use the NRQCD matching coefficients obtained in Sec. II.D, the potentials must be kept in d dimensions. This is not important as far as the soft or US factorization is concerned (it amounts to a change of subtraction scheme), but it becomes when the calculation is sensitive to divergences due to the hard or potential factorization. This occurs at order $m\alpha_s^6$ for the spectrum and in $\mathcal{O}(\alpha_s^2)$ corrections for the current. Note that any loop correction to a given (e.g., Coulomb) potential slightly changes its functional form [it gets multiplied by $(r\nu)^{(4-D)}$ for each loop]. The expressions for the potentials in three dimensions calculated at higher orders display small logarithms, which eventually cancel out in the full calculation, in addition to the large logarithms, which eventually become $\ln \alpha_s$, as discussed by Kniehl *et al.* (2002a) [note that in Brambilla *et al.* (1999a) only the large logarithms were displayed].

(5) The octet potential is also known at two-loop accuracy (Kniehl *et al.*, 2005),

$$V_o^{(0)}(r) \equiv \left(\frac{C_A}{2} - C_F \right) \frac{\alpha_{V_o}(r)}{r},$$

$$\alpha_{V_o}(r) = \alpha_{V_s}(r) - \left(\frac{3}{4} - \frac{\pi^2}{16} \right) C_A^2 \alpha_s^3 + \mathcal{O}(\alpha_s^4). \quad (103)$$

(6) At order $m\alpha_s^5$ for the spectrum and at $\mathcal{O}(\alpha_s^3)$ for the current US loops start to contribute. This implies that $V_A(r)$ is also needed. At tree level we have

$$V_A(r) = V_B(r) = 1. \quad (104)$$

(7) For the case $m_1 \neq m_2$, the $1/m^2$ potentials have only been calculated in the scheme described in Sec. IV.E for QED (Pineda and Soto, 1999). Earlier calculations for both QCD (Gupta and Radford, 1982) and QED (Gupta *et al.*, 1989) exist, which have been carried out by matching directly the fundamental theory to a quantum-mechanical Hamiltonian.

(8) RG-improved expressions for the potential can also be obtained. They are discussed in Sec. IV.H.

Finally, we would like to briefly discuss the matching of currents and the imaginary pNRQCD potential. Integrating out the soft scale when matching local currents produces scaleless integrals, which are zero in DR. This means that the matching coefficient remains the same at the matching scale. If we take the electromagnetic-vector current as an example, the matching condition is $b_{1,\text{pNR}}^v(\nu_p, \nu_{us} = \nu_s) = b_{1,\text{NR}}^v(\nu_p, \nu_s)$. In the case of $b_{1,\text{NR}}^v$, only a dependence on ν_p appears (at least at low orders). An equivalent discussion applies to the imaginary terms of the Lagrangian for which the general matching condition $\text{Im} f^{\text{NR}}(\nu_p, \nu_{us} = \nu_s) = \text{Im} f(\nu_p, \nu_s)$ holds. Nevertheless, one should keep in mind that the expressions for the matching coefficients will change once their running is considered (see Sec. IV.H).

F. Matching: Wilson-loop approach

We discuss here another way to perform the matching to pNRQCD which we sometimes denote as Wilson-loop matching. With respect to the previously discussed procedure, it is characterized by the following points.

- It is done in coordinate space.
- It is done with the pNRQCD Lagrangian in the form of Eq. (60). This means that the degrees of freedom that appear most naturally in the pNRQCD part of the matching are singlet and octet fields.
- As a consequence of (b), only one time appears in the computation.
- The gluon fields appear in the NRQCD part of the matching procedure in terms of Wilson-loop amplitudes. Therefore the formulation will be explicitly gauge invariant at each step.
- Gauge-invariant expressions can be obtained for the potentials that encode all the corrections in $\alpha_s(1/r)$ for a given order in $1/m$ and the multipole expansion.

The results obtained within this matching procedure will be equivalent (up to field redefinitions) to those obtained in the previous section.

From points (d) and (e) above, it is clear that the Wilson-loop matching is well suited for generalization to nonperturbative cases. Therefore it provides us with a bridge between the weak-coupling matching procedure of this section and the strong-coupling one of Sec. VII.

There, the language will be exactly the one introduced here in the framework of perturbative QCD.

In the following, we define our interpolating fields, set the basis of the matching, and illustrate the procedure by discussing the static matching up to and including order r^2 in the multipole expansion. We closely follow the work of Brambilla *et al.* (2000), to which we refer the reader for more details of the original derivation.

1. Interpolating fields

Our aim is to match, in coordinate space, amplitudes defined in terms of the fields of NRQCD with amplitudes defined in terms of the fields that appear in the pNRQCD Lagrangian (60), i.e., A_μ , S , and O^a fields. Therefore we need to identify some interpolating fields in NRQCD that have the same quantum numbers and the same transformation properties as S and O^a . The correspondence is not one to one. Given an interpolating field in NRQCD there are an infinite number of combinations of singlet and octet operators with US fields that have the same quantum numbers and therefore a nonvanishing overlap with the NRQCD operator. Fortunately, the operators in pNRQCD can be organized according to the counting of the multipole expansion. For instance, for the singlet we have

$$\begin{aligned} & \chi^\dagger(\mathbf{x}_2, t) \phi(\mathbf{x}_2, \mathbf{x}_1; t) \psi(\mathbf{x}_1, t) \\ & \rightarrow \sqrt{Z_s^{(0)}(r)} S(\mathbf{r}, \mathbf{R}, t) \\ & \quad + \sqrt{Z_{E,s}(r)} r\mathbf{r} \cdot g\mathbf{E}^a(\mathbf{R}, t) O^a(\mathbf{r}, \mathbf{R}, t) + \dots, \end{aligned} \quad (105)$$

and for the octet

$$\begin{aligned} & \chi^\dagger(\mathbf{x}_2, t) \phi(\mathbf{x}_2, \mathbf{R}; t) T^a \phi(\mathbf{R}, \mathbf{x}_1; t) \psi(\mathbf{x}_1, t) \\ & \rightarrow \sqrt{Z_o^{(0)}(r)} O^a(\mathbf{r}, \mathbf{R}, t) \\ & \quad + \sqrt{Z_{E,o}(r)} r\mathbf{r} \cdot g\mathbf{E}^a(\mathbf{R}, t) S(\mathbf{r}, \mathbf{R}, t) + \dots, \end{aligned} \quad (106)$$

where

$$\phi(\mathbf{y}, \mathbf{x}; t) \equiv P \exp \left\{ i \int_0^1 ds (\mathbf{y} - \mathbf{x}) \cdot g\mathbf{A}(\mathbf{x} - s(\mathbf{x} - \mathbf{y}), t) \right\}. \quad (107)$$

The arrows are a reminder that the two operators act on different Hilbert spaces and that the equalities hold only inside Green's functions. The factors Z are normalization factors. From Eqs. (105) and (106) it follows that the operators on the left-hand side overlap at leading order in the multipole expansion with the singlet and octet fields, respectively.

The matching for the octet in Eq. (106) does not make use of a gauge-invariant operator. In a perturbative matching this is not problematic since V_o is gauge invariant order by order in α_s . However, if one aims at taking advantage of nonperturbative techniques, it is preferable to work with a manifestly gauge-invariant quantity. The simplest solution consists in replacing the T^a color matrix on the left-hand side of Eq. (106) by a local gluonic operator $H^a(\mathbf{R}, t) T^a$ with the right transformation properties, e.g., $g\mathbf{B}^a(\mathbf{R}, t) T^a$. All $H^a(\mathbf{R}, t) T^a$ with the right

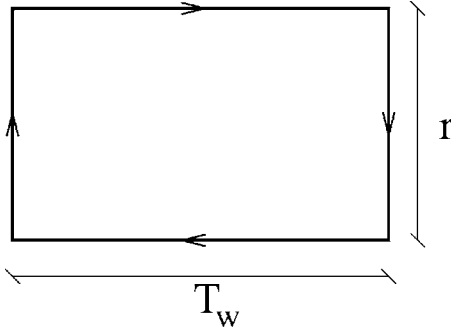


FIG. 8. A graphical representation of the static Wilson loop. We adopt the convention that the time direction is from the left to the right. Therefore the quark trajectories are represented by horizontal lines and the equal-time end-point Wilson lines by shorter vertical lines.

transformation properties will give the same potential in the weak-coupling regime corresponding to the perturbative octet potential. In the strong-coupling regime, where octet quark-antiquark fields do not exist as independent degrees of freedom, they identify different degrees of freedom and hence different potentials, corresponding to the different symmetry properties of H^a . We come back to this in full detail in Sec. VI.

2. Matching at $\mathcal{O}(r^0, 1/m^0)$

In order to get $V_s^{(0)}$ and $Z_s^{(0)}$, we choose the following Green's function in NRQCD (Susskind, 1977; Brown and Weisberger, 1979):

$$G_{\text{NRQCD}} = \langle \text{vac} | \chi^\dagger(x_2) \phi(x_2, x_1) \psi(x_1) \psi^\dagger(y_1) \phi(y_1, y_2) \chi(y_2) | \text{vac} \rangle = \delta^3(\mathbf{x}_1 - \mathbf{y}_1) \delta^3(\mathbf{x}_2 - \mathbf{y}_2) \langle W_\square \rangle + \dots, \quad (108)$$

where the dots stand for higher-order corrections in the $1/m$ expansion. The quantity W_\square is the rectangular Wilson loop (Wilson, 1974) with corners $x_1 = (T_W/2, \mathbf{r}/2)$, $x_2 = (T_W/2, -\mathbf{r}/2)$, $y_1 = (-T_W/2, \mathbf{r}/2)$, and $y_2 = (-T_W/2, -\mathbf{r}/2)$:

$$W_\square \equiv P \exp \left\{ -ig \oint_{r \times T_W} dz^\mu A_\mu(z) \right\}. \quad (109)$$

A graphical representation is given in Fig. 8. We also define

$$\langle \dots \rangle \equiv \langle \text{vac} | \text{Tr} \{ \dots \} | \text{vac} \rangle = \int DADqD\bar{q} e^{-iS^{(0)}} \text{Tr} \{ \dots \}, \quad (110)$$

where $S^{(0)}$ is the pure Yang-Mills plus light-quark action of QCD and the path integral is over all light fields.

Equation (105) states that the leading overlap of the Green's function (108) is with the singlet propagator in pNRQCD. Indeed, in pNRQCD we get in the static limit and at the zeroth order in the multipole expansion:

$$G_{\text{pNRQCD}} = Z_s^{(0)}(r) \delta^3(\mathbf{x}_1 - \mathbf{y}_1) \delta^3(\mathbf{x}_2 - \mathbf{y}_2) e^{-iT_W V_s^{(0)}(r)}. \quad (111)$$

In order to single out the soft scale, we consider the large T_W limit of the Wilson loop (equivalent to setting $E \rightarrow 0$):

$$\frac{i}{T_W} \ln \langle W_\square \rangle = u_0(r) + i \frac{u_1(r)}{T_W} + \mathcal{O}\left(\frac{1}{T_W^2}\right) \quad \text{for } T_W \rightarrow \infty, \quad (112)$$

then from the matching condition $G_{\text{NRQCD}} = G_{\text{pNRQCD}}$ we obtain

$$V_s^{(0)}(r) \equiv -C_F \frac{\alpha_s(r)}{r} = u_0(r), \quad (113)$$

$$\ln Z_s^{(0)}(r) = u_1(r). \quad (114)$$

The matching does not rely on any perturbative expansion in α_s . However, since we are concerned with the weak-coupling situation, the quantities on the right-hand side of Eqs. (113) and (114) can be evaluated expanding order by order in α_s . At LO in α_s we have

$$V_s^{(0)}(r) = -C_F \frac{\alpha_s}{r} \quad \text{or } \alpha_V = \alpha_s, \quad (115)$$

$$Z_s^{(0)}(r) = N_c. \quad (116)$$

In order to get $V_o^{(0)}$ and $Z_o^{(0)}$ one proceeds in a similar way. We choose the NRQCD Green's function:

$$G_{\text{NRQCD}}^{ab} = \langle \text{vac} | \chi^\dagger(x_2) \phi\left(\mathbf{x}_2, \frac{\mathbf{x}_1 + \mathbf{x}_2}{2}; \frac{T_W}{2}\right) T^a \times \phi\left(\frac{\mathbf{x}_1 + \mathbf{x}_2}{2}, \mathbf{x}_1; \frac{T_W}{2}\right) \psi(x_1) \psi^\dagger(y_1) \times \phi\left(\mathbf{y}_1, \frac{\mathbf{y}_1 + \mathbf{y}_2}{2}; -\frac{T_W}{2}\right) T^b \phi\left(\frac{\mathbf{y}_1 + \mathbf{y}_2}{2}, \mathbf{y}_2; -\frac{T_W}{2}\right) \times \chi(y_2) | \text{vac} \rangle = \delta^3(\mathbf{x}_1 - \mathbf{y}_1) \delta^3(\mathbf{x}_2 - \mathbf{y}_2) \langle T^a W_\square T^b \rangle + \dots, \quad (117)$$

where in the last line the color matrices are understood as inserted in the static Wilson loop at the points $(\mathbf{R}, T_W/2)$ and $(\mathbf{R}, -T_W/2)$. The dots stand for higher-order corrections in the $1/m$ expansion.

Equation (106) states that the leading overlap of the Green's function (117) is with the octet propagator in pNRQCD. Indeed, in pNRQCD we obtain in the static limit and at zeroth order in the multipole expansion

$$G_{\text{pNRQCD}}^{ab} = Z_o^{(0)}(r) \delta^3(\mathbf{x}_1 - \mathbf{y}_1) \delta^3(\mathbf{x}_2 - \mathbf{y}_2) e^{-iT_W V_o^{(0)}(r)} \times \langle \phi_{ab}^{\text{adj}}(T_W/2, -T_W/2) \rangle, \quad (118)$$

where the Wilson line,

$$\begin{aligned} \phi(T_W/2, -T_W/2) &\equiv \phi(T_W/2, \mathbf{R}, -T_W/2, \mathbf{R}) \\ &= P \exp \left\{ -ig \int_{-T_W/2}^{T_W/2} dt A_0(\mathbf{R}, t) \right\}, \end{aligned}$$

is evaluated in the adjoint representation. As in the singlet case, we define

$$\begin{aligned} \frac{i}{T_W} \ln \frac{\langle T^a W_{\square} T^b \rangle}{\langle \phi_{ab}^{\text{adj}}(T_W/2, -T_W/2) \rangle} \\ = v_0(r) + i \frac{v_1(r)}{T_W} + \mathcal{O}\left(\frac{1}{T_W^2}\right) \quad \text{for } T_W \rightarrow \infty. \end{aligned} \quad (119)$$

From the matching condition $G_{\text{NRQCD}}^{ab} = G_{\text{pNRQCD}}^{ab}$ we obtain

$$V_o^{(0)}(r) \equiv \left(\frac{C_A}{2} - C_F \right) \frac{\alpha_{V_o}(r)}{r} = v_0(r), \quad (120)$$

$$\ln Z_o^{(0)}(r) = v_1(r). \quad (121)$$

Again, the formulas above do not rely on any expansion in α_s . However, in the weak-coupling situation, the quantities on the right-hand sides of Eqs. (120) and (121) can be expanded order by order in α_s . At LO in α_s we obtain

$$V_o^{(0)}(r) = \left(\frac{C_A}{2} - C_F \right) \frac{\alpha_s}{r} \quad \text{or } \alpha_{V_o} = \alpha_s, \quad (122)$$

$$\ln Z_o^{(0)}(r) = T_F. \quad (123)$$

Note that, despite the octet matching procedure being gauge dependent, the octet static potential obtained in this way is not at any finite order in perturbation theory (it corresponds to the pole of the octet static propagator). All the gauge dependence goes into the normalization factor $Z_o^{(0)}$. In this respect, it is worthwhile to observe that the string $\langle \phi_{ab}^{\text{adj}}(T_W/2, -T_W/2) \rangle$ does not give contributions to the potential at any finite order in perturbation theory, but it does to $Z_o^{(0)}$.

3. Matching at $\mathcal{O}(r^1, 1/m^0)$ and $\mathcal{O}(r^2, 1/m^0)$

At $\mathcal{O}(r)$, there are no additional contributions to the singlet and octet matching potentials and to the normalization factors. At this order in the multipole expansion one finds V_A and V_B . In the weak-coupling regime at LO in α_s they are

$$V_A(r) = 1, \quad V_B(r) = 1. \quad (124)$$

At $\mathcal{O}(r^2)$, one finds the next-to-leading contributions to the singlet and octet static potentials and to the singlet static normalization factor.

The NLO correction in the multipole expansion to the singlet static propagator (111) is given by (see Fig. 9)

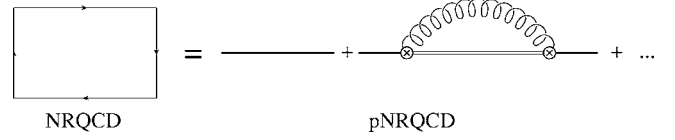


FIG. 9. The matching of $V_s^{(0)}$ and $Z_s^{(0)}$ at next-to-leading order (NLO) in the multipole expansion. On the left-hand side is the Wilson loop in NRQCD, on the right-hand side are the pNRQCD propagators. The first and second diagrams on the right-hand side symbolically represent the first and second terms in Eq. (125).

$$\begin{aligned} G_{\text{pNRQCD}} &= Z_s^{(0)}(r) \delta^3(\mathbf{x}_1 - \mathbf{y}_1) \delta^3(\mathbf{x}_2 - \mathbf{y}_2) e^{-iT_W V_s^{(0)}(r)} \\ &\times \left(1 - \frac{T_F}{N_c} V_A^2(r) \int_{-T_W/2}^{T_W/2} dt \int_{-T_W/2}^t dt' \right. \\ &\times e^{-i(t-t')(V_o^{(0)} - V_s^{(0)})} \\ &\left. \times \langle \mathbf{r} \cdot g \mathbf{E}^a(t) \phi_{ab}^{\text{adj}}(t, t') \mathbf{r} \cdot g \mathbf{E}^b(t') \rangle \right), \end{aligned} \quad (125)$$

where fields with only temporal arguments are evaluated in the center-of-mass coordinate. From the matching condition $G_{\text{NRQCD}} = G_{\text{pNRQCD}}$, we obtain $Z_s^{(0)}$ and $V_s^{(0)}$ at NLO in the multipole expansion:

$$\begin{aligned} V_s^{(0)}(r) &= u_0(r) + \frac{T_F}{N_c} V_A^2(r) \lim_{T_W \rightarrow \infty} \frac{i}{T_W} \int_{-T_W/2}^{T_W/2} dt \\ &\times \int_{-T_W/2}^t dt' e^{-i(t-t')(V_o^{(0)} - V_s^{(0)})} \\ &\times \langle \mathbf{r} \cdot g \mathbf{E}^a(t) \phi_{ab}^{\text{adj}}(t, t') \mathbf{r} \cdot g \mathbf{E}^b(t') \rangle, \end{aligned} \quad (126)$$

$$\begin{aligned} \ln Z_s^{(0)}(r) &= u_1(r) + \frac{T_F}{N_c} V_A^2(r) \int_{-\infty}^{\infty} dt \\ &\times \int_{-\infty}^t dt' e^{-i(t-t')(V_o^{(0)} - V_s^{(0)})} \\ &\times \langle \mathbf{r} \cdot g \mathbf{E}^a(t) \phi_{ab}^{\text{adj}}(t, t') \mathbf{r} \cdot g \mathbf{E}^b(t') \rangle. \end{aligned} \quad (127)$$

Equations (126) and (127) do not rely on any perturbative expansion in α_s . However, since we are considering the weak-coupling case, they can be evaluated order by order in α_s and one can obtain the leading logarithmic contribution to the static potential. This comes from the three-loop IR logarithmic divergence of the Wilson loop first noticed by Appelquist *et al.* (1978) (see also Kummer *et al.*, 1996). The calculation may be done in various ways depending on how divergences are regularized. Obviously the scheme adopted for calculating the Wilson loop must be the same as that adopted for calculating the loop diagram in pNRQCD. This study has been performed by Brambilla *et al.* (1999b, 2000) giving

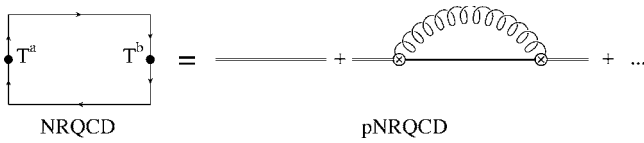


FIG. 10. The matching of $V_o^{(0)}$ and $Z_o^{(0)}$ at NLO in the multipole expansion. On the left-hand side is the Wilson loop in NRQCD with color matrix insertions, on the right-hand side are the pNRQCD propagators.

$$V_s^{(0)}(r, \nu_{us}) = -C_F \frac{\alpha_{V_s}(r)}{r} = (u_0(r))_{\text{two-loop}} - \frac{C_F C_A^3}{12} \frac{\alpha_s}{r} \frac{\alpha_s^3}{\pi} \ln(r\nu_{us}), \quad (128)$$

$$\ln Z_s^{(0)}(r, \nu_{us}) = (u_1(r))_{\text{two-loop}} + \frac{C_F C_A^2}{2} \frac{\alpha_s^3}{\pi} \ln(r\nu_{us}). \quad (129)$$

The two-loop expression for $u_0(r)$ is given by $-C_F \alpha_{V_s}(r)_{\text{two-loop}}/r$ and the two-loop expression for α_{V_s} can be found in Eq. (101). The contributions proportional to $\ln(r\nu_{us})$ in Eqs. (128) and (129) would be zero in QED. The fact that α_{V_s} depends on the IR behavior of the theory is therefore a distinct feature of QCD, more specifically, of the non-Abelian nature of QCD, which allows gluons to interact with themselves at arbitrarily small energy scales. We stress that in order to match the normalization factor (129), it is necessary to take into account contributions coming from the end-point Wilson lines, which can be considered irrelevant only at order $(1/T_W)^0$, i.e., for the potential (note that this does not require any special assumption about the large-time behavior of the gluon fields).

The NLO correction to Eq. (118) in the multipole expansion comes from the graph shown in Fig. 10. We omit a term proportional to V_B^2 of the type shown in Fig. 11 and terms which contain operators like $\text{Tr}\{\mathbf{r}^i [\mathbf{D}^i, \mathbf{E}^j] O O^\dagger\}$, because in perturbation theory they neither contribute to the octet matching potential nor to the normalization. The reason is that in contrast to the nonperturbative regime where we may have dependencies on the scale Λ_{QCD} , in perturbation theory loops on octet lines are scaleless and vanish in DR. With a calculation analogous to that in the singlet case we obtain at leading logarithmic three-loop accuracy

$$V_o^{(0)}(r, \nu_{us}) = \left(\frac{C_A}{2} - C_F \right) \frac{\alpha_{V_o}(r)}{r} = (v_0(r))_{\text{two-loop}} + \left(\frac{C_A}{2} - C_F \right) \frac{C_A^3}{12} \frac{\alpha_s}{r} \frac{\alpha_s^3}{\pi} \ln r\nu_{us}. \quad (130)$$

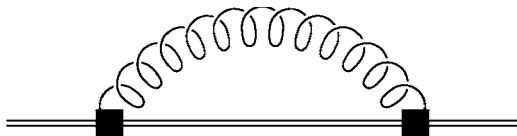


FIG. 11. Octet self-energy graph proportional to V_B^2 .

The two-loop expression for $v_0(r)$ is given by $(C_A - C_F/2)\alpha_{V_o}(r)_{\text{two-loop}}/r$ and for the two-loop expression of α_{V_o} , see Eq. (103). Similarly $Z_o^{(0)}$ may also be calculated, but only in a specific gauge.

4. Matching at order r^0 ($1/m$, $1/m^2$, and beyond)

Following this method, one may consider $1/m$ corrections. If one works at LO in the multipole expansion, the singlet and octet fields decouple. If we further focus on the singlet sector, the computations would be similar to those that appear in Sec. VII.E.4 for the strong-coupling regime. This is the case because we are actually performing the matching order by order in $1/m$ and to any order in α_s . Therefore the expressions obtained in the strong-coupling regime also hold here up to corrections due to US effects. This reasoning also applies to what in Sec. VII is called the “quantum-mechanical matching” (see Sec. VII.E), where explicit expressions in terms of Wilson-loop amplitudes for the real and imaginary parts of the pNRQCD potentials are derived. Those expressions are also valid in the perturbative regime, if they are understood to be at $\mathcal{O}(r^0)$ in the multipole expansion. Note that the Wilson loops multiplying delta functions of \mathbf{r} or derivatives of them are zero in the perturbative regime since they become dimensionless objects and vanish in DR. In particular, this applies to the gluonic correlators that appear in the imaginary part of the potential. Finally, we note that nonanalytic terms due to the scale $\sqrt{m\Lambda_{\text{QCD}}}$ do not appear here since for $\Lambda_{\text{QCD}} \leq E$, this three-momentum scale has not been integrated out.

G. Observables: spectrum and inclusive decay widths

We have finally built the pNRQCD Lagrangian and are in the position to calculate observables with it. We consider observables (being the theoretically cleanest ones) that only involve the calculation of the NR propagator (Green’s function) of the system projected onto the colorless sector of a quark-antiquark pair (with P_s the corresponding projector) and the gluonic vacuum,

$$\Pi(E, \mathbf{r}, \mathbf{r}') \equiv i \int dt d^3\mathbf{R} e^{iEt} \langle \text{vac} | T \{ S(\mathbf{r}', 0, 0) S^\dagger(\mathbf{r}, \mathbf{R}, t) \} | \text{vac} \rangle = \langle \mathbf{r}' | G_s(E) | \mathbf{r} \rangle, \quad (131)$$

$$G_s(E) \equiv P_s \langle \text{vac} | \frac{1}{H - E} | \text{vac} \rangle P_s = G_c(E) + \delta G_s, \quad (132)$$

where H is the pNRQCD Hamiltonian, G_c the Coulomb Green’s function defined in Fig. 5, and E the energy measured from the threshold $2m$.

Besides the heavy-quarkonium spectrum (i.e., the poles of the Green’s function), we consider inclusive (electromagnetic) decay widths, NR sum rules, and t - \bar{t}

production near threshold. For these the normalization at the origin will be important,¹² i.e., the object $\langle \mathbf{r}=0 | G_s(E) | \mathbf{r}=0 \rangle$ has to be computed.

In pNRQCD, there are only potential and US loops. Within pNRQCD, talking about potential loops is nothing but talking about quantum-mechanical perturbation theory:

$$\delta G_s^{\text{pot.}} \text{---} \blacksquare \text{---} \delta V_s + \dots \sim G_c \delta V_s G_c + \dots,$$

where the black square represents a generic δV_s correction to the singlet Coulomb Hamiltonian.

US loops can be computed using standard Feynman-diagram techniques, where it is sometimes convenient to work in momentum space for the US momenta and in position space for the soft scale [this is certainly so if one wants to do standard (finite) quantum-mechanical perturbation theory, although it is clearly possible to do it in momentum space]. We illustrate the procedure with the first US contribution to G_s :

$$\begin{aligned} \delta G_s^{\text{us}} &= \text{---} \text{---} \text{---} \text{---} \text{---} \sim G_c(E) \int \frac{d^d \mathbf{k}}{(2\pi)^d} \mathbf{r} \frac{k}{k + h_o^{(0)} - E} \mathbf{r} G_c(E) \\ &\sim G_c(E) \mathbf{r} (h_o^{(0)} - E)^3 \left\{ \frac{1}{\epsilon} + \gamma + \ln \frac{(h_o^{(0)} - E)^2}{v_{us}^2} \right. \\ &\quad \left. + C \right\} \mathbf{r} G_c(E), \end{aligned} \quad (133)$$

where $d=3+2\epsilon$. We can see that the result is UV divergent. This is not a problem in an EFT in which such divergences can (and should) be absorbed in the matching coefficients of the EFT, i.e., in the potentials. Moreover, there are other sources of logarithmic UV divergences, proportional to $\ln v_p$, coming from potential loops. They show up either by going to high enough orders in quantum-mechanical perturbation theory [for instance, if we are interested in computing the spectrum at $\mathcal{O}(m\alpha_s^6)$],

$$G_c(E) \delta V_s G_c(E) \cdots \delta V_s G_c(E), \quad (134)$$

or by inserting sufficiently singular operators in the computation (as is the case for the renormalization of the matching coefficient of the electromagnetic current). These divergences can be absorbed in the matching coefficients of the local potentials [those proportional to $\delta^{(3)}(\mathbf{r})$ or its derivatives] or in the matching coefficients associated with the currents. Let us explain in detail how this works. Since the singular behavior of the potential loops appears for $|\mathbf{p}| \gg \alpha_s/r$, a perturbative expansion in

¹²Other observables that do not belong to this category are semi-inclusive radiative decay widths, which have been studied by Garcia i Tormo and Soto (2004) and are considered in Sec. VIII.G, or heavy-quarkonium production, for which an analysis in the weak-coupling regime is available (Beneke *et al.*, 2000).

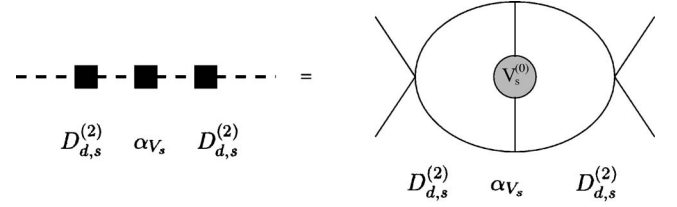


FIG. 12. One possible contribution to the running of $D_{d,s}^{(2)}$ at next-to-leading-logarithm order (NLL). The first picture represents the calculation in terms of the free quark-antiquark propagator $G_c^{(0)}$ and the potentials (the small rectangles). The picture on the right is the representation within a more standard diagrammatic interpretation in terms of quarks and antiquarks. The delta potentials are displayed as local interactions and the Coulomb potential as an extended object in space (but not in time).

α_s is allowed in $G_c(E)$, which can be approximated by the free propagator:

$$\text{---} \text{---} \text{---} \equiv G_c^{(0)}(E) = \frac{1}{E - \mathbf{p}^2/m}.$$

Therefore a practical simplification follows from the fact that the Coulomb potential $-C_F \alpha_s/r$ can be considered a perturbation as far as the computation of the $\ln v_p$ UV divergences is concerned. Moreover, each $G_c^{(0)}$ produces a potential loop and one extra power of m in the numerator, which eliminates the powers of $1/m$ in the denominator. This allows the mixing of potentials with different powers of $1/m$. One typical example is the diagram in Fig. 12, which corresponds to

$$\begin{aligned} G_c^{(0)}(E) \frac{\pi C_F D_{d,s}^{(2)}}{m^2} \delta^{(3)}(\mathbf{r}) G_c^{(0)}(E) C_F \frac{\alpha_{V_s}}{r} G_c^{(0)}(E) \\ \times \frac{\pi C_F D_{d,s}^{(2)}}{m^2} \delta^{(3)}(\mathbf{r}) G_c^{(0)}(E). \end{aligned} \quad (135)$$

The relevant computation gives

$$\begin{aligned} \langle \mathbf{r}=0 | G_c^{(0)}(E) C_F \frac{\alpha_{V_s}}{r} G_c^{(0)}(E) | \mathbf{r}=0 \rangle \\ \sim \int \frac{d^d p'}{(2\pi)^d} \int \frac{d^d p}{(2\pi)^d} \frac{m}{\mathbf{p}'^2 - mE} C_F \frac{4\pi \alpha_{V_s}}{\mathbf{q}^2} \frac{m}{\mathbf{p}^2 - mE} \\ \sim -C_F \frac{m^2 \alpha_{V_s}}{16\pi \epsilon}, \end{aligned} \quad (136)$$

where $\mathbf{q} = \mathbf{p} - \mathbf{p}'$. This divergence can be absorbed in $D_{d,s}^{(2)}$ contributing to its running as follows:

$$v_p \frac{d}{dv_p} D_{d,s}^{(2)}(v_p) \sim \alpha_{V_s}(v_p) D_{d,s}^{(2)2}(v_p) + \dots \quad (137)$$

It is particularly appealing how the EFT framework gives a solution to the problem of the UV divergences one finds in standard quantum-mechanical perturbation-theory calculations. When potential divergences are found it can be more convenient to work in a momen-

tum representation [see, for instance, Czarnecki *et al.* (1999b)]. Nevertheless, it is also possible to handle the UV divergences in position space (Yelkhovsky, 2001). Either way, the computation should be performed in the same scheme used to compute the potentials (see Sec. IV.E for details).

1. Heavy-quarkonium mass

After this discussion and taking into account the power-counting rules given in Sec. IV.B, one can obtain the different observables up to some order in $v \sim \alpha_s$. For instance, the level of precision of the perturbative computation for the heavy-quarkonium mass,

$$M_{nlj}^{\text{pert.}} = 2m + \sum_{m=2}^{\infty} A_{nlj}^{(m)} \alpha_s^m, \quad (138)$$

is as follows (some results were actually computed prior to the existence of pNRQCD). The $\mathcal{O}(m\alpha_s^2)$ result is nothing but the positroniumlike result with the proper color factor. The $\mathcal{O}(m\alpha_s^3)$ contribution was computed by Billoire (1980). The $\mathcal{O}(m\alpha_s^4)$ term was computed by Melnikov and Yelkhovsky (1998), Pineda and Yndurain (1998, 2000), Penin and Pivovarov (1999); the one at $\mathcal{O}(m\alpha_s^5 \ln \alpha_s)$ by Brambilla *et al.* (1999a), Kniehl and Penin (2000c), Hoang, Manohar, and Stewart (2001); the next-to-next-to-next-to-leading-order (NNNLO) large- β_0 result by Hoang (2000), Kiyo and Sumino (2000); and the computations that complete the NNNLO result for the ground state (but without the static-potential three-loop coefficient) by Kniehl *et al.* (2002a), Penin and Steinhauser, (2002).¹³ Logarithms have also been resummed for the heavy-quarkonium mass (see Sec. IV.H for details).

In principle, for the bottomonium ground state, finite charm-mass effects have to be taken into account since the soft scale is of the order of the charm mass. They can be found in the articles by Eiras and Soto (2000); Hoang (2000); Melles (2000); Wang and Yao (2004).

So far, nonperturbative effects have not been discussed. Therefore it was implicitly assumed that $\Lambda_{\text{QCD}} \ll mv^2$, which makes them relevant at $\mathcal{O}(m\alpha_s^5)$ where US modes appear for the first time. This assumption may be reasonable for $t\bar{t}$ systems, but for bottomonium and charmonium it is more questionable. In the situation $\Lambda_{\text{QCD}} \approx mv^2$, one cannot compute using perturbation theory at the US scale. In this situation (which may be relevant for bottomonium), the energy of the heavy quarkonium reads as follows:

$$M_{nlj} = 2m + \sum_{m=2}^{\infty} A_{nlj}^{(m)}(v_{us}) \alpha_s^m + \delta M_{nlj}^{\text{US}}(v_{us}), \quad (139)$$

where the v_{us} scale dependence of the different pieces cancels in the overall sum (for the perturbative sum, this dependence first appears in $A_{nlj}^{(5)}$) and ($E_n \equiv A_{nlj}^{(2)} \alpha_s^2$)

$$\begin{aligned} \delta M_{nlj}^{\text{US}}(v_{us}) &\simeq \delta M_{nl}^{\text{US}}(v_{us}) \\ &= \frac{T_F}{3N_c} \int_0^\infty dt \langle n, l | \mathbf{r} e^{-t(h_o^{(0)} - E_n)} \mathbf{r} | n, l \rangle \\ &\quad \times \langle g \mathbf{E}^a(t) \phi(t, 0)_{ab}^{\text{adj}} g \mathbf{E}^b(0) \rangle (v_{us}), \end{aligned} \quad (140)$$

for which one can think of several possibilities depending on the relative size between mv^2 and Λ_{QCD} . In the limit $mv^2 \gg \Lambda_{\text{QCD}}$, the result obtained by Penin and Steinhauser (2002) is the combination

$$A_{nlj}^{(5)}(v_{us}) \alpha_s^5 + \delta M_{nlj}^{\text{US}}(v_{us}) | \mathcal{O}(\alpha_s^5)_{\text{pert.}}. \quad (141)$$

The expression for the nonperturbative object looks similar to Eq. (140) but with an UV cutoff Λ such that $mv^2 \gg \Lambda \gg \Lambda_{\text{QCD}}$. Therefore we have

$$\delta M_{nlj}^{\text{US}}(v_{us}) = \delta M_{nlj}^{\text{pert.,US}}(v_{us}; \Lambda) + \delta M_{nlj}^{\text{US}}(\Lambda). \quad (142)$$

The study of the nonperturbative effects in this limit, often called the Voloshin-Leutwyler limit, has a long history starting from Voloshin (1979) and Leutwyler (1981). $\delta M_{nlj}^{\text{US}}(\Lambda)$ reads [this expression follows by Fourier transforming to energy space Eq. (140) and setting $v_{us} = \Lambda$]

$$\begin{aligned} \delta M_{nlj}^{\text{US}}(\Lambda) &= \frac{g^2}{6N_c} \langle \text{vac} | E_j^a(0) \\ &\quad \times \langle n, l | \mathbf{r} \left[\frac{1}{E_n - h_o^{(0)} - iD_0^{\text{adj}}} \right]_{ab} \mathbf{r} | n, l \rangle \\ &\quad \times E_j^b(0) | \text{vac} \rangle. \end{aligned} \quad (143)$$

A notation closer to the one used by Voloshin (1979) can be obtained by going to a Hamiltonian formulation (for instance, fixing the gauge $A_0=0$). This corresponds to replacing iD_0^{adj} by $H^{(0)}$, where $H^{(0)}$ is defined in Eq. (196) and the physical states are constrained to satisfy the Gauss law (projected to the octet sector),

$$\begin{aligned} \mathbf{D} \cdot \mathbf{\Pi}^a | \text{phys} \rangle &= \left(\int d^3R \text{Tr} \{ \mathcal{O}^\dagger [g T^a, \mathcal{O}] \right. \\ &\quad \left. + \bar{q} \gamma^0 T^a q \right) | \text{phys} \rangle, \end{aligned} \quad (144)$$

where $\mathbf{\Pi}^a$ is the canonical momentum conjugated to \mathbf{A}^a . As long as we do not study the fine and hyperfine splittings (see Leutwyler, 1981; Curci *et al.*, 1983; Campostrini *et al.*, 1986; Krämer *et al.*, 1992; Titard and Yndurain, 1995; Pineda, 1997a, for such studies in the Voloshin-Leutwyler limit), the corrections do not depend on j (total angular momentum) and s (spin) so we shall not display these indices in the states. The octet propagator mixes low $\mathcal{O}(iD_0^{\text{adj}} \sim \Lambda_{\text{QCD}})$ and high energies $\mathcal{O}(h_o^{(0)} \sim E_n \sim mv^2)$. Therefore an operator product ex-

¹³The application of pNRQED (the QED version of pNRQCD) and, in general, of factorization with DR, has also led to a plethora of results for the spectra of positronium (Czarnecki *et al.*, 1999a; Melnikov and Yelkhovsky, 1999b, 2001; Pineda and Soto, 1999; Kniehl and Penin, 2000b).

pansion can be performed whose expansion parameter is of order

$$\left(\frac{iD_0^{\text{adj}}}{E_n - h_o}\right)^2 \sim \left(\frac{\Lambda_{\text{QCD}}}{m\beta_n^2}\right)^2, \quad (145)$$

and one obtains

$$\delta M_{nl}^{\text{US}}(\Lambda) = \sum_{r=0}^{\infty} C_r O_r \equiv \sum_{r=0}^{\infty} \delta E_{nl}^{(r)}, \quad (146)$$

where

$$C_r = \langle n, l | \mathbf{r} \left(\frac{1}{E_n - h_o} \right)^{2r+1} \mathbf{r} | n, l \rangle, \quad (147)$$

$$O_r = \frac{g^2}{54} \langle \text{vac} | \text{Tr}([D_0(0), [\dots [D_0(0), \mathbf{E}(0)] \dots]] | \text{vac} \rangle, \quad (148)$$

and the trace is in the adjoint representation. $\delta E_{nl}^{(0)}$ has been obtained by Leutwyler (1981); Voloshin (1982); Pineda (1997b) and $\delta E_{nl}^{(1)}$ by Pineda (1997b). For further details, we refer the reader to these works.

What we have discussed applies for $t\bar{t}$ production near threshold. In the case of bottomonium or charmonium, it is more likely that the kinematical situations $mv^2 \sim \Lambda_{\text{QCD}}$ (in which the whole functional form of the chromoelectric correlator is needed) or $\Lambda_{\text{QCD}} \gg mv^2$ apply. This last situation is discussed in Sec. VII. A phenomenological analysis is presented in Sec. VIII.A.

2. Inclusive decay widths

It is rather easy, after the matching has been performed, to calculate in pNRQCD the inclusive decay width of a heavy quarkonium H into light particles. This is the imaginary part of the singlet propagator pole in the complex plane and may be calculated as (at LO in $\text{Im } H$)

$$\Gamma(H \rightarrow \text{light particles}) = -2 \langle n, l, s, j | \text{Im } H | n, l, s, j \rangle. \quad (149)$$

The imaginary part of the pNRQCD Hamiltonian has been written in Eqs. (75) and (76). It depends on delta (or derivatives of delta) potentials and does not mix singlet and octet fields. The states $|n, l, s, j\rangle$ are the eigenstates of the pNRQCD Hamiltonian. For electromagnetic inclusive decays, $\text{Im } f_{\text{EM}}^{\text{NR}}(^3S_1)$ is needed (or equivalently the matching coefficient of the electromagnetic current, $b_{1,\text{pNR}}^v$ for the decay into e^+e^- and $\text{Im } f_{\text{EM}}^{\text{NR}}(^1S_0)$, for the decay into $\gamma\gamma$). The first matching coefficient is known at present with two-loop accuracy (Källen and Sarby, 1955; Beneke *et al.*, 1998; Czarnecki and Melnikov, 1998) in a closed analytic form. For the second, besides the one-loop result by Harris and Brown (1957), a semianalytic two-loop result was obtained by Czarnecki and Melnikov (2002). Apart from the electromagnetic matching coefficients, the relevant calculation is that of the residue of the NR propagator at the origin:

$$\text{Res}_{E=E_{\text{pole}}} \langle \mathbf{r} = 0 | G_s(E) | \mathbf{r} = 0 \rangle = |\phi_n^{(0)}|^2 (1 + \delta\phi_n)^2, \quad (150)$$

where

$$|\phi_n^{(0)}|^2 = \frac{1}{\pi} \left(\frac{m C_F \alpha_s}{2n} \right)^3 \equiv \rho_n, \quad (151)$$

and E_{pole} is the energy for which $G_s(E)$ has a pole. Explicit expressions for the purely perturbative computation at NNLO can be found in the articles of Melnikov and Yelkhovsky (1999a) and Penin and Pivovarov (1999). Note that at this order the LO expressions for $\text{Im } g_{\text{EM}}^{\text{pNR}}(^3S_1)$ and $\text{Im } g_{\text{EM}}^{\text{pNR}}(^1S_0)$ are also needed. Therefore, with NNLO precision, the electromagnetic decays can be written in the following way:

$$\Gamma(V_Q(nS) \rightarrow e^+e^-) = \frac{4C_A}{m^2} \rho_n \left[\text{Im } f_{\text{EM}}^{\text{NR}}(^3S_1) (1 + \delta\phi_n)^2 + \text{Im } g_{\text{EM}}^{\text{pNR}}(^3S_1) \frac{E_n}{m} \right], \quad (152)$$

$$\Gamma(P_Q(nS) \rightarrow \gamma\gamma) = \frac{4C_A}{m^2} \rho_n \left[\text{Im } f_{\text{EM}}^{\text{NR}}(^1S_0) (1 + \delta\phi_n)^2 + \text{Im } g_{\text{EM}}^{\text{pNR}}(^1S_0) \frac{E_n}{m} \right], \quad (153)$$

where V and P stand for the vector and pseudoscalar heavy quarkonium. Some higher-order corrections are also known. The $\mathcal{O}(\alpha_s^3 \ln \alpha_s)$ term has been computed by Kniehl *et al.* (2003); Hoang (2004), the $\mathcal{O}(\alpha_s^3 \ln^2 \alpha_s)$ term by Kniehl and Penin (2000c).¹⁴ For RG-improved expressions, see Sec. IV.H.

For the nonperturbative corrections, a discussion similar to the mass case applies to the relative size between Λ_{QCD} and mv^2 . Near the pole E_n , we have the expansion (we only consider nonperturbative corrections in what follows)

$$\begin{aligned} \langle \mathbf{r} = 0 | G_s(E) | \mathbf{r} = 0 \rangle &= \frac{\rho_n + \delta\rho_n^{\text{np}}}{E_n + \delta E_{n0}^{\text{np}} - E} + \mathcal{O}((E_n + \delta E_{n0}^{\text{np}} - E)^0) \\ &= \frac{\rho_n}{E_n - E} - \frac{\rho_n \delta E_{n0}^{\text{np}}}{(E_n - E)^2} + \frac{\delta\rho_n^{\text{np}}}{E_n - E} + \mathcal{O}((E_n - E)^0) \\ &\quad + \mathcal{O}(\delta^{\text{np}} E_{n0}^2). \end{aligned} \quad (154)$$

On the other hand, one obtains

$$\begin{aligned} \langle \mathbf{r} = 0 | G_s(E) | \mathbf{r} = 0 \rangle &\simeq \langle \mathbf{r} = 0 | G_c(E) | \mathbf{r} = 0 \rangle + \langle \mathbf{r} = 0 | \delta G_s^{\text{np}}(E) | \mathbf{r} = 0 \rangle, \end{aligned} \quad (155)$$

where

¹⁴Major progress has also been made in QED for positronium decays using these techniques. See Kniehl and Penin, 2000a; Melnikov and Yelkhovsky, 2000.

$$\begin{aligned}
\langle \mathbf{r}=0 | \delta G_s^{\text{np}}(E) | \mathbf{r}=0 \rangle &= \frac{g^2}{18} \langle \text{vac} | E_j^a(0) | \mathbf{r}=0 \rangle \frac{1}{h_s^{(0)} - E} \mathbf{r} \left[\frac{1}{h_o^{(0)} + iD_0^{\text{adj}} - E} \right]_{ab} \mathbf{r} \\
&\times \frac{1}{h_s^{(0)} - E} | \mathbf{r}=0 \rangle E_j^b(0) | \text{vac} \rangle \\
&= -\frac{\rho_n \delta E_{n0}^{\text{np}}}{(E_n - E)^2} + \frac{\delta \rho_n^{\text{np}}}{E_n - E} + \mathcal{O}((E_n - E)^0). \quad (156)
\end{aligned}$$

Proceeding in the same way as before, we can factorize mv^2 from Λ_{QCD} effects:

$$\langle \mathbf{r}=0 | \delta G_s^{\text{np}}(E) | \mathbf{r}=0 \rangle = \sum_{r=0}^{\infty} C_r^G O_r, \quad (157)$$

where

$$\begin{aligned}
C_r^G &= \langle \mathbf{r}=0 | \frac{1}{h_s^{(0)} - E} \mathbf{r} \left(\frac{1}{h_o^{(0)} - E} \right)^{2r+1} \frac{1}{h_s^{(0)} - E} | \mathbf{r}=0 \rangle \\
&= \frac{A_{-2}^{(r)}}{(E_n - E)^2} + \frac{A_{-1}^{(r)}}{(E_n - E)} + \mathcal{O}((E_n - E)^0), \quad (158)
\end{aligned}$$

and O_r is defined in Eq. (148). Now, from these expressions, we can read off the observables we are interested in, namely,

$$\delta \rho_n^{\text{np}} \equiv \sum_{r=0}^{\infty} \delta \rho_n^{(r)} = \sum_{r=0}^{\infty} A_{-1}^{(r)} O_r, \quad \delta E_{n0}^{\text{np}} = \frac{-1}{\rho_n} \sum_{r=0}^{\infty} A_{-2}^{(r)} O_r. \quad (159)$$

This also provides a new method of obtaining the energy corrections for $l=0$ states, which can be used to check the results of the previous subsection. $\delta \rho_n^{(0)}$ and $\delta E_{n0}^{(0)}$ were calculated by Voloshin (1982) and $\delta \rho_n^{(1)}$ by Pineda (1997b). We refer the reader to these works for further details.

NR sum rules and $t\bar{t}$ production near threshold will be discussed in Secs. VIII.E and VIII.F, respectively. For those, the relevant objects to be computed are again $\langle \mathbf{r}=0 | G_s(E) | \mathbf{r}=0 \rangle$, but for arbitrary energy $E \sim mv^2$, and the electromagnetic matching coefficients considered before. Finally, it is also possible to obtain RG-improved expressions, which we consider in the next section.

H. Renormalization group

Schematically, we can write the pNRQCD Lagrangian as an expansion in r and $1/m$ in the following way:

$$\mathcal{L}_{\text{pNRQCD}} = \sum_{n=-1}^{\infty} r^n \tilde{V}_n O_n + \frac{1}{m} \sum_{n=-2}^{\infty} r^n \tilde{V}_n^{(1)} O_n^{(1)} + \mathcal{O}\left(\frac{1}{m^2}\right), \quad (160)$$

where $\tilde{V}_n^{(\ell)}$ ($\tilde{V}_n^{(0)} \equiv \tilde{V}_n$) are dimensionless constants (in four dimensions). Since they reabsorb the divergences of the EFT in the way explained in Sec. IV.G, they will

depend on ν_p and ν_{us} . One can obtain RG-improved expressions for $\tilde{V}_n^{(\ell)}$ in the following way.

One first performs the matching from QCD to NRQCD. The latter depends on some matching coefficients, $c(\nu_s)$ and $f(\nu_p, \nu_s)$, which can be obtained order by order in α_s (with $\nu_p = \nu_s$) following the procedure described in Sec. II.D. In Sec. II.E, we discussed the procedure to get the running of c and the soft (ν_s) running of f at any finite order (basically using HQET techniques). Nevertheless, the running of $f(\nu_p, \nu_s)$ is more complicated beyond one loop since a dependence on ν_p appears. As we shall see, it can be obtained within pNRQCD.

The second step is the matching from NRQCD to pNRQCD. The latter depends on some matching coefficients (potentials), which typically have the following structure: $\tilde{V}(c(\nu_s), f(\nu_p, \nu_s), \nu_s, \nu_{us}, r)$. These potentials can be obtained order by order in α_s following the procedure described in Secs. IV.E and IV.F. The integrals in the matching calculation depend on a factorization scale ν , which corresponds either to ν_s or to ν_{us} . In an explicit calculation, they can be distinguished by looking at the UV and IR behavior of the diagrams: UV divergences are proportional to $\ln \nu_s$, which cancel the ν_s scale dependence inherited from the NRQCD matching coefficients, and IR divergences are proportional to ν_{us} . However, since we only want to perform a matching calculation at some given scale $\nu = \nu_s = \nu_{us}$ (or when working order by order in α_s without attempting any resummation of logarithms), it is not necessary to distinguish between ν_s and ν_{us} .

The third step is to obtain the RG equations of the potentials. ν_s provides us with the starting point of the RG evolution with respect to ν_{us} (up to a constant of order 1). The running with respect to ν_{us} can then be obtained following the procedure described by Pineda and Soto (2000) and Pineda (2002b). Formally, the RG equations of the matching coefficients due to the ν_{us} dependence read

$$\nu_{us} \frac{d}{d\nu_{us}} \tilde{V} = B_{\tilde{V}}(\tilde{V}). \quad (161)$$

From a practical point of view, one can organize the RG equations within an expansion in $1/m$ and $\alpha_s(\nu_{us})$. At $\mathcal{O}(1/m^0)$, the analysis corresponds to the study of the static limit of pNRQCD, which has been carried out by Pineda and Soto (2000). Since $\tilde{V}_{-1} \neq 0$, there are relevant operators (super-renormalizable terms) in the Lagrangian and the US RG equations lose the triangular structure that they exhibited for the RG equations of ν_s . Still, if $\tilde{V}_{-1} \ll 1$, the RG equations can be obtained as a double expansion in \tilde{V}_{-1} and \tilde{V}_0 , where the latter corresponds to the marginal operators (renormalizable interactions). At short distances ($1/r \gg \Lambda_{\text{QCD}}$), this is the case for the static limit of pNRQCD. Specifically, we have $\tilde{V}_{-1} = \{\alpha_{V_s}, \alpha_{V_o}\}$, which fulfills $\tilde{V}_{-1} \sim \alpha_s(r) \ll 1$, $\tilde{V}_0 = \alpha_s(\nu_{us})$, and

$\tilde{V}_1 = \{V_A, V_B\} \sim 1$. Therefore we can calculate the anomalous dimensions order by order in $\alpha_s(\nu_{us})$. In addition, we also have an expansion in \tilde{V}_{-1} . Moreover, the specific form of the pNRQCD Lagrangian severely constrains the RG equations' general structure. Therefore, for instance, the leading nontrivial RG equation for α_{V_s} reads

$$\nu_{us} \frac{d}{d\nu_{us}} \alpha_{V_s} = \frac{2}{3} \frac{\alpha_s}{\pi} V_A^2 \left[\left(\frac{C_A}{2} - C_F \right) \alpha_{V_o} + C_F \alpha_{V_s} \right]^3 + \mathcal{O}(\tilde{V}_{-1}^4 \tilde{V}_0, \tilde{V}_0^2 \tilde{V}_{-1}^3). \quad (162)$$

At higher orders in $1/m$ the analysis has been carried out by Pineda (2002b). The same considerations as for the static limit apply here as far as the nontriangularity of the RG equations is concerned. In general, one has the structure

$$\nu_{us} \frac{d}{d\nu_{us}} \tilde{V}_n^{(\ell)} \sim \sum_{\{n_i\} \{ \ell_i \}} \tilde{V}_{n_1}^{(\ell_1)} \tilde{V}_{n_2}^{(\ell_2)} \dots \tilde{V}_{n_j}^{(\ell_j)},$$

with $\sum_{i=1}^j \ell_i = \ell, \quad \sum_{i=1}^j n_i = n, \quad (163)$

and one has to pick up the leading contributions from all possible terms. Actually, as far as the NNLL heavy-quarkonium mass is concerned, the relevant US running can be obtained by computing the diagram displayed in Eq. (133) (one also has to consider the running of V_A , which happens to be zero). Working in DR, one should note that the potentials have to be understood in D dimensions [see, for instance, Eq. (3.1) of Schröder's thesis (1999a)]. Therefore powers of g_B^2 (the bare coupling) have dimensions and have to be compensated by powers of $k^{2\epsilon}$ in α_{V_s} . This means that the US divergences ($1/\epsilon$ poles) generated by the right-hand side of Eq. (162) are absorbed by the terms in α_{V_s} proportional to g_B^8 or to a higher power. Finally, by solving Eq. (161) between ν_s and ν_{us} , we have $\tilde{V}(c(\nu_s), f(\nu_p, \nu_s), \nu_s, \nu_{us}, r)$, where the running with respect to ν_{us} is known. Note that the running with respect to ν_s is also known, since we demand that the potential be independent of it:

$$\nu_s \frac{d}{d\nu_s} \tilde{V} = 0, \quad (164)$$

which can be solved by setting $\nu_s = 1/r$. Therefore one can also deduce the dependence of \tilde{V} on r .

The final step is to obtain the RG equation for ν_p . In pNRQCD, integrals over the relative three-momentum of the heavy quarks occur. When these integrals are finite no dependence on ν_p occurs and one has $|\mathbf{p}| \sim 1/r \sim m\alpha_s$ and $\mathbf{p}^2/m \sim m\alpha_s^2$. Therefore one can reduce ν_{us} down to $\sim m\alpha_s^2$ reproducing the results obtained by Pineda (2002b). In general, the integrals over \mathbf{p} are divergent, and the structure of the logarithms is dictated by the UV behavior of \mathbf{p} and $1/r$. This means that we cannot replace $1/r$ and ν_{us} by their physical expectation values but rather by their cutoffs within the integral over \mathbf{p} , i.e., ν_p . Therefore besides the potential's explicit de-

pendence on ν_p , which appears in f , it also implicitly depends on ν_p through the requirement $1/r \sim |\mathbf{p}| \ll \nu_p$, and also through ν_{us} since ν_{us} has to fulfill $\mathbf{p}^2/m \ll \nu_{us} \ll |\mathbf{p}|$ in order to ensure that only soft degrees of freedom have been integrated out for a given $|\mathbf{p}|$. This latter requirement holds if we fix the final point of the evolution of the ultrasoft RG equation to be $\nu_{us} = \nu_p^2/m$. At this stage, a single cutoff ν_p exists and the correlation of cutoffs becomes manifest. Therefore for the RG equation for ν_p , the anomalous dimension of $\tilde{V}(c(1/r), f(\nu_p, 1/r), 1/r, \nu_p^2/m, r)$ is at LO the same as the one of $\tilde{V}(c(\nu_p), f(\nu_p, \nu_p), \nu_p, \nu_p^2/m, \nu_p)$.¹⁵ It appears through the divergences induced by the iteration of the potentials in the way explained by Pineda (2002a) and Sec. IV.G. In particular, the computation of the anomalous dimension can be organized within an expansion in α_s and using the free propagators $G_c^{(0)}$. Finally, the running will go from $\nu_p \sim m$ down to $\nu_p \sim m\alpha_s$. A similar discussion applies to the running of the matching coefficients of the currents (or, in other words, of the imaginary terms of the potential). This completes the procedure to obtain the RG equations for the hard, soft, and US scales. An example is given below.

This line of investigation has led to several new results in heavy-quarkonium physics. They can be summarized as follows (we omit all numerical coefficients that can be found in the quoted literature):

- The NNLL correction to the heavy-quarkonium energy (Pineda, 2002b), i.e., corrections of order

$$\delta E \sim m\alpha_s^4 + m\alpha_s^5 \ln \alpha_s + m\alpha_s^6 \ln^2 \alpha_s + \dots \quad (166)$$

- The LL (Pineda, 2002b) (first obtained by Hoang, Manohar, and Stewart, 2001) and NLL (Kniehl *et al.*, 2004; Penin *et al.*, 2004a) correction to the heavy-quarkonium hyperfine splitting,

$$\delta E_{\text{HF}} \sim m\alpha_s^4 + m\alpha_s^5 \ln \alpha_s + m\alpha_s^6 \ln^2 \alpha_s + \dots + m\alpha_s^5 + m\alpha_s^6 \ln \alpha_s + m\alpha_s^7 \ln^2 \alpha_s + m\alpha_s^8 \ln^3 \alpha_s + \dots \quad (167)$$

¹⁵Roughly speaking, this result can be thought of as expanding $\ln r$ around $\ln \nu_p$ in the potential, i.e.,

$$\tilde{V}(c(1/r), f(\nu_p, 1/r), 1/r, \nu_p^2/m, r) \simeq \tilde{V}(c(\nu_p), f(\nu_p, \nu_p), \nu_p, \nu_p^2/m, \nu_p) + \ln(\nu_p r) \frac{d}{dr} \tilde{V} \Big|_{1/r=\nu_p} + \dots \quad (165)$$

The $\ln(\nu_p r)$ terms give subleading contributions to the anomalous dimension when introduced in divergent integrals over \mathbf{p} . An explicit example of this type of correction appears in the computation of the hyperfine splitting of heavy quarkonium at NLL (Kniehl *et al.*, 2004; Penin *et al.*, 2004a).

- The NLL (Pineda, 2002a) correction to the inclusive electromagnetic decays (this result can be applied to \bar{t} - t production at threshold or NR sum rules since the running of the electromagnetic current matching coefficient is the only nontrivial object that appears in the NLL running),

$$\Gamma(V_Q(nS) \rightarrow e^+e^-) \sim m\alpha_s^3(1 + \alpha_s^2 \ln \alpha_s + \alpha_s^3 \ln^2 \alpha_s + \dots),$$

$$\Gamma(P_Q(nS) \rightarrow \gamma\gamma) \sim m\alpha_s^3(1 + \alpha_s^2 \ln \alpha_s + \alpha_s^3 \ln^2 \alpha_s + \dots), \quad (168)$$

and for the ratio the NNLL correction (Penin *et al.*, 2004b)

$$\frac{\Gamma(V_Q(nS) \rightarrow e^+e^-)}{\Gamma(P_Q(nS) \rightarrow \gamma\gamma)} \sim 1 + \alpha_s^2 \ln \alpha_s + \alpha_s^3 \ln^2 \alpha_s + \dots + \alpha_s^3 \ln \alpha_s + \alpha_s^4 \ln^2 \alpha_s + \dots. \quad (169)$$

The resummation of logarithms using EFTs was first addressed within the velocity NRQCD framework (Luke *et al.*, 2000; see also Manohar and Stewart, 2000c, 2001; Hoang, Manohar, and Stewart, 2001; Hoang and Stewart, 2003; Hoang, 2004), where the relevance of the cutoff correlation for the RG was first realized. Nevertheless, the early formulations of this theory had some problems (in particular, concerning the treatment of US modes), which led to incorrect results for the heavy-quarkonium mass at NNLL (Hoang, Manohar, and Stewart, 2001) and the electromagnetic-current matching coefficient at NLL (Manohar and Stewart, 2001). They have been resolved by Hoang and Stewart (2003) and their results now agree with those obtained in pNRQCD (Pineda, 2002a, 2002b). The application of the RG to QED bound states has also been considered in both formalisms; see Manohar and Stewart (2000a); Pineda (2002a, 2002c); Penin *et al.* (2004b).

Finally, we illustrate the method in the simplest possible situation where all the scales appear. We consider the corrections to the heavy-quarkonium spectrum for the non-equal-mass case in the limit where one of the masses (m_2) goes to infinity, and in the Abelian limit with zero light flavors ($C_F \rightarrow 1, C_A \rightarrow 0, T_F \rightarrow 1, n_f \rightarrow 0$). This is nothing but the hydrogen-atom case. We compute some NNLL corrections to the Lamb shift of $\mathcal{O}(m\alpha_s^8 \ln^3 \alpha_s)$, which were first computed using the RG by Manohar and Stewart (2000a). Here we follow the discussion in the articles of Pineda (2002a, 2002c). In this limit, α_s does not run and we can neglect the four-fermion matching coefficients since they are suppressed by powers of $1/m_2$. Therefore we only have to consider the running of the matching coefficients of the heavy-quark bilinear terms. At $\mathcal{O}(1/m^2)$, c_D is the only matching coefficient with nontrivial running. By solving Eq. (35) in this limit, one obtains

$$c_D(\nu_s) = 1 - \frac{8}{3} \frac{\alpha_s}{\pi} \ln \frac{\nu_s}{m}. \quad (170)$$

At the pNRQED level, we have to consider first the US RG running of $D_{d,s}^{(2)}$, which follows from Eq. (133). It reads (we use $V_A=1$ and $c_S^{(1,-2)}=1$)

$$\nu_{us} \frac{d}{d\nu_{us}} D_{d,s}^{(2)} = -\frac{4}{3} \frac{\alpha_s^2}{\pi}. \quad (171)$$

By using the initial matching condition

$$D_{d,s}^{(2)}(\nu_s) = \alpha_s \frac{c_D(\nu_s)}{2}, \quad (172)$$

we can solve Eq. (171). The solution is

$$D_d^{(2)}(\nu_{us}) = \frac{\alpha_s}{2} \left(1 - \frac{8}{3} \frac{\alpha_s}{\pi} \ln \frac{\nu_{us}}{m} \right), \quad (173)$$

which gives the full NNLL contribution to the spectrum of $\mathcal{O}(m\alpha_s^5 \ln \alpha_s)$ and nothing else. At NNNLL, we can obtain the $\mathcal{O}(m\alpha_s^8 \ln^3 \alpha_s)$ contribution from Eq. (137), which is due to the diagram in Fig. 12. This is because the $\mathcal{O}(m\alpha_s^8 \ln^3 \alpha_s)$ term has the highest power of logarithm that could appear from this evaluation of the energy and that in order to achieve such power it is necessary to mix with its NNLL-terms. As we have seen, the latter only appear in the LL evaluation of $D_d^{(2)}$ (173), which, indeed, only produces a single logarithm. The other point is that the NLL evaluation of the potentials only produces single logarithms unless mixed with LL running. Therefore the diagrams with the highest power of $D_d^{(2)}$ will give the highest logarithmic power in the spectrum of the NNNLL. Thus we only have to solve Eq. (137) (note the replacement $\nu_{us} = \nu_p^2/m$), which in the limit considered here reads

$$\nu_p \frac{d}{d\nu_p} D_{d,s}^{(2)}(\nu_p) = \alpha_s D_{d,s}^{(2)2}(\nu_p) + \dots. \quad (174)$$

The solution is

$$\delta D_d^{(2)} = \frac{64}{27} \alpha_s^3 \left(\frac{\alpha_s}{\pi} \right)^2 \ln^3 \frac{\nu_p}{m}. \quad (175)$$

V. RENORMALONS AND THE DEFINITION OF THE HEAVY-QUARK MASS

A. The pole mass and static singlet potential renormalon

The pole mass of a heavy quark can be related to the MS mass by the series

$$m = m_{\overline{\text{MS}}} + \sum_{n=0}^{\infty} r_n \alpha_s^{n+1}, \quad (176)$$

where $\alpha_s \equiv \alpha_s(\nu)$, $m_{\overline{\text{MS}}}$ is calculated at the normalization point $\nu = m_{\overline{\text{MS}}}$ (in this way logarithms that are not associated with the renormalon are resummed), and the first three coefficients r_0 , r_1 , and r_2 are known (Gray *et al.*, 1990; Chetyrkin and Steinhauser, 2000; Melnikov and

Ritbergen, 2000). The pole mass is also known to be IR finite and scheme independent at any finite order in α_s (Kronfeld, 1998). We then define the Borel transform

$$m = m_{\overline{\text{MS}}} + \int_0^\infty dt e^{-t/\alpha_s} B[m](t), \quad B[m](t) \equiv \sum_{n=0}^\infty r_n \frac{t^n}{n!}. \quad (177)$$

We denote by renormalons the singularities on the real axis of the Borel plane.¹⁶ The perturbative expansion behavior of Eq. (176) at large orders is dictated by the closest renormalon to the origin of its Borel transform, which happens to be located at $t=2\pi/\beta_0$ (Beneke and Braun, 1994; Bigi *et al.*, 1994; Neubert and Sachrajda, 1995). More precisely, the behavior of the Borel transform near the closest renormalon at the origin is (we define $u = \beta_0 t/4\pi$)

$$B[m](t(u)) = B[\delta m_{\text{RS}}](t(u)) + (\text{term analytic at } u = 1/2), \quad (178)$$

where

$$B[\delta m_{\text{RS}}](t(u)) \equiv N_m \nu \frac{1}{(1-2u)^{1+b}} [1 + c_1(1-2u) + c_2(1-2u)^2 + \dots]. \quad (179)$$

This dictates that the behavior of the perturbative expansion at large orders be

$$r_n = N_m \nu \left(\frac{\beta_0}{2\pi} \right)^n \frac{\Gamma(n+1+b)}{\Gamma(1+b)} \left(1 + \frac{b}{(n+b)} c_1 + \frac{b(b-1)}{(n+b)(n+b-1)} c_2 + \dots \right). \quad (180)$$

The different b , c_1 , c_2 , etc. can be obtained from the procedure used by Beneke (1995). The coefficients b and c_1 were computed by Beneke (1995), and c_2 by Beneke (1999) and Pineda (2001). They are

$$b = \frac{\beta_1}{2\beta_0^2}, \quad c_1 = \frac{1}{4b\beta_0^3} \left(\frac{\beta_1^2}{\beta_0} - \beta_2 \right), \quad (181)$$

and

$$c_2 = \frac{1}{b(b-1)} \times \frac{\beta_1^4 + 4\beta_0^3\beta_1\beta_2 - 2\beta_0\beta_1^2\beta_2 + \beta_0^2(-2\beta_1^3 + \beta_2^2) - 2\beta_0^4\beta_3}{32\beta_0^8}. \quad (182)$$

Approximate determinations for N_m have been obtained by Pineda (2001); Lee (2003b); Cvetic (2004); see also Pineda (2003b).

One can perform the same analysis with the singlet static potential when $\Lambda_{\text{QCD}} \ll 1/r$. Its perturbative expansion reads

$$V_s^{(0)}(r; \nu_{us}) = \sum_{n=0}^\infty V_{s,n}^{(0)} \alpha_s^{n+1}. \quad (183)$$

The potential, however, is not an IR safe object since it depends on the IR cutoff ν_{us} , which first appears at $\mathcal{O}(\alpha_s^4)$ (for more details see Sec. IV.F). Nevertheless, these US logarithms are not associated with the first IR renormalon since they also appear in momentum space (see also the discussion below). They will not be considered further in this section.

We now use the observation that the first IR renormalon of the singlet static potential cancels with (twice) the renormalon of the pole mass. This has been proven in the (one-chain) large- β_0 approximation by Pineda (1998) and Hoang, Smith, *et al.* (1999b) and at any loop (disregarding possible effects due to ν_{us}) by Beneke (1998). It can also be argued to hold from an EFT approach where any renormalon ambiguity should cancel between operators and matching coefficients. Let us consider, for instance, $1/r \gg \Lambda_{\text{QCD}}$. If we understand the quantity $2m + V_s^{(0)}$ as an observable up to $\mathcal{O}(r^2 \Lambda_{\text{QCD}}^3, \Lambda_{\text{QCD}}^2/m)$ renormalon (and/or nonperturbative) contributions, then this proves the (first IR) renormalon cancellation at any loop (as well as the IR-renormalon independence of ν_{us}).

One can now read off the asymptotic behavior of the static potential from the one of the pole mass and work analogously. We define the Borel transform

$$V_s^{(0)} = \int_0^\infty dt e^{-t/\alpha_s} B[V_s^{(0)}](t), \quad B[V_s^{(0)}](t) \equiv \sum_{n=0}^\infty V_{s,n}^{(0)} \frac{t^n}{n!}. \quad (184)$$

The closest renormalon to the origin is located at $t=2\pi/\beta_0$. This dictates that the behavior of the perturbative expansion at large orders be

$$V_{s,n}^{(0)} = N_{V_s} \nu \left(\frac{\beta_0}{2\pi} \right)^n \frac{\Gamma(n+1+b)}{\Gamma(1+b)} \left(1 + \frac{b}{(n+b)} c_1 + \frac{b(b-1)}{(n+b)(n+b-1)} c_2 + \dots \right), \quad (185)$$

and the Borel transform near the singularity reads

$$B[V_s^{(0)}](t(u)) = N_{V_s} \nu \frac{1}{(1-2u)^{1+b}} [1 + c_1(1-2u) + c_2(1-2u)^2 + \dots] + (\text{analytic term}). \quad (186)$$

In this case, by *analytic term* we mean an analytic function up to the next IR renormalon at $u=3/2$ (Aglietti and Ligeti, 1995).

For N_{V_s} some approximate determinations exist (Pineda, 2001; Lee, 2003b; see also Pineda, 2003b). Actually, the best determinations come from N_m using the cancellation of the pole mass and static singlet potential renormalon, i.e.,

$$2N_m + N_{V_s} = 0. \quad (187)$$

¹⁶We shall not consider singularities due to instantons (Le Guillou and Zinn-Justin 1990).

B. Renormalon-subtracted scheme and power counting

In EFTs with heavy quarks, the inverse of the heavy-quark mass becomes one of the expansion parameters (and of the matching coefficients). A natural choice in the past has been the pole mass because it is the natural definition in processes where the particles eventually measured in the detectors correspond to the fields in the Lagrangian (as in QED). This is not the case in QCD. One consequence of this is that the pole mass suffers from renormalon singularities. Moreover, since these renormalon singularities lie close to the origin of the Borel plane and perturbative calculations have gone very far for systems with heavy quarks, they manifest themselves as a poor convergence of the perturbative series. It is then natural to try to define a new mass parameter, which replaces the pole mass, but is still adequate for threshold problems. Several choices have been proposed in the literature: the kinetic mass (Bigi *et al.*, 1994), the potential-subtracted (PS) mass (Beneke, 1998), the $1S$ mass (Hoang, Ligeti, and Manohar, 1999), the $\overline{\text{PS}}$ -mass (Yakovlev and Groote, 2001), and the RS (RS) mass (Pineda, 2001). All of them achieve the renormalon cancellation and share the following structure:

$$m_X = m - \delta m_X, \quad (188)$$

where $X = \{\text{PS}, 1S, \dots\}$ and δm_X is an object such that

$$B[\delta m_X] = B[\delta m_{\text{RS}}] + (\text{analytic term at } u = 1/2). \quad (189)$$

The different definitions have different analytic terms. δm_{kin} is defined as the self-energy of a static quark computed with a hard cutoff, δm_{PS} is defined as 1/2 the self-energy of the Coulomb potential computed with a hard cutoff much smaller than $1/r$, $\delta m_{\overline{\text{PS}}}$ is defined as the soft part of the heavy-quark self-energy computed with a hard cutoff, and δm_{1S} is 1/2 the perturbative binding energy of the ground state of heavy quarkonium (note that in this case the renormalon cancellation is achieved between different powers of α_s). We shall not discuss further all these threshold masses. Instead, we focus on one, the RS mass, which better matches with the analyses of the previous section. In any case, a large part of the discussion also holds when replacing RS by X . It should be noted that since different masses implement the renormalon cancellation in different ways, different systematic errors appear. For instance, the major error in the RS mass comes from N_m [see Eq. (180)]. For the kinetic and PS masses, it seems difficult to compute higher-order terms. The PS and $1S$ masses depend on the US scale at NNNLO, which may be problematic once this precision is needed (for instance, in B physics). Finally, the $1S$ mass assumes that the ground state of heavy quarkonium is mainly a perturbative system. Therefore having at one's disposal several masses may help to better handle the errors, e.g., in the extraction of the MS quark masses.

The RS definition tries to cancel the poor perturbative behavior associated with the renormalon, which is due to the nonanalytic terms in $1-2u$ in the Borel transform

of the pole mass. These terms also exist in the effective theory. Therefore the procedure followed by Pineda (2001) was to subtract the pure renormalon contribution in the new mass definition,¹⁷ the RS mass m_{RS} ,

$$m_{\text{RS}}(\nu_f) = m - \sum_{n=1}^{\infty} N_m \nu_f \left(\frac{\beta_0}{2\pi} \right)^n \alpha_s^{n+1}(\nu_f) \times \sum_{k=0}^{\infty} c_k \frac{\Gamma(n+1+b-k)}{\Gamma(1+b-k)}, \quad (190)$$

where $c_0=1$. We expect that with this renormalon-free definition, the coefficients multiplying the expansion parameters in the effective-theory calculation will have a natural size and that the same holds for the coefficients multiplying the powers of α_s in the perturbative expansion relating m_{RS} to $m_{\overline{\text{MS}}}$. Therefore we do not lose accuracy if we first obtain m_{RS} and later on use the perturbative relation between m_{RS} and $m_{\overline{\text{MS}}}$ in order to obtain the latter. Nevertheless, since we work order by order in α_s , in the relation between m_{RS} and $m_{\overline{\text{MS}}}$ it is important to expand everything in terms of α_s , specifically $\alpha_s(\nu_f)$, in order to achieve the renormalon cancellation order by order in α_s . Then, the perturbative expansion in terms of the $\overline{\text{MS}}$ mass reads

$$m_{\text{RS}}(\nu_f) = m_{\overline{\text{MS}}} + \sum_{n=0}^{\infty} r_n^{\text{RS}} \alpha_s^{n+1}, \quad (191)$$

where $r_n^{\text{RS}} = r_n^{\text{RS}}(m_{\overline{\text{MS}}}, \nu, \nu_f)$. These r_n^{RS} are the ones expected to be of natural size (or at least not to be artificially enlarged by the first IR renormalon).

These definitions significantly improve the convergence of the perturbative series in comparison with the pole mass. We refer the reader to the work of Pineda (2001) for numerical details.

The shift from the pole mass to the RS mass affects the explicit expression of the effective Lagrangians. In particular, in HQET at LO, a residual mass term appears in the Lagrangian

$$\mathcal{L} = \bar{h}(iD_0 - \delta m_{\text{RS}})h + \mathcal{O}\left(\frac{1}{m_{\text{RS}}}\right), \quad (192)$$

where $\delta m_{\text{RS}} = m - m_{\text{RS}}$ and similarly for the NRQCD Lagrangian.

If we consider the LO in $1/m$ for pNRQCD when $\Lambda_{\text{QCD}} \ll m\alpha_s$, the residual mass term is absorbed into the static potential (in going from NRQCD to pNRQCD, one runs down the scale ν_f to $\nu_f \lesssim m\alpha_s$). We can then, analogous to the RS mass, define a singlet static RS potential

$$V_{s,\text{RS}}^{(0)}(\nu_f) = V_s^{(0)} + 2\delta m_{\text{RS}}, \quad (193)$$

where the coefficients multiplying the perturbative series should be of $\mathcal{O}(1)$ (provided that we expand $V_s^{(0)}$ and

¹⁷One could also choose not to include terms proportional to c_n for $n \geq 2$ since these terms actually go to zero for $u \rightarrow 1/2$ for the physical value of $b \sim 0.4$.

δm_{RS} in the same parameter, namely, α_s). Notice also the trivial fact that the scheme dependence of m_{RS} cancels with the scheme dependence of V_{RS} . This definition significantly improves the perturbative expansion in the potential. For a numerical analysis we refer the reader to the work of Pineda (2001, 2003b).

The pNRQCD Lagrangian for weak coupling in the RS scheme is formally equal to the one in the on-shell scheme [see Eq. (60)] with the modifications $m_{1(2)} \rightarrow m_{1,\text{RS}(2,\text{RS})}$, $V \rightarrow V_{\text{RS}}$, and so on. Note, in particular, that now the expansion is in terms of $1/m_{\text{RS}}$.¹⁸ One can then compute observables along the lines of Sec. IV.G (at the practical level one can work with the pole mass and change to the RS mass at the end). For instance, one would obtain the following expression for the heavy-quarkonium spectrum [see Eq. (138)]:

$$M_{n\bar{l}j} = 2m_{\text{RS}} + \sum_{m=2}^{\infty} A_{n\bar{l}j}^{m,\text{RS}}(\nu_{us})\alpha_s^m + \delta M_{n\bar{l}j}^{\text{US}}(\nu_{us}), \quad (194)$$

where the ν_{us} scale dependence of the different pieces cancels in the overall sum (for the perturbative sum, this dependence first appears in $A_{n\bar{l}j}^{5,\text{RS}}$).

We expect that by working with the RS scheme the coefficients multiplying the powers of α_s will now be of natural size and therefore the convergence is improved compared with the on-shell scheme. Actually, this appears to be the case. See Sec. VIII for details and a phenomenological discussion.

Finally, we discuss some theoretical issues (see also Beneke, 1999). First, once one agrees to give up using the pole mass as an expansion parameter, one may still wonder why not use the $\overline{\text{MS}}$ mass instead. There are several answers to this question. One is that due to the fact that there is another scale, $m\alpha_s$, besides m , one would not achieve the renormalon cancellation order by order in α_s but rather between different orders in α_s , jeopardizing in this way the convergence of the perturbative expansion. This can be resolved by using the ϵ -expansion (Hoang, Ligeti, and Manohar, 1999). Nevertheless, some other problems may remain. Working with $m_{\overline{\text{MS}}}$ would mean introducing a large shift in the pNRQCD Lagrangian of $\mathcal{O}(m\alpha_s)$ thereby compromising the power-counting rules.¹⁹ Furthermore, by expanding everything in terms of α_s , we may introduce a potentially

¹⁸Note that the definition of the RS scheme in the octet sector is more involved since there are some renormalons left at $u = 1/2$ in $V_o^{(0)} + 2\delta m_{\text{RS}}$. The reason is that even at LO in $1/m$, $2m + V_o^{(0)}$ is not an observable due to the fact that there is still interaction with low-energy gluons. Therefore one expects $2m + V_o^{(0)}$ to be ambiguous by an amount of $\mathcal{O}(\Lambda_{\text{QCD}})$. We elaborate on this in section VI.

¹⁹This is certainly so for $t\bar{t}$ physics. Nevertheless, for the bottom quark, the $\mathcal{O}(m\alpha_s)$ term does not seem to be that large numerically, being much smaller than the typical values of the soft scale in the Y(1S). Therefore it may be that working with the $\overline{\text{MS}}$ mass does not destroy the power-counting rules or pNRQCD (or HQET) at the practical level.

large logarithm, $\ln m/\nu$ [note that we cannot minimize this logarithm except at the price of introducing another large logarithm, $\ln(m\alpha_s/\nu)$].

VI. (P)NRQCD: THE STATIC LIMIT

Although NRQCD and pNRQCD were originally designed to study $Q\bar{Q}$ systems of large but finite mass, it is very interesting to consider their static limit (where $m \rightarrow \infty$ while keeping all the other scales finite). On the one hand, the static energy spectra are the main ingredients for the potentials both in the strong- and in the weak-coupling regimes. On the other hand, the study of the energy spectrum is interesting in itself. For instance, a linear dependence on r for the ground-state energy at long distances is usually considered a proof of confinement. The abundant lattice data (at least of quenched simulations) make it possible to study quantitatively for which distances the potentials are in the perturbative or nonperturbative regime, providing a controlled framework for discerning when to use the weak- or the strong-coupling version, of pNRQCD. To answer this question, the proper handling of the renormalon singularities will be crucial.

A. NRQCD in the static limit

The Hamiltonian associated with the Lagrangian (4) is

$$H = H^{(0)} + \mathcal{O}(1/m), \quad (195)$$

$$H^{(0)} = \int d^3\mathbf{x} \frac{1}{2} (\mathbf{\Pi}^a \mathbf{\Pi}^a + \mathbf{B}^a \mathbf{B}^a) - \sum_{j=1}^{n_f} \int d^3\mathbf{x} \bar{q}_j i \mathbf{D} \cdot \boldsymbol{\gamma} q_j, \quad (196)$$

and the physical states are constrained to satisfy the Gauss law:

$$\mathbf{D} \cdot \mathbf{\Pi}^a | \text{phys} \rangle = g \left(\psi^\dagger T^a \psi + \chi^\dagger T^a \chi + \sum_{j=1}^{n_f} \bar{q}_j \gamma^0 T^a q_j \right) | \text{phys} \rangle. \quad (197)$$

We are interested in the one-quark–one-antiquark sector of the Fock space. In the static limit it is spanned by

$$| \mathbf{n}; \mathbf{x}_1, \mathbf{x}_2 \rangle^{(0)} \equiv \psi^\dagger(\mathbf{x}_1) \chi_c^\dagger(\mathbf{x}_2) | n; \mathbf{x}_1, \mathbf{x}_2 \rangle^{(0)}, \quad \forall \mathbf{x}_1, \mathbf{x}_2, \quad (198)$$

where $| \mathbf{n}; \mathbf{x}_1, \mathbf{x}_2 \rangle^{(0)}$ is a gauge-invariant (since it satisfies the Gauss law) eigenstate (up to a phase) of $H^{(0)}$ with energy $E_n^{(0)}(\mathbf{x}_1, \mathbf{x}_2)$. For convenience, we use here the field $\chi_c(\mathbf{x}) = i\sigma^2 \chi^*(\mathbf{x})$, instead of $\chi(\mathbf{x})$, because it is the one to which a particle interpretation can easily be given: it corresponds to a Pauli spinor that annihilates a fermion in the 3^* representation of color SU(3) with the standard, particlelike, spin structure. $| n; \mathbf{x}_1, \mathbf{x}_2 \rangle^{(0)}$ encodes the gluonic content of the state, namely, it is annihilated by $\chi_c(\mathbf{x})$ and $\psi(\mathbf{x})$ for all \mathbf{x} . It transforms as a $3_{\mathbf{x}_1} \otimes 3_{\mathbf{x}_2}^*$ under

TABLE I. Operators H for the Σ , Π , and Δ gluonic excitations between static quarks in pNRQCD up to dimension 3. The covariant derivative is understood in the adjoint representation. $\mathbf{D}\cdot\mathbf{B}$ and $\mathbf{D}\cdot\mathbf{E}$ do not appear, the first because it is identically zero after using the Jacobi identity, while the second gives vanishing contributions after using the equations of motion. From Brambilla *et al.*, 2000.

Gluelumps	$L=1$	$L=2$
$O^a H^a$		
$\Sigma_g^{+'}$	$\mathbf{r}\cdot\mathbf{E}, \mathbf{r}\cdot(\mathbf{D}\times\mathbf{B})$	
Σ_g^-		$(\mathbf{r}\cdot\mathbf{D})(\mathbf{r}\cdot\mathbf{B})$
Π_g	$\mathbf{r}\times\mathbf{E}, \mathbf{r}\times(\mathbf{D}\times\mathbf{B})$	
Π'_g		$\mathbf{r}\times[(\mathbf{r}\cdot\mathbf{D})\mathbf{B}+\mathbf{D}(\mathbf{r}\cdot\mathbf{B})]$
Δ_g		$(\mathbf{r}\times\mathbf{D})^i(\mathbf{r}\times\mathbf{B})^j+(\mathbf{r}\times\mathbf{D})^j(\mathbf{r}\times\mathbf{B})^i$
Σ_u^+		$(\mathbf{r}\cdot\mathbf{D})(\mathbf{r}\cdot\mathbf{E})$
Σ_u^-	$\mathbf{r}\cdot\mathbf{B}, \mathbf{r}\cdot(\mathbf{D}\times\mathbf{E})$	
Π_u	$\mathbf{r}\times\mathbf{B}, \mathbf{r}\times(\mathbf{D}\times\mathbf{E})$	
Π'_u		$\mathbf{r}\times[(\mathbf{r}\cdot\mathbf{D})\mathbf{E}+\mathbf{D}(\mathbf{r}\cdot\mathbf{E})]$
Δ_u		$(\mathbf{r}\times\mathbf{D})^i(\mathbf{r}\times\mathbf{E})^j+(\mathbf{r}\times\mathbf{D})^j(\mathbf{r}\times\mathbf{E})^i$

$$\begin{aligned} \Sigma_g^{+'} &\sim \Pi_g, & \Sigma_g^- &\sim \Pi'_g \sim \Delta_g, \\ \Sigma_u^- &\sim \Pi_u, & \Sigma_u^+ &\sim \Pi'_u \sim \Delta_u. \end{aligned} \quad (202)$$

Similar observations have also been made by Foster and Michael (1999). In pNRQCD they emerge in a quite clear and straightforward way and one can explicitly write down the relevant operators. For higher excitations the expected degeneracies have been obtained by Bali and Pineda (2004). We discuss them further when comparing with lattice data in Sec. VI.D.

So far only the symmetries of pNRQCD at lowest order in the multipole expansion have been used. In fact one can go beyond that and predict the shape of the static energies by calculating the singlet and gluelump (static hybrid) correlators,

$$\begin{aligned} \langle \text{vac} | H(\mathbf{R}, \mathbf{r}, T/2) H^\dagger(\mathbf{R}', \mathbf{r}', -T/2) | \text{vac} \rangle \\ \sim \delta^3(\mathbf{R} - \mathbf{R}') \delta^3(\mathbf{r} - \mathbf{r}') e^{-iTV_H(r)}, \end{aligned} \quad (203)$$

$$\begin{aligned} \langle \text{vac} | S(\mathbf{R}, \mathbf{r}, T/2) S^\dagger(\mathbf{R}', \mathbf{r}', -T/2) | \text{vac} \rangle \\ \sim \delta^3(\mathbf{R} - \mathbf{R}') \delta^3(\mathbf{r} - \mathbf{r}') e^{-iTV_s^{(0)}(r)}, \end{aligned} \quad (204)$$

for large T . At lowest order in the multipole expansion the spectrum of the singlet state reads²⁰

$$E_s(r) = 2m + V_s^{(0)}(r) + \mathcal{O}(r^2). \quad (205)$$

For the static hybrids, the spectrum reads $[V_H = V_o^{(0)}(r) + \Lambda_H]$

$$E_H(r) = 2m + V_o^{(0)}(r) + \Lambda_H + \mathcal{O}(r^2), \quad (206)$$

where

$$\Lambda_H \equiv \lim_{T \rightarrow \infty} \frac{i}{T} \ln \langle H^a(T/2) \phi_{ab}^{\text{adj}}(T/2, -T/2) H^b(-T/2) \rangle. \quad (207)$$

Note that Eq. (207) allows us to relate the correlation length of some gluonic correlators to the behavior of the spectrum of the static hybrids at short distances. Note also that Λ_H is the same for operators corresponding to states that are degenerate.

The potentials $V_s^{(0)}$ and $V_o^{(0)}$ can be computed within perturbation theory. One could then perform a detailed comparison with lattice data. We will see that in order to do so we have to deal first with the renormalon ambiguities as explained in Sec. V.

C. The singlet static potential at short distances versus lattice

In the last few years, lattice simulations (Bali *et al.*, 1997; Necco and Sommer, 2002) have improved their predictions at short distances allowing very accurate comparisons between perturbation theory and lattice simulations. In order to perform this comparison, we cannot work in the on-shell scheme due to the presence of the renormalon, which destroys the convergence of the perturbative series. Therefore schemes were introduced to make the renormalon cancellation explicit. In the work of Recksiegel and Sumino (2002) and Sumino (2002) the renormalon cancellation is achieved order by order in α_s by expanding both m and $V_s^{(0)}$ in terms of the same $\alpha_s(\nu)$. A potential problem of this method is the appearance of large logarithms in the mass expansion. In the results of Necco and Sommer (2001), lattice data were shown to agree with perturbation theory at short distances if the force was used instead of the potential. It was shown by Pineda (2003b) that this is equivalent to working in a renormalon-free scheme, and a first quantitative comparison of the (quenched) lattice data with the RS potential $V_{s,\text{RS}}^{(0)}(r)$ was done (see also Lee, 2003b). This analysis allowed us to put quantitative bounds on nonperturbative effects at short distances and, in particular, it ruled out a linear potential with slope $\sigma = 0.21 \text{ GeV}^2$ at short distances (see also Pineda, 2004). It also showed that today lattice data are precise enough to be sensitive to three-loop perturbation theory (see Fig. 14). Overall, up to distances of around $(0.4-0.5)r_0$, perturbation theory is convergent with small errors and agrees with lattice data in all of the previous analyses. For larger distances the analysis done by Pineda (2003b) shows agreement with the lattice data (within errors) up to distances of $\sim 0.8r_0$ if large logarithms are resummed. In the paper by Recksiegel and Sumino (2003) it was argued that by fine-tuning the renormalization scale, agreement with lattice data could be reached (within errors) up to $3r_0$. Nevertheless, for such large distances, the use of perturbation theory is quite doubtful. There-

²⁰By taking the arbitrary subtraction constant as twice the pole mass of a heavy quark in Eqs. (205) and (206), these equations become renormalon-free.

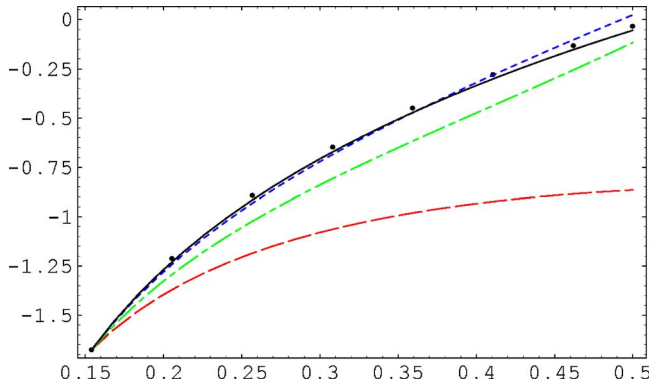


FIG. 14. (Color online) Plot of $r_0[V_{\text{RS}}(r) - V_{\text{RS}}(r') + E_{\text{latt.}}(r')]$ vs r at tree (dashed line), one-loop (dash-dotted line), two-loop (dotted line), and three-loop level (estimate) plus the renormalization-group (RG) expression for the ultrasoft (US) logarithms (solid line) compared with the lattice simulations $E_{\text{latt.}}(r)$ (Necco and Sommer, 2002). For the scale of $\alpha_s(\nu)$, we set $\nu=1/r$. Further, $\nu_f=\nu_{\text{us}}=2.5r_0^{-1}$, $\Lambda_{\overline{\text{MS}}}=0.602r_0^{-1}$ (Capitani *et al.*, 1999), and $r'=0.15399r_0$. From Pineda, 2003b.

fore further studies are needed to see whether this agreement is purely accidental or a theoretical explanation can be given.

D. Gluelumps versus lattice

We compare the predictions of pNRQCD for the static hybrids in the weak-coupling regime with lattice data. We first explore at which distances the expected degeneracies start to be fulfilled and whether the glue-lump mass and hybrid potential splittings agree with each other (see Fig. 13). On a qualitative level the short-distance data are consistent with the expected degeneracies. In any case, at best one can imagine perturbation theory to be valid for the left-most two data points. With the exception of the Π_u , Π'_u , and Φ_u potentials there are also no clear signs of the onset of the short-distance $1/r$ behavior with a positive coefficient as expected from perturbation theory. Furthermore, most of the gaps within multiplets of hybrid potentials, which at leading order depend on the size of the nonperturbative r^2 term, are still quite significant, even at $r=0.4r_0$; for instance, the difference between the Σ_u^- and Π_u potentials at this distance is about $0.28r_0^{-1} \approx 110$ MeV.

From the above considerations it is clear that for a more quantitative study one needs lattice data at shorter distances. These have been provided by Bali and Pineda (2004) for the lowest two gluonic excitations, Π_u and Σ_u^- . We display their differences in the continuum limit in Fig. 15. We see how these approach zero at small r , as expected from the short-distance expansion. pNRQCD predicts that the next effects should be of $\mathcal{O}(r^2)$ (and renormalon-free). The lattice data are fitted rather well by a $\Delta E_{\Pi_u-\Sigma_u^-} = A_{\Pi_u-\Sigma_u^-} r^2$ ansatz for short distances, with slope (see Fig. 15)

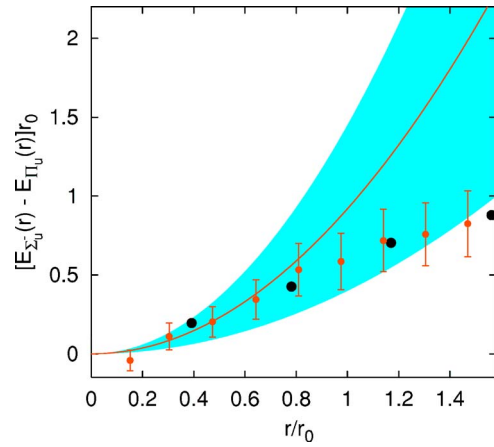


FIG. 15. (Color online) Splitting between the Σ_u^- and Π_u potentials extrapolated to the continuum limit and comparison with a quadratic fit to the $r \leq 0.5r_0$ data points ($r_0^{-1} \approx 0.4$ GeV). The big circles correspond to the data obtained by Juge *et al.* (2003). The errors in this case are smaller than the symbols. The smaller circles correspond to the data obtained by Bali and Pineda, 2004. From Bali and Pineda, 2004.

$$A_{\Pi_u-\Sigma_u^-} = 0.92^{+0.53}_{-0.52} r_0^{-3}, \quad (208)$$

where the error is purely statistical (lattice), the systematic error being negligible. We remark that within the framework of static pNRQCD and to second order in the multipole expansion, one can relate the slope $A_{\Pi_u-\Sigma_u^-}$ to gluonic correlators of QCD.

One can go beyond these analyses and use lattice data plus the knowledge of the (perturbative) octet potential to obtain numerical values for glue-lump masses in a particular scheme. However, analogous to the situation with the static singlet potential, the convergence of the octet potential perturbative series is poor. The solution to this problem comes again from working in a RS scheme properly generalized to the hybrid case. The hybrid energy is

$$E_H(r) = 2m_{\text{RS}}(\nu_f) + V_{o,\text{RS}}(r; \nu_f) + \Lambda_H^{\text{RS}}(\nu_f) + \mathcal{O}(r^2). \quad (209)$$

In the RS scheme the octet potential is

$$V_{o,\text{RS}}(\nu_f) = V_o - \delta V_{o,\text{RS}} = \sum_{n=0}^{\infty} V_{o,n}^{\text{RS}} \alpha_s^{n+1}, \quad (210)$$

where

$$\delta V_{o,\text{RS}} = \sum_{n=1}^{\infty} N_{V_o} \nu_f \left(\frac{\beta_0}{2\pi} \right)^n \alpha_s^{n+1}(\nu_f) \sum_{k=0}^{\infty} c_k \frac{\Gamma(n+1+b-k)}{\Gamma(1+b-k)}. \quad (211)$$

This specifies the glue-lump mass

$$\Lambda_H^{\text{RS}}(\nu_f) = \Lambda_H - \delta \Lambda_{\text{RS}}(\nu_f), \quad (212)$$

where

TABLE II. Absolute values for the gluelump masses in the continuum limit in the RS scheme at $\nu_f=2.5r_0^{-1}\approx 1$ GeV, in r_0 units and in GeV. Note that an additional uncertainty of about 10% should be added to the last column to account for the quenched approximation. We also display examples of creation operators H for these states. The curly braces denote complete symmetrization of the indices. From Bali and Pineda, 2004.

J^{PC}	H	$\Lambda_H^{\text{RS}} r_0$	$\Lambda_H^{\text{RS}}/\text{GeV}$
1^{+-}	B_i	2.25 (39)	0.87 (15)
1^{--}	E_i	3.18 (41)	1.25 (16)
2^{--}	$D_{\{i} B_{\beta\}}$	3.69 (42)	1.45 (17)
2^{+-}	$D_{\{i} E_{\beta\}}$	4.72 (48)	1.86 (19)
3^{+-}	$D_{\{i} D_j B_{k\}}$	4.72 (45)	1.86 (18)
0^{++}	\mathbf{B}^2	5.02 (46)	1.98 (18)
4^{--}	$D_{\{i} D_j D_k B_{l\}}$	5.41 (46)	2.13 (18)
1^{++}	$(\mathbf{B} \wedge \mathbf{E})_i$	5.45 (51)	2.15 (20)

$$\delta\Lambda_{\text{RS}}(\nu_f) = \sum_{n=1}^{\infty} N_{\Lambda} \nu_f \left(\frac{\beta_0}{2\pi}\right)^n \alpha_s^{n+1}(\nu_f) \times \sum_{k=0}^{\infty} c_k \frac{\Gamma(n+1+b-k)}{\Gamma(1+b-k)}. \quad (213)$$

Note that factorization requires

$$2N_m + N_{V_o} + N_{\Lambda} = 0. \quad (214)$$

N_m is already known and N_{V_o} can also be obtained approximately from low orders in perturbation theory following the same procedure as in Sec. V.A. One now has a convergent series in perturbation theory and can obtain absolute values for the masses of the gluelumps, in particular, for the lowest gluelump using the splitting of the Σ_g^+ and the Π_u potential. Then using the lattice data obtained by Foster and Michael (1999), it is possible to calculate the absolute values for the masses of all gluelump excitations in a given scheme (in this case, the RS scheme). The results are summarized in Table II. For a comparison with other determinations, see the work of Bali and Pineda (2004).

VII. POTENTIAL NRQCD. THE STRONG-COUPLED REGIME

In this section we discuss pNRQCD when $\Lambda_{\text{QCD}} \gg E$. In Sec. III we have called this situation the strong-coupling regime of pNRQCD, and some general features of the physical picture have already been discussed. Since the EFT does not tell us anything about the nonperturbative dynamics of QCD, we have to rely on some assumptions in order to identify the relevant degrees of freedom. The assumptions will be minimal, supported by general considerations and lattice data, but clearly we are on less solid ground here than in the weak-coupling regime.

A. Degrees of freedom

If we consider the case without light quarks, the physical states made by a heavy quark and antiquark are heavy-quarkonium states or hybrids or both of them in the presence of glueballs. Quenched lattice data show that the static energy of the lowest state is separated by a gap of order Λ_{QCD} from the higher ones. This feature is preserved in going to unquenched simulations (see Fig. 4). We assume that this feature is also preserved in the dynamical case of heavy quarks with finite masses. This leads to identifying the heavy quarkonium with the solution of the Schrödinger equation on which the static potential corresponds to the ground-state static energy.

Once light fermions have been incorporated, however, new gauge-invariant states appear besides the heavy quarkonium, hybrids, and glueballs. First, we have states with no heavy-quark content. Due to chiral symmetry, there is a mass gap of $\mathcal{O}(\Lambda_{\text{QCD}})$ between the Goldstone bosons, which are massless in the chiral limit, and the rest of the spectrum. Therefore the Goldstone bosons are US degrees of freedom, while the rest of the spectrum is integrated out at the scale Λ_{QCD} . Besides these, we also have bound states made of one heavy quark and light quarks. In practice, we are considering the $Q\bar{q}-\bar{Q}q$ system. The energy of this system is, according to the HQET counting rules (Neubert, 1994), $m_{Q\bar{q}} + m_{\bar{Q}q} = 2m + 2\bar{\Lambda}$. Therefore since $\bar{\Lambda} \sim \Lambda_{\text{QCD}}$, we assume that these states are also integrated out at the scale Λ_{QCD} . This cannot be done for heavy-quarkonium states near threshold, since in this case there is no mass gap between the heavy quarkonium and the creation of a $Q\bar{q}-\bar{Q}q$ pair. Thus if we want to study the heavy quarkonium near threshold, we should include these degrees of freedom in the spectrum [for a model-dependent approach to this situation see, for instance, Eichten *et al.* (1978)]. We assume here that the heavy-quarkonium

states under construction are safely far from threshold.²¹

In summary, the pNRQCD degrees of freedom in the regime $\Lambda_{\text{QCD}} \gg E$ for quarkonium states far from threshold are a singlet field S , describing the heavy-quarkonium state, and Goldstone boson fields. In the following, we shall not consider the Goldstone boson fields. If one switches off the light fermions, only the singlet survives and pNRQCD reduces to a pure two-particle nonrelativistic quantum-mechanical system, usually referred to as a pure potential model.

B. Power counting

The structure of the pNRQCD Lagrangian under the above conditions is very simple: it is just a bilinear in the singlet field. Therefore establishing the power counting means to estimate the size of the terms multiplying the bilinear.

The soft scale $|\mathbf{p}|$ must be assigned to $-i\nabla_{\mathbf{r}}$ and $1/r$, the US scale $E \sim \mathbf{p}^2/m$ to the time derivatives $i\partial_0$ and $V_s^{(0)}$. This last condition follows from the consistency of the theory that requires the virial theorem be met. In other words, all the terms in the Schrödinger equation,

$$i\partial_0\phi = E\phi = (\mathbf{p}^2/m + V_s^{(0)})\phi, \quad (215)$$

must count the same. Note that the normalization condition of the wave function $[\int d^3\mathbf{r}|\phi(\mathbf{r})|^2=1]$ sets $|\phi|^2 \sim |\mathbf{p}|^3$. In general, the $1/m$ corrections to the potential (real and imaginary) will be a combination of α_s calculated at different scales, derivatives with respect to the relative coordinate $-i\nabla_{\mathbf{r}}$, $1/r$, and expectation values of the fields of the light degrees of freedom. The quantities m and $\alpha_s(m)$ are inherited from the hard matching and have well-known values, in particular $\alpha_s(m) \ll 1$. The strong-coupling constant also appears evaluated at the scales $\sqrt{m\Lambda_{\text{QCD}}}$, $1/r$, Λ_{QCD} , and E . At the scale $\sqrt{m\Lambda_{\text{QCD}}}$, which appears in loop calculations (see below), $\alpha_s(m) \ll \alpha_s(\sqrt{m\Lambda_{\text{QCD}}}) \ll 1$ since $\sqrt{m\Lambda_{\text{QCD}}} \gg \Lambda_{\text{QCD}}$. At the scales Λ_{QCD} and E , $\alpha_s(\Lambda_{\text{QCD}}) \sim 1$ and $\alpha_s(E) \sim 1$ by definition of the strong-coupling regime. If $|\mathbf{p}| \sim \Lambda_{\text{QCD}}$, then $\alpha_s(1/r) \sim 1$. If $|\mathbf{p}| \gg \Lambda_{\text{QCD}} \gg E$, then $\alpha_s(\sqrt{m\Lambda_{\text{QCD}}}) \ll \alpha_s(1/r) \ll 1$. In the situation $|\mathbf{p}| \sim \Lambda_{\text{QCD}}$, the expectation values of the fields of the light degrees of freedom depend on \mathbf{r} and Λ_{QCD} , while in the situation $|\mathbf{p}| \gg \Lambda_{\text{QCD}} \gg E$, the $1/r \sim |\mathbf{p}|$ dependence factorizes and the expectation values of the fields of the light degrees of freedom depend only on Λ_{QCD} .²² In both cases their natural counting is Λ_{QCD} to the power of their dimension.

²¹One may think of relaxing this condition in the large- N_c limit, where the mixing between the heavy quarkonium and the $Q\bar{q}-\bar{Q}q$ is suppressed by powers of $1/N_c$.

²²This is certainly so for states with low principal quantum number n . For higher excitations one should keep in mind that \mathbf{p} and $1/r$ could scale differently with n .

C. Lagrangian and symmetries

The pNRQCD Lagrangian (without Goldstone bosons) is given by

$$L_{\text{pNRQCD}} = \int d^3\mathbf{R} \int d^3\mathbf{r} S^\dagger [i\partial_0 - h_s(\mathbf{x}_1, \mathbf{x}_2, \mathbf{p}_1, \mathbf{p}_2, \mathbf{S}_1, \mathbf{S}_2)] S, \quad (216)$$

where

$$h_s(\mathbf{x}_1, \mathbf{x}_2, \mathbf{p}_1, \mathbf{p}_2, \mathbf{S}_1, \mathbf{S}_2) = \frac{\mathbf{p}_1^2}{2m_1} + \frac{\mathbf{p}_2^2}{2m_2} + V_s(\mathbf{x}_1, \mathbf{x}_2, \mathbf{p}_1, \mathbf{p}_2, \mathbf{S}_1, \mathbf{S}_2), \quad (217)$$

$\mathbf{p}_j = -i\nabla_{\mathbf{x}_j}$, $\mathbf{r} = \mathbf{x}_1 - \mathbf{x}_2$, $\mathbf{R} = (\mathbf{x}_1 + \mathbf{x}_2)/2$, and \mathbf{S}_j is the spin operator of particle j . In the following, unless stated differently, we assume $m_1 \neq m_2$. However, we shall not exploit a possible hierarchy between the two masses, which for our purposes are of the same order $\sim m \gg \Lambda_{\text{QCD}}$. The potential V_s contains a real and an imaginary part, with the real part responsible for the binding and the imaginary part for the decay width of the heavy-quarkonium state. The imaginary part of V_s comes from the matching coefficients of the four-fermion operators of NRQCD. The potential V_s is, in general, a nonperturbative quantity, even if to some degree it may be obtained with perturbation theory, as the matching coefficients of NRQCD, or in general any contribution coming from scales larger than Λ_{QCD} . It is the aim of the matching procedure, which we discuss in the following sections, to provide the factorization formulas and the exact expressions for the nonperturbative pieces. These may eventually be calculated on the lattice or in QCD vacuum models, which will be the subject of Sec. VII.G.

The symmetries of the singlet field are those already discussed for the pNRQCD Lagrangian in the weak-coupling regime. In particular, the potential and kinetic energies satisfy the Poincaré invariance constraints (85) and (86) (for the singlet potential). Note that Poincaré invariance may also constrain the natural power counting discussed in Sec. VII.B.

D. Matching: analytic and nonanalytic mass terms

Despite the fact that the strong-coupling Lagrangian (216) looks quite simple, the matching procedure that leads to it may be complicated. This is due to the fact that we have to integrate out, and therefore to make explicit, all the degrees of freedom (or momentum regions) that appear in the range from the hard to the US scale within a nonperturbative environment.

Since we are also integrating out Λ_{QCD} , new momentum regions (apart from Λ_{QCD} itself) that do not appear in the weak-coupling matching show up. Let us consider, for instance, the diagram of Fig. 16. Suppose that the incoming (outcoming) particle is an off-shell particle of energy $\sim \Lambda_{\text{QCD}}$ and three-momentum $p(q) \sim mv$ [for in-

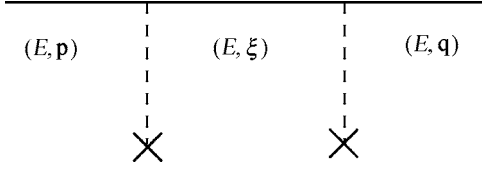


FIG. 16. The incoming energy E is of order Λ_{QCD} , p , and q of order mv . The vertex describes the interaction with an external potential V .

stance, an on-shell particle that just emitted (absorbed) a soft gluon of energy Λ_{QCD}]. The diagram corresponds to the integral

$$\int \frac{d^3\xi}{(2\pi)^3} V(\mathbf{p}-\xi) \frac{1}{E-\xi^2/m+i\epsilon} V(\xi-\mathbf{q}). \quad (218)$$

This integral also receives a contribution from the three-momentum region $\xi \sim \sqrt{mE} \sim \sqrt{m\Lambda_{\text{QCD}}}$. Since $\sqrt{m\Lambda_{\text{QCD}}} \gg \Lambda_{\text{QCD}}$, the potential is perturbative, and since $\sqrt{m\Lambda_{\text{QCD}}} \gg p, q$, we may expand in p and q and the integral effectively reduces to

$$\alpha_s^2 \int \frac{d^3\xi}{(2\pi)^3} \frac{1}{\xi^4} \frac{1}{E-\xi^2/m+i\epsilon} \sim \alpha_s^2 \frac{1}{\Lambda_{\text{QCD}}} \frac{1}{\sqrt{m\Lambda_{\text{QCD}}}}, \quad (219)$$

where α_s is calculated at the (perturbative) scale $\sqrt{m\Lambda_{\text{QCD}}}$. From the above example we may draw the following conclusions. First, in the strong-coupling regime new degrees of freedom show up in loops, namely, quark-antiquark pairs with relative three-momentum of order $\sqrt{m\Lambda_{\text{QCD}}}$ and on-shell energy of order Λ_{QCD} . Since the scale $\sqrt{m\Lambda_{\text{QCD}}} \gg |\mathbf{p}|$ for $\Lambda_{\text{QCD}} \gg E$, this is the largest scale below m and thus the first to be integrated out. The only reason this otherwise dominant contribution to the potential is suppressed is that it appears only in loops. Second, since we expand in the external momenta, which are small compared to $\sqrt{m\Lambda_{\text{QCD}}}$, the effective interaction that arises is local. Third, this kind of contribution is nonanalytic in m .

It is convenient to split the potential (imaginary and real parts) into a part that gets contributions only from scales that are analytic in the mass, $V^{1/m}$, and another, $V^{1/\sqrt{m}}$, that contains any contribution coming from the scale $\sqrt{m\Lambda_{\text{QCD}}}$:

$$V_s = V^{1/m} + V^{1/\sqrt{m}}. \quad (220)$$

We often refer to $V^{1/\sqrt{m}}$ as the part of the potential that is nonanalytic in $1/m$. This is only true at LO, which is, however, the order at which we work here. The matching for the $V^{1/m}$ part may be performed in a strict $1/m$ expansion. The matching for the $V^{1/\sqrt{m}}$ part may be done by integrating out quark-antiquark pairs with relative three-momenta of order $\sqrt{m\Lambda_{\text{QCD}}}$.

We next discuss the matching procedures for $V^{1/m}$ and $V^{1/\sqrt{m}}$ when $|\mathbf{p}| \sim \Lambda_{\text{QCD}}$ and $|\mathbf{p}| \gg \Lambda_{\text{QCD}} \gg E$. We will first consider the case $|\mathbf{p}| \sim \Lambda_{\text{QCD}}$ in Sec. VII.E. The potential will be a function of \mathbf{r} and Λ_{QCD} . This is the most general

case. The particular case $|\mathbf{p}| \gg \Lambda_{\text{QCD}} \gg E$ may be derived by factorizing the potential in a high-energy part dependent on $1/r \sim |\mathbf{p}|$ and a low-energy part dependent on Λ_{QCD} . In this case, however, it is more practical and consistent with the general philosophy of the EFT to achieve factorization directly by integrating out the scales $|\mathbf{p}|$ and Λ_{QCD} in two different steps of the matching procedure. We consider this situation in Sec. VII.F. We note here that local terms that appear when $|\mathbf{p}| \sim \Lambda_{\text{QCD}}$ are already factorized and therefore will be reproduced (up to field redefinitions) when $|\mathbf{p}| \gg \Lambda_{\text{QCD}} \gg E$. This describes the imaginary part of the potential, which comes from the four-fermion contact terms of the NRQCD Lagrangian and the part of the potential that is nonanalytic in $1/m$.

Finally, we mention that soft light fermions will not be explicitly considered in the matching computation. If we want to incorporate them, the procedure would be analogous. One would have to consider the matrix elements and Wilson loops with dynamical light fermions incorporated and new terms appearing in the energies at $\mathcal{O}(1/m^2)$ due to operators involving light fermions that appear in the NRQCD Lagrangian at $\mathcal{O}(1/m^2)$ and the Gauss law.

E. Matching for $|\mathbf{p}| \sim \Lambda_{\text{QCD}}$

In Sec. VI.A, we discussed the static limit of NRQCD. The spectrum consists of the static energies $E_0^{(0)} \ll E_1^{(0)} \ll \dots$. We assume a gap of order Λ_{QCD} between $E_0^{(0)}$ and the higher excitations. pNRQCD is, by definition, the EFT that describes the lowest excitation of the NRQCD spectrum. From Eq. (216) it follows that pNRQCD in the static limit consists of a singlet field S with static energy $V^{(0)}$. Since the static energy is an observable, the matching condition in the static limit is

$$E_0^{(0)}(r) = V^{(0)}(r). \quad (221)$$

Note that the left-hand side is a quantity defined in NRQCD, while the right-hand side is a matching coefficient of pNRQCD.

We may think of generalizing the matching condition (221) to the nonstatic case. Similar to what was done in Sec. VI.A, we introduce the normalized eigenstates, $|\underline{n}; \mathbf{x}_1, \mathbf{x}_2\rangle$, and eigenvalues, $E_n(\mathbf{x}_1, \mathbf{x}_2; \mathbf{p}_1, \mathbf{p}_2)$, of the full NRQCD Hamiltonian H . They satisfy the equations

$$\begin{aligned} H|\underline{n}; \mathbf{x}_1, \mathbf{x}_2\rangle &= \int d^3x'_1 d^3x'_2 |\underline{n}; \mathbf{x}'_1, \mathbf{x}'_2\rangle \\ &\times E_n(\mathbf{x}'_1, \mathbf{x}'_2; \mathbf{p}'_1, \mathbf{p}'_2; \mathbf{S}_1, \mathbf{S}_2) \\ &\times \delta^{(3)}(\mathbf{x}'_1 - \mathbf{x}_1) \delta^{(3)}(\mathbf{x}'_2 - \mathbf{x}_2), \end{aligned} \quad (222)$$

$$\langle \underline{m}; \mathbf{x}_1, \mathbf{x}_2 | \underline{n}; \mathbf{y}_1, \mathbf{y}_2 \rangle = \delta_{nm} \delta^{(3)}(\mathbf{x}_1 - \mathbf{y}_1) \delta^{(3)}(\mathbf{x}_2 - \mathbf{y}_2), \quad (223)$$

where the states are labeled with the positions \mathbf{x}_1 and \mathbf{x}_2 of the static solution even if the position operator does not commute with H beyond the static limit. The eigenvalues E_n are, in general, functions of the momentum

and spin operators and therefore should be understood as operators as well. We assume a gap of order Λ_{QCD} between (the levels of) E_0 and (the levels of) E_n for $n > 0$. Under this circumstance, and arguing as in the static case above, it follows that the matching condition is

$$E_0(\mathbf{x}_1, \mathbf{x}_2, \mathbf{p}_1, \mathbf{p}_2, \mathbf{S}_1, \mathbf{S}_2) = h_s(\mathbf{x}_1, \mathbf{x}_2, \mathbf{p}_1, \mathbf{p}_2, \mathbf{S}_1, \mathbf{S}_2). \quad (224)$$

Again, this equation expresses the (real and imaginary parts of the) pNRQCD Hamiltonian in terms of a quantity

$$E_0(\mathbf{x}_1, \mathbf{x}_2, \mathbf{p}_1, \mathbf{p}_2, \mathbf{S}_1, \mathbf{S}_2) \delta^{(3)}(\mathbf{x}_1 - \mathbf{y}_1) \delta^{(3)}(\mathbf{x}_2 - \mathbf{y}_2) = \langle \underline{0}; \mathbf{x}_1, \mathbf{x}_2 | H | \underline{0}; \mathbf{y}_1, \mathbf{y}_2 \rangle, \quad (225)$$

defined in NRQCD. The aim of the matching is to calculate this quantity. As discussed above, it will contain a part that is analytic in $1/m$ and another that is not.

1. Matching of the analytic terms: quantum-mechanical matching

The analytic part of E_0 can be calculated, by definition, in a strict $1/m$ expansion. The idea is to split the NRQCD Hamiltonian as

$$H = H^{(0)} + H_I, \quad (226)$$

where $H^{(0)}$ is the static Hamiltonian, whose eigenstates and eigenvalues have been discussed in Sec. VI.A, and

$$H_I = \frac{H^{(1,0)}}{m_1} + \frac{H^{(0,1)}}{m_2} + \frac{H^{(2,0)}}{m_1^2} + \frac{H^{(0,2)}}{m_2^2} + \frac{H^{(1,1)}}{m_1 m_2} + \dots \quad (227)$$

is the sum of all higher-order terms in the $1/m$ expansion of the NRQCD Hamiltonian. Then solve Eq. (222) using quantum-mechanical perturbation theory around the static solution. Calculated in this way, the eigenstates (and eigenvalues) of Eq. (222) result as expansions in powers of $1/m$:

$$\begin{aligned} |\underline{n}; \mathbf{x}_1, \mathbf{x}_2 \rangle &= |\underline{n}; \mathbf{x}_1, \mathbf{x}_2 \rangle^{(0)} + \frac{1}{m_1} |\underline{n}; \mathbf{x}_1, \mathbf{x}_2 \rangle^{(1,0)} \\ &+ \frac{1}{m_2} |\underline{n}; \mathbf{x}_1, \mathbf{x}_2 \rangle^{(0,1)} + \frac{1}{m_1^2} |\underline{n}; \mathbf{x}_1, \mathbf{x}_2 \rangle^{(2,0)} \\ &+ \frac{1}{m_2^2} |\underline{n}; \mathbf{x}_1, \mathbf{x}_2 \rangle^{(0,2)} + \frac{1}{m_1 m_2} |\underline{n}; \mathbf{x}_1, \mathbf{x}_2 \rangle^{(1,1)} \\ &+ \dots \end{aligned} \quad (228)$$

A complete derivation can be found in the original literature (Brambilla, Pineda, *et al.*, 2001; Pineda and Vairo, 2001; Brambilla, Eiras, *et al.*, 2003).²³ Here we only make a few remarks. First, the expressions for $|\underline{n}; \mathbf{x}_1, \mathbf{x}_2 \rangle^{(1,0)}$ and $|\underline{n}; \mathbf{x}_1, \mathbf{x}_2 \rangle^{(2,0)}$ look similar to the well-known formulas of time-independent perturbation

theory in quantum mechanics, the only difference being the fact that the energies $E_n^{(0)}$ depend on spatial coordinates and that the matrix elements of $H^{(1,0)}$ and $H^{(2,0)}$ are operators in the quantum-mechanical sense. Second, as usually done in quantum mechanics, we have set the relative phase between $|\underline{n}; \mathbf{x}_1, \mathbf{x}_2 \rangle$ and $|\underline{n}; \mathbf{x}_1, \mathbf{x}_2 \rangle^{(0)}$ to 1 in Eq. (228). This choice is arbitrary. The freedom of choice reflects the fact that the eigenvalues and eigenstates solution of Eq. (222) are defined up to a unitary transformation e^{iO_n} (with $O_n^\dagger = O_n$):

$$\begin{aligned} |\underline{n}; \mathbf{x}_1, \mathbf{x}_2 \rangle &\rightarrow \int d^3 \mathbf{x}'_1 d^3 \mathbf{x}'_2 |\underline{n}; \mathbf{x}'_1, \mathbf{x}'_2 \rangle e^{iO_n(\mathbf{x}'_1, \mathbf{x}'_2, \mathbf{p}'_1, \mathbf{p}'_2, \mathbf{S}_1, \mathbf{S}_2)} \\ &\times \delta^{(3)}(\mathbf{x}'_1 - \mathbf{x}_1) \delta^{(3)}(\mathbf{x}'_2 - \mathbf{x}_2), \end{aligned} \quad (229)$$

$$E_n(\mathbf{x}_1, \mathbf{x}_2, \mathbf{p}_1, \mathbf{p}_2, \mathbf{S}_1, \mathbf{S}_2)$$

$$\begin{aligned} &\rightarrow \int d^3 \mathbf{x}'_1 d^3 \mathbf{x}'_2 e^{iO_n(\mathbf{x}'_1, \mathbf{x}'_2, \mathbf{p}'_1, \mathbf{p}'_2, \mathbf{S}_1, \mathbf{S}_2)} E_n(\mathbf{x}'_1, \mathbf{x}'_2, \mathbf{p}'_1, \mathbf{p}'_2, \mathbf{S}_1, \mathbf{S}_2) \\ &\times e^{-iO_n(\mathbf{x}'_1, \mathbf{x}'_2, \mathbf{p}'_1, \mathbf{p}'_2, \mathbf{S}_1, \mathbf{S}_2)} \delta^{(3)}(\mathbf{x}'_1 - \mathbf{x}_1) \delta^{(3)}(\mathbf{x}'_2 - \mathbf{x}_2). \end{aligned} \quad (230)$$

Our choice preserves the power counting and allows us to obtain rather compact expressions for the potentials. Third, from the expression for the state $|\underline{0}; \mathbf{x}_1, \mathbf{x}_2 \rangle$, the expression for the energy E_0 may be derived straightforwardly, order by order in $1/m$, from Eq. (225). Finally, the matching condition (224) gives the pNRQCD Hamiltonian.

In order to transform the quantum-mechanical expressions into expressions that only contain expectation values of gluon fields, the following steps are necessary.

(i) The first step is to integrate out the fermion fields. They appear in the matrix elements of $H^{(1)}$ and $H^{(2)}$ either in the states [see Eq. (198)] or in the Hamiltonian itself as two- or four-fermion interaction terms. In the first case, we have, for instance,

$$\begin{aligned} &{}^{(0)} \langle \underline{n}; \mathbf{x}_1, \mathbf{x}_2 | \int d^3 \xi \psi^\dagger(\xi) O(\xi) \psi(\xi) | \underline{m}; \mathbf{y}_1, \mathbf{y}_2 \rangle^{(0)} \\ &= {}^{(0)} \langle n; \mathbf{x}_1, \mathbf{x}_2 | O(\mathbf{x}_1) | m; \mathbf{x}_1, \mathbf{x}_2 \rangle^{(0)} \delta^{(3)}(\mathbf{x}_1 - \mathbf{y}_1) \\ &\times \delta^{(3)}(\mathbf{x}_2 - \mathbf{y}_2), \end{aligned} \quad (231)$$

in the second case

$$\begin{aligned} &{}^{(0)} \langle \underline{n}; \mathbf{x}_1, \mathbf{x}_2 | \int d^3 \xi \psi^\dagger(\xi) O_A(\xi) \psi(\xi) \chi_c^\dagger(\xi) O_B(\xi) \chi_c(\xi) \\ &\times | \underline{m}; \mathbf{y}_1, \mathbf{y}_2 \rangle^{(0)} \\ &= \delta^{(3)}(\mathbf{x}_1 - \mathbf{x}_2) {}^{(0)} \langle n; \mathbf{x}_1, \mathbf{x}_2 | O_A(\mathbf{x}_1) O_B(\mathbf{x}_2) \\ &\times | m; \mathbf{x}_1, \mathbf{x}_2 \rangle^{(0)} \delta^{(3)}(\mathbf{x}_1 - \mathbf{y}_1) \delta^{(3)}(\mathbf{x}_2 - \mathbf{y}_2), \end{aligned} \quad (232)$$

where O , O_A , and O_B are combinations of gluon fields. In the last case, the interaction is local [$\sim \delta^{(3)}(\mathbf{r})$]. At this stage, the expressions only contain matrix elements of gluon fields on the pure gluonic states $|n; \mathbf{x}_1, \mathbf{x}_2 \rangle^{(0)} \equiv |n \rangle^{(0)}$. At this point, it is also possible to use the Gauss law (197). It allows us to write all the terms of the type $[\mathbf{D}, g\mathbf{E}]$ in terms of $\delta^{(3)}(\mathbf{r})$ times some color matrices, up

²³A similar approach has been used by Szczepaniak and Swanson (1997) in order to derive, from the QCD Hamiltonian in the Coulomb gauge, the spin-dependent part of the potential up to $\mathcal{O}(1/m^2)$.

to terms proportional to $\delta^{(3)}(\mathbf{0})$ that vanish in DR. We shall assume this regularization scheme from now on.

(ii) Further simplifications may be achieved using the identities [$F_{1,2} \equiv F(\mathbf{x}_{1,2})$]

$${}^{(0)}\langle n|\mathbf{D}_1|n\rangle^{(0)} = \nabla_1, \quad {}^{(0)}\langle n|\mathbf{D}_{c2}|n\rangle^{(0)} = \nabla_2, \quad (233)$$

$${}^{(0)}\langle n|\mathbf{D}_1|j\rangle^{(0)} = \frac{{}^{(0)}\langle n|g\mathbf{E}_1|j\rangle^{(0)}}{E_n^{(0)} - E_j^{(0)}}, \quad (234)$$

$${}^{(0)}\langle n|\mathbf{D}_{c2}|j\rangle^{(0)} = -\frac{{}^{(0)}\langle n|g\mathbf{E}_2^T|j\rangle^{(0)}}{E_n^{(0)} - E_j^{(0)}} \quad \forall n \neq j,$$

$${}^{(0)}\langle n|g\mathbf{E}_1|n\rangle^{(0)} = -(\nabla_1 E_n^{(0)}), \quad {}^{(0)}\langle n|g\mathbf{E}_2^T|n\rangle^{(0)} = (\nabla_2 E_n^{(0)}), \quad (235)$$

where \mathbf{D}_c is the charge conjugate of \mathbf{D} . The first equality follows from symmetry considerations, the second and the third may be derived from ${}^{(0)}\langle n|[H^{(0)}, \mathbf{D}]|j\rangle^{(0)} = E_n^{(0)} {}^{(0)}\langle n|\mathbf{D}|j\rangle^{(0)} - {}^{(0)}\langle n|\mathbf{D}|j\rangle^{(0)} E_j^{(0)}$ and the canonical commutation relations.

(iii) The last step consists in rewriting the quantum-mechanical expressions in terms of Wilson-loop amplitudes. We proceed by considering an interpolating state (in the Heisenberg representation) that has a nonvanishing overlap with the ground state:

$$\psi^\dagger(\mathbf{x}_1)\phi(\mathbf{x}_1, \mathbf{x}_2)\chi_c^\dagger(\mathbf{x}_2)|\text{vac}\rangle, \quad (236)$$

where ϕ makes the above state overlap with the ground state $|0; \mathbf{x}_1, \mathbf{x}_2\rangle^{(0)}$. We use here the popular choice (107), which assumes that the ground state has the Σ_g^+ quantum numbers. We also define $\phi(\mathbf{y}, \mathbf{x}; t=0) \equiv \phi(\mathbf{y}, \mathbf{x})$. Then we have

$$\psi^\dagger(\mathbf{x}_1)\phi(\mathbf{x}_1, \mathbf{x}_2)\chi_c^\dagger(\mathbf{x}_2)|\text{vac}\rangle = \sum_n a_n(\mathbf{x}_1, \mathbf{x}_2)|\underline{n}; \mathbf{x}_1, \mathbf{x}_2\rangle^{(0)}, \quad (237)$$

or, without fermion fields,

$$\phi(\mathbf{x}_1, \mathbf{x}_2)|\text{vac}\rangle = \sum_n a_n(\mathbf{x}_1, \mathbf{x}_2)|n; \mathbf{x}_1, \mathbf{x}_2\rangle^{(0)}, \quad (238)$$

with $a_0 \neq 0$. At this point, we define the Wilson-loop average $\langle \cdots \rangle_\square \equiv \langle \cdots W_\square \rangle$. The gauge fields are, in general, localized on the static quark lines of the Wilson loop. Therefore $\langle \cdots \rangle_\square$ is gauge invariant. Inserting the identity operator $\Sigma|n\rangle^{(0)(0)}\langle n|$ into the Wilson-loop averages, from Eq. (238) it follows that

$$\langle W_\square \rangle = \sum_n e^{-iE_n^{(0)}T_W} |a_n|^2, \quad (239)$$

$$\begin{aligned} & \langle F^{(1)}(t_1) \cdots F^{(n)}(t_n) \rangle_\square \\ &= \sum_{n, m, s_1, \dots, s_{n-1}} a_n^* a_m {}^{(0)}\langle n|F^{(1)}|s_1\rangle^{(0)} \cdots {}^{(0)}\langle s_{n-1}|F^{(n)}|m\rangle^{(0)} \\ & \quad \times e^{-i(E_n^{(0)} + E_m^{(0)})(T_W/2)} e^{i(E_n^{(0)} - E_{s_1}^{(0)})t_1} \cdots e^{i(E_{s_{n-1}}^{(0)} - E_m^{(0)})t_n}, \end{aligned} \quad (240)$$

$$\begin{aligned} & \langle\langle F^{(1)}(t_1) \cdots F^{(n)}(t_n) \rangle\rangle \\ & \equiv \lim_{T_W \rightarrow \infty} \frac{\langle F^{(1)}(t_1) \cdots F^{(n)}(t_n) \rangle_\square(0)}{\langle W_\square \rangle} \\ &= \sum_{s_1, \dots, s_{n-1}} {}^{(0)}\langle 0|F^{(1)}|s_1\rangle^{(0)} \cdots {}^{(0)}\langle s_{n-1}|F^{(n)}|0\rangle^{(0)} \\ & \quad \times e^{i(E_0^{(0)} - E_{s_1}^{(0)})t_1} \cdots e^{i(E_{s_{n-1}}^{(0)} - E_0^{(0)})t_n}, \end{aligned} \quad (241)$$

where $T_W/2 \geq t_1 \geq t_2 \geq \cdots \geq t_n \geq -T_W/2$ and $F^{(n)}$ are gluon fields localized on the static Wilson loop. All the quantum-mechanical expressions obtained at the end of step (ii) may be expressed as combinations of

$$\int_0^\infty dt_1 \cdots \int_0^{t_{n-1}} dt_n t_1^{j_1} \cdots t_n^{j_n} \langle\langle F^{(1)}(t_1) \cdots F^{(n)}(t_n) \rangle\rangle_c, \quad (242)$$

where $\langle\langle \cdots \rangle\rangle_c$ stands for the connected part of $\langle\langle \cdots \rangle\rangle$.

2. Matching of the analytic terms: the real pNRQCD potential

We give here and in the following section the explicit formulas for the part of the pNRQCD potential that is analytic in $1/m$. For the real part, we give formulas up to (and including) order $1/m^2$, for the imaginary part up to (and including) order $1/m^4$. The formulas are given in four dimensions. Divergences have been regularized, if necessary, in DR. We have explicitly used the Gauss-law constraint (197). Note that we would need to generalize these formulas to d dimensions to work in a MS-like scheme and consistently use the same scheme used for renormalizing the NRQCD matching coefficients.

Up to (and including) order $1/m^2$, the real part of the potential $V^{1/m}$ may be written as in Eq. (63) and the $1/m^2$ potentials may be decomposed in terms of their momentum and spin content as in Eqs. (65)–(71). The different pieces are given by Brambilla, Pineda, *et al.* (2001); Pineda and Vairo (2001):

$$V^{(0)}(r) = \lim_{T_W \rightarrow \infty} \frac{i}{T_W} \ln \langle W_\square \rangle, \quad (243)$$

$$V^{(1,0)}(r) = -\frac{1}{2} \int_0^\infty dt t \langle\langle g\mathbf{E}_1(t) \cdot g\mathbf{E}_1(0) \rangle\rangle_c, \quad (244)$$

$$V^{(0,1)}(r) = V^{(1,0)}(r), \quad (245)$$

$$V_{\mathbf{p}^2}^{(2,0)}(r) = \frac{i}{2} \hat{\mathbf{r}}^i \hat{\mathbf{r}}^j \int_0^\infty dt t^2 \langle\langle g\mathbf{E}_1^i(t) g\mathbf{E}_1^j(0) \rangle\rangle_c, \quad (246)$$

$$V_{\mathbf{L}^2}^{(2,0)}(r) = \frac{i}{4} (\delta^{ij} - 3\hat{\mathbf{r}}^i \hat{\mathbf{r}}^j) \int_0^\infty dt t^2 \langle\langle g\mathbf{E}_1^i(t) g\mathbf{E}_1^j(0) \rangle\rangle_c, \quad (247)$$

$$\begin{aligned} V_r^{(2,0)}(r) &= \frac{\pi C_F \alpha_s c_D^{(1)}}{2} \delta^{(3)}(\mathbf{r}) - \frac{ic_F^{(1)2}}{4} \int_0^\infty dt \langle\langle g\mathbf{B}_1(t) \cdot g\mathbf{B}_1(0) \rangle\rangle_c + \frac{1}{2} (\nabla_{\mathbf{r}}^2 V_{\mathbf{p}^2}^{(2,0)}) - \frac{i}{2} \int_0^\infty dt_1 \int_0^{t_1} dt_2 \int_0^{t_2} dt_3 (t_2 - t_3)^2 \\ &\quad \times \langle\langle g\mathbf{E}_1(t_1) \cdot g\mathbf{E}_1(t_2) g\mathbf{E}_1(t_3) \cdot g\mathbf{E}_1(0) \rangle\rangle_c + \frac{1}{2} \left(\nabla_{\mathbf{r}}^i \int_0^\infty dt_1 \int_0^{t_1} dt_2 (t_1 - t_2)^2 \langle\langle g\mathbf{E}_1^i(t_1) g\mathbf{E}_1(t_2) \cdot g\mathbf{E}_1(0) \rangle\rangle_c \right) \\ &\quad - \frac{i}{2} (\nabla_{\mathbf{r}}^i V^{(0)}) \int_0^\infty dt_1 \int_0^{t_1} dt_2 (t_1 - t_2)^3 \langle\langle g\mathbf{E}_1^i(t_1) g\mathbf{E}_1(t_2) \cdot g\mathbf{E}_1(0) \rangle\rangle_c + \frac{1}{4} \left(\nabla_{\mathbf{r}}^i \int_0^\infty dt t^3 \langle\langle g\mathbf{E}_1^i(t) g\mathbf{E}_1^j(0) \rangle\rangle_c (\nabla_{\mathbf{r}}^j V^{(0)}) \right) \\ &\quad - \frac{i}{12} \int_0^\infty dt t^4 \langle\langle g\mathbf{E}_1^i(t) g\mathbf{E}_1^j(0) \rangle\rangle_c (\nabla_{\mathbf{r}}^i V^{(0)}) (\nabla_{\mathbf{r}}^j V^{(0)}) - \frac{c_1^{g(1)}}{4} f_{abc} \int d^3\mathbf{x} \langle\langle gG_{\mu\nu}^a(x) G_{\mu\alpha}^b(x) G_{\nu\alpha}^c(x) \rangle\rangle, \end{aligned} \quad (248)$$

$$V_{\mathbf{p}^2}^{(0,2)}(r) = V_{\mathbf{p}^2}^{(2,0)}(r), \quad V_{\mathbf{L}^2}^{(0,2)}(r) = V_{\mathbf{L}^2}^{(2,0)}(r), \quad V_r^{(0,2)}(r) = V_r^{(2,0)}(r; m_2 \leftrightarrow m_1), \quad (249)$$

$$V_{\mathbf{p}^2}^{(1,1)}(r) = i \hat{\mathbf{r}}^i \hat{\mathbf{r}}^j \int_0^\infty dt t^2 \langle\langle g\mathbf{E}_1^i(t) g\mathbf{E}_2^j(0) \rangle\rangle_c, \quad (250)$$

$$V_{\mathbf{L}^2}^{(1,1)}(r) = i \frac{\delta^{ij} - 3\hat{\mathbf{r}}^i \hat{\mathbf{r}}^j}{2} \int_0^\infty dt t^2 \langle\langle g\mathbf{E}_1^i(t) g\mathbf{E}_2^j(0) \rangle\rangle_c, \quad (251)$$

$$\begin{aligned} V_r^{(1,1)}(r) &= -\frac{1}{2} (\nabla_{\mathbf{r}}^i V_{\mathbf{p}^2}^{(1,1)}) \delta^{(3)}(\mathbf{r}) - i \int_0^\infty dt_1 \int_0^{t_1} dt_2 \int_0^{t_2} dt_3 (t_2 - t_3)^2 \langle\langle g\mathbf{E}_1(t_1) \cdot g\mathbf{E}_1(t_2) g\mathbf{E}_2(t_3) \cdot g\mathbf{E}_2(0) \rangle\rangle_c \\ &\quad + \frac{1}{2} \left(\nabla_{\mathbf{r}}^i \int_0^\infty dt_1 \int_0^{t_1} dt_2 (t_1 - t_2)^2 \langle\langle g\mathbf{E}_1^i(t_1) g\mathbf{E}_2(t_2) \cdot g\mathbf{E}_2(0) \rangle\rangle_c \right) \\ &\quad + \frac{1}{2} \left(\nabla_{\mathbf{r}}^i \int_0^\infty dt_1 \int_0^{t_1} dt_2 (t_1 - t_2)^2 \langle\langle g\mathbf{E}_2^i(t_1) g\mathbf{E}_1(t_2) \cdot g\mathbf{E}_1(0) \rangle\rangle_c \right) \\ &\quad - \frac{i}{2} (\nabla_{\mathbf{r}}^i V^{(0)}) \int_0^\infty dt_1 \int_0^{t_1} dt_2 (t_1 - t_2)^3 \langle\langle g\mathbf{E}_1^i(t_1) g\mathbf{E}_2(t_2) \cdot g\mathbf{E}_2(0) \rangle\rangle_c - \frac{i}{2} (\nabla_{\mathbf{r}}^i V^{(0)}) \int_0^\infty dt_1 \int_0^{t_1} dt_2 (t_1 \\ &\quad - t_2)^3 \langle\langle g\mathbf{E}_2^i(t_1) g\mathbf{E}_1(t_2) \cdot g\mathbf{E}_1(0) \rangle\rangle_c + \frac{1}{4} \left(\nabla_{\mathbf{r}}^i \int_0^\infty dt t^3 \{ \langle\langle g\mathbf{E}_1^i(t) g\mathbf{E}_2^j(0) \rangle\rangle_c + \langle\langle g\mathbf{E}_2^i(t) g\mathbf{E}_1^j(0) \rangle\rangle_c \} (\nabla_{\mathbf{r}}^j V^{(0)}) \right) \\ &\quad - \frac{i}{6} \int_0^\infty dt t^4 \langle\langle g\mathbf{E}_1^i(t) g\mathbf{E}_2^j(0) \rangle\rangle_c (\nabla_{\mathbf{r}}^i V^{(0)}) (\nabla_{\mathbf{r}}^j V^{(0)}), - \frac{C_A}{2} [\text{Re } f_1(^1S_0) + 3 \text{Re } f_1(^3S_1)] \delta^{(3)}(\mathbf{r}), \end{aligned} \quad (252)$$

$$V_{LS}^{(2,0)}(r) = -\frac{c_F^{(1)}}{r^2} i\mathbf{r} \cdot \int_0^\infty dt t \langle\langle g\mathbf{B}_1(t) \times g\mathbf{E}_1(0) \rangle\rangle + \frac{c_S^{(1)}}{2r^2} \mathbf{r} \cdot (\nabla_{\mathbf{r}} V^{(0)}), \quad (253)$$

$$V_{LS}^{(0,2)}(r) = V_{LS}^{(2,0)}(r; m_2 \leftrightarrow m_1), \quad (254)$$

$$V_{L_2 S_1}^{(1,1)}(r) = -\frac{c_F^{(1)}}{r^2} i\mathbf{r} \cdot \int_0^\infty dt t \langle\langle g\mathbf{B}_1(t) \times g\mathbf{E}_2(0) \rangle\rangle, \quad (255)$$

$$V_{L_1 S_2}^{(1,1)}(r) = V_{L_2 S_1}^{(1,1)}(r; m_1 \leftrightarrow m_2), \quad (256)$$

$$V_{S^2}^{(1,1)}(r) = \frac{2c_F^{(1)}c_F^{(2)}}{3}i \int_0^\infty dt \langle\langle \mathbf{g}\mathbf{B}_1(t) \cdot \mathbf{g}\mathbf{B}_2(0) \rangle\rangle + 2C_A[\text{Re} f_1(^1S_0) - \text{Re} f_1(^3S_1)]\delta^{(3)}(\mathbf{r}), \quad (257)$$

$$V_{S_{12}}^{(1,1)}(r) = \frac{c_F^{(1)}c_F^{(2)}}{4}i\hat{\mathbf{r}}^i\hat{\mathbf{r}}^j \int_0^\infty dt \left[\langle\langle \mathbf{g}\mathbf{B}_1^i(t)\mathbf{g}\mathbf{B}_2^j(0) \rangle\rangle - \frac{\delta^{ij}}{3}\langle\langle \mathbf{g}\mathbf{B}_1(t) \cdot \mathbf{g}\mathbf{B}_2(0) \rangle\rangle \right]. \quad (258)$$

Equations (245), (249), (254), and (256) follow from invariance under simultaneous charge conjugation and $m_1 \leftrightarrow m_2$ exchange.

Equation (243) is the well-known formula that gives the static potential in terms of the static Wilson loop (Susskind, 1977; Brown and Weisberger, 1979). In the weak-coupling case, this formula requires corrections from US degrees of freedom (in that case, US gluons). Here, by assumption, we do not have other US degrees of freedom besides the heavy-quarkonium singlet field, hence there are no corrections. Once Goldstone bosons are taken into account, their contribution will eventually correct Eq. (243). With respect to the power counting, for dimensional reasons $V^{(0)}$ would count as $|\mathbf{p}|$. In Sec. VII.B we have argued, however, that the NR dynamics constrains $V^{(0)}$ to count as E . The extra suppression of order $E/|\mathbf{p}| \sim v$ has to arise on dynamical grounds. In the perturbative case, it originates from the factor $\alpha_s \sim v$ in the potential. In the nonperturbative case little can be said and some other mechanism must be responsible.

Equation (244) gives the $1/m$ corrections to the static potential. They were first calculated by Brambilla, Pineda, *et al.* (2001). In accordance with the power counting of Sec. VII.B, these corrections are of the order $\Lambda_{\text{QCD}}^2/m \sim E$ when $|\mathbf{p}| \sim \Lambda_{\text{QCD}}$. Therefore they may, in principle, be as large as the static potential. In the weak-coupling regime, the first nonvanishing contribution to $V^{(1,0)}$ is of order α_s^2 and gives $V^{(1,0)}(r) = -C_F C_A \alpha_s^2 / 4r^2$, which is suppressed by α_s^2 with respect to the static potential.

Equations (246), (247), (250), and (251) are momentum-dependent $1/m^2$ potentials. They were first derived using a quantum-mechanical path-integral approach by Barchielli *et al.* (1988). Equations (248) and (252) are momentum- and spin-independent $1/m^2$ potentials. Their calculation was first done by Pineda and Vairo (2001). Note that they are necessary in order to solve the ordering ambiguity that plagues the calculation of the momentum-dependent potentials. The momentum- and spin-independent $1/m^2$ potentials also depend on some of the matching coefficients of NRQCD. The last term of Eq. (248) comes from the $1/m^2$ corrections to the Yang-Mills Lagrangian of NRQCD. It is somehow different from the other terms since the fields are not localized on the Wilson-loop lines. Moreover, it exhibits a fictitious dependence on the time at which the operator insertion is made, which disappears in the limit $T_W \rightarrow \infty$. However, the term is not as peculiar as it may at first appear if we notice that $V^{(0)}$

could also be written in a similar way: $V^{(0)} = \frac{1}{2} \int d^3\mathbf{x} \langle\langle (\mathbf{\Pi}^a \mathbf{\Pi}^a + \mathbf{B}^a \mathbf{B}^a)(x) \rangle\rangle$.

Equation (255) gives the spin-orbit, Eq. (257) the spin-spin, and Eq. (258) the spin-tensor $1/m^2$ potential. These potentials were first derived, by Eichten and Feinberg (1981), in the approach that we discuss in Sec. VII.E.4 and rederived later by several authors in similar or different approaches, for instance, by Peskin (1983); Gromes (1984); Barchielli *et al.* (1988). None of the early derivations included the NRQCD matching coefficients, which were first included by Chen *et al.* (1995); see also Brambilla and Vairo (1999b). Pineda and Vairo (2001) corrected an error in the formula of the spin-orbit potential $V_{L_2 S_1}^{(1,1)}$ that can be found in the original papers (Eichten and Feinberg, 1981; Gromes, 1984; Barchielli *et al.*, 1988; Chen *et al.*, 1995). For a detailed analysis and comments on this, see Brambilla, Gromes, and Vairo (2001) and Pineda and Vairo (2001).

In the $|\mathbf{p}| \sim \Lambda_{\text{QCD}}$ regime, the leading terms contributing to the $1/m^2$ potentials are of the order Λ_{QCD}^3/m . Not all the terms contribute, however, to the same order. Terms involving $\nabla_{\mathbf{r}} V^{(0)}$ have an extra $\mathcal{O}(v)$ suppression coming from the specific counting of $V^{(0)}$. Terms involving matching coefficients of NRQCD also have an expansion in α_s . Since the matching coefficients of the four-fermion and of the pure Yang-Mills operators of NRQCD start at order α_s , terms involving them are suppressed by a factor α_s . In particular, if we consider the potentials with more terms, $V_r^{(2,0)}$ and $V_r^{(1,1)}$, only the terms in the first two and three lines listed in Eqs. (248) and (252), respectively, are expected to contribute at LO. In the weak-coupling regime, there is an extra α_s suppression coming from the g^2 in the Wilson-loop amplitudes and the $1/m^2$ potentials give the familiar $m\alpha_s^4$ relativistic, fine, and hyperfine corrections to the perturbative spectrum.

The Poincaré invariance constraints (86) become in the present case with different masses

$$V_{LS}^{(2,0)}(r) - V_{L_2 S_1}^{(1,1)}(r) + \frac{V^{(0)'}(r)}{2r} = 0, \quad (259)$$

$$V_{L^2}^{(2,0)}(r) + V_{L^2}^{(0,2)}(r) - V_{L^2}^{(1,1)}(r) + \frac{r}{2} V^{(0)'}(r) = 0, \quad (260)$$

$$-2[V_{\mathbf{p}^2}^{(2,0)}(r) + V_{\mathbf{p}^2}^{(0,2)}(r)] + 2V_{\mathbf{p}^2}^{(1,1)}(r) - V^{(0)}(r) + rV^{(0)'}(r) = 0. \quad (261)$$

These are general symmetry relations, independent of the dynamics. However, due to the potentials given above, they now impose specific relations among the Wilson-loop amplitudes and the matching coefficients of NRQCD, which can be tested independently. Taking at tree level the NRQCD matching coefficients, Eq. (259) was proved by Gromes (1984), and Eqs. (260) and (261) by Barchielli *et al.* (1990). A way to proceed is the following (Brambilla, Gromes, and Vairo, 2001). Consider a chromoelectric- or a chromomagnetic-field insertion in a static Wilson loop and then apply an infinitesimal Lorentz boost with velocity \mathbf{v} . The following identities hold:

$$\langle\langle g\mathbf{B}(\mathbf{x}_1, t) \rangle\rangle^{\text{boosted}} + \langle\langle [\mathbf{v} \times g\mathbf{E}(\mathbf{x}_1, t)] \rangle\rangle^{\text{boosted}} - \langle\langle g\mathbf{B}(\mathbf{x}_1, t) \rangle\rangle = 0, \quad (262)$$

$$\langle\langle ig\hat{\mathbf{v}} \cdot \mathbf{E}(\mathbf{x}_1, t) \rangle\rangle - \langle\langle ig\hat{\mathbf{v}} \cdot \mathbf{E}(\mathbf{x}_1, t) \rangle\rangle^{\text{boosted}} = 0. \quad (263)$$

Expanding both equations at order v and v^2 , respectively, and considering that the difference between the boosted and the static Wilson loop corresponds to insertions of chromoelectric fields, we obtain from the first equation

$$-i \int_0^\infty dt [\langle\langle g\mathbf{B}(\mathbf{x}_1, t) \times g\mathbf{E}(\mathbf{x}_1, 0) \rangle\rangle - \langle\langle g\mathbf{B}(\mathbf{x}_1, t) \times g\mathbf{E}(\mathbf{x}_2, 0) \rangle\rangle] + \hat{\mathbf{v}}V^{(0)'}(r) = 0, \quad (264)$$

and from the second equations (260) and (261). These relations have also been tested on the lattice, as we shall discuss in Sec. VII.G.

Finally, we emphasize that the freedom we noticed at the level of NRQCD to perform a unitary transformation of the states and energies, Eqs. (229) and (230), is obviously preserved at the level of pNRQCD. The effect of a unitary field redefinition U of the singlet field is to transform $h_s \rightarrow U^\dagger h_s U$, where h_s is the pNRQCD Hamiltonian. This means that no special physical meaning is associated with a single potential term, which may be reshuffled into another by means of a suitable unitary transformation. In other words, unlike physical observables, which are unambiguous, potentials depend on the specific scheme adopted. The potentials listed in Eqs. (243)–(258) are given in the scheme defined by Eq. (228), which fixes the relative phase to 1 between $|\underline{n}; \mathbf{x}_1, \mathbf{x}_2\rangle$ and $|\underline{n}; \mathbf{x}_1, \mathbf{x}_2\rangle^{(0)}$. We refer the reader to Brambilla, Pineda, *et al.* (2001); see also Brambilla, Gromes, and Vairo (2001) for more details.

3. Matching of the analytic terms: the imaginary pNRQCD potential

Let us consider heavy quarkonia made of a quark and an antiquark of the same flavor ($m_1 = m_2 = m$). Annihilation

processes happen in QCD at the scale of the mass m . Integrating them out in the matching from QCD to NRQCD gives rise to imaginary contributions to the four-fermion matching coefficients. Under the assumptions that led to Eq. (216), they are the only source of contribution to the imaginary pNRQCD Hamiltonian, which can be calculated in the same way as the real part. In practice, the calculation reduces to picking up from the right-hand side of Eq. (225) only contributions that involve four-fermion operators.

From the above general considerations, the imaginary part of the potential $V^{1/m}$ is

$$\text{Im } V^{1/m} = \frac{\text{Im } V^{(2)}}{m^2} + \frac{\text{Im } V^{(4)}}{m^4} + \dots \quad (265)$$

The functions $\text{Im } V^{(2)}$ and $\text{Im } V^{(4)}$ encode the information from the dimension-6 and the dimension-8 four-fermion operators of NRQCD, respectively. They will have the following structure:

$$(\text{spin}) \times (\text{delta}) \times (\text{Im } f) \times (\text{nonperturbative matrix element}). \quad (266)$$

The first factor, which is one of the projectors (77)–(81), accounts for the spin structure. The second is a delta function or (for $\text{Im } V^{(n>2)}$) consists of derivatives of delta functions due to the fact that the four-fermion operators are local. The third is the imaginary part of a four-fermion matching coefficient of NRQCD. Note that, in general, the potential may also depend on some real matching coefficients of NRQCD. Finally, the last term is a matrix element that contains all soft gluons integrated out from NRQCD. These matrix elements are Wilson amplitudes, similar to those that appear in the real part of the pNRQCD potentials, taken in the $r \rightarrow 0$ limit due to the delta function. In other words, they are nonlocal (in time) correlators of gluonic fields F : $\langle F^{(1)}(t_1, \mathbf{0}) \phi(t_1, t_2) \dots F^{(n)}(t_n, \mathbf{0}) \phi(t_n, t_1) \rangle$. In the following we omit the Wilson lines ϕ connecting the fields and the spatial location of the fields which are irrelevant. The correlators that show up at order $1/m^2$ and $1/m^4$ are encoded in the nonperturbative parameters \mathcal{E}_1 , \mathcal{E}_3 , \mathcal{B}_1 , $\mathcal{E}_3^{(2,t)}$, and $\mathcal{E}_3^{(2,EM)}$, where

$$\mathcal{E}_n \equiv \frac{1}{N_c} \int_0^\infty dt t^n \langle g\mathbf{E}(t) \cdot g\mathbf{E}(0) \rangle, \quad (267)$$

$$\mathcal{B}_n \equiv \frac{1}{N_c} \int_0^\infty dt t^n \langle g\mathbf{B}(t) \cdot g\mathbf{B}(0) \rangle,$$

and the definitions of $\mathcal{E}_3^{(2,t)}$ and $\mathcal{E}_3^{(2,EM)}$, which involve four chromoelectric fields, can be found in the article by Brambilla, Eiras, *et al.* (2003).

The explicit expression for $\text{Im } V^{(2)}$ is equal to Eq. (75), while $\text{Im } V^{(4)}$ is given by Brambilla, Eiras, *et al.* (2002, 2003):

$$\begin{aligned}
\text{Im } V^{(4)} = & C_A T_{Sj}^{ij} \nabla_{\mathbf{r}}^i \delta^{(3)}(\mathbf{r}) \nabla_{\mathbf{r}}^j [\text{Im } f_1^{(2S+1)P_J} + \text{Im } f_{\text{EM}}^{(2S+1)P_J}] + \frac{C_A}{2} \Omega_{Sj}^{ij} \left\{ \nabla_{\mathbf{r}}^i \nabla_{\mathbf{r}}^j + \frac{\delta_{ij}}{3} \mathcal{E}_1, \delta^{(3)}(\mathbf{r}) \right\} [\text{Im } g_1^{(2S+1)S_J} \\
& + \text{Im } g_{\text{EM}}^{(2S+1)S_J}] + \frac{T_F}{3} T_{Sj}^{ii} \delta^{(3)}(\mathbf{r}) \text{Im } f_8^{(2S+1)P_J} \mathcal{E}_1 + \frac{T_F}{9} \nabla_{\mathbf{r}} \delta^{(3)}(\mathbf{r}) \nabla_{\mathbf{r}} \{ 4 \text{Im } f_8^{(1)S_0} - 2\mathbf{S}^2 [\text{Im } f_8^{(1)S_0} \\
& - \text{Im } f_8^{(3)S_1}] \} \mathcal{E}_3 + 2T_F c_F^2 \delta^{(3)}(\mathbf{r}) \left(\text{Im } f_8^{(3)S_1} + \frac{1}{6} \mathbf{S}^2 [\text{Im } f_8^{(1)S_0} - 3 \text{Im } f_8^{(3)S_1}] \right) \mathcal{B}_1 + \frac{T_F}{3} \delta^{(3)}(\mathbf{r}) \{ 4 \text{Im } f_8^{(1)S_0} \\
& - 2\mathbf{S}^2 [\text{Im } f_8^{(1)S_0} - \text{Im } f_8^{(3)S_1}] \} \mathcal{E}_3^2 - \frac{C_A}{3} \delta^{(3)}(\mathbf{r}) \{ 4 \text{Im } f_1^{(1)S_0} - 2\mathbf{S}^2 [\text{Im } f_1^{(1)S_0} - \text{Im } f_1^{(3)S_1}] \} \mathcal{E}_3^{(2,t)} \\
& - C_A \frac{2}{9} \{ \nabla_{\mathbf{r}}^2, \delta^{(3)}(\mathbf{r}) \} \left(\text{Im } f_1^{(1)S_0} + \text{Im } f_{\text{EM}}^{(1)S_0} + \frac{\mathbf{S}^2}{2} [\text{Im } f_1^{(3)S_1} - \text{Im } f_1^{(1)S_0} + \text{Im } f_{\text{EM}}^{(3)S_1} - \text{Im } f_{\text{EM}}^{(1)S_0}] \right) \mathcal{E}_3 \\
& - 2C_A c_F^2 \delta^{(3)}(\mathbf{r}) \left(\text{Im } f_1^{(1)S_0} + \text{Im } f_{\text{EM}}^{(1)S_0} + \frac{\mathbf{S}^2}{6} [\text{Im } f_1^{(3)S_1} - 3 \text{Im } f_1^{(1)S_0} + \text{Im } f_{\text{EM}}^{(3)S_1} - 3 \text{Im } f_{\text{EM}}^{(1)S_0}] \right) \mathcal{B}_1 \\
& - \frac{C_A}{3} \delta^{(3)}(\mathbf{r}) \{ 4 \text{Im } f_{\text{EM}}^{(1)S_0} - 2\mathbf{S}^2 [\text{Im } f_{\text{EM}}^{(1)S_0} - \text{Im } f_{\text{EM}}^{(3)S_1}] \} \mathcal{E}_3^{(2,\text{EM})}. \tag{268}
\end{aligned}$$

Note that there are more terms in Eq. (268) than in Eq. (76) due to the nonperturbative counting. Similar to the real case, the quantities $\text{Im } V^{(2)}$, $\text{Im } V^{(4)}$, ... are defined up to unitary transformations. A discussion and an explicit example may be found in the article of Brambilla, Eiras, *et al.* (2003).

4. Matching of the analytic terms: direct matching of Wilson-loop amplitudes

In the previous sections we performed the matching to pNRQCD first by deriving quantum-mechanical expressions, then by translating them into Wilson-loop amplitudes. Hence one may wonder whether it would be possible to directly perform the matching to Wilson-loop amplitudes. This is possible and simply requires applying to the strong-coupling regime the Wilson-loop matching used in Sec. IV.F for the weak-coupling regime. The only difference will be that no US corrections have to be subtracted from the Wilson-loop amplitudes in this case. It should be noted that historically the first derivation of some of the heavy-quarkonium potentials was done by direct computation of Wilson-loop amplitudes, namely, the static potential (Susskind, 1977; Brown and Weisberger, 1979) the $1/m^2$ spin-dependent potentials (Eichten and Feinberg, 1981; Gromes, 1984), and the $\mathbf{p}^i \mathbf{p}^j / m^2$ spin-independent potentials (Barchielli *et al.*, 1988). We now (re)derive the heavy-quarkonium potential up to (and including) order $1/m$ by directly matching Wilson-loop amplitudes to pNRQCD Green's functions (Brambilla, Pineda, *et al.*, 2001).

Let us consider the following Green's function of NRQCD:

$$\begin{aligned}
G_{\text{NRQCD}} = & \langle \text{vac} | \chi_c(\mathbf{x}_2, T_W/2) \phi(\mathbf{x}_2, \mathbf{x}_1; T_W/2) \psi(\mathbf{x}_1, T_W/2) \\
& \times \psi^\dagger(\mathbf{y}_1, -T_W/2) \phi(\mathbf{y}_1, \mathbf{y}_2; -T_W/2) \\
& \times \chi_c^\dagger(\mathbf{y}_2, -T_W/2) | \text{vac} \rangle. \tag{269}
\end{aligned}$$

Expanding G_{NRQCD} order by order in $1/m$, $G_{\text{NRQCD}} = G_{\text{NRQCD}}^{(0)} + (1/m_1) G_{\text{NRQCD}}^{(1,0)} + (1/m_2) G_{\text{NRQCD}}^{(0,1)} + \dots$, and integrating out the fermion fields we obtain

$$G_{\text{NRQCD}}^{(0)} = \langle W_\square \rangle \delta^{(3)}(\mathbf{x}_1 - \mathbf{y}_1) \delta^{(3)}(\mathbf{x}_2 - \mathbf{y}_2), \tag{270}$$

$$G_{\text{NRQCD}}^{(1,0)} = \frac{i}{2} \int_{-T_W/2}^{T_W/2} dt \langle \mathbf{D}_1^2(t) \rangle_\square \delta^{(3)}(\mathbf{x}_1 - \mathbf{y}_1) \delta^{(3)}(\mathbf{x}_2 - \mathbf{y}_2). \tag{271}$$

For simplicity we shall not display here and in the following the analogous formulas for $G_{\text{NRQCD}}^{(0,1)}$. From time reversal it follows that $\langle \mathbf{B}_1(t) \rangle_\square = -\langle \mathbf{B}_1(-t) \rangle_\square$, which eliminates the spin-dependent term in Eq. (271). After some algebra it follows that

$$\begin{aligned}
G_{\text{NRQCD}}^{(1,0)} = & \frac{i}{2} \left\{ \frac{T_W}{2} \nabla_{\mathbf{x}_1}^2 \langle W_\square \rangle + \frac{T_W}{2} \langle W_\square \rangle \nabla_{\mathbf{x}_1}^2 \right. \\
& + T_W \langle \mathbf{O}_f(T_W/2) \cdot \mathbf{O}_i(-T_W/2) \rangle_\square \\
& + ig \int_{-T_W/2}^{T_W/2} dt \left(\frac{T_W}{2} - t \right) \langle \mathbf{O}_f(T_W/2) \cdot \mathbf{E}(t) \rangle_\square \\
& - ig \int_{-T_W/2}^{T_W/2} dt \left(\frac{T_W}{2} + t \right) \langle \mathbf{E}(t) \cdot \mathbf{O}_i(-T_W/2) \rangle_\square \\
& + \frac{g^2}{2} \int_{-T_W/2}^{T_W/2} dt \int_{-T_W/2}^{T_W/2} dt' |t - t'| \\
& \left. \times \langle \mathbf{E}(t) \cdot \mathbf{E}(t') \rangle_\square \right\} \delta^{(3)}(\mathbf{x}_1 - \mathbf{y}_1) \delta^{(3)}(\mathbf{x}_2 - \mathbf{y}_2), \tag{272}
\end{aligned}$$

where the explicit form of the operators \mathbf{O}_i and \mathbf{O}_f does not matter here and can be found in the article by Brambilla, Pineda, *et al.* (2001).

As discussed in the previous section, the state $\psi^\dagger(\mathbf{x}_1)\phi(\mathbf{x}_1, \mathbf{x}_2)\chi_c^\dagger(\mathbf{x}_2)|\text{vac}\rangle$ has a nonvanishing overlap with the NRQCD ground state $|\mathcal{0}; \mathbf{x}_1, \mathbf{x}_2\rangle$:

$$Z^{1/2}(\mathbf{x}_1, \mathbf{x}_2, -i\nabla_{\mathbf{x}_1}, -i\nabla_{\mathbf{x}_2})\delta^{(3)}(\mathbf{x}_1 - \mathbf{y}_1)\delta^{(3)}(\mathbf{x}_2 - \mathbf{y}_2) = \langle \text{vac} | \chi_c(\mathbf{x}_2)\phi(\mathbf{x}_2, \mathbf{x}_1)\psi(\mathbf{x}_1) | \mathcal{0}; \mathbf{y}_1, \mathbf{y}_2 \rangle. \quad (273)$$

Since we are only interested in the analytic terms in $1/m$, the normalization factor Z may also be expanded in $1/m$:

$$Z(\mathbf{x}_1, \mathbf{x}_2, -i\nabla_{\mathbf{x}_1}, -i\nabla_{\mathbf{x}_2}) = Z^{(0)}(r) + \left(\frac{1}{m_1} + \frac{1}{m_2} \right) Z^{(1)}(r) + iZ^{(1,p)}(r) \times \mathbf{r} \cdot \left(\frac{-i\nabla_{\mathbf{x}_1}}{m_1} - \frac{-i\nabla_{\mathbf{x}_2}}{m_2} \right) + \dots \quad (274)$$

The NRQCD ground state is the degree of freedom that we identify with the singlet field of pNRQCD. Therefore

the Green's function in pNRQCD that matches G_{NRQCD} is

$$G_{\text{pNRQCD}} = \langle \text{vac} | Z^{1/2}(\mathbf{x}_1, \mathbf{x}_2, -i\nabla_{\mathbf{x}_1}, -i\nabla_{\mathbf{x}_2}) \times S(\mathbf{x}_1, \mathbf{x}_2, T_W/2) S^\dagger(\mathbf{y}_1, \mathbf{y}_2, -T_W/2) \times Z^{\dagger 1/2}(\mathbf{y}_1, \mathbf{y}_2, -i\nabla_{\mathbf{y}_1}, -i\nabla_{\mathbf{y}_2}) | \text{vac} \rangle = Z^{1/2} e^{-iT_W h_s} Z^{\dagger 1/2} \delta^{(3)}(\mathbf{x}_1 - \mathbf{y}_1) \delta^{(3)}(\mathbf{x}_2 - \mathbf{y}_2). \quad (275)$$

Matching Eq. (275) with Eq. (269) we obtain at $\mathcal{O}(1/m^0)$

$$V^{(0)} = \lim_{T_W \rightarrow \infty} \frac{i}{T_W} \ln \langle W_\square \rangle, \quad (276)$$

$$\ln Z^{(0)} = \lim_{T_W \rightarrow \infty} (\ln \langle W_\square \rangle + iV^{(0)} T_W). \quad (277)$$

Equation (276) coincides with Eq. (243) and is equivalent (up to US corrections) to the weak-coupling result of Sec. IV.F.2. Matching at $\mathcal{O}(1/m)$ we obtain

$$V^{(1,0)} + \frac{1}{2} (\nabla_{\mathbf{r}} V^{(0)}) \cdot \mathbf{r} \frac{Z^{(1,p)}}{Z^{(0)}} = \lim_{T_W \rightarrow \infty} \left\{ -\frac{1}{8} \left(\frac{(\nabla_{\mathbf{r}} Z^{(0)})}{Z^{(0)}} \right)^2 + i \frac{T_W (\nabla_{\mathbf{r}} Z^{(0)})}{4 Z^{(0)}} \cdot (\nabla_{\mathbf{r}} V^{(0)}) + \frac{T_W^2 (\nabla_{\mathbf{r}} V^{(0)})^2}{12} - \frac{g}{4} \int_{-T_W/2}^{T_W/2} dt \left[\left(1 - \frac{2t}{T_W} \right) \times \frac{\langle \mathbf{O}(T_W/2) \cdot \mathbf{E}(t) \rangle_\square}{\langle W_\square \rangle} - \left(1 + \frac{2t}{T_W} \right) \frac{\langle \mathbf{E}(t) \cdot \mathbf{O}_i(-T_W/2) \rangle_\square}{\langle W_\square \rangle} \right] - \frac{1}{2} \frac{\langle \mathbf{O}(T_W/2) \mathbf{O}_i(-T_W/2) \rangle_\square}{\langle W_\square \rangle} - \frac{g^2}{4T_W} \int_{-T_W/2}^{T_W/2} dt \int_{-T_W/2}^{T_W/2} dt' |t - t'| \frac{\langle \mathbf{E}(t) \cdot \mathbf{E}(t') \rangle_\square}{\langle W_\square \rangle} \right\}. \quad (278)$$

From Eq. (278) we cannot disentangle $V^{(1,0)}$ from $Z^{(1,p)}$. This reflects, in the framework of the Wilson-loop matching, the freedom to perform unitary field redefinitions on the pNRQCD Lagrangian. Indeed, the Green's function (275) does not uniquely define h_s , but only up to a unitary transformation of Z and h_s . Note that Eq. (273) allows one to calculate $Z^{(1,p)}$ only after a procedure that fixes $|\mathcal{0}; \mathbf{x}_1, \mathbf{x}_2\rangle$, which is defined up to a transformation (229), has been given. A possible choice of $Z^{(1,p)}$ is the one that fixes $V^{(1,0)}$ to the value found in Eq. (244). Here this choice appears arbitrary and no obvious criteria to prefer it seem to be at hand. Naturally, the same result would follow by calculating $Z^{(1,p)}$ from Eq. (273) with the ‘‘quantum-mechanical’’ procedure (228).

In the same way we perform the matching at order $1/m^2$. In that case, the Wilson amplitude to match would be the sum of all amplitudes made by an insertion of a $1/m^2$ or of two $1/m$ NRQCD operators. In order to fix the ambiguity between Z and h_s at order $1/m^2$, some prescription for the $1/m^2$ terms in Z is required. Again we have no obvious criteria to guide us. However, with a suitable choice we would reproduce the potentials (246)–(258).

In concluding, we remark that there appear to be some advantages in using the quantum-mechanical matching rather than the direct matching of Wilson-loop amplitudes. The first one is that it provides a natural and physical procedure for calculating the potentials and the normalization factors which works for all orders in the $1/m$ expansion. It is physical because the potentials come out independent of the initial and final interpolating fields, while dependence is encoded in the normalization factor. Moreover, the power counting is preserved. The second one is that the quantum-mechanical expressions come out manifestly finite in the large-time limit. This is not obvious for an expression similar to Eq. (278), which contains several divergent pieces that eventually cancel each other. Finally, we mention that the calculation of $V^{1/\sqrt{m}}$ using the direct matching of Wilson-loop amplitudes has not been addressed yet.

5. Matching of the nonanalytic terms

In this section, we calculate $V^{1/\sqrt{m}}$, which is the part of the potential that is nonanalytic in $1/m$. We consider real and imaginary contributions at the same time and therefore restrict ourselves to the case $m_1 = m_2 = m$. In

Sec. VII.D, we have shown that $V^{1/\sqrt{m}}$ arises from quark-antiquark pairs of relative three-momentum of order $\sqrt{m}\Lambda_{\text{QCD}}$. This momentum region shows up in loops where gluons of energy Λ_{QCD} are involved (see Fig. 16). When $p \sim \Lambda_{\text{QCD}}$, the scale $\sqrt{m}\Lambda_{\text{QCD}}$ is the largest after m and therefore the first to be integrated out from NRQCD.

Following the procedure of Brambilla, Pineda, *et al.* (2004), we go through these three steps.

(i) The first step is to make explicit at the level of NRQCD the existence of different degrees of freedom by splitting the quark (antiquark) field into two: a semihard field for the (three-momentum) fluctuations of $\mathcal{O}(\sqrt{m}\Lambda_{\text{QCD}})$, ψ_{sh} (χ_{sh}), and a potential field for the (three-momentum) fluctuations of $\mathcal{O}(p)$, ψ_p (χ_p):

$$\psi = \psi_p + \psi_{\text{sh}}, \quad \chi = \chi_p + \chi_{\text{sh}}. \quad (279)$$

The NRQCD Lagrangian then reads

$$L_{\text{NRQCD}} = L_{\text{NRQCD}}^{\text{sh}} + L_{\text{NRQCD}}^p + L_{\text{mixing}} + L_g + L_l, \quad (280)$$

where the Lagrangians $L_{\text{NRQCD}}^{\text{sh}}$ and L_{NRQCD}^p are identical to the NRQCD Lagrangian expressed in terms of semihard and potential fields, respectively, the quantities L_g and L_l are the NRQCD Lagrangians for gluons and light quarks, respectively, and L_{mixing} contains the mixing terms.

(ii) The second step is to integrate out gluons and quarks of energy or three-momentum of $\mathcal{O}(\sqrt{m}\Lambda_{\text{QCD}})$. This leads to the EFT NRQCD':

$$\begin{aligned} L_{\text{NRQCD}} \rightarrow L_{\text{NRQCD}'} &= L_{\text{pNRQCD}'}^{\text{sh}} + L_{\text{NRQCD}}^p \\ &+ \text{Re } L_{\text{mixing}}^{(0)} + \text{Im } L_{\text{mixing}}^{(0)} \\ &+ \text{Re } L_{\text{mixing}}^{(1)} + \dots + L_g + L_l. \end{aligned} \quad (281)$$

Let us discuss the different terms.

(ii.a) $L_{\text{pNRQCD}'}^{\text{sh}}$ comes from integrating out gluons and quarks of energy or three-momentum of $\mathcal{O}(\sqrt{m}\Lambda_{\text{QCD}})$ from $L_{\text{NRQCD}}^{\text{sh}}$. The scale $\sqrt{m}\Lambda_{\text{QCD}} \gg \Lambda_{\text{QCD}}$ is perturbative and therefore we can use weak-coupling techniques. If we further project onto the quark-antiquark sector, the Lagrangian $L_{\text{pNRQCD}'}^{\text{sh}}$ will formally coincide with Eq. (60). The multipole-expanded gluons in $L_{\text{pNRQCD}'}^{\text{sh}}$ have (four-) momentum much smaller than $\sqrt{m}\Lambda_{\text{QCD}}$.

(ii.b) In order to simplify the calculation of L_{mixing} , we assume

$$\sqrt{m}\Lambda_{\text{QCD}} \gg m\alpha_s(\sqrt{m}\Lambda_{\text{QCD}}), \quad (282)$$

which implies that whenever a momentum of order $\sqrt{m}\Lambda_{\text{QCD}}$ flows into a Coulomb potential (note that at the scale $\sqrt{m}\Lambda_{\text{QCD}}$ the potential is perturbative), the potential can be expanded about the kinetic energy. If this is not the case, then a Coulomb resummation is needed. Here we avoid the technical complications connected with this case. However, there may be situations in

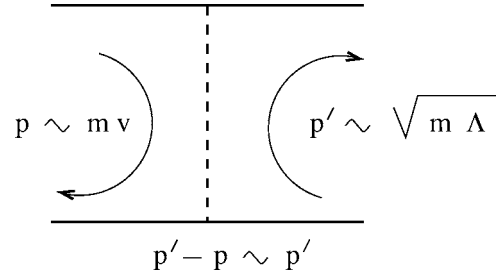


FIG. 17. The Coulomb-exchange graph contributing to the leading mixing interaction between semihard and potential fields.

which this cannot be avoided. For instance, this may be the case for the Y system if the following attribution of scales holds for the $Y(1S)$: $p_{Y(1S)} \sim m_b \alpha_s(p_{Y(1S)})$ and $\Lambda_{\text{QCD}} \sim m_b \alpha_s^2(p_{Y(1S)})$, where $p_{Y(1S)}$ is the typical momentum transfer of the $Y(1S)$ and m_b the bottom-quark mass. In this case one would have $\sqrt{m_b \Lambda_{\text{QCD}}} \sim p_{Y(1S)}$ instead of Eq. (282).

The leading-order contribution to the real part of L_{mixing} comes from the one-Coulomb-exchange graph of Fig. 17:

$$\begin{aligned} \text{Re } L_{\text{mixing}}^{(0)} &= - \int d^3\mathbf{R} \int d^3\mathbf{r} \text{Tr} \{ J^\dagger(\mathbf{R}) V_s^{(0)}(\mathbf{r}) S_{\text{sh}}(\mathbf{R}, \mathbf{r}) \} \\ &+ \text{H.c.} - \int d^3\mathbf{R} \int d^3\mathbf{r} \text{Tr} \{ J^\dagger(\mathbf{R}) V_o^{(0)}(\mathbf{r}) \\ &\times O_{\text{sh}}(\mathbf{R}, \mathbf{r}) \} + \text{H.c.}, \end{aligned} \quad (283)$$

$$J^\dagger(\mathbf{R}) \equiv \chi_p(\mathbf{R}) \psi_p^\dagger(\mathbf{R}), \quad (284)$$

where S_{sh} and O_{sh} are semihard singlet and octet quark-antiquark fields, respectively. The potentials $V_s^{(0)}$ and $V_o^{(0)}$ are perturbative: $V_s^{(0)} = -C_F \alpha_s / r$ and $V_o^{(0)} = (1/2N_c) \alpha_s / r$. The coupling constant is calculated at the semihard scale $\sqrt{m}\Lambda_{\text{QCD}}$.

The leading contribution to the imaginary part of L_{mixing} may be read off from the imaginary part of the pNRQCD Lagrangian at order $1/m^2$ in the weak-coupling regime:

$$\begin{aligned} \text{Im } L_{\text{mixing}}^{(0)} &= - \int d^3\mathbf{R} \int d^3\mathbf{r} \text{Tr} \left\{ S_{\text{sh}}^\dagger(\mathbf{R}, \mathbf{0}) \frac{K_s}{m^2} \delta^{(3)}(\mathbf{r}) J(\mathbf{R}) \right\} \\ &+ \text{H.c.} - \int d^3\mathbf{R} \int d^3\mathbf{r} \text{Tr} \left\{ O_{\text{sh}}^\dagger(\mathbf{R}, \mathbf{0}) \frac{K_o}{m^2} \delta^{(3)}(\mathbf{r}) \right. \\ &\left. \times J(\mathbf{R}) \right\} + \text{H.c.}, \end{aligned} \quad (285)$$

where

$$\begin{aligned} K_s &= - \frac{C_A}{2} \{ 4 \text{Im } f_1(^1S_0) - 2\mathbf{S}^2 [\text{Im } f_1(^1S_0) - \text{Im } f_1(^3S_1)] \\ &+ 4 \text{Im } f_{\text{EM}}(^1S_0) - 2\mathbf{S}^2 [\text{Im } f_{\text{EM}}(^1S_0) - \text{Im } f_{\text{EM}}(^3S_1)] \}, \end{aligned} \quad (286)$$

$$K_o = -\frac{T_F}{2}\{4 \operatorname{Im} f_8(^1S_0) - 2S^2[\operatorname{Im} f_8(^1S_0) - \operatorname{Im} f_8(^3S_1)]\}. \quad (287)$$

The NLO term of the real part of L_{mixing} in the $p/\sqrt{m}\Lambda_{\text{QCD}}$ expansion is given by

$$\begin{aligned} \operatorname{Re} L_{\text{mixing}}^{(1)} = & - \int d^3\mathbf{R} \int d^3\mathbf{r} \operatorname{Tr}\{\mathbf{J}^\dagger(\mathbf{R}) \cdot \mathbf{r} V_s^{(0)}(\mathbf{r}) S_{\text{sh}}(\mathbf{R}, \mathbf{r})\} \\ & + \text{H.c.} - \int d^3\mathbf{R} \int d^3\mathbf{r} \operatorname{Tr}\{\mathbf{J}^\dagger(\mathbf{R}) \cdot \mathbf{r} V_o^{(0)}(\mathbf{r}) \\ & \times O_{\text{sh}}(\mathbf{R}, \mathbf{r})\} + \text{H.c.}, \end{aligned} \quad (288)$$

$$\mathbf{J}^\dagger(\mathbf{R}) \equiv \chi_p(\mathbf{R}) \frac{\vec{\mathbf{D}}}{2} \psi_p^\dagger(\mathbf{R}), \quad (289)$$

which can be obtained by expanding the Coulomb potential of Fig. 17 in p/p' . In a similar way higher-order terms may be obtained. Note that, as expected, the potential fields always appear as local currents in L_{mixing} .

(iii) The final step consists of integrating out degrees of freedom of $\mathcal{O}(\Lambda_{\text{QCD}})$. This leads to the pNRQCD Lagrangian (216). How to calculate the analytic part of the potential $V^{1/m}$ has been discussed in Secs. VII.E.1, VII.E.2, and VII.E.3. For the explicit computation of $V^{1/\sqrt{m}}$, we refer the reader to the work of Brambilla, Pineda, *et al.* (2004). The results for $\operatorname{Re} V^{1/\sqrt{m}}(r)$ and $\operatorname{Im} V^{-1/\sqrt{m}}(r)$ turn out to be

$$\operatorname{Re} V^{1/\sqrt{m}}(r) = (2C_F + C_A)^2 \frac{4}{3\Gamma(9/2)} \pi \alpha_s^2 \mathcal{E}_{7/2}^E \frac{\delta^{(3)}(\mathbf{r})}{m^{3/2}}, \quad (290)$$

$$\operatorname{Im} V^{1/\sqrt{m}}(r) = (2C_F + C_A) \frac{4}{3\Gamma(7/2)} K_s \alpha_s \mathcal{E}_{5/2}^E \frac{\delta^{(3)}(\mathbf{r})}{m^{5/2}}, \quad (291)$$

where, in order to avoid the phase ambiguity in the definition of the fractional power of a complex number, we have written the chromoelectric correlator of Eq. (267) in Euclidean space,

$$\mathcal{E}_n^E \equiv \frac{1}{N_c} \int_0^\infty d\tau \tau^n \langle \mathbf{g}\mathbf{E}(t) \cdot \mathbf{g}\mathbf{E}(0) \rangle_E. \quad (292)$$

In accordance with the power counting of Sec. VII.B, Eq. (290) gives a contribution of order $p^3/m^2 \times m\alpha_s/\sqrt{m}\Lambda_{\text{QCD}} \times \alpha_s$ and Eq. (291) gives one of order $p^3/m^2 \times m\alpha_s/\sqrt{m}\Lambda_{\text{QCD}} \times \Lambda_{\text{QCD}}/m$. Therefore the correction (290) is suppressed with respect to the largest $1/m^2$ potentials calculated in Sec. VII.E.2. The correction (291) is suppressed with respect to the imaginary part of the $1/m^2$ potential, given in Eq. (75). However, its size relative to the imaginary part of the $1/m^4$ potential, given in Eq. (268), depends on the size of $\alpha_s(\sqrt{m}\Lambda_{\text{QCD}})$ about which no definite statement can be made at this point.

F. Matching for $|\mathbf{p}| \gg \Lambda_{\text{QCD}} \gg E$

Although it is not clear whether quarkonia states fulfilling $|\mathbf{p}| \gg \Lambda_{\text{QCD}} \gg E$ exist in nature, this situation is worth investigating. The reason is that the calculation in the $|\mathbf{p}| \gg \Lambda_{\text{QCD}} \gg E$ case can be divided into two steps, the first of which can be carried out by a perturbative calculation in α_s . The second step, even if it is nonperturbative in α_s , admits a diagrammatic representation which makes the calculation somewhat more intuitive.

1. pNRQCD'

We shall call pNRQCD' the EFT for energies below $|\mathbf{p}|$. Since $|\mathbf{p}| \gg \Lambda_{\text{QCD}}$, integrating out the energy scale $|\mathbf{p}|$, namely, the matching between NRQCD and pNRQCD', can be carried out perturbatively in α_s . The resulting EFT Lagrangian entirely coincides with the pNRQCD one in the weak-coupling regime, which at lower orders has been displayed in Eqs. (60) and (74). Here we need higher-order terms in the multipole expansion (at tree level):

$$\begin{aligned} \delta\mathcal{L}_{\text{pNRQCD}'} = & \frac{1}{8} \operatorname{Tr}\{O^\dagger \mathbf{r} \mathbf{r}^j \mathbf{g} \mathbf{D}^i \mathbf{E}^j O - O^\dagger O \mathbf{r}^i \mathbf{r}^j \mathbf{g} \mathbf{D}^i \mathbf{E}^j\} \\ & + \frac{1}{24} \operatorname{Tr}\{O^\dagger \mathbf{r}^i \mathbf{r}^j \mathbf{r}^k \mathbf{g} \mathbf{D}^i \mathbf{D}^j \mathbf{E}^k S + \text{H.c.}\} \\ & + \frac{c_F}{2m} \operatorname{Tr}\{O^\dagger (\boldsymbol{\sigma}_1 - \boldsymbol{\sigma}_2) \cdot \mathbf{g} \mathbf{B} S + \text{H.c.}\}, \end{aligned} \quad (293)$$

where the traces are in color space only. S and O are chosen to transform as a $1/2 \otimes 1/2$ representation in spin space (hence $\boldsymbol{\sigma}_1 - \boldsymbol{\sigma}_2 = \boldsymbol{\sigma}_1 \otimes \mathbf{1}_2 - \mathbf{1}_1 \otimes \boldsymbol{\sigma}_2$).

2. Matching pNRQCD to pNRQCD'

The matching of pNRQCD' to pNRQCD can no longer be done perturbatively in α_s , but it can, indeed, be done perturbatively in the following ratios of scales: $\Lambda_{\text{QCD}}/|\mathbf{p}|$ (multipole expansion), Λ_{QCD}/m , and E/Λ_{QCD} . Therefore the basic skeleton of the calculation consists of an expansion in $x = (\Lambda_{\text{QCD}}/|\mathbf{p}|)^2$ and $y = (\Lambda_{\text{QCD}}/m)^2$. This suggests writing the pNRQCD Hamiltonian as

$$h = h_s + h_x + h_{x^2} + h_y + \dots \quad (294)$$

The interpolating fields of pNRQCD' and pNRQCD will be related by

$$\begin{aligned} S|_{\text{pNRQCD}'} = & Z^{1/2} S|_{\text{pNRQCD}} \\ = & (1 + Z_x + Z_{x^2} + Z_y + \dots)^{1/2} S|_{\text{pNRQCD}}. \end{aligned} \quad (295)$$

The matching calculation is

$$\begin{aligned}
& \int_{-\infty}^{\infty} dt e^{-iEt} \int d^3\mathbf{R} \langle \text{vac} | T \{ S(\mathbf{x}, \mathbf{R}, t) S(\mathbf{x}', \mathbf{0}, 0) \} \\
& \quad \times | \text{vac} \rangle \Big|_{\text{pNRQCD}'} \\
& = \int_{-\infty}^{\infty} dt e^{-iEt} \int d^3\mathbf{R} Z^{1/2} \langle \text{vac} | T \{ S(\mathbf{x}, \mathbf{R}, t) S(\mathbf{x}', \mathbf{0}, 0) \} \\
& \quad \times | \text{vac} \rangle \Big|_{\text{pNRQCD}} Z^{(1/2)\dagger}. \tag{296}
\end{aligned}$$

The right-hand side of the matching calculation has the following structure:

$$\begin{aligned}
& \frac{1}{E-h_s} + \frac{1}{E-h_s} (h_x + h_{x^2} + h_y) \frac{1}{E-h_s} + \frac{1}{2} \left(Z_x + Z_{x^2} \right. \\
& \quad \left. + Z_y - \frac{Z_x^2}{4} \right) \frac{1}{E-h_s} + \frac{1}{E-h_s} \frac{1}{2} \left(Z_x + Z_{x^2} + Z_y \right. \\
& \quad \left. - \frac{Z_x^2}{4} \right)^\dagger + \left(\frac{Z_x}{2} \right) \frac{1}{E-h_s} \left(\frac{Z_x}{2} \right)^\dagger \\
& \quad + \frac{1}{E-h_s} h_x \frac{1}{E-h_s} h_x \frac{1}{E-h_s} \\
& \quad + \left(\frac{Z_x}{2} \right) \frac{1}{E-h_s} h_x \frac{1}{E-h_s} + \frac{1}{E-h_s} h_x \frac{1}{E-h_s} \left(\frac{Z_x}{2} \right)^\dagger. \tag{297}
\end{aligned}$$

Hence once we have made sure that, up to contact terms, the left-hand side of Eq. (296) has exactly the same structure, we can easily identify the contributions to the pNRQCD Hamiltonian from the second term of expression (297).

Let us illustrate how the calculation of the left-hand side of Eq. (296) proceeds by concentrating on the following contribution:

$$\frac{1}{E-h_s} \frac{i}{N_c} \int_0^\infty dt \langle i\mathbf{r} \cdot g\mathbf{E}(t) e^{-i(h_o-E)t} i\mathbf{r} \cdot g\mathbf{E}(0) \rangle \frac{1}{E-h_s}. \tag{298}$$

One might naively think that because E/Λ_{QCD} is small, it can be implemented by expanding the exponential (t takes the typical value of $1/\Lambda_{\text{QCD}}$) (Brambilla, Eiras, *et al.*, 2002, 2003). However, this is not entirely correct. Whereas it is true that h_o , between the heavy quarkonium states we are considering, has size E , it may experience fluctuations of a larger size, for instance, $\sim \Lambda_{\text{QCD}}$ since the cutoff of the relative three-momentum is only constrained to be smaller than m , and hence it may well reach values $\sim \sqrt{m\Lambda_{\text{QCD}}}$. Nevertheless, the energy E can indeed always be expanded, which guarantees that we eventually get usual, energy-independent, potentials. If h_o could not be expanded, we obtain potentials which are nontrivial functions of m , Λ_{QCD} , and \mathbf{r} . Fortunately, we can do much better by exploiting the fact that the momenta, which prevent us from expanding, fulfill $|\mathbf{p}| \sim \sqrt{m\Lambda_{\text{QCD}}} \gg \Lambda_{\text{QCD}}$. We shall proceed as follows. We split the relative momentum into two regions. The first region fulfills $|\mathbf{p}| \ll \sqrt{m\Lambda_{\text{QCD}}}$ and h_o can be expanded and

the second region contains the momentum fluctuations $\sim \sqrt{m\Lambda_{\text{QCD}}}$.

(i) The matching in the region $|\mathbf{p}| \ll \sqrt{m\Lambda_{\text{QCD}}}$.

(i.a) The real part of the potential.

At LO in the expansion, the exponential in Eq. (298) reduces to 1 and we obtain the leading nonperturbative correction to the Coulomb potential:

$$\delta V_s = -i \frac{g^2}{N_c} T_F \frac{r^2}{3} \int_0^\infty dt \langle \mathbf{E}^a(t) \phi(t, 0)_{ab}^{\text{adj}} \mathbf{E}^b(0) \rangle. \tag{299}$$

This expression was first derived by Balitsky (1985). Higher orders in the E/Λ_{QCD} expansion can be easily calculated. They induce contributions to potentials which are higher order in $1/m$ as well as further contributions to the static potential. Some of these have been calculated by Brambilla *et al.* (2000).

(i.b) The imaginary part of the potential.

Since the imaginary parts, which are inherited from NRQCD, are contained in local $[\delta^{(3)}(\mathbf{r}), \nabla \delta^{(3)}(\mathbf{r}) \nabla, \text{etc.}]$ terms in the pNRQCD' Lagrangian, they tend to vanish when being multiplied by the \mathbf{r} 's arising from the multipole expansion. Hence for an imaginary part to contribute, it must have a sufficient number of derivatives (usually arising from the E/Λ_{QCD} expansion) in order to cancel all the \mathbf{r} 's. Since derivatives are always accompanied by powers of $1/m$, it implies that at a given order in $1/m$, only a finite number of terms in the multipole expansion contributes. We are only interested in collecting the imaginary parts that contribute up to order $1/m^4$ in order to provide an independent calculation to support the results of Sec. VII.E. Consider again the contribution of Eq. (298). The first imaginary terms arise at $\mathcal{O}(E/\Lambda_{\text{QCD}})$ from the $\mathcal{O}(1/m^4)$ parts of the singlet and octet potentials displayed in Eq. (76):

$$\begin{aligned}
& \frac{i}{E-h_s} \left(\frac{T_F T_{SJ}^{ii} \text{Im} f_8^{(2S+1)P_J}}{3N_c m^4} \right. \\
& \quad \left. + \frac{\mathcal{T}_S [\text{Im} g_1^{(2S+1)S_S} + \text{Im} g_{\text{EM}}^{(2S+1)S_S}]}{m^4} \right) \\
& \quad \times \int_0^\infty dt \langle g\mathbf{E}(t) \cdot g\mathbf{E}(0) \rangle \frac{\delta^{(3)}(\mathbf{r})}{E-h_s}, \tag{300}
\end{aligned}$$

where \mathcal{T}_{SJ}^{ij} are defined as defined in Eqs. (77)–(80) and $\mathcal{T}_S = \Omega_{SS}^{ii}/3$. The calculation may be systematically extended to higher orders. Details are given by Brambilla, Eiras, *et al.* (2003). Here we just point out two subtleties. First, ill-defined expressions arise in the calculation from products of distributions (both products of two delta functions and products of delta functions with nonlocal potentials, which diverge as $\mathbf{r} \rightarrow 0$). It is most convenient to use DR in this case, which sets all these terms to zero. This is shown in Appendix D in the article by Brambilla, Eiras, *et al.* (2003), where the relation to other regularization schemes is also discussed. Second, there is a freedom in organizing the calculation, which may lead to different forms of the potentials. Let us consider, as an example, the term

$$\frac{1}{E-h_s} \mathbf{r} (E-h_s)^2 \mathbf{r} \frac{1}{E-h_s}. \quad (301)$$

If we decide to take one power $(E-h_s)$ to the right and one to the left, we have

$$\begin{aligned} & \mathbf{r}^2 + \mathbf{r}[\mathbf{r}, h_s] \frac{1}{E-h_s} + \frac{1}{E-h_s} [h_s, \mathbf{r}] \mathbf{r} + \frac{1}{E-h_s} [h_s, \mathbf{r}] \\ & \times [\mathbf{r}, h_s] \frac{1}{E-h_s}, \end{aligned} \quad (302)$$

which does not produce any imaginary part. However, an equally acceptable expression is

$$\begin{aligned} & \mathbf{r}^2 + \frac{1}{2} [\mathbf{r}, [\mathbf{r}, h_s]] \frac{1}{E-h_s} + \frac{1}{E-h_s} \frac{1}{2} [[h_s, \mathbf{r}], \mathbf{r}] \\ & + \frac{1}{E-h_s} \frac{1}{2} \{ [[\mathbf{r}, h_s], h_s], \mathbf{r} \} \frac{1}{E-h_s}, \end{aligned} \quad (303)$$

which does produce an imaginary part. The apparent paradox only reflects the fact that expression (301) by itself (as well as others from the calculation) does not determine uniquely its contribution to the potential. It leads to contact terms, wave-function normalization and potential, as is apparent in Eqs. (302) and (303), but depending on how we decide to organize the calculation, the terms associated with each of these pieces change. For instance, when matched to Eq. (297), Eq. (302) gives $h_x = [h_s, \mathbf{r}] [\mathbf{r}, h_s]$, $Z_x = \mathbf{r} [\mathbf{r}, h_s]$, whereas Eq. (303) gives $h_x = \frac{1}{2} \{ [[\mathbf{r}, h_s], h_s], \mathbf{r} \}$, $Z_x = \frac{1}{2} [\mathbf{r}, [\mathbf{r}, h_s]]$. This should not be a surprise. It corresponds to the freedom of making unitary transformations in a quantum-mechanical Hamiltonian already discussed in the previous sections, and does not affect any physical observables. In order to fix the contribution to the potential of any term once and forever, we use the prescription described in detail in Sec. V of Brambilla, Eiras, *et al.* (2003). With this prescription, Eq. (301) gives rise to the potential obtained in Eq. (302) and hence to no imaginary part. Eventually, combining all the contributions, we obtain for the imaginary part of the pNRQCD potential when $p \gg \Lambda_{\text{QCD}} \gg E$ the same result, up to a unitary transformation, as obtained in Sec. VII.E when $p \sim \Lambda_{\text{QCD}}$ and explicitly listed in Eqs. (75) and (268). The explicit form of the unitary transformation can be found in the article by Brambilla, Eiras, *et al.* (2003).

(ii) The matching in the region $|\mathbf{p}| \sim \sqrt{m\Lambda_{\text{QCD}}}$.

The contributions due to heavy quarks of three-momentum of order $\sqrt{m\Lambda_{\text{QCD}}}$ may be calculated similar to Sec. VII.E.5. The main difference is that now potential and semihard degrees of freedom need not be separated at the level of NRQCD, but of pNRQCD'.

(ii.a) The first step consists in rewriting the pNRQCD' Lagrangian in terms of semihard fields S_{sh} and O_{sh}^a associated with three-momentum fluctuations of $\mathcal{O}(\sqrt{m\Lambda_{\text{QCD}}})$ and potential fields S_p and O_p^a associated with three-momentum fluctuations of $\mathcal{O}(p)$:

$$S = S_p + S_{\text{sh}}, \quad O^a = O_p^a + O_{\text{sh}}^a. \quad (304)$$

The pNRQCD' Lagrangian is then

$$\begin{aligned} L_{\text{pNRQCD}'} &= L_{\text{pNRQCD}'}^{\text{sh}} + L_{\text{pNRQCD}'}^p + L_{\text{mixing}} + L_g \\ &+ L_l, \end{aligned} \quad (305)$$

where $L_{\text{pNRQCD}'}^{\text{sh}}$ and $L_{\text{pNRQCD}'}^p$ are identical to the pNRQCD' Lagrangian in the heavy-quarkonium bilinear sector except for the changes $S, O^a, V_s, V_o \rightarrow S_{\text{sh}}, O_{\text{sh}}^a, V_s^{\text{sh,sh}}, V_o^{\text{sh,sh}}$, and $S, O^a, V_s, V_o \rightarrow S_p, O_p^a, V_s^{p,p}, V_o^{p,p}$, respectively. L_g and L_l are the parts of the pNRQCD' Lagrangian that contain only gluons and light quarks, respectively, and L_{mixing} contains the mixing terms. We recall that the gluons left dynamical have energies of $\mathcal{O}(\Lambda_{\text{QCD}})$ and that analytic terms in \mathbf{r} do not mix semihard and potential fields. Therefore the multipole expansion in Eq. (293) is an expansion in either the scale $\mathbf{r} \sim 1/\sqrt{m\Lambda_{\text{QCD}}}$ in $L_{\text{pNRQCD}'}^{\text{sh}}$, or the scale $\mathbf{r} \sim 1/p$ in $L_{\text{pNRQCD}'}^p$.

(ii.b) The second step consists of integrating out gluons and quarks of energy and three-momentum of $\mathcal{O}(\sqrt{m\Lambda_{\text{QCD}}})$. We assume, as in Eq. (282) and for the same reasons as discussed there, that $\sqrt{m\Lambda_{\text{QCD}}} \gg m\alpha_s(\sqrt{m\Lambda_{\text{QCD}}})$. As an example, we consider the real part of the singlet mixing term due to the static Coulomb potential. The matching works exactly as in paragraph (ii.b) of Sec. VII.E.5 and leads to

$$\begin{aligned} & \text{Re } L_{\text{mixing}|_{\text{singlet}}} \\ &= - \int d^3\mathbf{R} \int d^3\mathbf{r} S_p^\dagger(\mathbf{R}, \mathbf{r}) V_s^{(0)}(\mathbf{r}) S_{\text{sh}}(\mathbf{R}, \mathbf{r}) + \text{H.c.} \\ &\rightarrow - \int d^3\mathbf{R} \int d^3\mathbf{r} [S_p^\dagger(\mathbf{R}, \mathbf{0}) + \mathbf{r} \cdot \nabla_{\mathbf{r}} S_p^\dagger(\mathbf{R}, \mathbf{0}) + \dots] \\ &\quad \times V_s^{(0)}(\mathbf{r}) S_{\text{sh}}(\mathbf{R}, \mathbf{r}) + \text{H.c.} \end{aligned} \quad (306)$$

At the order of interest, we have $V_s^{(0)} = -C_F \alpha_s / r$ and $\alpha_s = \alpha_s(\sqrt{m\Lambda_{\text{QCD}}})$. Analogous results hold for the real part of the octet mixing term due to the static Coulomb potential.

The leading contribution to the imaginary part of L_{mixing} is given by

$$\begin{aligned} \text{Im } L_{\text{mixing}} &= - \int d^3\mathbf{R} \int d^3\mathbf{r} \text{Tr} \left\{ S_{\text{sh}}^\dagger(\mathbf{R}, \mathbf{0}) \frac{K_s}{m^2} \delta^{(3)}(\mathbf{r}) \right. \\ &\quad \left. \times S_p(\mathbf{R}, \mathbf{0}) + \text{H.c.} \right\} \\ &\quad - \int d^3\mathbf{R} \int d^3\mathbf{r} \text{Tr} \left\{ O_{\text{sh}}^\dagger(\mathbf{R}, \mathbf{0}) \frac{K_o}{m^2} \delta^{(3)}(\mathbf{r}) \right. \\ &\quad \left. \times O_p(\mathbf{R}, \mathbf{0}) + \text{H.c.} \right\}, \end{aligned} \quad (307)$$

where K_s and K_o have been defined in Eqs. (286) and (287), respectively.

(ii.c) The final step consists in integrating out from pNRQCD' all fluctuations that appear at the energy

scale Λ_{QCD} . These are light quarks and gluons of energy or three-momentum of order Λ_{QCD} , and singlet and octet fields of energy of order Λ_{QCD} or three-momentum of order $\sqrt{m\Lambda_{\text{QCD}}}$. We are then left with pNRQCD. The part $V^{1/m}$ of the potential [see Eq. (220)] has been calculated in paragraph (i) of this section. The part $V^{1/\sqrt{m}}$ of the potential develops a real and an imaginary part. They turn out to be equal to Eqs. (290) and (291), respectively, i.e., to the results obtained in the kinematical situation $p \sim \Lambda_{\text{QCD}}$. We refer the reader to Brambilla, Pineda, *et al.* (2004) for a detailed diagrammatical calculation.

In summary, we have presented a derivation of the pNRQCD potential (real and imaginary) in a kinematical situation and with a technical procedure that are quite different from the ones of Sec. VII.E. The agreement of the results (up to unitary transformations) in the case when the potentials are local (nonanalytic and imaginary terms) is reassuring and confirms in an explicit calculation what is expected in Sec. VII.D on general grounds. Despite this, it should be noted that the matching coefficients of the terms in the multipole expansion in pNRQCD' (293) were only calculated at tree level here, whereas the expressions in Sec. VII.E correspond to an all-order result. This indicates that there must be a symmetry protecting these terms against higher-loop corrections.²⁴ This symmetry does not appear to be Poincaré invariance (Brambilla, Gromes, and Vairo, 2003).

G. Potentials and spectra: lattice and models

The heavy-quarkonium spectrum is obtained by solving the Schrödinger equation for the pNRQCD Hamiltonian h_s :

$$h_s \phi_{njls}(\mathbf{r}) = E_{njls} \phi_{njls}(\mathbf{r}). \quad (308)$$

Since h_s is known from Eqs. (243)–(258), (75), (268), (290), and (291), the Schrödinger equation (308) is completely defined in terms of QCD quantities.

At LO, Eq. (308) becomes

$$\begin{aligned} h_s^{(0)} \phi_{njls}^{(0)}(\mathbf{r}) &= \left(\frac{\mathbf{p}_1^2}{2m_1} + \frac{\mathbf{p}_2^2}{2m_2} + V_{\text{LO}} \right) \phi_{njls}^{(0)}(\mathbf{r}) \\ &= E_{njls}^{(0)} \phi_{njls}^{(0)}(\mathbf{r}). \end{aligned} \quad (309)$$

What V_{LO} depends on the power counting. We have argued in Sec. VII.E.2 that when $p \sim \Lambda_{\text{QCD}}$ and in the most conservative power counting, we have $V_{\text{LO}} = V^{(0)} + V^{(1)}/m$. On the other hand, if $p \gg \Lambda_{\text{QCD}}$, we have $V_{\text{LO}} = V^{(0)}$. In both cases, at this order the potential is spin independent ($E_{njls}^{(0)} \equiv E_{nl}^{(0)}$) and therefore the leading-order S - and P -wave functions read

$$\phi_{ns0s}^{(0)}(\mathbf{r}) = R_{n0}^{(0)}(r) \frac{1}{\sqrt{4\pi}} |s\rangle_{\text{spin}} \quad \text{and}$$

$$\phi_{nl1s}^{(0)}(\mathbf{r}) = R_{n1}^{(0)}(r) \langle \hat{\mathbf{r}} | js \rangle, \quad (310)$$

where $|s\rangle_{\text{spin}}$ denotes the normalized spin component, $|\hat{\mathbf{r}}\rangle$ the normalized eigenstate of the position, and $|js\rangle$ the J (total angular momentum) and S eigenstate such that $\langle \hat{\mathbf{r}} | j0 \rangle = Y_j^m(\hat{\mathbf{r}}) |0\rangle_{\text{spin}}$ ($j=l=1$) and $\langle \hat{\mathbf{r}} | j1 \rangle = \mathcal{Y}_{jm}^1(\hat{\mathbf{r}})$. The label m denotes the third component of the angular momentum.

At NLO, the $1/m^2$ potentials calculated in Sec. VII.E.2 have to be considered, except for the ones that may have extra suppression. The contribution to the spectrum that comes from the $V^{1/\sqrt{m}}$ potential given in Eq. (289) also turns out to be suppressed. Indeed, we have (m^{red} is the reduced mass)

$$\delta E_{njls}^{1/\sqrt{m}} = (2C_F + C_A)^2 \frac{1}{3\Gamma(9/2)} \alpha_s^2 \mathcal{E}_{7/2}^E \frac{|R_{n1}(0)|^2}{(2m^{\text{red}})^{3/2}} \delta_{l0}, \quad (311)$$

which is of order $|\mathbf{p}|^3/m^2 \times m\alpha_s/\sqrt{m\Lambda_{\text{QCD}}} \times \alpha_s$, i.e., suppressed with respect to the contribution coming from the $1/m^2$ potentials of Eqs. (243)–(258), which in the conservative counting is of order p^3/m^2 .

We would like to emphasize that in order to be consistent with the power counting, subleading terms in the expansion of the kinetic energy and the potential should be treated as perturbations when solving Eq. (309). This differs from the common practice in potential models. In an EFT framework, the calculation of the spectrum is not plagued by the inconsistencies emerging in higher-order calculations in potential models. It is, for instance, known that at second order in quantum-mechanical perturbation theory the spin-dependent terms result in a contribution that is ill defined. Regulating it requires the introduction of a cutoff (or DR). A large cutoff gives rise to a linear and to a logarithmic divergence. These divergences can be renormalized by redefining the coupling constant of a delta potential (Lepage, 1997). On the other hand, when one matches QCD to NRQCD, one expands in the energy and the three-momentum. In general, this induces IR divergences in the matching coefficients and, in particular, in the calculation of a matching coefficient of a four-fermion operator at two loops, which leads to the delta potential mentioned above. If one uses a consistent regularization scheme for both the QCD-NRQCD matching calculation and the quantum-mechanical calculation in pNRQCD, the divergences exactly cancel and eventually a totally consistent scale-independent result is obtained [for a QED example, see Czarnecki *et al.* (1999a, 1999b)]. Notice that an EFT framework is crucial for understanding this second-order calculation and for making the result meaningful.

For a determination of the spectrum at order p^3/m^2 in the conservative counting, one needs to consider, besides the static and the $1/m$ potential, the $\mathcal{O}(1/m^2)$ potentials given in Eq. (63), of which for $V_r^{(2,0)}$ and $V_r^{(1,1)}$ only the terms in the first three lines of Eqs. (248) and (252) need to be considered. How can one get the ex-

²⁴For the leading-order term, the nonrenormalization was verified at one loop by Pineda and Soto (2001).

licit form of these potentials? The EFT provides the expressions for such potentials in terms of Wilson-loop amplitudes typically involving chromoelectric- and chromomagnetic-field insertions. In the case of the imaginary parts, they reduce to chromoelectric and chromomagnetic correlators. These are low-energy objects that do not depend on the quarkonium state, involve only integrations over gluon fields and light quarks, are gauge invariant, and perfectly suited for lattice calculations. We emphasize that the EFT approach greatly reduces the lattice effort necessary to produce heavy-quarkonium spectra and decay widths. This is for two reasons. The first reason is that the objects to be calculated on the lattice involve only integrations over low-energy gluons and light quarks. The second is that one does not need to repeat a lattice evaluation for each quarkonium state (with the problems related to the mass extraction of the excited states) but only to extract the form of all the potentials with one simulation. These, once inserted in the Schrödinger equation (309), will produce the spectrum. One should check *a posteriori* which states in the obtained spectrum fulfill the hypothesis of the strong-coupling regime. The ones that do will be the ones for which the calculation is reliable.

1. Potentials and spectrum from the lattice

If DR is used in the continuum, the Wilson-loop amplitudes involved in the static and $1/m$ potentials can be renormalized by the counterterms of light degrees of freedom only, and hence they do not display a factorization scale dependence. For the $1/m^2$ and higher potentials, counterterms involving local potentials are also necessary and the Wilson-loop amplitudes depend on the factorization scale. In a physical observable, this scale dependence, together with the one induced by the quantum-mechanical perturbation theory, will cancel against the scale dependence of the NRQCD matching coefficients. In the strong-coupling regime, there are no US divergences, at least when the US degrees of freedom (pseudo-Goldstone bosons) are neglected.

In a lattice regularization scheme, the situation is more complicated for several reasons. The Wilson-loop amplitudes contain additive $1/a$ -dependent self-energy contributions (a being the lattice spacing), even in the static case. This dependence on $1/a$ is canceled by the quark-mass shift and is removed by a suitable renormalization condition (see the discussion on the static potential in Sec. VI and below). Moreover, large terms are generated having their origin in self-interactions within the plaquette as well as between plaquette and static propagator (to higher orders). These affect all Wilson-loop amplitudes. They would be canceled by NRQCD matching coefficients calculated in a lattice regularization. Without those the scale dependence can be dramatic and several *ad hoc* lattice methods have been applied to get rid of it without actually calculating the matching coefficients, which would be the definite solution. In addition, the Wilson-loop amplitudes will generate a - and r -dependent terms which are specific to the

lattice. On top of this, Lorentz invariance is broken on the lattice. Thus order a corrections to coefficients otherwise protected by Lorentz invariance may appear.

All these issues are related to the lattice regularization and renormalization. A proper treatment would require the calculation of both the NRQCD matching coefficients and the Wilson-loop amplitudes in a proper lattice regularization and renormalization scheme. The Schrödinger equation would also need to be solved in the same scheme, due to the quantum-mechanical divergences. The NRQCD matching coefficients are known at different accuracy in the continuum and in DR, see Sec. II.D, but up to now no calculation of the coefficients here relevant exists within a lattice scheme apart from the one in the work of Trotter and Lepage (1998). Another strategy would be to use a nonperturbative renormalization (Martinelli *et al.*, 1997) on both parts in lattice regularization. Alternatively, if the available MS NRQCD matching coefficients are to be used, one should change the Wilson-loop amplitudes from the lattice renormalization scheme to MS. This can be done in lattice perturbation theory since the cutoff of these divergences is close to m (Bodwin *et al.*, 2002). Then the divergences arising in the quantum-mechanical perturbation theory should also be MS renormalized.

A proper lattice treatment of pNRQCD has so far not been implemented. NRQCD matching coefficients were never considered in the lattice calculation of the potentials with the exception of the work of Bali *et al.* (1997) and Bali (2001), in which an estimate of the NRQCD matching coefficients was used. Therefore this work may be considered the closest to a lattice treatment of pNRQCD. We shall mainly refer to it in the following.

The static potential is given only in terms of the static Wilson loop (243) and it has been one of the first objects to be evaluated on the lattice in relation to quark confinement (Wilson, 1974). Today the static potential is known with great accuracy (Bali *et al.*, 1997; Bali, 2001; Lüscher and Weisz, 2002; Necco and Sommer, 2002) even in the unquenched case (Bali *et al.*, 2000; Bolder *et al.*, 2001). In Fig. 4, the curve labeled Σ_g^+ displays the static-potential data obtained by Bali *et al.* (2000) in units of $r_0 \approx 0.5$ fm. The squares refer to a quenched simulation at $\beta=6.2$ and the bullets to unquenched simulations at $\beta=5.6$ with two mass-degenerate quark flavors. The value of the mass parameter is $\kappa=0.1575$. The physical units follow from a choice of the lattice spacing a . This is often fixed on the bottomonium spectrum (Bali *et al.*, 1997; Bali, 2001). This procedure may potentially introduce large uncertainties if the set of potentials at our disposal is not complete, if the power counting not consistent, or if as is usually done, lower and higher bottomonium states are fitted with the same confining potentials. However, such a determination seems to be numerically in agreement with others obtained from the m_π/m_ρ ratio. The continuous curve in Fig. 4 represents the Cornell parametrization $V^{(0)}(r)=-e/r+\sigma r$ with $e \approx 0.368$ and $\sigma \approx (445 \text{ MeV})^2$. An additive self-energy contribution, associated with the static sources and di-

verging in the continuum limit, has been removed by normalizing the data to $V(r_0)=0$. This corresponds to the elimination of the static-potential renormalon described in Sec. V. As shown in Sec. VI, QCD perturbation theory perfectly agrees with the lattice data up to about 0.25 fm [actually the analysis done by Pineda (2003b) shows agreement up to 0.4 fm], while from about 0.5 fm on the data are described very well by an effective string theory at NLO (Lüscher and Weisz, 2002). However, this seems to be specific to the ground-state energy: the energy spectrum is still far from being stringlike at such distances (Lüscher and Weisz, 2004). This is more apparent for the excited-state energies (Baker and Steinke, 2001).

For the potential at order $1/m$ given in Eqs. (244) and (245), no lattice evaluation is available yet. The spin-dependent $1/m^2$ potentials instead have a quite long record of calculations (Campostrini, 1985; Michael, 1986; Huntley and Michael, 1987; Born *et al.*, 1994; Bali *et al.*, 1997). In the absence of a proper implementation of the NRQCD matching coefficients, the method proposed by Huntley and Michael (1987) was to obtain lattice spacing and scale-independent results for the spin-dependent Wilson-loop potentials based on the substitutions $\langle\langle FF \rangle\rangle \rightarrow \langle\langle FF \rangle\rangle / \langle FF \rangle$, F being the gluon field strength. The notations used by Bali (2001) for the spin-dependent and momentum-dependent Wilson-loop potentials differ from what we presented in Sec. VII.E.2. The objects that were evaluated on the lattice were $V'_1(r)$ [equal to $-r$ times the first term on the right-hand side of Eq. (253) with $c_F=1$] and $V'_2(r)$ [equal to $-r$ times the right-hand side of Eq. (255) with $c_F=1$] for the spin-orbit, $V_3(r)$ [equal to the first term on the right-hand side of Eq. (257) with $c_F=1$] for the spin-spin, and $V_d(r)$ [equal to the right-hand side of Eq. (258) with $c_F=1$] for the tensor potential. All the lattice determinations of the spin-dependent potentials use the correct expression for the spin-orbit potential (see comments in Sec. VII.E.2). An example is shown in Fig. 18(a). For the momentum-dependent part, the objects evaluated on the lattice were $V_b = -2/3 V_{\mathbf{L}^2}^{(1,1)} - V_{\mathbf{p}^2}^{(1,1)}$, $V_c = -V_{\mathbf{L}^2}^{(1,1)}$, $V_d = V_{\mathbf{p}^2}^{(2,0)} + 2/3 V_{\mathbf{L}^2}^{(2,0)}$, and $V_e = V_{\mathbf{L}^2}^{(2,0)}$. An example is shown in Fig. 18(b). The spin-independent and momentum-independent potentials at order $1/m^2$ have not yet been calculated.

The Poincaré invariance constraints (259)–(261) (which in the above notation are $V'_2 - V'_1 = V'_0$, $V_b + 2V_d = rV^{(0)}/6 - V^{(0)}/2$, and $V_c + 2V_e = -rV^{(0)}/2$) have been used to test the quality and the continuum limit of the lattice simulation by Bali *et al.* (1997). The lattice data satisfy well the relations especially in the short and medium range. For the long range, the data become noisy. We refer the reader to the original literature for more details.

More lattice plots may be found in the articles of Bali *et al.* (1997) and Bali (2001). In general the lattice curves appear to be quite noisy for large interquark separations. This calls for new determinations in a fully consistent lattice renormalization context. The lattice data have been compared with fits motivated in the short

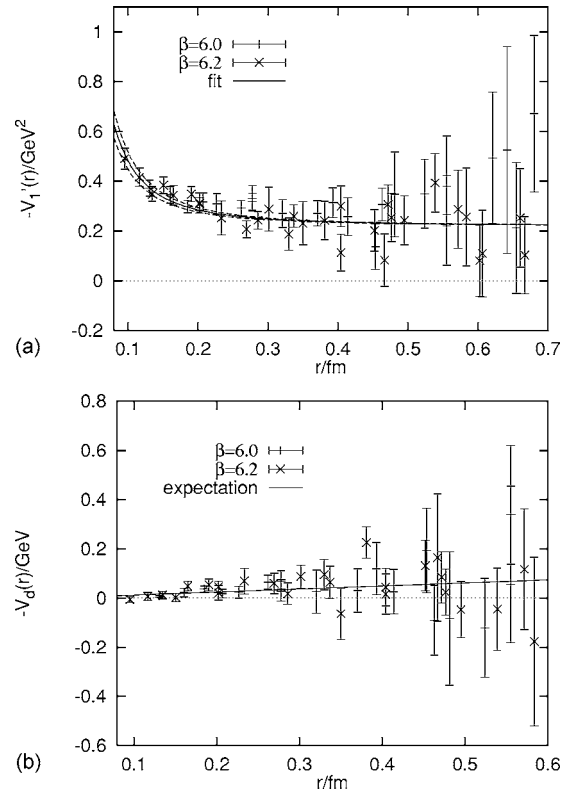


FIG. 18. (a) The spin-orbit potential $-V'_1$ with the fit $\sigma+h/r^2$ and (b) the potential V_d together with the curve $-\sigma/9r$. The lattice simulations are quenched. The fitting parameters are $\sigma \approx (468 \text{ MeV})^2$ and $h \approx 0.067$. From Bali *et al.*, 1997.

range by the perturbative behavior and in the long range by QCD vacuum-model calculations. We briefly mention some of them in the next subsection.

2. QCD vacuum models

The EFT has allowed us to systematically encode the low-energy contributions to the potentials into Wilson-loop amplitudes. These are also very convenient objects for evaluation in a QCD vacuum model. A QCD vacuum model may be defined by the behavior that it attributes to (not necessarily static) Wilson-loop expectation values in the large-distance region. Once this is known, it is possible to obtain all Wilson-loop amplitudes with field-strength insertions by means of functional derivatives of the Wilson loop (Migdal, 1983; Brambilla *et al.*, 1994). In this way the nonperturbative form of all potentials is derived from only one assumption on the Wilson-loop behavior. The lattice data on the potentials can be compared with the expectations from different QCD vacuum models. We note that more knowledge may be gained here on the mechanism of confinement. Indeed, while all models predict confinement and thus a linear increase of the static potential, the predictions for the relativistic corrections to the static potential vary and give nontrivial information. We refer the reader to Brambilla and Vairo (1997) for calculations within the stochastic vacuum model (Dosch and Simonov, 1988), to Baker, Ball, Brambilla, Prospero, *et al.*

(1996) and Baker, Ball, Brambilla, and Vairo (1996) for calculations inside dual QCD (dual superconductor mechanism of confinement; Baker *et al.*, 1991), to Baker *et al.* (1998) for a comparison between the two, and to Brambilla (1998) for a comparison also with the flux-tube model (Isgur and Paton, 1985) and the Bethe-Salpeter NR reduction of a scalar confining kernel. In the articles of Brambilla and Vairo (1999a, 2000b), one will find reviews of several QCD vacuum models and results relevant to the nonperturbative behavior of the potentials.

H. Inclusive decay widths into light particles

The inclusive decay width of a heavy quarkonium H into light particles is (at LO in $\text{Im } h_s$)

$$\Gamma(H \rightarrow \text{light particles}) = -2\langle n, l, s, j | \text{Im } h_s | n, l, s, j \rangle. \quad (312)$$

The imaginary part of the pNRQCD Hamiltonian has been written in Eqs. (75), (268), and (291), and the wave functions $\phi_{njl_s}(\mathbf{r}) = \langle \mathbf{r} | n, l, s, j \rangle$ have been discussed in Sec. VII.G. For present purposes, a LO calculation is sufficient for P -wave functions, while a NLO analysis, which involves the $1/m^2$ potentials, is necessary for S -wave ones.

With the above specifications and from Eq. (312), we can now list the pNRQCD expressions for S - and P -wave decays. We proceed as follows. First, we give the expressions for the matrix elements of NRQCD that appear in Eqs. (42)–(47) distinguishing between terms that are analytic in $1/m$ and terms that are not ($\langle H | O | H \rangle = \langle H | O | H \rangle^{1/m} + \langle H | O | H \rangle^{1/\sqrt{m}}$), since as we have seen in the previous sections they have been calculated in pNRQCD to different precision. Finally, we explicitly give the decay widths in pNRQCD at the precision to which they are presently known.

The analytic contributions in $1/m$ to the NRQCD matrix elements have been calculated up to (once normalized to m^0) $\mathcal{O}(p^3/m^3 \times (\Lambda_{\text{QCD}}^2/m^2, E/m))$ for S -wave (Brambilla, Eiras, *et al.*, 2003) and up to $\mathcal{O}(p^5/m^5)$ for P -wave matrix elements (Brambilla, Eiras, *et al.*, 2002):

$$\langle V_Q(nS) | O_1(^3S_1) | V_Q(nS) \rangle^{1/m} = C_A \frac{|R_{n0}^V(0)|^2}{2\pi} \left(1 - \frac{E_{n0}^{(0)}}{m} \frac{2\mathcal{E}_3}{9} + \frac{2\mathcal{E}_3^{(2,t)}}{3m^2} + \frac{c_F^2 \mathcal{B}_1}{3m^2} \right), \quad (313)$$

$$\langle P_Q(nS) | O_1(^1S_0) | P_Q(nS) \rangle^{1/m} = C_A \frac{|R_{n0}^P(0)|^2}{2\pi} \left(1 - \frac{E_{n0}^{(0)}}{m} \frac{2\mathcal{E}_3}{9} + \frac{2\mathcal{E}_3^{(2,t)}}{3m^2} + \frac{c_F^2 \mathcal{B}_1}{m^2} \right), \quad (314)$$

$$\langle V_Q(nS) | O_{\text{EM}}(^3S_1) | V_Q(nS) \rangle^{1/m} = C_A \frac{|R_{n0}^V(0)|^2}{2\pi} \left(1 - \frac{E_{n0}^{(0)}}{m} \frac{2\mathcal{E}_3}{9} + \frac{2\mathcal{E}_3^{(2,\text{EM})}}{3m^2} + \frac{c_F^2 \mathcal{B}_1}{3m^2} \right), \quad (315)$$

$$\langle P_Q(nS) | O_{\text{EM}}(^1S_0) | P_Q(nS) \rangle^{1/m} = C_A \frac{|R_{n0}^P(0)|^2}{2\pi} \left(1 - \frac{E_{n0}^{(0)}}{m} \frac{2\mathcal{E}_3}{9} + \frac{2\mathcal{E}_3^{(2,\text{EM})}}{3m^2} + \frac{c_F^2 \mathcal{B}_1}{m^2} \right), \quad (316)$$

$$\begin{aligned} \langle \chi_Q(nJS) | O_1(^{2S+1}P_J) | \chi_Q(nJS) \rangle^{1/m} \\ = \langle \chi_Q(nJS) | O_{\text{EM}}(^{2S+1}P_J) | \chi_Q(nJS) \rangle^{1/m} \\ = \frac{3}{2} \frac{C_A}{\pi} |R_{n1}^{(0)'}(0)|^2, \end{aligned} \quad (317)$$

$$\begin{aligned} \langle V_Q(nS) | \mathcal{P}_1(^3S_1) | V_Q(nS) \rangle^{1/m} \\ = \langle P_Q(nS) | \mathcal{P}_1(^1S_0) | P_Q(nS) \rangle^{1/m} \\ = \langle V_Q(nS) | \mathcal{P}_{\text{EM}}(^3S_1) | V_Q(nS) \rangle^{1/m} \\ = \langle P_Q(nS) | \mathcal{P}_{\text{EM}}(^1S_0) | P_Q(nS) \rangle^{1/m} \\ = C_A \frac{|R_{n0}^{(0)}(0)|^2}{2\pi} (mE_{n0}^{(0)} - \mathcal{E}_1), \end{aligned} \quad (318)$$

$$\begin{aligned} \langle V_Q(nS) | O_8(^3S_1) | V_Q(nS) \rangle^{1/m} \\ = \langle P_Q(nS) | O_8(^1S_0) | P_Q(nS) \rangle^{1/m} \\ = C_A \frac{|R_{n0}^{(0)}(0)|^2}{2\pi} \left(-\frac{2(C_A/2 - C_F)\mathcal{E}_3^{(2)}}{3m^2} \right), \end{aligned} \quad (319)$$

$$\begin{aligned} \langle V_Q(nS) | O_8(^1S_0) | V_Q(nS) \rangle^{1/m} \\ = \frac{\langle P_Q(nS) | O_8(^3S_1) | P_Q(nS) \rangle^{1/m}}{3} \\ = C_A \frac{|R_{n0}^{(0)}(0)|^2}{2\pi} \left(-\frac{(C_A/2 - C_F)c_F^2 \mathcal{B}_1}{3m^2} \right), \end{aligned} \quad (320)$$

$$\begin{aligned} \frac{\langle V_Q(nS) | O_8(^3P_J) | V_Q(nS) \rangle^{1/m}}{2J+1} \\ = \frac{\langle P_Q(nS) | O_8(^1P_1) | P_Q(nS) \rangle^{1/m}}{9} \\ = C_A \frac{|R_{n0}^{(0)}(0)|^2}{2\pi} \left(-\frac{(C_A/2 - C_F)\mathcal{E}_1}{9} \right), \end{aligned} \quad (321)$$

$$\langle \chi_Q(nJS) | O_8(^1S_0) | \chi_Q(nJS) \rangle^{1/m} = \frac{T_F |R_{n1}^{(0)'}(0)|^2}{3 \pi m^2} \mathcal{E}_3, \quad (322)$$

where the radial part of the vector S -wave function is $R_{n101} \equiv R_{n0}^V$ and the radial part of the pseudoscalar S -wave function is $R_{n000} \equiv R_{n0}^P$. The quantity $R_{n1}^{(0)'}$ is the derivative of the radial part of the LO P -wave function. Any other dimension-6 and dimension-8 S -wave matrix elements are 0 at the order considered here.

The nonanalytic contributions in $1/m$ to the NRQCD matrix elements have been calculated up to (once normalized to m^0) $\mathcal{O}(p^3/m^3 \times \Lambda_{\text{QCD}}/m \times m\alpha_s/\sqrt{m\Lambda_{\text{QCD}}})$ for S -wave matrix elements (Brambilla, Pineda, *et al.*, 2004):

$$\begin{aligned}
& \langle V_Q(nS) | O_1(^3S_1) | V_Q(nS) \rangle^{1/\sqrt{m}} \\
&= \langle V_Q(nS) | O_{EM}(^3S_1) | V_Q(nS) \rangle^{1/\sqrt{m}} \\
&= C_A \frac{|R_{n0}^V(0)|^2}{2\pi} \left(1 + \frac{4(2C_F + C_A) \alpha_s \mathcal{E}_{5/2}^E}{3\Gamma(7/2) m^{1/2}} \right), \quad (323)
\end{aligned}$$

$$\begin{aligned}
& \langle P_Q(nS) | O_1(^1S_0) | P_Q(nS) \rangle^{1/\sqrt{m}} \\
&= \langle P_Q(nS) | O_{EM}(^1S_0) | P_Q(nS) \rangle^{1/\sqrt{m}} \\
&= C_A \frac{|R_{n0}^P(0)|^2}{2\pi} \left(1 + \frac{4(2C_F + C_A) \alpha_s \mathcal{E}_{5/2}^E}{3\Gamma(7/2) m^{1/2}} \right). \quad (324)
\end{aligned}$$

All other matrix elements receive contributions which are $\mathcal{O}(m\alpha_s/\sqrt{m\Lambda_{\text{QCD}}})$ suppressed, under the condition (282), with respect to those listed in Eqs. (313)–(322).

Some comments are in order. All matrix elements are factorized into a part that is the wave function at the origin and a combination of gluon-field correlators. The wave function carries the dependence on the state and flavor content of the decaying heavy quarkonium (apart from the residual dependence on m and n in the binding energy and on m in the logarithms in c_F), while the correlators only depend on the low-energy properties of QCD and are in this sense universal. They may be calculated once and forever, by means of lattice simulations (D’Elia *et al.*, 1997; Bali *et al.*, 1998; Foster and Michael, 1999; Bali and Pineda, 2004), specific models of the QCD vacuum (Baker *et al.*, 1998; Brambilla, 2000; Di Giacomo *et al.*, 2002), or extracted from experimental data (Brambilla, Eiras, *et al.*, 2002; see also Sec. VIII.D). We emphasize that the factorization holds only if $\Lambda_{\text{QCD}} \gg E$, otherwise it would not be possible to disentangle the heavy quarkonium, whose energy is E , from the non-perturbative gluons.

The factorization is also the reason for the reduction in the number of nonperturbative parameters in going from NRQCD to pNRQCD. In pNRQCD these are the wave functions and the gluon-field correlators. Among these only the wave functions depend on the specific heavy-quarkonium state that we are considering. As discussed at the beginning of the section, the wave function may be calculated, in principle, in terms of QCD quantities by solving the Schrödinger equation (308). At the order at which they are given, Eqs. (313)–(316) are sensitive to the difference between the pseudoscalar and the vector S -wave function. For the other S -wave operators, the difference is not important at the present level of accuracy. The reduction in the number of parameters is more evident if we consider ratios of matrix elements of hadronic operators and electromagnetic ones. The wave-function dependence drops out and we are left with a combination of a few universal gluon-field correlators. In Sec. VIII.D, we discuss the phenomenological relevance of this for the calculation of bottomonium and charmonium inclusive decay widths.

Finally, we recall that, apart from the matrix elements $\langle V_Q(nS) | O_1(^3S_1) | V_Q(nS) \rangle$ and $\langle P_Q(nS) | O_1(^1S_0) | P_Q(nS) \rangle$ that are affected at relative order Λ_{QCD}/m

$\times m\alpha_s/\sqrt{m\Lambda_{\text{QCD}}}$, all other matrix elements listed above receive nonanalytic contributions from the three-momentum scale $\sqrt{m\Lambda_{\text{QCD}}}$ at relative order $m\alpha_s/\sqrt{m\Lambda_{\text{QCD}}}$ with respect to the leading piece. It may turn out that these contributions are numerically important since the suppression factor $m\alpha_s/\sqrt{m\Lambda_{\text{QCD}}}$ may not be that small. In this case it would be important to have the leading nonanalytic contributions for all matrix elements. As long as this is not the case, nonanalytic contributions give the dominant source of uncertainty for the factorization formulas (317)–(322).

We conclude by giving the explicit formulas in pNRQCD for the electromagnetic and inclusive decay widths of heavy quarkonium into light particles at the present level of knowledge. This means that S -wave decay widths are given up to and including $\mathcal{O}(\text{Im}f \times p^3/m^2 \times \Lambda_{\text{QCD}}/m \times m\alpha_s/\sqrt{m\Lambda_{\text{QCD}}})$ and P -wave decay widths up to and including $\mathcal{O}(\text{Im}f \times p^5/m^4)$:

$$\begin{aligned}
\Gamma(V_Q(nS) \rightarrow LH) &= \frac{C_A |R_{n0}^V(0)|^2}{\pi m^2} \text{Im} f_1(^3S_1) \\
&\times \left(1 + \frac{4(2C_F + C_A) \alpha_s \mathcal{E}_{5/2}^E}{3\Gamma(7/2) m^{1/2}} \right), \quad (325)
\end{aligned}$$

$$\begin{aligned}
\Gamma(P_Q(nS) \rightarrow LH) &= \frac{C_A |R_{n0}^P(0)|^2}{\pi m^2} \text{Im} f_1(^1S_0) \\
&\times \left(1 + \frac{4(2C_F + C_A) \alpha_s \mathcal{E}_{5/2}^E}{3\Gamma(7/2) m^{1/2}} \right), \quad (326)
\end{aligned}$$

$$\begin{aligned}
\Gamma(\chi_Q(nJ) \rightarrow LH) &= \frac{C_A |R_{n1}^{(0)'}(0)|^2}{\pi m^4} \left(3 \text{Im} f_1(^{2S+1}P_J) \right. \\
&\left. + \frac{2T_F}{3C_A} \text{Im} f_8(^{2S+1}S_S) \mathcal{E}_3 \right), \quad (327)
\end{aligned}$$

$$\begin{aligned}
\Gamma(V_Q(nS) \rightarrow e^+e^-) &= \frac{C_A |R_{n0}^V(0)|^2}{\pi m^2} \text{Im} f_{ee}(^3S_1) \\
&\times \left(1 + \frac{4(2C_F + C_A) \alpha_s \mathcal{E}_{5/2}^E}{3\Gamma(7/2) m^{1/2}} \right), \quad (328)
\end{aligned}$$

$$\begin{aligned}
\Gamma(P_Q(nS) \rightarrow \gamma\gamma) &= \frac{C_A |R_{n0}^P(0)|^2}{\pi m^2} \text{Im} f_{\gamma\gamma}(^1S_0) \\
&\times \left(1 + \frac{4(2C_F + C_A) \alpha_s \mathcal{E}_{5/2}^E}{3\Gamma(7/2) m^{1/2}} \right), \quad (329)
\end{aligned}$$

$$\begin{aligned}
\Gamma(\chi_Q(nJ) \rightarrow \gamma\gamma) &= 3 \frac{C_A |R_{n1}^{(0)'}(0)|^2}{\pi m^4} \text{Im} f_{\gamma\gamma}(^3P_J) \\
&\text{for } J = 0, 2. \quad (330)
\end{aligned}$$

TABLE III. Recent determinations of \bar{m}_b and \bar{m}_c in the $\overline{\text{MS}}$ scheme from the $Y(1S)$ and $J/\psi(1S)$ masses.

Reference	Order	$\bar{m}_b(\bar{m}_b)$ (GeV)
Beneke and Signer, 1996	NNLO	4.24 ± 0.09
Hoang, 1999	NNLO	4.21 ± 0.09
Pineda, 2001	NNLO	$4.210 \pm 0.090 \pm 0.025$
Brambilla, Sumino, and Vairo, 2002	NNLO	$4.190 \pm 0.020 \pm 0.025$
Penin and Steinhäuser, 2002	NNNLO	4.349 ± 0.070
Lee, 2003a	NNNLO	4.20 ± 0.04
Contreras <i>et al.</i> , 2004	NNNLO	4.241 ± 0.070
Reference	Order	$\bar{m}_c(\bar{m}_c)$ (GeV)
Brambilla, Sumino, and Vairo, 2001	NNLO	1.24 ± 0.020

VIII. PHENOMENOLOGICAL APPLICATIONS

A. Determinations of m_b and m_c from the $1S$ resonances

Here we present state-of-the-art determinations of the bottom and charm masses from the ground-state bottomonium and charmonium masses.

For precise determinations of those parameters, we need a situation where the dynamics can be described by a weak-coupling analysis (at least in a first approximation) and where nonperturbative effects are small. Therefore the first question we should answer is are we in such a dynamical situation? For the bottomonium and charmonium systems, we believe that the masses m_b and m_c are much larger than Λ_{QCD} . This is not enough, however, since we also need $mv \gg \Lambda_{\text{QCD}}$. If this is the case then we are dealing (in a first approximation) with a Coulomb-type bound state. In this situation we can apply the results of Sec. IV.G once the renormalon cancellation along the lines of Sec. V has been used. In other words, our starting point will be Eq. (194). Let us see whether the assumption $mv \gg \Lambda_{\text{QCD}}$ is reasonable for bottomonium and charmonium ground states. The momentum transfer in the first case is around $\lesssim 2$ GeV whereas in the second case it is around $\lesssim 1$ GeV. The momentum transfer between the heavy quark and anti-quark lies in the deep Euclidean domain. Therefore the computation does not rely on local duality (at least to low orders in perturbation theory). The assumption $mv \gg \Lambda_{\text{QCD}}$ then becomes equivalent to believing in perturbative calculations in the Euclidean domain in the above range of energies. We report on work in which this assumption is taken for the bottomonium as well as for the charmonium ground state. The relative size between the US scale and Λ_{QCD} remains to be fixed.

Let us now consider recent determinations available in the literature, which we cite in Table III. In the first three references, as well as in the article by Penin and Steinhäuser (2002), finite charm-mass effects due to the potential and self-energy, calculated by Gray *et al.*

(1990); Eiras and Soto (2000); Hoang (2000); Melles (2000), were not included. In all the references except Beneke and Signer (1999) (at the moment of that computation the conversion from the pole to the $\overline{\text{MS}}$ masses was not known with the required accuracy), the conversion from the threshold (or pole) masses to the $\overline{\text{MS}}$ has been performed to three loops. The NNNLO analyses should be understood only as almost complete, since the three-loop static-potential coefficient was only estimated. In the work of Beneke and Signer (1999), a NNLO analysis was done in the PS scheme. In that of Hoang (1999), a NNLO analysis was done in the $1S$ scheme. In Pineda's work (2001), a NNLO analysis was done in the RS scheme as well as an analysis at NNNLO including the logarithms at this order and the large- β_0 result. In Brambilla, Sumino, and Vairo (2002), a NNLO analysis was done in the $\overline{\text{MS}}$ scheme using the epsilon expansion. Penin and Steinhäuser (2002) used a NNNLO analysis in the on-shell scheme. We believe that the difference with respect to the other results is due to the presence of the renormalon, as well as the way US and nonperturbative effects were implemented since the authors assume $mv^2 \gg \Lambda_{\text{QCD}}$. In the work of Lee (2003a) a NNNLO analysis was done in a scheme similar to the RS one. He included the US contribution within perturbation theory. Contreras *et al.* (2004) also used a NNNLO analysis in a scheme similar to the RS one. In this case, the US contribution was also treated perturbatively but in a different way from the soft one. It would be extremely interesting to repeat these analyses without the US contribution. Actually, in the Contreras *et al.* (2004) analysis, it is easy to separate out the US contribution (although it is not fully clear in which scheme). If one eliminates the US contribution in this case, the bottom mass goes down by around 50 MeV leading to good agreement with previous analyses. Nevertheless, it remains to be seen what would happen (Lee, 2003a) if a similar approach were applied.

We would also like to mention the determination of the charm mass from the $J/\psi(1S)$ mass (Brambilla, Sumino, and Vairo, 2001). The authors perform a complete NNLO analysis in the $1S$ scheme. It would be very interesting to perform a similar analysis with a different threshold mass, as well as to do the NNNLO analysis in order to see whether the result remains stable.

In the above analyses, with the exception of that of Penin and Steinhäuser (2002), the nonperturbative effects have been left unevaluated. In some cases the nonperturbative results obtained in the limit $mv^2 \gg \Lambda_{\text{QCD}}$ have been used to estimate their size.

The main sources of errors and possible improvements are the following. None of the above analyses has yet incorporated the resummation of logarithms available at NNLO. It would be interesting to see its effect on the mass of the heavy quarkonium. So far all (almost complete) NNNLO evaluations have been done assuming that the US contribution can be computed within perturbation theory. It would be most interesting to perform the NNNLO analysis without the US piece. Two of the (potentially) major sources of errors in these kinds of

evaluations of the heavy-quarkonium mass are the non-perturbative contribution (140) and possible effects due to subleading renormalons [see the discussion by Pineda (2001)]. Any reliable determination of Eq. (140) will have an immediate impact on our understanding of the theoretical errors. On the one hand, it would put on more solid ground our implicit assumption that the LO solution corresponds to a Coulomb-type bound state. Once this is achieved, it would bring the error estimates of the nonperturbative effects from a qualitative level to a quantitative one, (hopefully) decreasing their size significantly. On the other hand, one may think of cross-checking these results with other determinations. The fact that the difference happens to be relatively small supports the belief that (perturbative and nonperturbative) higher-order effects are indeed not very large. In order to have an independent handle on the size of the nonperturbative corrections, one may consider the difference between the lattice simulation of the static potential and the perturbative prediction (Pineda, 2003b). If one neglects possible effects of unquenching, one gets (in the static limit) nonperturbative contributions, which are not larger than ~ 100 MeV. A precise determination would require an accurate determination of the chromoelectric correlator which appears in Eq. (140) from the lattice. In this respect, we note that by using the data on the gluelump masses reported in Table II one obtains $\Lambda_E \approx 1.25$ GeV, which is much larger than the US scale. This may indicate that the actual situation, even for the ground-state bottomonium, is $mv \gg \Lambda_{\text{QCD}} \gg mv^2$, at least as far as the computation of Eq. (140) is concerned. Then the results of Sec. VII.F would apply.

B. Spectroscopy in the weak-coupling regime

Along the lines of the previous section, once it is assumed that the $Y(1S)$ can be described by the weak-coupling version of pNRQCD, it should be possible to give a prediction for the $\eta_b(1S)$ mass. If this belief is extended to the $J/\psi(1S)$, it should also be possible to give predictions for the $B_c(1S)^{25}$ and $B_c(1S)^*$ masses, as well as to check the theory by comparing them with the experimental value of the $\eta_c(1S)$ mass.

Working in the $1S$ scheme at NNLO, Brambilla and Vairo (2000a) obtained a prediction for the $B_c(1S)$ mass:

$$M(B_c) = 6326_{-9}^{+29} \text{ MeV}, \quad (331)$$

where the error accounts only for higher-order perturbative corrections and uncertainties in $\alpha_s(M_Z)$. The error due to nonperturbative contributions has been estimated to be 40–100 MeV. It is argued there that the nonperturbative contributions to the B_c mass in the $1S$ -mass scheme come out as the following combination of nonperturbative contributions in the pole-mass scheme: $-\delta E(J/\psi)^{\text{np}}/2 - \delta E(Y(1S))^{\text{np}}/2 + \delta E(B_c)^{\text{np}}$.

²⁵Although its mass has been measured to be $6.40 \pm 0.39 \pm 0.13$ GeV (Abe *et al.*, 1998), the precision is not good enough to test the theory.

Therefore cancellations may occur if all three corrections are of the same type and size. This may substantially reduce the total size of the nonperturbative corrections to the B_c in the $1S$ -mass scheme. Brambilla, Sumino, and Vairo (2001) made a similar determination using the $\overline{\text{MS}}$ c and b masses. The result is very similar: $M(B_c) = 6324 \pm 23$ MeV. Again the error only accounts for higher-order perturbative corrections and uncertainties in $\alpha_s(M_Z)$. The error due to nonperturbative contributions has not been estimated there. Brambilla, Sumino, and Vairo (2002) also included charm-mass effects in the analysis. They lower slightly the central value: $M(B_c) = 6309 \pm 17$ MeV. The error is as above.

In the case of bottomonium, Kniehl *et al.* (2004) calculated the hyperfine splitting of the ground state at NLL0 in the on-shell scheme (the effects due to the pole-mass renormalon are subleading). For this observable, the resummation of the logarithms along the lines discussed in Sec. IV.H seems important. The authors have given a rather precise prediction for the mass of the $\eta_b(1S)$, which uses the experimental value of $M_{Y(1S)}$,

$$M(\eta_b(1S)) = 9421 \pm 11(\text{th})_{-8}^{+9}(\delta\alpha_s) \text{ MeV}, \quad (332)$$

where the errors due to the higher-order perturbative corrections and the nonperturbative effects are added up in quadrature in “th,” whereas “ $\delta\alpha_s$ ” stands for the uncertainty in $\alpha_s(M_Z) = 0.118 \pm 0.003$. They also obtained a value for the charmonium ground-state hyperfine splitting, $M(J/\psi(1S)) - M(\eta_c(1S)) \approx 104$ MeV, to be compared with the experimental value of 117.7 MeV. Recksiegel and Sumino (2004) have performed a numerical NLO analysis of these hyperfine splittings. For bottomonium they get ≈ 44 MeV, which compares well with the above number, and for charmonium ≈ 88 MeV, which is somewhat lower.

Penin *et al.* (2004a) have also calculated the hyperfine splitting of the B_c ground state at NLL0 in a way similar to that of Kniehl *et al.* (2004). They obtain

$$M(B_c^*) - M(B_c) = 65 \pm 24(\text{th})_{-16}^{+19}(\delta\alpha_s) \text{ MeV}, \quad (333)$$

where the errors are as in Eq. (332). This result, combined with Eq. (331), or, eventually, with a more accurate experimental determination of the B_c mass, provides a prediction for the B_c^* mass.

Brambilla, Sumino, and Vairo (2001, 2002) considered higher excitations of the bottomonium system at NNLO in the $\overline{\text{MS}}$ mass scheme using the epsilon expansion (the latter reference also included finite charm-mass effects). It is not obvious *a priori* that these can be described under the kinematical assumption $mv \gg \Lambda_{\text{QCD}}$, however, it is worth investigating this possibility. The results for the levels that turn out to be stable in this analysis are shown in Table IV. We note that at least a part of the higher bottomonium levels seems to be reasonably well described in perturbation theory. In particular, the equal level spacing, characteristic for the quarkonium spectrum, is reasonably well reproduced without making use of a confining potential. This behavior seems to originate from self-energy contribution remnants of the

TABLE IV. Comparison of the theoretical predictions of some of the bottomonium levels obtained by Brambilla, Sumino, and Vairo (2002) with the experimental data. The errors come from summing quadratically uncertainties in α_s , higher-order corrections, and finite charm-mass corrections (Brambilla *et al.*, 2004).

Y	$M(Y)^{\text{exp}}$ (MeV)	$M(Y)$ (MeV)
$Y(1\ ^3P_0)$	9860	9995 (83)
$Y(1\ ^3P_1)$	9893	10 004 (86)
$Y(1\ ^3P_2)$	9913	10 012 (89)
$Y(2\ ^3S_1)$	10023	10 084 (102)
$Y(1\ ^3P_0)$	10232	10 548 (239)
$Y(1\ ^3P_1)$	10255	10 564 (247)
$Y(1\ ^3P_2)$	10269	10 578 (258)
$Y(3\ ^3S_1)$	10355	10 645 (298)

renormalon cancellation and may reflect, from the point of view of the spectrum, the numerical agreement mentioned in Sec. VI that is found in some situations between the perturbative static potential and the lattice data up to very large distances. Indeed, it was this phenomenological analysis that triggered part of the subsequent analysis of the static potential measured on the lattice in terms of perturbative QCD. Moreover, since for higher levels the experimental data agree with the theoretical results within the uncertainties, we may expect this to be the case also for the bottomonium ground state, suggesting very small nonperturbative corrections to it. Along similar lines, but within a numerical analysis, fine splittings of bottomonium and charmonium levels have been considered at NLO by Recksiegel and Sumino (2004).

C. Electromagnetic inclusive decay widths in the weak-coupling regime

The electromagnetic inclusive decay widths are known at NNLO (see Sec. IV.G). Nevertheless, they suffer from large-scale uncertainties, which have so far prevented their use in phenomenological analysis. This also affects the accuracy of sum rules (see the discussion in Sec. VIII.E).

Recently, there have been a few phenomenological analyses including the resummation of logarithms (see Sec. IV.H). The impact of these logarithms appears to be large and the overall convergence of the series seems to improve. For bottomonium, Penin *et al.* (2004b) considered the complete result with NNLO accuracy for the ratio of the spin-1 and spin-0 production in the on-shell scheme (at this order effects due to the pole-mass renormalon are subleading). The logarithmic expansion shows nice convergence and stability [see Fig. 19(a)] despite the presence of US contributions with α_s evaluated at a rather low scale ν^2/m_b . At the same time, the perturbative corrections are important and reduce the LO result by approximately 40%. For illustration, at the scale of

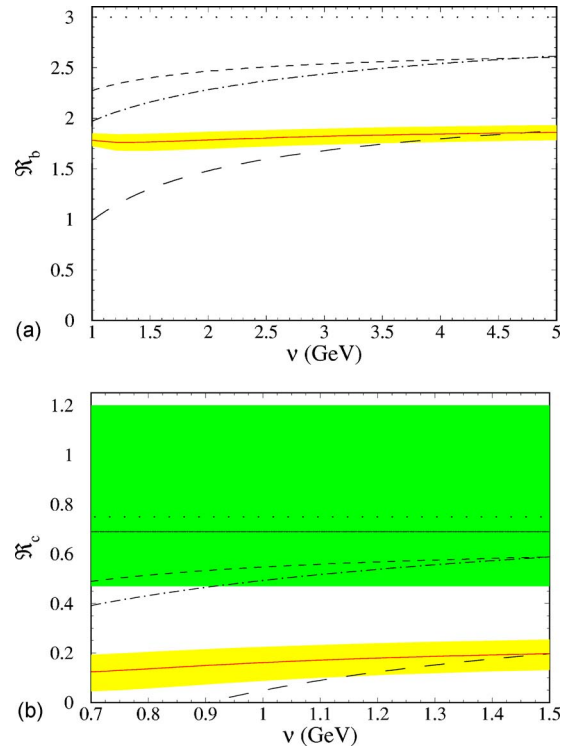


FIG. 19. (Color online) The spin ratio as a function of the renormalization scale ν in LO \equiv LL (dotted line), NLO (short-dashed line), NNLO (long-dashed line), NLL (dot-dashed line), and NNLL (solid line) approximation. For the NNLL result the band reflects the errors due to $\alpha_s(M_Z) = 0.118 \pm 0.003$. (a) The bottomonium ground-state case for which $\nu_h = m_b$. (b) The charmonium ground-state case for which $\nu_h = m_c$. In the charmonium case, the upper band represents the experimental error of the ratio (Eidelman *et al.*, 2004), where the central value is given by the horizontal solid line. From Penin *et al.*, 2004b.

minimal sensitivity, $\nu = 1.295$ GeV, one has the following series:

$$\mathcal{R}_b \equiv \frac{\Gamma(Y(1S) \rightarrow e^+e^-)}{\Gamma(\eta_b(1S) \rightarrow \gamma\gamma)} = \frac{1}{3e_b^2} (1 - 0.302 - 0.111). \quad (334)$$

In contrast, the fixed-order expansion blows up at the scale of the inverse Bohr radius. Nonperturbative effects contribute in the next-to-next-to-next-to-next-to-leading-logarithmic approximation, which is far beyond the precision of this computation. Note that the nonperturbative contribution to the ratio of decay rates is suppressed by a factor ν^2 in comparison to the binding energy and decay rates, where the leading nonperturbative effect is due to chromoelectric dipole interaction. Thus by using the available experimental data on the Y meson as input, one can predict the production and annihilation rates of the yet undiscovered η_b meson. In particular, one can predict the $\eta_b(1S)$ decay rate using the experimental value for the $Y(1S)$ decay rate (Penin *et al.*, 2004b):

$$\begin{aligned} \Gamma(\eta_b(1S) \rightarrow \gamma\gamma) \\ = 0.659 \pm 0.089(\text{th})_{-0.018}^{+0.019}(\delta\alpha_s) \pm 0.015(\text{expt}) \text{ keV}, \end{aligned} \quad (335)$$

where $\nu=1.295$ GeV was taken as the central value, the difference between the NNLO and NNLLO result for the theoretical error, and $\alpha_s(M_Z)=0.118\pm 0.003$. The last error in Eq. (335) reflects the experimental error of $\Gamma(Y(1S)\rightarrow e^+e^-)=1.314\pm 0.029$ keV (Eidelman *et al.*, 2004). This value considerably exceeds the result for the absolute value of the decay width obtained by Pineda (2003a) on the basis of a full NNLO analysis including the spin-independent part: $\Gamma(\eta_b(1S)\rightarrow \gamma\gamma)=0.35\pm 0.1(\text{th})\pm 0.05(\delta\alpha_s)$ keV. This can be a signal of slow convergence of the logarithmic expansion for the spin-independent contribution, which is more sensitive to the dynamics of the bound state and in particular to the US contribution, as has been discussed above. On the other hand, renormalon effects (Braaten and Chen, 1998; Bodwin and Chen, 1999) could produce some systematic errors in the purely perturbative evaluations of the production or annihilation rates. The problem is expected to be more severe for the charmonium case discussed below.

We would like to point out that the one-loop result for $\nu=m_b$ overshoots the NNLLO result by approximately 30%. This casts some doubts on the accuracy of the existing α_s determination from the $\Gamma(Y\rightarrow \text{light hadrons})/\Gamma(Y\rightarrow e^+e^-)$ decay rate ratio, which gives $\alpha_s(m_b)=0.177\pm 0.01$, well below the “world average” value (Eidelman *et al.*, 2004). The theoretical uncertainty in the analysis is estimated through the scale dependence of the one-loop result. The analysis of the photon-mediated annihilation rates indicates that the actual magnitude of the higher-order corrections is most likely quite far beyond such an estimate and the theoretical uncertainty given by Eidelman *et al.* (2004) should be increased by a factor of 2. This brings the result for α_s into a 1σ distance from the world average value.

For charmonium, the same analysis was performed by Penin *et al.* (2004b). The NNLO approximation becomes negative at an intermediate scale between $\alpha_s m_c$ and m_c [see Fig. 19(b)] and the use of the RG is mandatory in order to get a sensible perturbative approximation. The NNLLO approximation has good stability against the scale variation but the logarithmic expansion does not converge well. This is the main factor that limits the theoretical accuracy since the nonperturbative contribution is expected to be under control. For illustration, at the scale of minimal sensitivity, $\nu=0.645$ GeV, one obtains

$$\mathcal{R}_c \equiv \frac{\Gamma(J/\psi(1S) \rightarrow e^+e^-)}{\Gamma(\eta_c(1S) \rightarrow \gamma\gamma)} = \frac{1}{3e^2}(1 - 0.513 - 0.326). \quad (336)$$

The central value is 2σ below the experimental one. The discrepancy may be explained by large higher-order contributions. This should not be surprising because of the

rather large value of α_s at the inverse Bohr radius of charmonium. For the charmonium hyperfine splitting, however, the logarithmic expansion converges well and the prediction of the RG is in agreement with the experimental data. One can try to improve the convergence of the series for the production or annihilation rates by accurately taking into account the renormalon-related contributions. One point to note is that with a potential-model evaluation of the wave-function correction the sign of the NNLO term is reversed in the charmonium case (Czarnecki and Melnikov, 2001). At the same time the subtraction of the pole-mass renormalon from the perturbative static potential makes explicit that the potential is steeper and closer to lattice results and to phenomenological potential models, as we have seen in Sec. VI. Therefore the incorporation of higher-order effects from the static potential may improve the agreement with experiment. Finally, we mention that a NNLO evaluation for the $\eta_c(1S)\rightarrow \gamma\gamma$ decay reproduces in the minimal sensitivity region the experimental value (Pineda, 2003a).

D. Inclusive decay widths in the strong-coupling regime

At the end of Sec. II, we pointed out that the application of the NRQCD factorization formulas to inclusive annihilation widths of quarkonium was somehow limited by the large number and poor knowledge of the NRQCD four-fermion matrix elements. The pNRQCD factorization formulas presented in Sec. VII.H make both problems less severe by reducing the number of nonperturbative parameters and by factorizing the wave-function dependence. As a consequence, for systems to which it may be applied, pNRQCD in the strong-coupling regime has more predictive power than NRQCD. In the following, we present some of the predictions that are specific to pNRQCD. We remark that the problem of the poor convergence of the perturbative series for the NRQCD matching coefficients, also pointed out at the end of Sec. II, is specific to the hard-scale factorization and will persist at the level of pNRQCD.

Let us consider the following ratios of hadronic and electromagnetic annihilation widths for states with the same principal quantum number ($J=0,2$):

$$\begin{aligned} R_n^V &= \frac{\Gamma(V_Q(nS) \rightarrow LH)}{\Gamma(V_Q(nS) \rightarrow e^+e^-)}, \\ R_n^P &= \frac{\Gamma(P_Q(nS) \rightarrow LH)}{\Gamma(P_Q(nS) \rightarrow \gamma\gamma)}, \quad R_n^X = \frac{\Gamma(\chi_Q(nJ1) \rightarrow LH)}{\Gamma(\chi_Q(nJ1) \rightarrow \gamma\gamma)}. \end{aligned} \quad (337)$$

It is a specific prediction of pNRQCD that for states for which the assumption $\Lambda_{\text{QCD}} \gg E$ holds, the wave-function dependence drops out of the right-hand side of the above equations. The residual flavor dependence is encoded in the powers of $1/m$, in $E_{n0}^{(0)}$, and in the Wilson coefficients, while the residual dependence on the principal quantum number is encoded in the LO binding

energy $E_{n0}^{(0)}$. The Wilson coefficients may be calculated in perturbation theory and the binding energy may be derived from the quarkonium mass $M(nS)$: $M(nS) - 2m \simeq E_{n0}^{(0)}$. The only unknown quantities are the gluon-field correlators. The crucial point is that these do not depend on the flavor and the quarkonium quantum numbers. Therefore on the whole set of quarkonium states for which the pNRQCD formulas apply the number of non-perturbative parameters has decreased with respect to NRQCD. As discussed in Sec. VII.H, the gluon-field correlators may be extracted either from lattice simulations or specific models of the QCD vacuum or from experimental data. We shall come back to this last possibility at the end of the section.

Here we consider combinations of ratios in which even the dependence on the correlators drops out and predictions based purely on perturbative QCD are possible. Let us consider the ratios between R_n^V and R_n^P with different principal quantum numbers at order E/m . Contributions coming from the nonanalytic scale $\sqrt{m}\Lambda_{\text{QCD}}$ have not been calculated to that order, however, they appear to be suppressed in the ratio. We obtain

$$\frac{R_n^V}{R_m^V} = 1 + \left(\frac{\text{Im } g_1(^3S_1)}{\text{Im } f_1(^3S_1)} - \frac{\text{Im } g_{ee}(^3S_1)}{\text{Im } f_{ee}(^3S_1)} \right) \frac{M(nS) - M(mS)}{m}, \quad (338)$$

$$\frac{R_n^P}{R_m^P} = 1 + \left(\frac{\text{Im } g_1(^1S_0)}{\text{Im } f_1(^1S_0)} - \frac{\text{Im } g_{\gamma\gamma}(^1S_0)}{\text{Im } f_{\gamma\gamma}(^1S_0)} \right) \frac{M(nS) - M(mS)}{m}. \quad (339)$$

Due to the pNRQCD factorization, the octet-type contributions cancel in the ratio, differently from what is predicted in NRQCD within the standard power counting (Gremm and Kapustin, 1997). In the vector case we get for the $Y(2S)$ and $Y(3S)$ state ($m_b \simeq 5$ GeV) $R_2^Y/R_3^Y \simeq 1.3$, which is close to the experimental central value of about 1.4 from Eidelman *et al.* (2004). In the pseudoscalar case, since $\text{Im } g_1(^1S_0)/\text{Im } f_1(^1S_0) - \text{Im } g_{\gamma\gamma}(^1S_0)/\text{Im } f_{\gamma\gamma}(^1S_0)$ is of $\mathcal{O}(\alpha_s)$, we find that, at order E/m , R_n^P is the same for all radial excitations.

As mentioned above, it is possible to fix the gluon-field correlators on some experimental set of data and use them on some other. For instance, one may extract them from charmonium data and calculate bottomonium widths. This is particularly useful since at present, bottomonium data are less abundant than charmonium ones. The program has been carried out for P -wave decays by Brambilla, Eiras, *et al.* (2002). These depend on just one correlator, \mathcal{E}_3 , which may be extracted from P -wave charmonium decay data. The result is shown in Fig. 20. At the scale of 1 GeV one finds

$$\mathcal{E}_3(1 \text{ GeV}) = 5.3_{-2.2}^{+3.5}(\text{expt}), \quad (340)$$

where errors refer only to experimental uncertainties on the charmonium decay widths (in particular, uncertainties related to higher orders in the perturbative series,

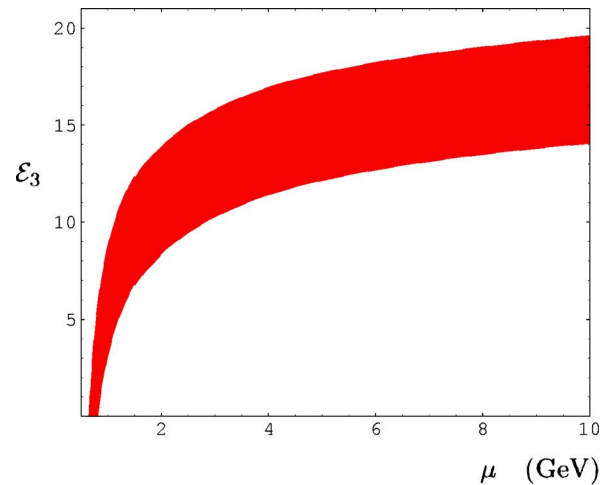


FIG. 20. (Color online) Plot of the one-loop RG-improved expression for \mathcal{E} vs μ : $\mathcal{E}(\mu) = \mathcal{E}(m) + (24N_c C_F / \beta_0) \ln[\alpha_s(m) / \alpha_s(\mu)]$. $\mathcal{E}(m)$ has been extracted from charmonium P -wave data. The error band accounts only for the uncertainties inherited from the charmonium data. From Vairo, 2003.

which may be potentially large, have not been included). In any case, the given value is compatible with the values that are usually assigned to the NRQCD octet and singlet matrix elements [e.g., from the fit given by Maltoni (2000) one obtains $\mathcal{E}_3(1 \text{ GeV}) = 3.6_{-2.9}^{+3.6}(\text{expt})$], while the bottomonium lattice data given by Bodwin *et al.* (1996, 2002) appear to give a lower value. Once \mathcal{E}_3 is known it may be inserted into Eqs. (327) and (330) to get the ratios of annihilation widths of bottomonium P waves. In practice, in pNRQCD at the order at which Eqs. (327) and (330) are valid, the 12 P -wave bottomonium and charmonium states that lie below threshold depend on 4 nonperturbative parameters (3 wave functions + 1 chromoelectric correlator \mathcal{E}_3). The reduction of the number of unknown nonperturbative parameters by 2 with respect to NRQCD allows one to formulate two specific new predictions of pNRQCD:

$$\frac{\Gamma(\chi_{b0}(1P) \rightarrow LH)}{\Gamma(\chi_{b1}(1P) \rightarrow LH)} = \frac{\Gamma(\chi_{b0}(2P) \rightarrow LH)}{\Gamma(\chi_{b1}(2P) \rightarrow LH)} = 8.0 \pm 1.3, \quad (341)$$

or alternatively

$$\frac{\Gamma(\chi_{b1}(1P) \rightarrow LH)}{\Gamma(\chi_{b2}(1P) \rightarrow LH)} = \frac{\Gamma(\chi_{b1}(2P) \rightarrow LH)}{\Gamma(\chi_{b2}(2P) \rightarrow LH)} = 0.50_{-0.04}^{+0.06}, \quad (342)$$

where \mathcal{E}_3 is taken from Fig. 20 and the NRQCD matching coefficients are taken at NLO. The errors refer only to the uncertainty in \mathcal{E}_3 . In Fig. 21 we plot the above ratios as functions of the factorization scale μ . We note that the scale dependence of \mathcal{E}_3 (see Fig. 20) has been smoothed out in the plots of Fig. 21, as expected in a physical quantity [compare the cancellation of the leading-order IR divergences between the singlet matching coefficients and the octet matrix elements discussed

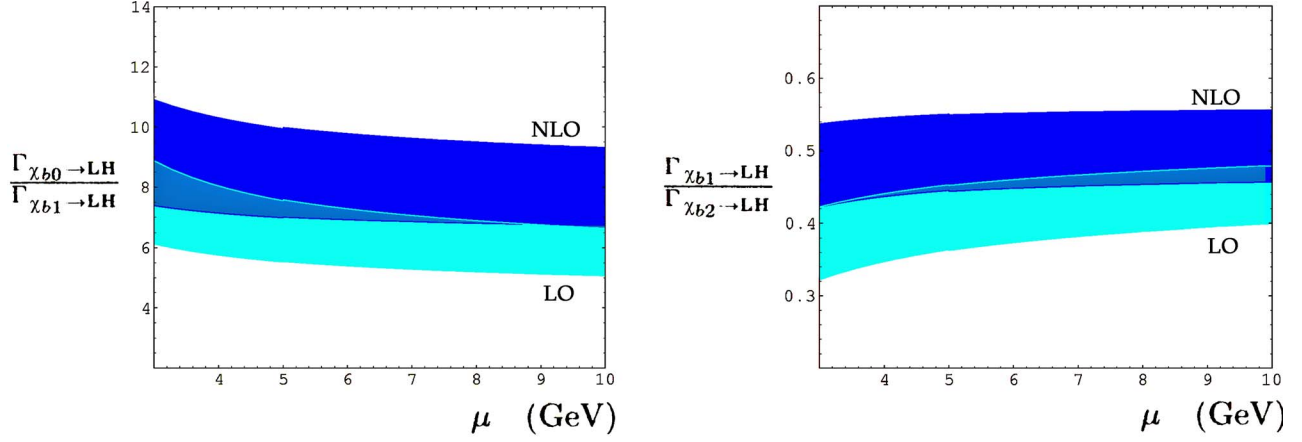


FIG. 21. (Color online) The left-hand side of Eqs. (341) and (342) plotted vs μ . We have taken \mathcal{E}_3 from Fig. 20. The LO and NLO bands refer to the Wilson coefficients at LO and NLO, respectively. From Vairo, 2003.

in the paragraph after Eq. (47)]. The large NLO corrections are reflected by the extension of the nonoverlapping regions in the two bands in Fig. 21. Recent CLEO measurements give [see Cinabro *et al.* (2002), corrected by Brambilla *et al.* (2004)] $\Gamma(\chi_{b0}(2P) \rightarrow LH)/\Gamma(\chi_{b2}(2P) \rightarrow LH) = 6.1 \pm 2.8$, which agree inside the large errors with the above predictions, and $\Gamma(\chi_{b1}(2P) \rightarrow LH)/\Gamma(\chi_{b2}(2P) \rightarrow LH) = 0.25 \pm 0.09$, which is somewhat lower than above.

The above approach may eventually be extended to a global fit of all correlators appearing in S - and P -wave annihilation widths. The obtained values could then be used to predict annihilation ratios of quarkonium states that are unknown or to improve present determinations. This program still requires the calculation of the contribution coming from the nonanalytic scale $\sqrt{m}\Lambda_{\text{QCD}}$, at least at relative order E/m and $\Lambda_{\text{QCD}}^2/m^2$, for S waves (that is with the same accuracy as the contributions coming from the analytic scales listed in Sec. VII.H) and the resummation of large contributions in the perturbative series of the four-fermion matching coefficients.

E. Nonrelativistic sum rules

NR sum rules are a classical example for the application of NR EFTs and the determination of the heavy-quark masses such as charm and bottom. The key point is the relation between $\Pi(q^2)$ at $q^2=0$ to moments of the total cross section $\sigma(e^+e^- \rightarrow Q\bar{Q})$. $\Pi(q^2)$ is defined in terms of the correlator of two electromagnetic heavy-quark currents in the following way:

$$(q_\mu q_\nu - g_{\mu\nu} q^2) \Pi(q^2) = i \int d^4x e^{iq \cdot x} \langle 0 | T \{ j_\mu^\nu(x) j_\nu^\nu(0) \} | 0 \rangle, \quad (343)$$

where $j_\mu^\nu(x) \equiv \bar{Q} \gamma_\mu Q(x)$. Using causality and the optical theorem one obtains

$$P_n = \frac{12\pi^2 e_Q^2}{n!} \left(\frac{d}{dq^2} \right)^n \Pi(q^2) |_{q^2=0} = \int_{\sqrt{s_{\min}}}^{\infty} \frac{ds}{s^{n+1}} R_{Q\bar{Q}}(s), \quad (344)$$

where $R_{Q\bar{Q}} \equiv \sigma(e^+e^- \rightarrow Q\bar{Q})/\sigma(e^+e^- \rightarrow \mu^+\mu^-)$ and e_Q is the quark electric charge. For low values of n , the left-hand side of Eq. (344) can be computed using perturbation theory due to the fact that the energy necessary to reach the threshold for heavy-quark production is much larger than Λ_{QCD} ,²⁶ whereas the right-hand side can be obtained from the experimental data. However, we are concerned here with the NR sum rules. These are defined by taking n large. This implies the existence of new scales in the problem besides m and Λ_{QCD} , such as m/\sqrt{n} , m/n , and so on. Therefore it is not so clear that one can actually perform computations within perturbation theory. For n large enough, one will have $\sqrt{n}\alpha_s \sim 1$ and a complete resummation of these terms should be achieved. The quantity $\sqrt{n}\alpha_s$ appears in the computation through the ratio of two different scales: $m\alpha_s/(m/\sqrt{n})$. Hence we see the following analogy with the NR situation: $1/\sqrt{n}$ plays the same role as v , the velocity of the heavy quark, and by taking $\sqrt{n}\alpha_s \sim 1$ we are considering the NR limit.

There is also another problem. For sufficiently large n , we can no longer claim that the induced scales are much larger than Λ_{QCD} and nonperturbative effects need to be considered. How to handle them is a delicate issue. Here, we only consider $m/\sqrt{n} \gg \Lambda_{\text{QCD}}$. This seems to be a safe requirement (at least for bottomonium). It is not clear, however, that we can also assume $m/n \gg \Lambda_{\text{QCD}}$. In practical applications the boundary for doing so is usu-

²⁶One should not forget, however, that potential problems may appear beyond NNLO due to the appearance of physical decay channels of the heavy quarkonium (Groote and Pivovarov, 2002; Portoles and Ruiz-Femenia, 2002).

TABLE V. Recent determinations of \bar{m}_b and \bar{m}_c in the $\overline{\text{MS}}$ scheme from NR sum rules.

Reference	Order	$\bar{m}_b(\bar{m}_b)$ (GeV)
Melnikov and Yelkhovsky, 1999a	NNLO (kinetic mass)	4.20±0.10
Penin and Pivovarov, 1999	NNLO (pole mass)	4.21±0.11
Beneke and Signer, 1999	NNLO (PS mass)	4.26±0.09
Hoang, 2000	NNLO (1S mass)	4.17±0.05
Eidemüller, 2003	NNLO (PS mass)	4.24±0.10
Reference	Order	$\bar{m}_c(\bar{m}_c)$ (GeV)
Eidemüller, 2003	NNLO (PS mass)	1.19±0.11

ally taken around $n \sim 10$. We discuss this issue further below.

In spite of the above remarks, the NR sum rules are ideal from the experimental point of view. By taking n large on the right-hand side of Eq. (344), the contribution from high momenta (the continuum region) is suppressed. Actually, this is the region which is less well known on the experimental side. Therefore by using NR sum rules, the experimental errors are significantly reduced. In practice, the following parametrization is used:

$$P_n^{\text{ex}} = \sum_{k=1}^6 \frac{9\pi}{\alpha^2(2m)} \frac{\Gamma_{Y(k)}}{M_{Y(k)}^{(2n+1)}} + \int_{\sqrt{s_{BB}}} ds s^{n+1} r_{\text{cont}}(s). \quad (345)$$

The theoretical expressions for the moments P_n^{th} can be computed order by order in the NR expansion in $1/\sqrt{n}$ and α_s , which at each order resums all the terms proportional to $\alpha_s \sqrt{n}$ to any power. Nowadays they are known in the on-shell scheme at NNLO in the NR expansion, which includes all corrections up to order $1/n$, α_s/\sqrt{n} , and α_s^2 (Kuhn *et al.*, 1998; Penin and Pivovarov, 1998; Beneke and Signer, 1999; Hoang, 1999; Melnikov and Yelkhovsky, 1999a). With this accuracy, the dispersion integration for the moments P_n takes the form

$$P_n = \frac{18C_A}{4^n m^{2n+2} \alpha^2(2m)} \int_{E_1}^{\infty} \frac{dE}{m} \exp\left(-\frac{E}{m}\right) \times \left(1 - \frac{E}{2m} + \frac{E^2}{4m^2 n}\right) \text{Im}[\langle \mathbf{r} = 0 | G_s(E) | \mathbf{r} = 0 \rangle] \times \left(\text{Im} f_{\text{EM}}^{\text{pNR}}({}^3S_1) + \text{Im} g_{\text{EM}}^{\text{pNR}}({}^3S_1) \frac{E}{m} \right), \quad (346)$$

where $E \equiv \sqrt{s} - 2m$ and E_1 is the binding energy of the lowest-lying resonance. The exponential form of the LO NR contribution to the energy integration has to be chosen because E scales as $v^2 \sim 1/n$. For explicit expressions, we refer the reader to Hoang (1999).

As we have pointed out before, working in the on-shell scheme introduces large errors. Therefore most of the analyses nowadays use threshold masses, where the cancellation of the pole-mass renormalon is explicit (see Table V). In practical terms this amounts to re-expressing the results obtained in the on-shell scheme in terms of the threshold masses. Nevertheless, even if

some improvement is obtained, large uncertainties remain due to a rather strong scale dependence. This scale dependence can be traced back to the fact that the decay width of the heavy quarkonium to e^+e^- is strongly scale dependent. For a more detailed discussion of this point, see Beneke and Signer (1999). In this respect, RG techniques have not yet been applied to these computations. It would be most interesting to do that and to see whether a more stable result is obtained.

Nonperturbative effects in sum rules are parametrically of the same size as in the $Y(1S)$ mass in the standard counting $1/\sqrt{n} \sim \alpha_s$. Nevertheless, it may happen that they are numerically suppressed. This is indeed the case considering that one can describe the nonperturbative effects by local condensates (Voloshin, 1995; Onishchenko, 2000). However, one can use the expression in terms of local condensates only when $m/n \gg \Lambda_{\text{QCD}}$ (although one can use that result as an order of magnitude estimate of the nonperturbative effects). This would be analogous to the assumption $m\alpha_s^2 \gg \Lambda_{\text{QCD}}$, which may be difficult to fulfill. Therefore it is more likely that the nonperturbative corrections will also depend on a non-local condensate of the same type (chromoelectric correlator) as the $Y(1S)$ mass does. Thus in order to estimate the nonperturbative errors in sum-rules evaluations, it would be most welcome to have at least the explicit expression of the nonperturbative effects when $m/n \sim \Lambda_{\text{QCD}}$, which is still lacking. In that way one could relate the nonperturbative effects for different moments in the sum rules to each other or to the nonperturbative effects in the $Y(1S)$ mass.

F. $t\bar{t}$ production near threshold

Future linear electron-positron colliders will produce large samples of $t\bar{t}$ pairs near threshold (Bagger *et al.*, 2000; Abe *et al.*, 2001a, 2001b; Aguilar-Saavedra *et al.*, 2001). In this regime, the top and the antitop will move slowly with respect to each other and pNRQCD becomes applicable. Since the top-quark mass $m_t \sim 175$ GeV and the expected (electroweak) decay width $\Gamma_t \sim 1.5$ GeV are large in comparison with Λ_{QCD} , nonperturbative effects due to Λ_{QCD} are expected to be small in the whole threshold region and hence a weak-

coupling analysis is very reliable. In addition, since $\Gamma_t \sim m_t \alpha_s^2$, which is the US scale, a remnant of the would-be toponium $1S$ state is expected to show up as a bump in the total cross section. This will serve to obtain the top-quark mass with a high accuracy.

The $t\bar{t}$ pair will be dominantly produced via $e^+e^- \rightarrow \gamma^*, Z^* \rightarrow t\bar{t}$. The total production cross section may be written as (Hoang *et al.*, 2000)

$$\sigma_{\text{tot}}^{\gamma, Z}(s) = \frac{4\pi\alpha^2}{3s} [F^v(s)R^v(s) + F^a(s)R^a(s)], \quad (347)$$

where $F^v(s)$ and $F^a(s)$ contain electroweak parameters (Hoang *et al.*, 2002) and

$$R^v(s) = \frac{4\pi}{s} \text{Im} \left(-i \int d^4x e^{iq \cdot x} \langle 0 | T j_\mu^v(x) j^{\nu\mu}(0) | 0 \rangle \right),$$

$$R^a(s) = \frac{4\pi}{s} \text{Im} \left(-i \int d^4x e^{iq \cdot x} \langle 0 | T j_\mu^a(x) j^{a\mu}(0) | 0 \rangle \right), \quad (348)$$

where $q = (\sqrt{s}, 0)$ and j_μ^v (j_μ^a) is the vector (axial-vector) current that produces a quark-antiquark pair defined by Eq. (12) [Eq. (13)]. Hence the full QCD calculation can be split into (i) calculating the matching coefficients $b_1^v(m_t, \nu)$, $b_2^v(m_t, \nu)$, and $b_1^a(m_t, \nu)$, and (ii) calculating current correlators in pNRQCD. Up to NNLO [$\mathcal{O}(\alpha_s^2)$ corrections], the latter reduces to a purely quantum-mechanical calculation along the lines of Sec. IV.G (US gluons do not play any role). The potential is only needed at the order displayed in Eqs. (101) and (102). This calculation has been carried out by several groups²⁷ and the final outcome is summarized by Hoang *et al.* (2000) [previous computations at LO (Fadin and Khoze, 1988) and NLO (Strassler and Peskin, 1991) relied on potential models which needed phenomenological input]. Several comments are in order.

(1) At NNLO, the scale dependence which appears in the matching coefficient $b_1^v(m_t, \nu)$ ($b_2^v = b_1^a = 1$ at this order) is compensated by the scale dependence introduced by regulating and renormalizing the UV divergences of the quantum-mechanical perturbation theory (*potential loops*).

(2) The top-quark width is introduced by replacing m_t by $m_t - i\Gamma_t/2$. A consistent inclusion of electroweak effects is still lacking.

(3) In order to obtain stable results for the top-quark mass in going from LO to NLO to NNLO, it is very important to use the so-called threshold masses rather than the pole mass. These are discussed in Sec. V.

(4) The large logarithms arising due to the various scales in the problem can be resummed using RG techniques as described in Sec. IV.H. This problem is non-trivial because all scales (hard, soft, potential, and US) play a role. It was first addressed within the velocity

NRQCD framework (Hoang, Manohar, Stewart, *et al.*, 2001). However, the correct result for $b_1^v(m_t, \mu)$ at NNLO was first given within pNRQCD by Pineda (2002a) and later reproduced within velocity NRQCD (Hoang and Stewart, 2003). Hoang and co-workers (2004); Hoang *et al.* (2002) computed some partial results for the NNLO contribution. The resulting series (Hoang, 2004) does not show a very good convergence (even if the absolute value of the corrections is small). This, however, may be due to the scheme dependence of the result. Penin *et al.* (2004b) have obtained a complete (and therefore scheme-independent) result with NNLO accuracy for the ratio of the spin-1 and spin-0 production. In this case good convergence is found, but one should keep in mind that this ratio is less sensitive to the US scale than the full current. Therefore it is premature to draw any definite conclusion about the convergence of the series before getting the complete NNLO evaluation, which, even if difficult, is within reach. This is of utmost importance for future determinations of the top mass and the Higgs-top coupling at a future linear collider (Martinez and Miquel, 2003).

(5) At NNNLO, as well as for the resummations above, US gluons start to play a role. The double logarithmic contributions were calculated by Kniehl and Penin (2000c) and the single logarithmic ones by Kniehl *et al.* (2003). The finite pieces are still missing. These can, in principle, be calculated with the potentials given by Kniehl, Penin, Smirnov, *et al.* (2002) together with the three-loop static potential (which is still missing), and the LO terms for the US gluons given by Eq. (60). The matching coefficients $b_1^v(m_t, \nu)$, $b_2^v(m_t, \nu)$, and $b_1^a(m_t, \nu)$ also need to be calculated to one order higher in α_s .

Figure 22 shows the current status of theoretical results for the total cross section for $e^+e^- \rightarrow \gamma^* \rightarrow t^+t^-$.

G. Semi-inclusive radiative decays

We have seen that NRQCD and pNRQCD are particularly suitable for describing inclusive decays of heavy quarkonia to light particles. Semi-inclusive and fully exclusive decays can also be addressed but they require additional theoretical considerations. Similar to what happens for inclusive decays, pNRQCD is expected to provide supplementary information here as well. Semi-inclusive radiative decays to light hadrons in which only the photon energy is measured are the simplest of them and will be briefly discussed in the following.

We shall restrict our discussion to the so-called direct contributions, for which the photon is emitted from a heavy-quark electromagnetic current. Fragmentation contributions also play an important role (Catani and Hautmann, 1995). The starting point is the QCD formula (Rothstein and Wise, 1997)

$$\frac{d\Gamma}{dz} = z \frac{M}{16\pi^2} \text{Im} T(z), \quad (349)$$

²⁷For an analytical expression for the $\gamma\gamma \rightarrow t\bar{t}$ cross section at NNLO, see Penin and Pivovarov (2001).

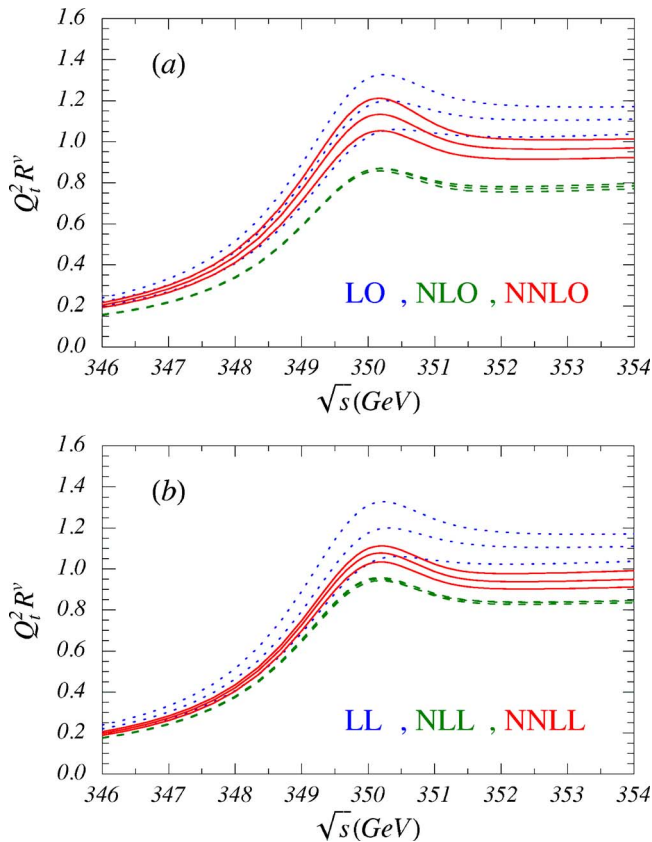


FIG. 22. (Color online) (a) The results for $e_t^2 R^v$ ($e_t=2/3$ is the top-quark electric charge) with $m_t=175$ GeV (the $1S$ threshold mass is used, see Sec. V) and $\Gamma_t=1.43$ GeV in fixed-order perturbation theory at LO (dotted lines), NLO (dashed lines), and NNLO (solid lines). (b) The results for $e_t^2 R^v$ with the same parameters in RG-improved perturbation theory at LL (dotted lines), NLL (dashed lines), and (partial) NNLL (solid lines) order. For each order, curves are plotted for $v_p/m_t=0.15, 0.20$, and 0.3 . From Hoang, 2003.

$$T(z) = -i \int d^4x e^{-iq \cdot x} \langle V_Q(nS) | T \{ J_\mu^v(x) j_\nu^v(0) \} \rangle \times |V_Q(nS)\rangle g_\perp^{\mu\nu},$$

where M is the heavy-quarkonium mass, and we have restricted ourselves to 3S_1 states. q is the photon momentum, which in the rest frame of the heavy quarkonium is $q=(q_+, q_-, q_\perp)=(zM, 0, 0)$. We have used light-cone coordinates $q_\pm=q^0 \pm q^3$. $z \in [0,1]$ is defined as $z=2E_\gamma/M$, namely, the fraction of the maximum energy that the photon may have in the heavy-quarkonium rest frame.

For z away from the lower and upper end points (0 and 1, respectively), no further scale is introduced beyond those inherent in the NR system. The integration of the scale m in the time-ordered product of currents in Eq. (349) leads to local NRQCD operators with matching coefficients which depend on m and z . At LO one obtains

$$\frac{1}{\Gamma_0} \frac{d\Gamma_{\text{LO}}}{dz} = \frac{2-z}{z} + \frac{z(1-z)}{(2-z)^2} + 2 \frac{1-z}{z^2} \ln(1-z) - 2 \frac{(1-z)^2}{(2-z)^3} \ln(1-z), \quad (350)$$

where

$$\Gamma_0 = \frac{32}{27} \alpha_s^2 e_Q^2 \frac{\langle V_Q(nS) | \mathcal{O}_1(^3S_1) | V_Q(nS) \rangle}{m^2}, \quad (351)$$

and e_Q is the charge of the heavy quark. The α_s correction to this rate was calculated numerically by Krämer (1999). The contribution of color-octet operators turns out to be strongly suppressed away from the upper endpoint region (the lowest-order color-octet contribution identically vanishes) (Maltoni and Petrelli, 1999). The expression corresponding to Eq. (351) in pNRQCD is obtained at lowest order in any of the possible regimes by just making the substitution

$$\langle V_Q(nS) | \mathcal{O}_1(^3S_1) | V_Q(nS) \rangle = \frac{N_c}{2\pi} |R_{n0}(0)|^2. \quad (352)$$

The final result coincides with the result of early QCD calculations (Brodsky *et al.*, 1978; Koller and Walsh, 1978).

For $z \rightarrow 0$, the emitted low-energy photon can only produce transitions within the NR bound state without destroying it. Hence the direct low-energy photon emission takes place in two steps: (i) the photon is emitted (dominantly by electric dipole and magnetic dipole transitions) and (ii) the remaining (off-shell) bound state is annihilated into light hadrons. It has a suppression $\sim z^3$ with respect to Γ_0 [see Manohar and Ruiz-Femenia (2004) and Voloshin (2004) for recent analyses of this region in QED]. Hence at some point the direct photon emission is overtaken by the so-called fragmentation contributions $\bar{Q}Q \rightarrow ggg \rightarrow gg\bar{q}q\gamma$ (Catani and Hautmann, 1995; Maltoni and Petrelli, 1999).

For $z \rightarrow 1$, momentum conservation implies that the gluons emitted in the short-distance annihilation process must have a direction roughly opposite to that of the photon. They produce a jetlike event with momentum $p_X=((1-z)M, M, 0)$ (in light-cone coordinates). This implies that two more scales become relevant, $p_{X^+}=(1-z)M$ and $p_{X^2}=(1-z)M^2$, producing an additional hierarchy $M \gg M\sqrt{1-z} \gg M(1-z)$. In recent years an EFT named soft-collinear effective theory (SEFT) has been introduced in order to efficiently exploit this hierarchy of scales. The main ideas which led to SEFT were outlined by Bauer, Fleming, and Luke (2001). Nowadays, it is being developed by several groups (Bauer, Fleming, Pirjol, *et al.*, 2001; Beneke *et al.*, 2002; Chay and Kim, 2002; Hill and Neubert, 2003) and it has been applied to $Y(1S)$ radiative decays by Bauer, Chaing, *et al.* (2001); Fleming and Leibovich (2003a, 2003b, 2004); Garcia i Tormo and Soto (2004). We shall not review SEFT here (a complete analysis connecting pNRQCD and SEFT is still lacking), but only mention its relevant features for the case we are concerned with. For $z \rightarrow 1$, upon inte-

grating out the scale m , the time-ordered product of currents in Eq. (349) does not reduce to local NRQCD operators anymore. Additional degrees of freedom are needed. These are collinear gluons (and collinear light quarks), which are defined as those having a typical momentum (in light-cone coordinates) $p \sim ((1-z)M, M, \sqrt{1-z}M)$. They are incorporated in SEFT together with the remaining degrees of freedom in NRQCD. Then one matches the QCD electromagnetic currents $j_\mu^\nu(x)$ (rather than the full time-ordered product) to SEFT currents. Next, the scale $\sqrt{1-z}M$ is integrated out (assuming that it is large enough to use perturbation theory) by matching the time-ordered product of currents in SEFT (now renamed SCET_I) to (nonlocal) operators of the so-called SCET_{II}, which does not contain collinear modes of virtuality $\sim(1-z)M^2$ anymore [see Beneke and Feldmann (2004) for a detailed description of the modes involved in SCET_I and in SCET_{II}]. By calculating the anomalous dimensions of the various operators appearing in both matchings and using standard RG techniques, one can resum large (Sudakov) logarithms $\ln(1-z)$. For the color-octet currents, this was done by Bauer, Chiang, *et al.* (2001) and for the color-singlet ones by results of Fleming and Leibovich (2003a, 2004). For the color-octet sector, the final outcome corrects the old results obtained by Photiadis (1985). For the color-octet sector, the final result may be given in terms of so-called shape functions (Rothstein and Wise, 1997), which involve expectation values in the heavy-quarkonium state of two color-octet NRQCD currents separated along a light-cone direction, for instance,

$$S(\ell^+) = \int \frac{dx^-}{4\pi} e^{-i/2\ell^+x^-} \langle V_Q(nS) | [\psi^\dagger T^b \chi](x^-) \phi_{bc}^{\text{adj}}(0, x^-) \times [\chi^\dagger T^c \psi](0) | V_Q(nS) \rangle. \quad (353)$$

If the heavy-quarkonium state is in the weak-coupling regime, as is likely in the case of the $Y(1S)$ system, one can use pNRQCD in that regime to calculate the shape functions. This was done by Garcia i Tormo and Soto (2004) [see also Beneke *et al.* (2000)]. When these results are combined with those of the singlet sector, an excellent description of data (Nemati *et al.*, 1997) is obtained (see Fig. 23) for the end-point region. Although, as discussed by Garcia i Tormo and Soto (2004), there are still some calculations missing in order to have a totally unambiguous theoretical result, the agreement with data is very encouraging. Indeed, the end-point region of the photon spectrum has been very elusive to theoretical descriptions. The color-singlet contribution (sometimes referred to as the color-singlet model) lies well above the data. For the color-octet contributions, different models were used in the past to estimate the shape functions, generically producing results incompatible with data (Bauer, Chiang, *et al.*, 2001; Wolf, 2001). These facts were used to argue that the introduction of a nonvanishing gluon mass was necessary in order to fit the experimental data (Field, 2002). This is no longer the case, at least as far as the $Y(1S)$ system is concerned.

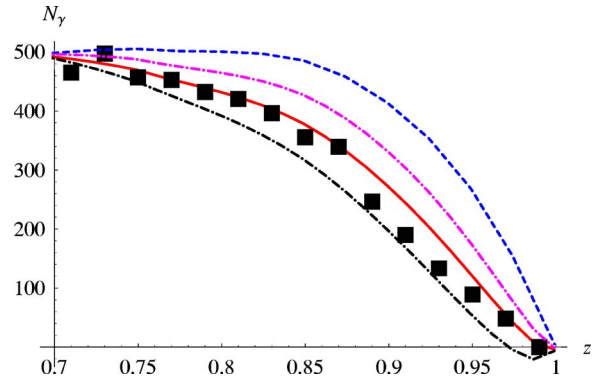


FIG. 23. (Color online) End-point region of the photon spectrum in semi-inclusive Y decay. The points are CLEO data (Nemati *et al.*, 1997), the dashed line is the (best) curve obtained by Fleming and Leibovich (2003a), and the solid and dot-dashed lines are the results of Garcia i Tormo and Soto (2004) (the solid line is the central value and the dot-dashed lines are obtained by a $2^{\pm 1}$ variation of the relevant scale). From Garcia i Tormo and Soto, 2004.

IX. CONCLUSIONS

The application of QCD EFTs to heavy quarkonia has considerably increased our understanding of those systems from a fundamental point of view. This has occurred at several levels.

- Long-standing puzzles have been resolved. For instance, the fate of IR divergences in the decay widths to light particles has been resolved in NRQCD by introducing color-octet operators, and the fate of the IR divergences in the QCD static potential has been resolved in pNRQCD by the explicit use of US gluons.
- Heavy-quarkonium physics in the strong-coupling regime has been brought into the realm of systematic calculations in QCD. This has led to the discovery of new terms in the potential which were missed in the past, both analytic and nonanalytic in $1/m$, and to express the color-octet NRQCD matrix elements in terms of wave functions at the origin and additional bound-state-independent nonperturbative parameters. This puts NR phenomenological potential models in a QCD context in the kinematic regime where this EFT description applies.
- In the weak-coupling regime, it has allowed higher-order calculations to be carried out in a systematic and much simpler manner. Errors are under parametric control. Moreover, it has made possible the application of RG techniques, which have been used to resum infinite series of IR QCD logarithms, being so far the only known way to carry out such resummations. This has opened up the possibility of having precision determinations of the Standard Model parameters to which the heavy quarkonium is sensitive: α_s and the heavy-quark masses.

Although the virtues by far exceed the drawbacks, the

latter are not absent in EFTs of heavy quarkonium. They are all related to the fact that the actual bottom and especially charm masses, are not so much larger than Λ_{QCD} (for toponiumlike states the EFT should work very well). This means that the scales $m \gg p \gg E$, which are assumed to be well separated, may actually not be that well separated, and hence expansions in various ratios may show a slow convergence. In the strong-coupling regime it is still too early to judge. For $Y(1S)$ in the weak-coupling regime, the convergence seems to be good. In addition, most of the matching coefficients of NRQCD show a poor convergence in $\alpha_s(m)$ for both bottom and charm masses, which is jeopardizing many practical applications of NRQCD. We may expect, however, that once the renormalon singularities in each series have been identified and properly subtracted, the situation will improve considerably, as has occurred with the introduction of threshold masses.

X. PROSPECTS

NR EFTs for heavy quarkonium still have an enormous potential and may evolve in many different directions. Some of them are more or less obvious improvements or extensions of what has been presented here. Others require the introduction of new concepts and techniques.

Among the obvious improvements are those which consist of calculating matching coefficients and observables to a higher accuracy in both NRQCD and pNRQCD. In NRQCD, it would be important to have the NNLO calculation of the imaginary parts of the matching coefficients of the four-fermion operators, at least for S and P waves. This would allow one to see whether the poor convergence observed at NLO is corrected or remains, and in either case it would facilitate renormalon-based improvements. It would also be important to have further and more accurate lattice calculations of the NRQCD matrix elements (see Sec. II.F.2). In the weak-coupling regime of pNRQCD, some perturbative calculations are missing, which seem to be in reach of the current computational power. Let us only mention the complete three-loop static potential, which is necessary for the complete NNNLO spectrum and for electromagnetic production processes (for instance, in $t\bar{t}$); the complete NNNLO resummation of the creation and annihilation currents; and the NNNLO calculation of electromagnetic production. These would allow an increase in the precision of the determinations of m_b , m_c , α_s , and, eventually, m_t (see Sec. VIII.A). For the case of $Y(1S)$, the accuracy is limited by the poor knowledge of the nonperturbative contributions, which are precisely given in terms of chromoelectric-field correlators. A proper lattice evaluation of the latter would be most welcome. For the $t\bar{t}$ system, the level of accuracy calls for the consistent inclusion of electroweak effects, which is also missing (see Sec. VIII.F).

In the strong-coupling regime of pNRQCD, on the one hand, it is necessary to update the early lattice

evaluations of the potentials including the more recently found $1/m$ and $1/m^2$ potentials. On the other hand, a systematic matching procedure of the potentials to the continuum limit and a rigorous lattice renormalization scheme should be developed (see Sec. VII.G). This will lead to a fully consistent lattice version of pNRQCD.

In the same regime, the inclusion of pseudo-Goldstone bosons (pions) and low-energy photons is still lacking. This would allow a description of electromagnetic and hadronic transitions in that situation.

Let us next mention some applications of EFTs to heavy quarkonium that require further theoretical elaborations.

The systematic study of semi-inclusive (see Sec. VIII.G) and exclusive decays may need the introduction of further degrees of freedom in addition to those of NRQCD or pNRQCD.

NRQCD production matrix elements should also have definite expressions in pNRQCD both in the weak- and in the strong-coupling regimes, which have not been worked out yet. It is expected that as for the decay matrix elements, new relations may appear and the number of nonperturbative parameters consequently reduced.

States close to or above the heavy-light meson pair threshold cannot be treated using pNRQCD, at least in its current formulations. Hence one has to stay at the NRQCD level. A hadronic version of NRQCD, including heavy-quarkonium states, heavy-light mesons, and pseudo-Goldstone bosons, in the spirit of Burdman and Donoghue (1992); Casalbuoni *et al.* (1997); Mannel and Urech (1997); Voloshin (2003), might prove useful and will eventually help to understand the nature of present (Choi *et al.*, 2003) and possibly future potential states in that region.

Including finite temperature in NRQCD and pNRQCD would make it possible to address important questions such as J/ψ suppression as a sign of deconfinement (Matsui and Satz, 1986) in current and future heavy-ion collision experiments.

Finally, by slightly changing the fundamental degrees of freedom, EFTs may be built which are similar to pNRQCD, but also suitable for describing bound states made of two heavy particles other than heavy quarkonium. An example is heavy baryons made of two heavy quarks, similar to those recently discovered at SELEX (Mattson *et al.*, 2002). These systems are theoretically quite interesting due to the interplay of HQET and NRQCD (Rösch, 2003; Soto, 2003). Quarkonia-quarkonia scattering may also be studied along the lines of the work of Bhanot and Peskin (1979); Peskin (1979); Fujii and Kharzeev (1999); Vairo (2000).

We feel that we are at the beginning of a time where most aspects of the physics of heavy quarkonium, and of similar systems, will be addressed in terms of EFTs of QCD. This is more than a change in language. It is moving this physics from being a battleground of competing models to being a source of some of the fundamental parameters of the Standard Model, a reliable test of its validity in the strong interaction sector, and a unique laboratory for the study of QCD properties.

ACKNOWLEDGMENTS

We are thankful to A. G. Grozin for comments on the manuscript and to C. Ewerz for a careful reading of the manuscript and many useful comments and suggestions. We gratefully acknowledge financial support from “Azioni Integrate Italia-Spagna 2004 (IT1824)/Acciones Integradas España-Italia (HI2003-0362),” and from the cooperation agreement INFN04-16 (CICYT-INFN). A.P. and J.S. are also funded by the MCyT and Feder (Spain) Grant No. FPA2001-3598, the CIRIT (Catalonia) Grant No. 2001SGR-00065, and the network EURIDICE (EU) HPRN-CT2002-00311. J.S. has been partially funded by the National Science Foundation under Grant No. PHY99-0794. A.V. acknowledges the financial support obtained inside the Italian MIUR program “Incentivazione alla Mobilità di Studiosi Stranieri e Italiani Residenti all’Estero.” N.B., J.S., and A.V. would like to thank the Benasque Center of Physics and J.S. the Kvali Institute of Theoretical Physics for hospitality while part of this work was written.

TABLE OF ACRONYMS

2PI	Two-particle irreducible
2PR	Two-particle reducible
DR	Dimensional regularization
EFT	Effective field theory
IR	Infrared
HQET	Heavy-quark effective theory
LO	Leading order
MS	Minimal subtraction
NLO	Next-to-leading order
NNLO	Next-to-next-to-leading order
NNNLO	Next-to-next-to-next-to-leading order
LL	Leading-logarithm order
NLL	Next-to-leading-logarithm order
NNLL	Next-to-next-to-leading-logarithm order
NR	Nonrelativistic
NRQCD	Nonrelativistic quantum chromodynamics
NRQED	Nonrelativistic quantum electrodynamics
pNRQCD	Potential NRQCD
PS	Potential subtracted
QFT	Quantum field theory
RG	Renormalization group
RS	Renormalon subtracted
SCET	Soft-collinear effective theory
US	Ultrasoft
vNRQCD	Velocity NRQCD

REFERENCES

Abe, F., *et al.* (CDF Collaboration), 1994, Phys. Rev. Lett. **73**, 225.
 Abe, F., *et al.* (CDF Collaboration), 1998, Phys. Rev. Lett. **81**, 2432.
 Abe, K., *et al.* (ACFA Linear Collider Working Group), 2001a, e-print hep-ph/0109166.
 Abe, T., *et al.* (American Linear Collider Working Group), 2001b, e-print hep-ex/0106057.

Aglietti, U., and Z. Ligeti, 1995, Phys. Lett. B **364**, 75.
 Aguilar-Saavedra, J. A., *et al.* (ECFA/DESY LC Physics Working Group), 2001, e-print hep-ph/0106315.
 Amoros, G., M. Beneke, and M. Neubert, 1997, Phys. Lett. B **401**, 81.
 Appelquist, T., M. Dine, and I. J. Muzinich, 1978, Phys. Rev. D **17**, 2074.
 Appelquist, T., and H. D. Politzer, 1975, Phys. Rev. Lett. **34**, 43.
 Aubert, J. J., *et al.*, 1974, Phys. Rev. Lett. **33**, 1404.
 Augustin, J. E., *et al.*, 1974, Phys. Rev. Lett. **33**, 1406.
 Bagger, J., *et al.* (American Linear Collider Working Group), 2000, e-print hep-ex/0007022.
 Baker, M., J. S. Ball, N. Brambilla, G. M. Prospero, and F. Zachariasen, 1996, Phys. Rev. D **54**, 2829.
 Baker, M., J. S. Ball, N. Brambilla, and A. Vairo, 1996, Phys. Lett. B **389**, 577.
 Baker, M., J. S. Ball, and F. Zachariasen, 1991, Phys. Rep. **209**, 73.
 Baker, M., N. Brambilla, H. G. Dosch, and A. Vairo, 1998, Phys. Rev. D **58**, 034010.
 Baker, M., and R. Steinke, 2001, e-print hep-ph/0101255.
 Bali, G. S., 2001, Phys. Rep. **343**, 1.
 Bali, G. S., N. Brambilla, and A. Vairo, 1998, Phys. Lett. B **421**, 265.
 Bali, G. S., and A. Pineda, 2004, Phys. Rev. D **69**, 094001.
 Bali, G. S., K. Schilling, and A. Wachter, 1997, Phys. Rev. D **56**, 2566.
 Bali, G. S., *et al.* (UKQCD Collaboration), 1993, Phys. Lett. B **309**, 378.
 Bali, G. S., *et al.* (TXL Collaboration), 2000, Phys. Rev. D **62**, 054503.
 Balitsky, I. I., 1985, Nucl. Phys. B **254**, 166.
 Balzereit, C., 1999, Phys. Rev. D **59**, 034006.
 Barbieri, R., M. Caffo, R. Gatto, and E. Remiddi, 1980, Phys. Lett. **B95**, 93.
 Barbieri, R., M. Caffo, R. Gatto, and E. Remiddi, 1981, Nucl. Phys. B **192**, 61.
 Barbieri, R., E. d’Emilio, G. Curci, and E. Remiddi, 1979, Nucl. Phys. B **154**, 535.
 Barbieri, R., R. Gatto, and E. Remiddi, 1976, Phys. Lett. **61B**, 465.
 Barchielli, A., N. Brambilla, and G. M. Prospero, 1990, Nuovo Cimento Soc. Ital. Fis., A **103A**, 59.
 Barchielli, A., E. Montaldi, and G. M. Prospero, 1988, Nucl. Phys. B **296**, 625.
 Bauer, C. W., C.-W. Chiang, S. Fleming, A. K. Leibovich, and I. Low, 2001, Phys. Rev. D **64**, 114014.
 Bauer, C. W., S. Fleming, and M. E. Luke, 2001, Phys. Rev. D **63**, 014006.
 Bauer, C. W., S. Fleming, D. Pirjol, and I. W. Stewart, 2001, Phys. Rev. D **63**, 114020.
 Bauer, C. W., and A. V. Manohar, 1998, Phys. Rev. D **57**, 337.
 Becher, T., and K. Melnikov, 2002, Phys. Rev. D **66**, 074508.
 Becher, T., and K. Melnikov, 2003, Phys. Rev. D **68**, 014506.
 Beneke, M., 1995, Phys. Lett. B **344**, 341.
 Beneke, M., 1997, e-print hep-ph/9703429.
 Beneke, M., 1998, Phys. Lett. B **434**, 115.
 Beneke, M., 1999, Phys. Rep. **317**, 1.
 Beneke, M., and V. M. Braun, 1994, Nucl. Phys. B **426**, 301.
 Beneke, M., A. P. Chapovsky, M. Diehl, and T. Feldmann, 2002, Nucl. Phys. B **643**, 431.
 Beneke, M., and T. Feldmann, 2004, Nucl. Phys. B **685**, 249.

- Beneke, M., G. A. Schuler, and S. Wolf, 2000, *Phys. Rev. D* **62**, 034004.
- Beneke, M., and A. Signer, 1999, *Phys. Lett. B* **471**, 233.
- Beneke, M., A. Signer, and V. A. Smirnov, 1998, *Phys. Rev. Lett.* **80**, 2535.
- Beneke, M., A. Signer, and V. A. Smirnov, 1999, *Phys. Lett. B* **454**, 137.
- Beneke, M., and V. A. Smirnov, 1998, *Nucl. Phys. B* **522**, 321.
- Bethe, H. A., and E. Salpeter, 1951, *Phys. Rev.* **84**, 1232.
- Bhanot, G., and M. E. Peskin, 1979, *Nucl. Phys. B* **156**, 391.
- Bigi, I. I. Y., M. A. Shifman, N. G. Uraltsev, and A. I. Vainshtein, 1994, *Phys. Rev. D* **50**, 2234.
- Billoire, A., 1980, *Phys. Lett.* **B92**, 343.
- Blok, B., J. G. Körner, D. Pirjol, and J. C. Rojas, 1997, *Nucl. Phys. B* **496**, 358.
- Bodwin, G. T., E. Braaten, and G. P. Lepage, 1992, *Phys. Rev. D* **46**, 1914.
- Bodwin, G. T., E. Braaten, and G. P. Lepage, 1995, *Phys. Rev. D* **51**, 1125.
- Bodwin, G. T., and Y.-Q. Chen, 1999, *Phys. Rev. D* **60**, 054008.
- Bodwin, G. T., and Y.-Q. Chen, 2001, *Phys. Rev. D* **64**, 114008.
- Bodwin, G. T., J. Lee, and R. Vogt, 2003, e-print hep-ph/0305034.
- Bodwin, G. T., and A. Petrelli, 2002, *Phys. Rev. D* **66**, 094011.
- Bodwin, G. T., D. K. Sinclair, and S. Kim, 1996, *Phys. Rev. Lett.* **77**, 2376.
- Bodwin, G. T., D. K. Sinclair, and S. Kim, 2002, *Phys. Rev. D* **65**, 054504.
- Bolder, B., *et al.*, 2001, *Phys. Rev. D* **63**, 074504.
- Born, K. D., E. Laermann, T. F. Walsh, and P. M. Zerwas, 1994, *Phys. Lett. B* **329**, 332.
- Braaten, E., and Y.-Q. Chen, 1998, *Phys. Rev. D* **57**, 4236.
- Braaten, E., S. Fleming, and T. C. Yuan, 1996, *Annu. Rev. Nucl. Part. Sci.* **46**, 197.
- Brambilla, N., 1998, e-print hep-ph/9809263.
- Brambilla, N., 2000, e-print hep-ph/0012211.
- Brambilla, N., P. Consoli, and G. M. Prospero, 1994, *Phys. Rev. D* **50**, 5878.
- Brambilla, N., D. Eiras, A. Pineda, J. Soto, and A. Vairo, 2002, *Phys. Rev. Lett.* **88**, 012003.
- Brambilla, N., D. Eiras, A. Pineda, J. Soto, and A. Vairo, 2003, *Phys. Rev. D* **67**, 034018.
- Brambilla, N., D. Gromes, and A. Vairo, 2001, *Phys. Rev. D* **64**, 076010.
- Brambilla, N., D. Gromes, and A. Vairo, 2003, *Phys. Lett. B* **576**, 314.
- Brambilla, N., A. Pineda, J. Soto, and A. Vairo, 1999a, *Phys. Lett. B* **470**, 215.
- Brambilla, N., A. Pineda, J. Soto, and A. Vairo, 1999b, *Phys. Rev. D* **60**, 091502.
- Brambilla, N., A. Pineda, J. Soto, and A. Vairo, 2000, *Nucl. Phys. B* **566**, 275.
- Brambilla, N., A. Pineda, J. Soto, and A. Vairo, 2001, *Phys. Rev. D* **63**, 014023.
- Brambilla, N., A. Pineda, J. Soto, and A. Vairo, 2004, *Phys. Lett. B* **580**, 60.
- Brambilla, N., Y. Sumino, and A. Vairo, 2001, *Phys. Lett. B* **513**, 381.
- Brambilla, N., Y. Sumino, and A. Vairo, 2002, *Phys. Rev. D* **65**, 034001.
- Brambilla, N., and A. Vairo, 1997, *Phys. Rev. D* **55**, 3974.
- Brambilla, N., and A. Vairo, 1999a, e-print hep-ph/9904330.
- Brambilla, N., and A. Vairo, 1999b, *Nucl. Phys. B, Proc. Suppl.* **74**, 201.
- Brambilla, N., and A. Vairo, 2000a, *Phys. Rev. D* **62**, 094019.
- Brambilla, N., and A. Vairo, 2000b, e-print hep-ph/0004192.
- Brambilla, N., *et al.*, 2004, e-print hep-ph/0412158.
- Brodsky, S. J., D. G. Coyne, T. A. DeGrand, and R. R. Horgan, 1978, *Phys. Lett.* **73B**, 203.
- Brown, L. S., and W. I. Weisberger, 1979, *Phys. Rev. D* **20**, 3239.
- Buchmüller, W., Y. J. Ng, and S. H. H. Tye, 1981, *Phys. Rev. D* **24**, 3003.
- Burdman, G., and J. F. Donoghue, 1992, *Phys. Lett. B* **280**, 287.
- Campostrini, M., 1985, *Nucl. Phys. B* **256**, 717.
- Campostrini, M., A. Di Giacomo, and S. Olejnik, 1986, *Z. Phys. C* **31**, 577.
- Capitani, S., M. Luscher, R. Sommer, and H. Wittig (ALPHA Collaboration), 1999, *Nucl. Phys. B* **544**, 669.
- Casalbuoni, R., *et al.*, 1997, *Phys. Rep.* **281**, 145.
- Caswell, W. E., and G. P. Lepage, 1986, *Phys. Lett.* **167B**, 437.
- Catani, S., and F. Hautmann, 1995, *Nucl. Phys. B, Proc. Suppl.* **39BC**, 359.
- Chay, J., and C. Kim, 2002, *Phys. Rev. D* **65**, 114016.
- Chen, Y.-Q., Y.-P. Kuang, and R. J. Oakes, 1995, *Phys. Rev. D* **52**, 264.
- Chetyrkin, K. G., and M. Steinhauser, 2000, *Nucl. Phys. B* **573**, 617.
- Chishtie, F. A., and V. Elias, 2001, *Phys. Lett. B* **521**, 434.
- Choi, S. K., *et al.* (Belle Collaboration), 2003, *Phys. Rev. Lett.* **91**, 262001.
- Cinabro, D., *et al.* (CLEO Collaboration), 2002, e-print hep-ex/0207062.
- Contreras, C., G. Cvetic, and P. Gaete, 2004, *Phys. Rev. D* **70**, 034008.
- Curci, G., A. Di Giacomo, and G. Paffuti, 1983, *Z. Phys. C* **18**, 135.
- Cvetic, G., 2004, *J. Phys. G* **30**, 863.
- Czarnecki, A., and A. G. Grozin, 1997, *Phys. Lett. B* **405**, 142.
- Czarnecki, A., and K. Melnikov, 1998, *Phys. Rev. Lett.* **80**, 2531.
- Czarnecki, A., and K. Melnikov, 2001, *Phys. Lett. B* **519**, 212.
- Czarnecki, A., and K. Melnikov, 2002, *Phys. Rev. D* **65**, 051501.
- Czarnecki, A., K. Melnikov, and A. Yelkhovsky, 1999a, *Phys. Rev. Lett.* **82**, 311.
- Czarnecki, A., K. Melnikov, and A. Yelkhovsky, 1999b, *Phys. Rev. A* **59**, 4316.
- De Rujula, A., and S. L. Glashow, 1975, *Phys. Rev. Lett.* **34**, 46.
- D'Elia, M., A. Di Giacomo, and E. Meggiolaro, 1997, *Phys. Lett. B* **408**, 315.
- Di Giacomo, A., H. G. Dosch, V. I. Shevchenko, and Y. A. Simonov, 2002, *Phys. Rep.* **372**, 319.
- Dirac, P. A. M., 1949, *Rev. Mod. Phys.* **21**, 392.
- Dosch, H. G., and Y. A. Simonov, 1988, *Phys. Lett. B* **205**, 339.
- Eichten, E., and F. Feinberg, 1981, *Phys. Rev. D* **23**, 2724.
- Eichten, E., K. Gottfried, T. Kinoshita, K. D. Lane, and T.-M. Yan, 1978, *Phys. Rev. D* **17**, 3090.
- Eichten, E., and B. Hill, 1990, *Phys. Lett. B* **243**, 427.
- Eichten, E. J., and C. Quigg, 1995, *Phys. Rev. D* **52**, 1726.
- Eidelman, S., *et al.* (Particle Data Group), 2004, *Phys. Lett. B* **592**, 1.
- Eidemüller, M., 2003, *Phys. Rev. D* **67**, 113002.
- Eiras, D., and J. Soto, 2000, *Phys. Lett. B* **491**, 101.
- Fadin, V. S., and V. A. Khoze, 1988, *Sov. J. Nucl. Phys.* **48**, 309.

- Falk, A. F., B. Grinstein, and M. E. Luke, 1991, Nucl. Phys. B **357**, 185.
- Field, J. H., 2002, Phys. Rev. D **66**, 013013.
- Fischler, W., 1977, Nucl. Phys. B **129**, 157.
- Fleming, S., and A. K. Leibovich, 2003a, Phys. Rev. D **67**, 074035.
- Fleming, S., and A. K. Leibovich, 2003b, Phys. Rev. Lett. **90**, 032001.
- Fleming, S., and A. K. Leibovich, 2004, Phys. Rev. D **70**, 094016.
- Fleming, S., I. Z. Rothstein, and A. K. Leibovich, 2001, Phys. Rev. D **64**, 036002.
- Foldy, L. L., 1961, Phys. Rev. **122**, 275.
- Foster, M., and C. Michael (UKQCD Collaboration), 1999, Phys. Rev. D **59**, 094509.
- Fujii, H., and D. Kharzeev, 1999, Phys. Rev. D **60**, 114039.
- Garcia i Tormo, X., and J. Soto, 2004, Phys. Rev. D **69**, 114006.
- Gray, A., *et al.* (HPQCD Collaboration), 2003, Nucl. Phys. B, Proc. Suppl. **119**, 592.
- Gray, N., D. J. Broadhurst, W. Grafe, and K. Schilcher, 1990, Z. Phys. C **48**, 673.
- Gremm, M., and A. Kapustin, 1997, Phys. Lett. B **407**, 323.
- Griesshammer, H. W., 1998, Phys. Rev. D **58**, 094027.
- Griesshammer, H. W., 2000, Nucl. Phys. B **579**, 313.
- Grinstein, B., and I. Z. Rothstein, 1998, Phys. Rev. D **57**, 78.
- Gromes, D., 1984, Z. Phys. C **26**, 401.
- Groote, S., and A. A. Pivovarov, 2002, JETP Lett. **75**, 221.
- Gupta, S. N., and S. F. Radford, 1981, Phys. Rev. D **24**, 2309.
- Gupta, S. N., and S. F. Radford, 1982, Phys. Rev. D **25**, 3430.
- Gupta, S. N., W. W. Repko, and I. C. J. Suchyta, 1989, Phys. Rev. D **40**, 4100.
- Hagiwara, K., C. B. Kim, and T. Yoshino, 1981, Nucl. Phys. B **177**, 461.
- Harris, I., and L. Brown, 1957, Phys. Rev. **105**, 1656.
- Herb, S. W., *et al.*, 1977, Phys. Rev. Lett. **39**, 252.
- Hill, R., and G. P. Lepage, 2000, Phys. Rev. D **62**, 111301.
- Hill, R. J., 2001, Phys. Rev. Lett. **86**, 3280.
- Hill, R. J., and M. Neubert, 2003, Nucl. Phys. B **657**, 229.
- Hoang, A. H., 1999, Phys. Rev. D **59**, 014039.
- Hoang, A. H., 2000, e-print hep-ph/0008102.
- Hoang, A. H., 2002, e-print hep-ph/0204299.
- Hoang, A. H., 2003, Acta Phys. Pol. B **34**, 4491.
- Hoang, A. H., 2004, Phys. Rev. D **69**, 034009.
- Hoang, A. H., P. Labelle, and S. M. Zebarjad, 1997, Phys. Rev. Lett. **79**, 3387.
- Hoang, A. H., Z. Ligeti, and A. V. Manohar, 1999, Phys. Rev. Lett. **82**, 277.
- Hoang, A. H., A. V. Manohar, and I. W. Stewart, 2001, Phys. Rev. D **64**, 014033.
- Hoang, A. H., A. V. Manohar, I. W. Stewart, and T. Teubner, 2001, Phys. Rev. Lett. **86**, 1951.
- Hoang, A. H., A. V. Manohar, I. W. Stewart, and T. Teubner, 2002, Phys. Rev. D **65**, 014014.
- Hoang, A. H., M. C. Smith, T. Stelzer, and S. Willenbrock, 1999, Phys. Rev. D **59**, 114014.
- Hoang, A. H., and I. W. Stewart, 2003, Phys. Rev. D **67**, 114020.
- Hoang, A. H., and T. Teubner, 1999, Phys. Rev. D **60**, 114027.
- Hoang, A. H., *et al.*, 2000, Eur. Phys. J. C **2**, 3.
- Huntley, A., and C. Michael, 1987, Nucl. Phys. B **286**, 211.
- Isgur, N., and J. Paton, 1985, Phys. Rev. D **31**, 2910.
- Juge, K. J., J. Kuti, and C. Morningstar, 2003, Phys. Rev. Lett. **90**, 161601.
- Källen, G., and A. Sarby, 1955, K. Dan. Vidensk. Selsk. Mat. Fys. Medd. **29 N17**, 1.
- Kinoshita, T., and M. Nio, 1996, Phys. Rev. D **53**, 4909.
- Kiyo, Y., and Y. Sumino, 2000, Phys. Lett. B **496**, 83.
- Kniehl, B. A., and A. A. Penin, 1999, Nucl. Phys. B **563**, 200.
- Kniehl, B. A., and A. A. Penin, 2000a, Phys. Rev. Lett. **85**, 1210.
- Kniehl, B. A., and A. A. Penin, 2000b, Phys. Rev. Lett. **85**, 5094.
- Kniehl, B. A., and A. A. Penin, 2000c, Nucl. Phys. B **577**, 197.
- Kniehl, B. A., A. A. Penin, A. Pineda, V. A. Smirnov, and M. Steinhauser, 2004, Phys. Rev. Lett. **92**, 242001.
- Kniehl, B. A., A. A. Penin, Y. Schroder, V. A. Smirnov, and M. Steinhauser, 2005, Phys. Lett. B **607**, 96.
- Kniehl, B. A., A. A. Penin, V. A. Smirnov, and M. Steinhauser, 2002a, Nucl. Phys. B **635**, 357.
- Kniehl, B. A., A. A. Penin, M. Steinhauser, and V. A. Smirnov, 2002b, Phys. Rev. D **65**, 091503.
- Kniehl, B. A., A. A. Penin, M. Steinhauser, and V. A. Smirnov, 2003, Phys. Rev. Lett. **90**, 212001.
- Koller, K., and T. Walsh, 1978, Nucl. Phys. B **140**, 449.
- Krajcik, R. A., and L. L. Foldy, 1974, Phys. Rev. D **10**, 1777.
- Krämer, A., H. G. Dosch, and R. A. Bertlmann, 1992, Fortschr. Phys. **40**, 93.
- Krämer, M., 1999, Phys. Rev. D **60**, 111503.
- Krämer, M., 2001, Prog. Part. Nucl. Phys. **47**, 141.
- Kronfeld, A. S., 1998, Phys. Rev. D **58**, 051501.
- Kronfeld, A. S., 2004, Nucl. Phys. B, Proc. Suppl. **129**, 46.
- Kuhn, J. H., A. A. Penin, and A. A. Pivovarov, 1998, Nucl. Phys. B **534**, 356.
- Kummer, W., W. Mödrtsch, and A. Vairo, 1996, Z. Phys. C **72**, 653.
- Labelle, P., 1998, Phys. Rev. D **58**, 093013.
- Labelle, P., S. M. Zebarjad, and C. P. Burgess, 1997, Phys. Rev. D **56**, 8053.
- Le Guillou, J. C., and J. Zinn-Justin, 1990, Eds., *Large Order Behavior of Perturbation Theory (Current Physics—Sources and Comments)* (North-Holland, Amsterdam).
- Lee, T., 2003a, J. High Energy Phys. **10**, 044.
- Lee, T., 2003b, Phys. Rev. D **67**, 014020.
- Lepage, G. P., 1997, e-print nucl-th/9706029.
- Lepage, G. P., 2005, Ann. Phys. (N.Y.) **315**, 193.
- Lepage, G. P., and B. A. Thacker, 1988, Nucl. Phys. B, Proc. Suppl. **4**, 199.
- Lepage, G. P., *et al.*, 1992, Phys. Rev. D **46**, 4052.
- Lepage, P., and C. Davies, 2004, Int. J. Mod. Phys. A **19**, 877.
- Leutwyler, H., 1981, Phys. Lett. **98B**, 447.
- Lucha, W., F. F. Schöberl, and D. Gromes, 1991, Phys. Rep. **200**, 127.
- Lucini, B., and M. Teper, 2001, J. High Energy Phys. **06**, 050.
- Luke, M. E., and A. V. Manohar, 1992, Phys. Lett. B **286**, 348.
- Luke, M. E., and A. V. Manohar, 1997, Phys. Rev. D **55**, 4129.
- Luke, M. E., A. V. Manohar, and I. Z. Rothstein, 2000, Phys. Rev. D **61**, 074025.
- Luke, M. E., and M. J. Savage, 1998, Phys. Rev. D **57**, 413.
- Lüscher, M., and P. Weisz, 2002, J. High Energy Phys. **07**, 049.
- Lüscher, M., and P. Weisz, 2004, J. High Energy Phys. **07**, 014.
- Ma, J. P., and Q. Wang, 2002, Phys. Lett. B **537**, 233.
- Mackenzie, P. B., and G. P. Lepage, 1981, Phys. Rev. Lett. **47**, 1244.
- Maltoni, F., 1999, Ph.D. thesis (University of Pisa).
- Maltoni, F., 2000, e-print hep-ph/0007003.
- Maltoni, F., and A. Petrelli, 1999, Phys. Rev. D **59**, 074006.

- Mannel, T., and R. Urech, 1997, *Z. Phys. C* **73**, 541.
- Manohar, A. V., 1997, *Phys. Rev. D* **56**, 230.
- Manohar, A. V., and P. Ruiz-Femenia, 2004, *Phys. Rev. D* **69**, 053003.
- Manohar, A. V., and I. W. Stewart, 2000a, *Phys. Rev. Lett.* **85**, 2248.
- Manohar, A. V., and I. W. Stewart, 2000b, *Phys. Rev. D* **62**, 074015.
- Manohar, A. V., and I. W. Stewart, 2000c, *Phys. Rev. D* **62**, 014033.
- Manohar, A. V., and I. W. Stewart, 2001, *Phys. Rev. D* **63**, 054004.
- Martinelli, G., *et al.*, 1997, *Phys. Lett. B* **411**, 141.
- Martinez, M., and R. Miquel, 2003, *Eur. Phys. J. C* **27**, 49.
- Matsui, T., and H. Satz, 1986, *Phys. Lett. B* **178**, 416.
- Mattson, M., *et al.* (SELEX Collaboration), 2002, *Phys. Rev. Lett.* **89**, 112001.
- Melles, M., 2000, *Phys. Rev. D* **62**, 074019.
- Melnikov, K., and T. v. Ritbergen, 2000, *Phys. Lett. B* **482**, 99.
- Melnikov, K., and A. Yelkhovsky, 1998, *Nucl. Phys. B* **528**, 59.
- Melnikov, K., and A. Yelkhovsky, 1999a, *Phys. Rev. D* **59**, 114009.
- Melnikov, K., and A. Yelkhovsky, 1999b, *Phys. Lett. B* **458**, 143.
- Melnikov, K., and A. Yelkhovsky, 2000, *Phys. Rev. D* **62**, 116003.
- Melnikov, K., and A. Yelkhovsky, 2001, *Phys. Rev. Lett.* **86**, 1498.
- Messiah, A., 1979, *Quantum Mechanics* (De Gruyter, Berlin), Vol. 2.
- Michael, C., 1986, *Phys. Rev. Lett.* **56**, 1219.
- Migdal, A. A., 1983, *Phys. Rep.* **102**, 199.
- Morningstar, C. J., and M. J. Peardon, 1999, *Phys. Rev. D* **60**, 034509.
- Necco, S., and R. Sommer, 2001, *Phys. Lett. B* **523**, 135.
- Necco, S., and R. Sommer, 2002, *Nucl. Phys. B* **622**, 328.
- Nemati, B., *et al.* (CLEO Collaboration), 1997, *Phys. Rev. D* **55**, 5273.
- Neubert, M., 1994, *Phys. Rep.* **245**, 259.
- Neubert, M., and C. T. Sachrajda, 1995, *Nucl. Phys. B* **438**, 235.
- Onishchenko, A. I., 2000, e-print hep-ph/0005127.
- Pantaleone, J., S. H. H. Tye, and Y. J. Ng, 1986, *Phys. Rev. D* **33**, 777.
- Pascual, P., and R. Tarrach, 1984, *Lect. Notes Phys.* **194**, 1.
- Penin, A. A., A. Pineda, V. A. Smirnov, and M. Steinhauser, 2004a, *Phys. Lett. B* **593**, 124.
- Penin, A. A., A. Pineda, V. A. Smirnov, and M. Steinhauser, 2004b, *Nucl. Phys. B* **699**, 183.
- Penin, A. A., and A. A. Pivovarov, 1998, *Phys. Lett. B* **435**, 413.
- Penin, A. A., and A. A. Pivovarov, 1999, *Nucl. Phys. B* **549**, 217.
- Penin, A. A., and A. A. Pivovarov, 2001, *Phys. At. Nucl.* **64**, 275.
- Penin, A. A., and M. Steinhauser, 2002, *Phys. Lett. B* **538**, 335.
- Peskin, M. E., 1979, *Nucl. Phys. B* **156**, 365.
- Peskin, M. E., 1983, presented at *11th International SLAC Summer Institute on Particle Physics*, Stanford, CA, July 18–26.
- Peter, M., 1997, *Phys. Rev. Lett.* **78**, 602.
- Petrelli, A., M. Cacciari, M. Greco, F. Maltoni, and M. L. Mangano, 1998, *Nucl. Phys. B* **514**, 245.
- Photiadis, D. M., 1985, *Phys. Lett.* **164B**, 160.
- Pineda, A., 1997a, *Phys. Rev. D* **55**, 407.
- Pineda, A., 1997b, *Nucl. Phys. B* **494**, 213.
- Pineda, A., 1998, Ph.D. thesis (University of Barcelona).
- Pineda, A., 2001, *J. High Energy Phys.* **06**, 022.
- Pineda, A., 2002a, *Phys. Rev. D* **66**, 054022.
- Pineda, A., 2002b, *Phys. Rev. D* **65**, 074007.
- Pineda, A., 2002c, *Phys. Rev. A* **66**, 062108.
- Pineda, A., 2003a, *Acta Phys. Pol. B* **34**, 5295.
- Pineda, A., 2003b, *J. Phys. G* **29**, 371.
- Pineda, A., 2004, *Nucl. Phys. B, Proc. Suppl.* **133**, 190.
- Pineda, A., and J. Soto, 1998a, *Nucl. Phys. B, Proc. Suppl.* **64**, 428.
- Pineda, A., and J. Soto, 1998b, *Phys. Lett. B* **420**, 391.
- Pineda, A., and J. Soto, 1998c, *Phys. Rev. D* **58**, 114011.
- Pineda, A., and J. Soto, 1999, *Phys. Rev. D* **59**, 016005.
- Pineda, A., and J. Soto, 2000, *Phys. Lett. B* **495**, 323.
- Pineda, A., and A. Vairo, 2001, *Phys. Rev. D* **63**, 054007.
- Pineda, A., and F. J. Yndurain, 1998, *Phys. Rev. D* **58**, 094022.
- Pineda, A., and F. J. Yndurain, 2000, *Phys. Rev. D* **61**, 077505.
- Portoles, J., and P. D. Ruiz-Femenia, 2002, *Eur. Phys. J. C* **24**, 439.
- Recksiegel, S., and Y. Sumino, 2002, *Phys. Rev. D* **65**, 054018.
- Recksiegel, S., and Y. Sumino, 2003, *Eur. Phys. J. C* **31**, 187.
- Recksiegel, S., and Y. Sumino, 2004, *Phys. Lett. B* **578**, 369.
- Rösch, T., 2003, Diploma thesis (University of Heidelberg).
- Rothstein, I. Z., and M. B. Wise, 1997, *Phys. Lett. B* **402**, 346.
- Scherer, S., and H. W. Fearing, 1995, *Phys. Rev. D* **52**, 6445.
- Schröder, Y., 1999a, Ph.D. thesis (University of Hamburg), DESY-THESIS-1999-021.
- Schröder, Y., 1999b, *Phys. Lett. B* **447**, 321.
- Sebastian, K. J., and D. Yun, 1979, *Phys. Rev. D* **19**, 2509.
- Skwarnicki, T., 2004, *Int. J. Mod. Phys. A* **19**, 1030.
- Sommer, R., 1994, *Nucl. Phys. B* **411**, 839.
- Soto, J., 2003, e-print hep-ph/0301138.
- Strassler, M. J., and M. E. Peskin, 1991, *Phys. Rev. D* **43**, 1500.
- Sumino, Y., 2002, *Phys. Rev. D* **65**, 054003.
- Susskind, L., 1977, in *Les Houches 1976, Proceedings, Weak and Electromagnetic Interactions at High Energies* (North-Holland, Amsterdam), pp. 207–308.
- Szczepaniak, A. P., and E. S. Swanson, 1997, *Phys. Rev. D* **55**, 3987.
- Thacker, B. A., and G. P. Lepage, 1991, *Phys. Rev. D* **43**, 196.
- Titard, S., and F. J. Yndurain, 1994, *Phys. Rev. D* **49**, 6007.
- Titard, S., and F. J. Yndurain, 1995, *Phys. Rev. D* **51**, 6348.
- Trottier, H. D., and G. P. Lepage, 1998, *Nucl. Phys. B, Proc. Suppl.* **63**, 865.
- Vairo, A., 2000, e-print hep-ph/0010191.
- Vairo, A., 2002, e-print hep-ph/0212271.
- Vairo, A., 2003, *Nucl. Phys. B, Proc. Suppl.* **115**, 166.
- Vairo, A., 2004a, *Nucl. Phys. B, Proc. Suppl.* **133**, 196.
- Vairo, A., 2004b, *Mod. Phys. Lett. A* **19**, 253.
- Voloshin, M. B., 1979, *Nucl. Phys. B* **154**, 365.
- Voloshin, M. B., 1982, *Sov. J. Nucl. Phys.* **36**, 143.
- Voloshin, M. B., 1995, *Int. J. Mod. Phys. A* **10**, 2865.
- Voloshin, M. B., 2003, *Phys. Lett. B* **562**, 68.
- Voloshin, M. B., 2004, *Mod. Phys. Lett. A* **19**, 181.
- Wang, H.-b., and Y.-P. Yao, 2004, *Phys. Rev. D* **70**, 094046.
- Wilson, K. G., 1974, *Phys. Rev. D* **10**, 2445.
- Wolf, S., 2001, *Phys. Rev. D* **63**, 074020.
- Yakovlev, O. I., and S. Groote, 2001, *Phys. Rev. D* **63**, 074012.
- Yelkhovsky, A., 2001, *Phys. Rev. A* **64**, 062104.
- Yndurain, F. J., 1999, *The Theory of Quark and Gluon Interactions* (Springer, Berlin).